Open Research Online

The Open University's repository of research publications
and other research outputs

Mechanisms and Factors Promoting Faithful Replication of Problematic Genomic Regions

Thesis

How to cite:

Agashe, Sumedha (2020). Mechanisms and Factors Promoting Faithful Replication of Problematic Genomic Regions. PhD thesis The Open University.

For guidance on citations see FAQs.

© 2020 Sumedha Agashe

https://creativecommons.org/licenses/by-nc-nd/4.0/

Version: Version of Record

Link(s) to article on publisher's website:
http://dx.doi.org/doi:10.21954/ou.ro.00011f56

Copyright and Moral Rights for the articles on this site are retained by the individual authors and/or other copyright owners. For more information on Open Research Online's data policy on reuse of materials please consult the policies page.

oro.open.ac.uk

Mechanisms and factors promoting faithful replication of problematic genomic regions

Sumedha Agashe
Student ID: F253085X

Supervisor: **Dr. Dana Branzei**
External Supervisor: Prof. Johanne Murray

Degree: Doctor of Philosophy
Program: Programme in Fundamentals of Cancer Biology
Discipline: School of Life, Health and Chemical Sciences
Registration owner: Affiliated Research Centre programme
Affiliated Research Centre: IFOM Fondazione- The FIRC Institute for Molecular Oncology
Submission: August 2020

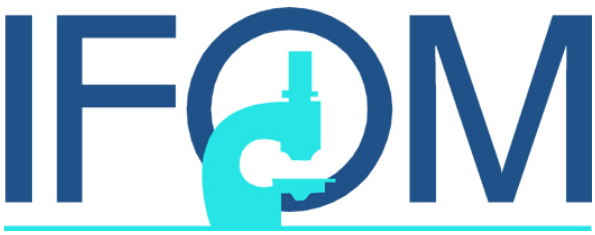

Abstract

Natural Pausing Sites (NPSs) are complex genomic regions predisposed to fragility. Our lab previously uncovered that the Smc5/6 complex is critical for replication through NPSs. We hypothesized that Smc5/6 maintains NPS integrity by coupling replication fork pausing at different repeat elements with recombination and recombination intermediate resolution. The Sgs1-Top3-Rmi1 (STR) complex and Smc5/6 co-localize genome-wide in G2/M, and prevent accumulation of recombination structures at damaged forks. Here we use several genome-wide and locus-specific methods to investigate the mechanisms and factors involved in NPS metabolism. We find evidence that Smc5/6 collaborates tightly with STR and coordinates various resolvases at NPSs to support replication completion.

Smc5/6 chromatin clusters overlap with the ones of Top3 and Rmi1 and are enriched at NPSs, where Smc5/6 facilitates Top3 retention. Further, we observe that Smc6 mutants that accumulate recombination intermediates at replication termination regions encode variants that bind less efficiently to NPSs. Both Smc5/6 dysfunction and STR depletion cause accumulation of recombination intermediates at stalled NPSs. A newly discovered intragenic mutation of *smc6-56* restores Top3 binding but causes additivity with various *sgs1* mutants, suggesting defects in other resolvases, possibly Mus81-Mms4. We further observe a role for Smc5/6, STR and DNA damage tolerance (DDT) pathways mediated by the polymerase clamp PCNA at topologically constrained regions along with Top2. We observe aggravated *top2-4* temperature sensitivity for mutants of the above-mentioned factors, which is independent of Rad51 dependent recombination.

Taken together, our results indicate a role for the STR complex in collaboration with Smc5/6 in NPS maintenance by resolving recombination intermediates to allow faithful segregation of these complex genomic regions. We further observe a role for STR, DDT and Smc5/6 along Top2 in facilitating resolution of topological stress before and during mitosis.

Acknowledgements

I would like to thank my supervisor Dr. Dana Branzei for her constant support and encouragement. Her supervision led both my PhD project and my scientific ambition in the right direction. I will always be thankful for her mentorship during this crucial period of my career. I feel lucky to have worked with a lab as diverse and unique as Branzei lab at IFOM. I thank each member of the lab for their contribution in my project and in discussions.

I would like to thank my external supervisor in the UK Dr. Jo Murray and third-party monitor at IFOM Dr. Stefano Casola for their help and discussions during my PhD. I am also grateful to Mio Sumie for her continuous support during my PhD, and Marina Properzi for her generous help as an International Students' Office staff and as an Italian teacher. I am grateful to IFOM for providing us the opportunity to focus on science while Marina and Mio took care of all the bureaucracy. I am also grateful to IFOM facilities and offices.

Lastly, I thank my family and friends for being with me during the time of my PhD, to help me get through the low points and celebrate with me during success.

List of Content:

List of Tables:

List of Figures:

List of abbreviations:

ARS	Autonomously Replicating Sequence
ChIP	Chromatin Immunoprecipitation
CFSs	Common Fragile Sites
CPT	Camptothecin
DDT	DNA Damage Tolerance
DSB	Double Strand Break
dHJs	Double Holliday Junctions
ERCc	Extrachromosomal rDNA Circles
FA	Fanconi Anaemia
GCRs	Gross Chromosomal Rearrangements
HR	Homologous Recombination
HU	Hydroxyurea
ICL	Inter-strand Crosslinking
LTRs	Long Terminal Repeats
MAGE	Melanoma-associated Antigen Gene
MMC	Mytomycin C
MMS	Methyl metansulfonate
NPSs	Natural Pausing Sites
NSE	Non SMC Element
PCNA	Proliferating Cell Nuclear Antigen
PFGE	Pulse Field Gel Electrophoresis
PRR	Post Replication Repair
RF	Replication fork
RFB	Replication Fork Barrier
SCIs	Sister Chromatid Intertwinings
SCJs	Sister Chromatid Junctions
SMC	Structural Maintenance of Chromosome
STR	Sgs1-Top3-Rmi1
SUMO	Small Ubiquitin-like Modifier
TERs	Termination Regions
TLS	Translesion synthesis
TS	Template Switching
WT	Wild Type

Chapter 1

Introduction

1.1 Introduction to replication fork pausing and natural pausing sites

1.1.1 Replication fork Pausing

Every cell undergoing mitotic division faithfully replicates its genome in a tedious and meticulous process to distribute identical genetic material to the two daughter cells. The process of replication needs to be accurate, rapid and restricted to only once per cell cycle. The cells activate several mechanisms to maintain the speed, accuracy and co-ordination of the process. Despite being tightly regulated, the replication process still faces obstacle that stall replication. Cells face high risk of DNA damage at stalled replication forks and such replication associated DNA damage is a major cause of mutagenesis as well as genomic instability leading to cancer.

Actively dividing cells initiate the cell cycle from G1 phase, where the cells prepare the machinery for duplicating its content. The replication is initiated in S-phase. Once initiated, the replication continues throughout the S-phase and during late S early G2/M phase the replication process terminates preventing the replication of the same region multiple times. The process of unwinding DNA, replicating leading/lagging strand and replication fork fusion is tightly coordinated. Genome replication is a tedious process and although the process of replication is conserved between prokaryotic and eukaryotic cells, there are differences in the details and in the variety of proteins involved.

While replication is a tightly regulated, there are several obstacles that are faced by a progressing replication fork (RF). Upon encountering regions of intrinsic replication complexity, the RF transiently pauses. The cells have established mechanisms to allow pausing of the RF until the replication obstacles are dealt with. RF continues through these regions upon removal of obstacles. The obstacles are either natural impediments, such as proteins bound to a certain sequence, secondary structures or spontaneous DNA lesions, or chemical obstacles arising due to external agents or metabolism.

1.1.2 Artificial vs Natural RF pausing

Several factors can cause impediments to progressing RFs. Chemical obstacles arise due to the treatment with DNA damaging agents such as UV light, Hydroxyurea (HU), Camptothecin (CPT) etc. These reagents cause either DNA damage and/or nucleotide pool depletion and result in transient fork pausing. Although such replication fork pausing is more severe and has effects on cell growth in certain mutant backgrounds, we are mainly interested in natural RF pausing for this thesis. The natural pausing of RF occurs due to the complex

nature of the genome. The progressing RF encounters an intrinsic obstacle and transiently pauses. The regions of such transient RF pausing in unperturbed replication are grouped under the category natural pausing sites (NPSs). They are similar to common fragile sites (CFSs) defined in mammalian cells. These regions are typical for being more prone to RF pausing and thus fragility in normal replicating cells. Both prokaryotes and eukaryotes have evolved mechanisms to deal with NPSs and even to take advantage of NPSs for replication termination.

1.1.3 Bacterial NPSs and replication termination

Starting from single cellular bacteria to multi-cellular complex organisms, the process of DNA replication is conserved. From the simple organism *E. coli*, we will begin our pursuit of understanding replication termination and RF pausing at NPSs. *E. coli* has a circular genome and employs a highly efficient strategy of polar arrest of RFs. These RFs emerge from one single origin of replication and converge at the termination region that is defined by the Tus-Ter complex. *E. coli* contains a Ter region in its genome composed of 14 to 16 base pair inverted repeats. To these Ter repeats, Tus protein binds forming a polar replication barrier. The binding of Tus to the Ter region is based on the conserved region within Ter composed of C6. When the RF approaches from the non-permissive side, it leads to tightening of the Tus-Ter complex and dislodging of the replication machinery until the other fork approaches from the permissive side. Only when the conserved C6 region is melted from both sides by advancing helicases, the Tus-Ter complex is destabilized leading to its removal from DNA and thus completion of replication. Preventing the binding of the Tus protein to the Ter region by mutagenesis of the region leads to failure of replication termination. Thus, this DNA-protein barrier is essential for termination (Kaplan, 2006; Sista et al., 1989). This is the simplest known example of termination where a single replication origin is active, leading to termination by fusion of two replication forks from opposite directions using RF pausing for their advantage.

1.1.4 Eukaryotic NPSs and replication stress associated with them

The factors involved in replication become more diverse as the genome gets more complex. One of the major challenges during replication in most of the organisms is replication termination. With the help of RF pausing and programmed fork block the cells have established mechanisms to terminate replication. The replication pausing however causes stress that cells have to deal with. Here we discuss how the replication stress is generated in eukaryotic cells at NPSs.

Replication in higher organisms is activated at multiple ARS (Autonomously Replicating Sequences), therefore terminated at multiple locations increasing the complexity of the process. These regions are often referred as Termination regions (TERs). There are 71 identified TERs in yeast (*Saccharomyces cerevisiae*). These regions often contain polar pausing elements that facilitate fork merging. The model for replication termination is believed to be asymmetric fork progression due to programmed fork pausing that completes the replication with pre-catenanes that can be resolved by topoisomerase Top2 post replication (Fachinetti et al., 2010). The programmed fork pausing at TERs is caused by several replication fork (RF) impediments. The DNA composition (such as repeats, putative hairpin formation, high transcription) is one responsible factor for pausing and fragility at these regions. A 2006 yeast study uncovered that inhibiting late replication origin firing resulted in small replication products arrested at specific sites. These sites were fragile and prone to breakage in natural conditions of replication without external DNA damage (Raveendranathan et al., 2006). Another interesting genome-wide approach was used in 2009 to understand replication pausing/slowing down. This study identified pausing sites by ChIP of RNA polymerase II. Interestingly, some of these regions were overlapping with RNA PolII genes that are highly transcribed and some other with previously identified DNA-protein complexes (Azvolinsky et al., 2009b; Takeuchi et al., 2003). The fragile sites in yeast were later also identified by mapping gamma H2A foci. One indicator of DNA damage or breaks is phosphorylation of histone H2A in Mec1/Tel1 dependent manner leading to formation of the gamma H2A foci. Half of these co-localized with silenced protein coding regions and other NPSs including tRNA, rRNA genes, telomeres, LTRs and replication origin (Szilard et al., 2010). Together these three studies identified various natural pausing sites (NPSs) of *S. cerevisiae* that cause RF pausing without DNA damaging conditions. There is overlap between TERs and NPSs as the pausing can mediate termination.

In fission yeast *Schizosaccharomyces pombe*, replication-recombination coupled pathways are used for Mat type switching. The Mat locus contains a known fragile site. Various studies have identified that this site is a polar replication barrier. Replication fork stalling at this barrier was studied and it was seen that the cells restore (or complete) replication through recombination mediated pathways (Ahn et al., 2005; Arcangioli and de Lahondes, 2000; Dalgaard and Klar, 2001; Lambert et al., 2005).

Several studies in higher eukaryotes involving chicken DT40 and human cell lines have addressed RF stalling at NPSs with interesting results. A class of fragile sites were identified in 1984 and termed as Common Fragile Sites (CFSs) in a mammalian study. These were sites of breakage upon metaphase spread after Aphidicolin treatment. Aphidicolin inhibits polymerase alpha and therefore was used as a tool to detect hot spots for fragility and breaks.

The 75 aphidicolin-induced common fragile sites identified in this study are listed in Genbank (Glover et al., 1984).

Our understanding so far indicates that the natural RF pausing can be caused by transcription-replication collision, protein-DNA complexes, DNA secondary structures and repeat elements. NPSs are often composed of clusters of secondary structures and repeat elements. NPSs are found in genomes of bacteria, yeast and higher eukaryotes causing RF pausing in a similar manner. We further discuss each of the above-mentioned types of RF pausing.

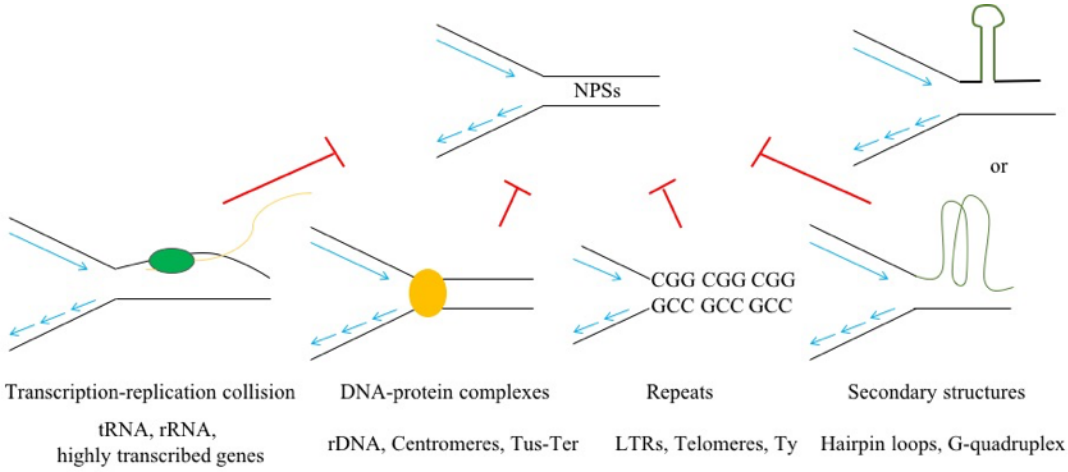

Fig1.1: Summary of major contributors of RF pausing

1.1.4.1 Transcription-replication collision

When replication and transcription are proceeding in the same direction, since the DNA polymerase is moving faster than the RNA polymerase, the replication can be slowed down by the ongoing transcription. The RNA polymerase travelling in opposite direction of DNA polymerase causes even more problems. The head-on collision between DNA and RNA polymerases leads to pausing of replication. Prolonged pausing of the replication fork is dangerous for cells as it can cause dissociation of the replication machinery from the fork, leading to gaps and/or unreplicated DNA that later on may cause segregation defects and aneuploidy (Liu and Alberts, 1995; Matsuzaki et al., 1994; Omont and Képès, 2004).

One of the most commonly studied case of transcription-replication collision is at rDNA regions. The rDNA genes are highly transcribed. Therefore, the cells have to come up with strategies to overcome the obstacles caused by ongoing transcription. Other than rDNA, also tRNA genes are highly expressed, the collision between replication and transcription machinery is likely at tRNA genes (Azvolinsky et al., 2009b; Takeuchi et al., 2003).

The active transcription of rDNA repeats causes replication barriers, cells employ fork pausing strategies in order to prevent replication-transcription head-on collision. Fob1 mediated protein-DNA complex causes a polar block of the RF. Prolonged pausing can cause

recombination at the rDNA region, which gives rise to extrachromosomal rDNA circles (ERCs) formation. ERCs lead to reduced rDNA copy number and are associated with yeast aging. Transcription of the rDNA region (in the absence of the RF block imposed by Fob1) also induces recombination leading to rDNA copy number variation and ERC formation. The torsional stress by high levels of transcription could lead to recombination events without RF pausing. Therefore, for smooth replication of the region, Fob1 mediated block is essential and is later removed by specialised helicases to complete replication through rDNA region (Brewer and Fangman, 1988; Defossez et al., 1999; Takeuchi et al., 2003). Furthermore, a study in 2014 using human patient cells showed that DNA-RNA hybrids at transcriptionally active rDNA region form R loops. These R loops (enhanced with camptothecin/CPT treatment) upregulate the repressive epigenetic marks silencing the genes which in turn causes Friedreich ataxia (FRDA) and Fragile X syndrome (FXS). This links R-loops (and excessive RF pausing) to several pathological conditions (Groh et al., 2014).
Another example of head-on replication-transcription collision is at tRNA genes and 3' LTRs of Ty elements. These sites are polar in nature and the RF barrier is dependent on active transcription. Interestingly, the similarity of these RF barriers to the polar barriers of *E coli* is very apparent (Deshpande and Newlon, 1996). *S. cerevisiae* chromosome site with multiple tRNA genes are prone to RF pausing and consecutive genomic rearrangements. Non-allelic recombination events take place upon excessive fork pausing. Removal of tRNA from this region reduces genome rearrangements indicating that the collision between replication and transcription is indeed responsible for genomic instability at this region (Admire et al., 2006).

1.1.4.2 Non-histone proteins bound to DNA

When a progressing RF encounters a non-histone protein bound to DNA, it tries to displace the protein and to continue replication. When the proteins are bound strongly to DNA, a moving RF is not able to displace the protein and it pauses at the barrier. The most common examples of RF block are at the rDNA region where the RF is blocked by programmed fork barrier Fob1 to systematically stall the replication fork (Kobayashi and Horiuchi, 1996). Specialized mechanisms come into play for rDNA replication to continue through the blocks without recombination and alterations in the repeat elements. Yeast centromeres and subtelomeres also contain pausing elements. The centromeres commonly contain protein-DNA complexes that cause transient replication fork barrier (Greenfeder and Newlon, 1992). Telomeric DNA is assembled differently from the rest of the genome. The DNA is assembled into telosomes instead of nucleosomes, making it difficult for replication machinery to access and replicate. Various non-histone proteins such as Sir proteins, Rif proteins, Cdc13

and other factors are bound to telomeres to protect them. This creates impediments to replication that relies on specialized helicases such as Pif1 to complete telomeric replication (Bourns et al., 1998; Tsukamoto et al., 2001; Wright et al., 1992).

1.1.4.3 Repeats

When a RF stalls close to repeats, the risk of losing or gaining repeat elements due to aberrant recombination is very high. The inverted repeats tend to form secondary structures and cause impediments to the ongoing replication. The repeat elements are at higher risk of alterations. Therefore, they are included in NPSs. The common example of repeat elements are rDNA repeats. When replication is perturbed in rDNA regions, the repeats can be lost by formation of ERCs as a result of aberrant recombination. Other examples of repeat elements include Ty transposable elements that contains repeats, CAG/CTG and other triplet repeats, telomeric repeats etc. Each example of DNA repeats poses a putative threat to unperturbed replication.

Almost 3% of the *S. cerevisiae* genome is retrotransposons and these are flanked by long terminal repeats (LTRs). The homology between Ty elements has potential to cause genetic variation by insertion at new regions or homologous recombination. Ectopic recombination between Ty repeats could lead to deletion or insertions in the genome. Elevated rate of transcription in these regions can lead to ectopic recombination through DSBs generated in replication-transcription collision. The genomic location with two Ty elements in opposite orientation (head-to-head Ty elements) is more prone to DSB formation (Lemoine et al., 2005; Mieczkowski et al., 2006). Along with Ty elements, telomeric pausing is largely dependent on TG1-3 repeats along with protein-DNA complexes (Makovets et al., 2004).

1.1.4.4 DNA secondary structures

Secondary structures also cause impediments to fork progression. Examples of such impediments include hairpin and cruciform structures formed by inverted repeats and G-quadruplex. Examples of inverted repeats include Ty elements and Alu quasi palindromes. Several studies from *E. coli*, *S. cerevisiae* and human cells have shown that the secondary structures ahead of RF can cause pausing and fragility dependent on recombination-based mechanisms.

The G-quadruplex structures formed due to telomeric elements are also responsible for RF pausing (Paeschke et al., 2013). Similar to G4 structures, palindromic sequences and long inverted repeats often cause DSBs due to secondary structures formed. However, the DSB formation and recombination often depends on the nature and chromosomal location of this fragile region (Lobachev et al., 2000; Narayanan et al., 2006). A genome-wide gene

expression analysis in DT40 cells (chicken B cell line) led to an interesting observation. The differential expression of several genes occurring after HU treatment (similar condition to prolonged RF pausing) were observed to resemble depletion of G4-unwinding helicases (FANCJ, WRN and BLM). At small scale, HU causes impaired replication of G-quadruplex structures leading to epigenetic changes and changes in gene expression ultimately resembling transcriptionally absence of certain helicases (Papadopoulou et al., 2015). This indicated a major contribution of DNA secondary structures to the natural pausing and putative DNA damage.

1.2 How do cells deal with replication fork pausing at NPSs?

So far, we understood problems faced by progressing RFs, leading to RF pausing and replication stress associated with it. The cells deal with RF pausing during each cell cycle. Excessive RF pausing is harmful for the cells and therefore specialized mechanisms have evolved to prevent recombination and repair machinery to attack stalled RFs at NPSs. Here we will summarize the known mechanisms of NPS maintenance preventing RF pausing to become harmful.

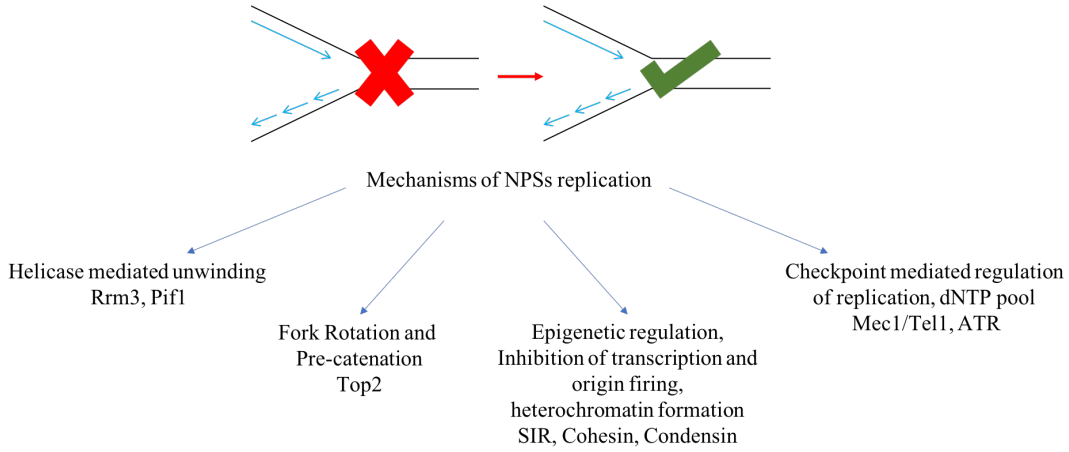

Fig1.2: Summary of pathways to deal with RF pausing for faithful NPS replication

S. cerevisiae cells rely on specialised helicases to allow replication through NPSs. The simplest strategy to remove a transcription-replication block, DNA secondary structures and hairpin structures formed due to DNA repeats is their unwinding by specialized helicases (Leon-Ortiz et al., 2014). However, this also needs to be complemented by other pathways. If the replication block is persistent, it can lead to damaged or broken forks causing genome instability. In such cases cells rely on efficient homologous recombination machinery for repair. The complexity of NPSs makes it difficult to perform efficient recombination. Therefore, cells employ many parallel strategies, including epigenetic changes, regulation of topology, heterochromatin formation, cohesion and condensation to avoid ectopic

recombination events at NPSs. Together these strategies maintain the replication through late replicating NPSs and allow successful replication termination (Lambert and Carr, 2005). Maintaining DNA topology is a critical task at NPSs. During replication elongation, topoisomerases release the stress ahead of the RF. The action of topoisomerases is complemented by fork rotation and subsequent resolution of precatenanes. However, fork rotation is primarily restricted to special regions such as termination zones and NPSs. At these regions, fork rotation and precatenation occurs as topoisomerase activity is restricted due to replication blocks. However, if fork rotation is not restricted to these regions, it can disrupt replication and cause DNA damage. This specialized approach complements topoisomerase action allowing faithful termination of replication and passage of RF through difficult to replicate regions (Schalbetter et al., 2015). Point mutants of topoisomerase *top1* and *top2* are synthetic sick, most likely due to reduction in DNA synthesis and RNA transcription. Major effect of this synthetic interaction is observed at the rDNA region where transcription and replication both is affected. Topoisomerases play a role to remove the torsional stress at rDNA (most likely at other NPSs as well) by acting in similar manner to a swivel. Either of topoisomerases can perform this function. Top2 is also involved in global replication termination (Brill et al., 1987).

Particularly at regions of rDNA genes, maintenance of rDNA repeats mainly relies on recombination, cohesion and condensation. rDNA is composed of various repetitive arrays prone to improper/deletional recombination. Fob1 mediated RF barrier allows proper replication of rDNA regions. The origins in *S. cerevisiae* rDNA region are largely clustered and silenced. The non-coding transcription in the spacer region of rDNA is also negatively regulated. Cohesin restricts the movement of the rDNA repeat regions to prevent unequal recombination. If transcription or origin firing is not regulated, cohesin in spacer regions will be displaced, increasing chances of recombination and rDNA copy number variation. Condensation is also involved in proper segregation of rDNA during mitosis and rDNA is a major target of condensin in *S. cerevisiae*. Furthermore, condensin is associated with maintenance of torsional stress during replication termination (Huang et al., 2006; Kobayashi, 2006; Pasero et al., 2002).

Replication stress at NPSs and other regions not only causes genome instability but also epigenetic changes and loss of chromatin integrity. Post replication, histone chaperones re-assemble and fold the chromatin for proper chromatin segregation. Absence of Rrm3 causes epigenetic changes in sub-telomeric region, which are dependent on specific histone chaperons. Stalling of RFs in the absence of Rrm3 predisposes the DNA to epigenetic changes. Rrm3 and CAF-1 compete for PCNA binding and thereby regulate histone reincorporation at the NPSs where the RF is paused after completion of replication (Wyse

et al., 2016). Replication stress has the potential to induce unscheduled silencing due to changes in epigenetic marks. The silencing complex SIR is enriched at NPSs, the replication stress due to tight protein-DNA complex formation enhances the silencing and heterochromatin-like structure formation at NPSs. This helps cells to prevent aberrant recombination (Dubarry et al., 2011; Jasencakova and Groth, 2010; Jasencakova et al., 2010; Nikolov and Taddei, 2016).

Upon replication stress, the checkpoint kinases promote replisome function in order to complete faithful replication especially at NPSs. Upon checkpoint activation, S-phase is slowed down allowing completion of replication, late origin firing is blocked and mitosis is delayed. The replication checkpoint thus stabilizes stalled forks and keeps them in a replication active state. Replisome stability is unaffected by defective checkpoint function, indicating that the checkpoint has no contribution in replisome stability but promotes replisome processivity. Without the checkpoint, there are higher chances of RF collapse (De Piccoli et al., 2012; Lambert and Carr, 2005). In a mammalian study, it was found that fork protection by ATR is crucial for fragile sites. In the absence of this checkpoint kinase mild replication stress can cause damage at fragile sites. However, cells still can progress to mitosis which leads to genomic instability (Koundrioukoff et al., 2013).

Together all these strategies work in parallel to protect NPSs against unequal recombination and genome instability. These mechanisms are key to successful NPS replication and termination. Although we know the array of strategies that play roles in NPS maintenance, the exact mechanisms underlying the strategies are still elusive. The interdependence between these pathways is also unknown. In this thesis we try to further understand the molecular mechanisms of NPS replication and maintenance.

1.3 What are the known molecular players of NPS replication?

Even though we do not completely understand all the molecular players involved in faithful replication of NPSs and successful replication termination, many proteins are known to play a role. Some of them are part of DNA replication and repair pathways, while some others are checkpoint proteins.

The most studied proteins involved in replication through so called ‘difficult to replicate’ regions like NPSs are specialized helicases such as Pif1 and Rrm3. Rrm3 travels with the replication machinery, but the rate of replication is not affected by Rrm3. Rrm3 dependent pause sites include tRNA and rRNA genes, centromeres, inactive replication origins, transcriptional silencers (NPSs in general). Without Rrm3 1400 regions accumulate breaks in unperturbed replicating cells. These included regions containing non-nucleosomal protein-DNA complexes. Indicating that Rrm3 plays an important role in allowing

replication through various non-histone protein-DNA complexes which are one of the natural replication barriers in unperturbed S-phase. The helicase/ATPase (or catalytic) activity of Rrm3 is required for this function of Rrm3 (Azvolinsky et al., 2006; Ivessa et al., 2003; Ivessa et al., 2002; Prado and Aguilera, 2005). *S. Pombe* encodes Pfh1 (Pif1 helicase family), this helicase is involved in replication through NPSs including rRNA, tRNA genes, Mat locus and highly transcribed RNA Pol II genes. Pfh1 prevents RF damage at these regions and stabilizes stalled forks to complete replication (Sabouri et al., 2012). A human cell lines study shows that the DNA damage and telomere instability associated with G-quadruplex (G4) structures are dealt by Pif1. Specialized helicase Pif1 unwinds these structures to prevent genome instability. Pif1 is a conserved helicase and human Pif1 is found to be able to rescue to phenotype of *pif1Δ* in *S. cerevisiae*. At *S. cerevisiae* telomeres, Pif1 helicase displaces the telomerase by reducing its processivity. Pif1 preferentially associates with wild-type length of telomeres preventing the telomerase activity. In the absence of Pif1 there is excess of telomerase and thus lengthening of telomeres. While overexpression of Pif1 reduces the amount of telomerase. Pif1 thus allows lengthening of short telomeres while maintaining long telomeres intact (Boule et al., 2005; Paeschke et al., 2013; Phillips et al., 2015). In mammalian cells, Fanconi anaemia protein FANCJ (helicase) is also known to prevent fork stalling at G4 structures. This however causes ssDNA gaps that are repaired later. The repair process prevents the early condensation of chromatin and unscheduled restart of stalled forks at G4 structures (Schwab et al., 2013). In another mammalian study, RecQ helicases are found to remove Rad51 filaments from CFSs and recruit Mus81/Eme1 to the fragile sites. Mus81/Mms4 endonuclease heterodimer starts the DNA repair post replication allowing faithful segregation of these regions during mitosis. Without RecQ, these regions have excessive Rad51 filaments, which prevent expression of CFSs therefore lead to their improper replication and segregation (Di Marco et al., 2017).

Apart from helicases, other specialised factors play a role to fine tune the process. MCM helicases are phosphorylated by DDK and form the CMG helicase complex, which binds to Tof1/Csm3 (also phosphorylated) allowing programmed fork pausing at NPSs. Tof1 and Csm3 protect stalled forks at TERs and rDNA from Rrm3, allowing Fob1 mediated pausing. They play a role in replication fork pausing at chromosomal sites where non-histone proteins are bound to DNA in general. Mrc1, Csm3 and Tof1 are mediators of replication check point activation (Rad53 phosphorylation). Without phosphorylation, Tof1/Csm3 is not retained by the replication machinery. In *rrm3Δ* cells, there is more pausing as there is no helicase to remove protein-DNA complex. While in the absence of *TOF1/CSM3* there is reduction in replication fork pausing as Rrm3 activity is deregulated (Bando et al., 2009; Bastia et al., 2016; Hodgson et al., 2007; Mohanty et al., 2006).

Mec1 facilitates replication through replication slow zones (that overlap majorly with NPSs) preventing breaks. In the absence of Mec1, the cells experience increased genome instability due to breaks generally in specific regions (Cha and Kleckner, 2002). Similar studies in mammals show that Tim/Tipin complex (Mec1/Ddc2 in *S. cerevisiae*) interacts with various DNA replication proteins. Tim interacts directly with the CMG helicase and affects its activity. Tim also interacts with DNA polymerases and stimulates their activity. In this way, the checkpoint can control replication (Cho et al., 2013). ATR (and not ATM) also plays a critical role in fragile site stability. Without ATR, there is increased expression of fragile sites (Casper et al., 2002). Another mammalian study showed that Mus81/Eme1 localizes to CFSs during early mitosis, causing breaks and gaps formation. This induces expression of CFSs signal and faithful segregation of chromosomes. Contrary to previous thinking, CFSs break in a systematic Mus81/Eme1 dependent manner to promote faithful segregation of sister chromatid avoiding lagging chromosome and bridge formation (Ying et al., 2013).

In *S. cerevisiae*, Top2 mediates stability of highly transcribed regions, maintaining these fragile regions. In the absence of Top2, Hmo1 becomes toxic for these regions. Top2 along Hmo1 is recruited to NPSs, preventing histone variant Htz1 recruitment to the region. Together, Top2 and Hmo1 mediate epigenetic regulation and facilitate smooth M/G1 transition. In the absence of functional Top2 (*top2-4* or *top2-1*), these loci accumulate gamma H2A modification (Bermejo et al., 2009a). Epigenetic modifications are associated with replication completion and may play a role in detecting replication termination. Methyltransferases associate with replication forks and restore histone methylation along with replication machinery (Abmayr and Workman, 2012). The histone chaperone FACT complex also interacts with the MCM helicase and allows fork progression and normal rate of replication in vertebrates (Abe et al., 2011). Several studies in *S. cerevisiae* show that, SIR transcriptional silencer complex is involved in silencing expression of Mat type and other genes. The components of the SIR complex are recruited to NPSs such as tRNA. When tRNA genes are placed ectopically, the genes around tRNA are silenced due to the SIR complex. The protein-DNA complex formed by SIR complex causes replication stress leading to heterochromatin status of the region. SIR proteins are recruited due to replication stress, once recruited they form a protein-DNA complex that is dislodged by Rrm3 to continue replication. Recombination in the rDNA regions depends on Sir2. Sir2 and rDNA copy numbers are the factors that regulate the transcription of rDNA genes. Once transcription is induced (by a bidirectional promoter in spacer region), cohesion removal regulates the recombination at rDNA region. Without Sir2, there is reduction in association of cohesin to rDNA. Sir2 thus restricts the accessibility of rDNA non-transcribed regions to modifications and prevents unequal recombination between the rDNA repeats allowing its

faithful replication (Dubarry et al., 2011; Fritze et al., 1997; Kobayashi and Ganley, 2005; Kobayashi et al., 2004). In *S. pombe*, Swi1 and Swi3 act at RF barriers at rDNA. These proteins, along with Rts1, allow faithful rDNA replication. When RTS1 mediated fork pausing occurs at an ectopic locus, for example between direct repeats, recombination mediated repair allows completion of replication avoiding deletions and breakage of the RF. This process is complemented by helicases (Ahn et al., 2005; Krings and Bastia, 2004). Several studies in mammalian cells uncover that RF response is fine-tuned by histone supply and demand mediated by Asf1 (histone chaperon with anti-silencing function). Asf1 is known to bind to excess histones (possibly created due to ssDNA formation) during replication stress. Certain modifications on Histone H3-H4 accumulate upon replication stress. The replication stress affects histone modifications and possibly epigenetic regulation through these proteins. Upon replication stress, histone recycling is inhibited leading to accumulation of methylated histones (also more so because of helicases unwinding and forming ssDNA displacing histones), which are buffered by Asf1. Upon replication restart these histones are consumed. This regulates the unwinding of DNA before replication and re-formation of nucleosomes after RF passes through the region (Groth et al., 2007; Jasencakova et al., 2010).

In 2004 two genetic screens of aimed to understand what pathways cause lethality or growth defects in combination with *rrm3Δ* cells. The outcome of these studies included intra-S checkpoint, Srs2, STR complex, MRX complex but not Mus81/Mms4. This hints at stalled forks being converted to Rad51 dependent recombination intermediates to be processed by STR. Genes for fork restart and intra-S checkpoint are required for *rrm3Δ* viability. Unlike *rrm3Δ*, *srs2Δ* and *sgs1Δ* do not lead to fork pausing at the rDNA region. Deletion of *RAD51* (but not *RAD52*) rescues the synthetic phenotype of *rrm3Δ sgs1Δ* or *rrm3Δ srs2Δ* indicating that toxic recombination intermediates are responsible for the lethality. However, the combinations of *rrm3Δ rad50Δ*, *rrm3Δ xrs2Δ*, *rrm3Δ mrc1Δ* were not rescued by *rad51Δ*, which could be due to these factors (Rad50, Xrs2 and Mrc1) acting upstream of recombination. But if recombination intermediates are prevented to form by deleting *RAD51*, there is still a recombination independent pathway allowing completion of replication through these regions. Activation of checkpoint in *rrm3Δ* cells is not affected by *sgs1Δ* or *rad51Δ*, meaning the structures that activate the checkpoint are stalled/broken/reversed forks and not toxic recombination intermediates. Post-replicative repair is not essential for proliferation in *rrm3Δ* cells (Schmidt and Kolodner, 2004; Torres et al., 2004). Cullin Rtt101 protein also plays a role along with Rrm3 in replication through NPSs. *rtt101Δ* is viable only in the presence of Rrm3, and it shows excessive recombination

at stalled forks. This mutant is also sensitive to fork pausing by DNA alkylating agents (but not by nucleotide depletion by HU) (Luke et al., 2006).

Work from our lab also uncovered a link between *S. cerevisiae* Smc5/6 and faithful replication of NPSs. Smc5/6 localizes at NPSs and protects their integrity by preventing fragility caused by extensive fork pausing mediated by Tof1-Csm3 fork protection complex and further recombination. Smc5/6 function is complementary to Rrm3, preventing DNA lesions/damage at NPSs (Branzei and Menolfi, 2016; Menolfi et al., 2015). Smc5/6 also plays a critical role in DDT by resolving recombination intermediates arising during endogenous replication. This role of Smc5/6 is similar to Sgs1/BLM, mutated in Bloom syndrome patients (Branzei et al., 2006; Räschle et al., 2015).

Together, these protein complexes deal with (or possibly prevent) replication stress at NPSs. The replication pausing is important but dealing with recombination intermediates arising at these regions is even more crucial for cell survival. The factors mentioned above, along with the strategies mentioned in the previous part prevent the fragility at these regions prone to breakage (Leon-Ortiz et al., 2014; Tourriere and Pasero, 2007).

1.4 What are the putative molecular players of NPS replication along with Smc5/6 complex?

In unperturbed S phase the RF pauses at difficult to replicate regions (NPSs) such as tRNA, repeats, centromeres and telomeres due to non-histone DNA-protein complexes, transcription-replication collision, DNA secondary structures etc. There are about 1400 known sites in *S. cerevisiae* genome where replication pauses. At these regions, specialized fork protection mechanisms play important role to prevent prolonged pausing and DNA damage. Cells usually prevent damage by protecting these regions against recombination machinery by several mechanisms. Various factors act in a coordinated fashion to facilitate replication of these regions. The accumulation of RF pausing elements at NPSs can lead to chromosomal rearrangements. However, the replication of these regions is not fully understood. We are particularly interested in role of Smc5/6 in the replication of NPSs and the proteins that cooperate with Smc5/6 to carry out its function. Since Smc5/6 does not have a known catalytic activity to deal with the intermediates that could form at NPSs, we are investigating the proteins that collaborate with Smc5/6 to carry out its role at NPSs. In particular, we are interested in the roles of the STR complex, Top2, PCNA and its modifiers along with Smc5/6 in maintenance and replication of NPSs.

1.4.1 The Smc5/6 complex

1.4.1.1 Structure of the Smc5/6 complex

The Smc5/6 complex is part of Structural Maintenance of Chromosomes (SMC) family of proteins. The major functions of SMC complexes revolve around regulation of chromosome architecture throughout cell cycle (reviewed in (Losada and Hirano, 2005)). The SMC protein family is conserved from prokaryotes to eukaryotes. However, the diversity of SMC complexes increases in higher eukaryotes. Bacteria possess only one SMC protein while the higher organisms have three independent SMC protein complexes namely Condensin, Cohesin and the Smc5/6 complex. The three SMC protein complexes show structural similarity and are conserved in eukaryotes from yeast to humans (reviewed in (Jeppsson et al., 2014b)).

The three SMC complexes, Cohesin, Condensin and Smc5/6 show striking similarity in their structure. Each of the SMC protein is roughly 1000-1500 amino acid in length, the SMC proteins have a typical structure where the nucleotide binding Walker A motif at N-terminus and Walker B motif at C-terminus are separated by coiled coil. The coiled coil folds on itself at the hinge forming an ATP binding globular head domain on the other end. The ATPase head domain and hinge domain in a single SMC protein are thus separated by intramolecular coiled-coil. Furthermore, the heterodimers of SMC proteins are formed by direct interaction between SMC proteins at the hinge domain. The heterodimer formation is a dynamic process. The heterodimer can form an open or closed V shaped structure that can be visualized by electron microscopy (Anderson et al., 2002). The ring formation of SMC proteins is guided by bridging the two globular head domains with the Kleisin subunit. The other non-SMC elements of the SMC protein complexes are bound on the SMC ring.

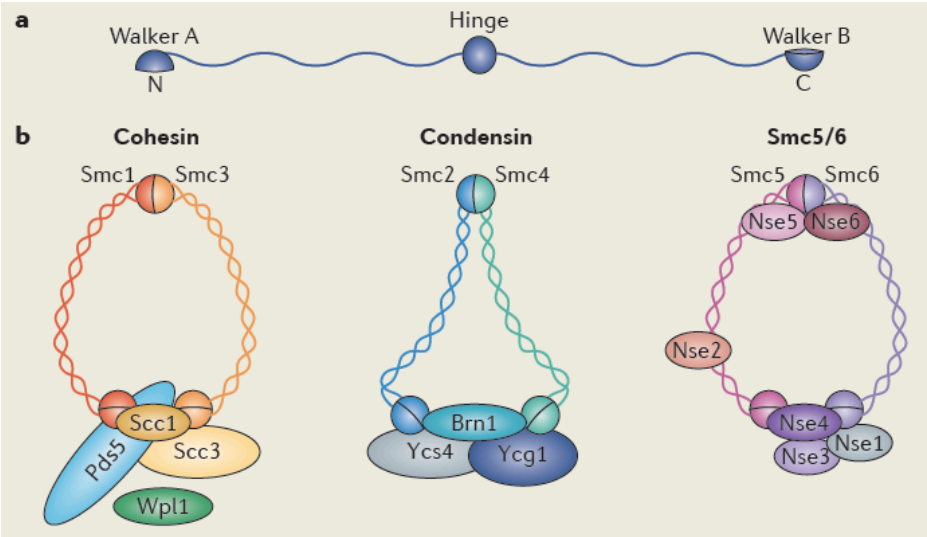

Fig1.3: The structural comparison of *S. cerevisiae* SMC complexes. Adapted from (Jeppsson et al., 2014b)

The *S. cerevisiae* Smc5/6 complex is composed of two SMC proteins, Smc5 and Smc6, and six additional non-SMC elements (Nse) Nse1, Nse2/Mms21, Nse3, Nse4/Qri2, Nse5, Nse6/Kre21 (Hu et al., 2005; McDonald et al., 2003; Pebernard et al., 2004; Pebernard et al., 2006). In *S. pombe* Smc6 is also known as Rad18 while Smc5 is called Spr18 (Lehmann et al., 1995; Sergeant et al., 2005). The human SMC5/6 complex is composed of orthologs SMC5, SMC6, NSE1, NSE2/MMS21, NSE3/MAGE1, NSE4 and NSE5-NSE6 (SLF1/SLF2) (Räschle et al., 2015; Taylor et al., 2008). All the subunits of *S. cerevisiae* complex are essential for cell viability (Zhao and Blobel, 2005) while Nse5 and Nse6 are not essential for *S. pombe* cell viability (Pebernard et al., 2006). Smc5 and Nse2-deficient chicken DT40 cells survive but are slow-growing (Kliszczak et al., 2012; Rossi et al., 2020; Stephan et al., 2011). In human cells, RNAi-dependent depletion of SMC5/6 components slows down cell cycle possibly due to incomplete depletion, (Behlke-Steinert et al., 2009), whereas *SMC6* knockout mouse are embryonic lethal (Ju et al., 2013). This suggests that the Smc5/6 complex has essential functions in various organisms.

In *S. cerevisiae* Smc5/6 complex, the central SMC ring is formed between Smc5 and Smc6 and Nse4, which is the kleisin component. Nse1-Nse3 forms a subcomplex that associates with Nse4, while Nse5-Nse6 forms a subcomplex that associates with Smc5/6 ring at the hinge domain. Nse2/Mms21 is associated with Smc5/6 ring at the coiled-coil of Smc5 (Duan et al., 2009a).

1.4.1.2 Activities of the Smc5/6 components

Previous studies showed that Smc5 and Smc6, along with ATPase activity, have the ability to bind ssDNA and dsDNA. Furthermore, *in vitro* studies showed that the affinity of Smc5 and Smc6 is more for ssDNA in the physiological conditions. The length of ssDNA required for the binding is much smaller (merely 40 to 50 nt) indicating the possibility of multiple Smc5/6 complexes being present at ssDNA generated during DNA replication and repair (Roy and D'Amours, 2011; Roy et al., 2011). Recent structural studies observed that human hNSE1/3/4 sub complex has DNA binding ability as well. While these studies confirmed hSMC5/6 core dimer binds preferentially to ssDNA as previously observed (also shown in (Alt et al., 2017)), they made interesting observations for the hSMC1/3 subcomplex. The EMSA results showed comparable DNA binding abilities of hNSE1/3 dimer to 45bp ssDNA and dsDNA, however at shorter lengths this sub complex preferred binding to dsDNA (Adamus et al., 2020; Zabrady et al., 2016).

Nse1 contains a RING domain (usually associated with E3 ubiquitin ligases), although it does not show any activity *in vitro* (Pebernard et al., 2008). Nse1 through its RING domain is thought to act as a structural component of Nse1-Nse3-Nse4 subcomplex and stabilize the

Smc5/6 complex through its interaction with Smc5 globular head. The interaction between Nse3 and Nse1 is important for the role of Smc5/6 in DNA repair and genome stability (Duan et al., 2009b; Palecek et al., 2006; Wani et al., 2018).

Nse2/Mms21 has a SP-RING (SIZ/PIAS-RING) motif in its C-terminus that is generally associated with E3 SUMO (small-ubiquitin like modifier) ligase activity. Nse2/Mms21 shows SUMO ligase activity both *in vitro* and *in vivo* experiments (Andrews et al., 2005; Potts and Yu, 2005; Zhao and Blobel, 2005). SUMO moiety (Smt3 in *S cerevisiae*, SUMO-1,-2,-3 in mammals) is similar to ubiquitin and can be covalently bound to the lysine of the target protein. The SUMOylation cascade relies on an E1 SUMO ligase (Uba2/Aos1 in *S cerevisiae*, SAE1/SAE2 in humans), E2 SUMO ligase (Ubc9) and several E3 ligases. *S cerevisiae* possesses four E3 SUMO ligases namely Siz1, Siz2, Mms21 and Zip3. SUMO moiety can be added as a single modification or as chains of multiple SUMO molecules on the target protein. In addition, initial SUMO molecules attached to targets can grow into chains (Jentsch and Psakhye, 2013). SUMOylation has been implicated in several pathways of cell and nuclear functions including DNA replication, DNA repair, DNA damage tolerance, checkpoint pathways etc. (reviewed in (Bergink and Jentsch, 2009; Jentsch and Psakhye, 2013)). The known targets of Mms21 SUMO ligase include *S cerevisiae* Smc5, Smc6, Ku70, Sgs1-Top3-Rmi1 (Bermúdez-López et al., 2016; Bonner et al., 2016; Zhao and Blobel, 2005), Scc1, Smc1, Smc3 (Almedawar et al., 2012; McAleenan et al., 2012) and the kinetochore proteins Ndc10 and Bir1 (Yong-Gonzales et al., 2012). In *S. pombe*, Nse2 targets Smc6, Nse3 and Nse4 (Andrews et al., 2005; Pebernard et al., 2008), and in human Smc6, Rap1, SA2, SCC1, TIN2, TRAX, TRF1 and TRF2 (Potts et al., 2006; Potts and Yu, 2005, 2007). Along with these targets, several *in vitro* and *in vivo* studies also showed that yeast and human Mms21 is able to self-SUMOylate, giving rise to heavier Mms21 molecules (Andrews et al., 2005; Potts and Yu, 2005; Zhao and Blobel, 2005). Although Mms21 is essential for cell survival, the SUMO ligase activity of Mms21 is not essential. Two mutants of Mms21 lacking SUMO ligase activity *mms21-11* (entire SP-RING is deleted) and *mms21-CH* (point mutations in SP-RING domain) are not lethal (Branzei et al., 2006; Zhao and Blobel, 2005).

Nse3 possesses a melanoma-associated antigen gene (MAGE) domain (Sergeant et al., 2005), making it a MAGE-like protein. The functions of MAGE proteins are poorly understood but they are implicated in gene expression, cell cycle regulation, pluripotency, differentiation and apoptosis. They are also linked to some cancers (Feng et al., 2011; Park et al., 2020). The MAGE proteins can also bind and enhance the function of ubiquitin E3 ligases (Doyle et al., 2010).

Nse4, the kleisin subunit, contains helix-turn-helix and winged-helix folds which are characteristic of SMC kleisin subunits such as Scc1, CAP-H and CAP-H2 (Palecek et al., 2006). The Human homolog of Nse4 is Nse4a but there is also a germ-line specific isoform Nse4b expressed only in testis. The homology between the two isoforms is 50% (Båvner et al., 2005; Taylor et al., 2008).

Nse5 and Nse6 forms a subcomplex and is important for the stability of the Smc5/6 complex. The association of this subcomplex to the Smc5/6 core ring is different in *S. cerevisiae* (at hinge domain) and *S. pombe* (at ATPase head with Nse1-Nse3-Nse4 complex), while the position of NSE4-NSE5 subcomplex is unclear in mammalian cells (Duan et al., 2009b; Pebernard et al., 2006; Räschle et al., 2015). The role of Nse5-Nse6 subcomplex is not fully understood. The mutants of this subcomplex affect the stability of the Smc5/6 complex and thus show phenotype similar to Smc5/6 dysfunction. Nse5-Nse6 subcomplex is less conserved in various species (Duan et al., 2009b).

1.4.1.3 Known roles of the Smc5/6 complex

Smc5/6 complex is known to bind to stalled RFs proximal to early replication origins in S-phase upon HU treatment. During G2/M phase the Smc5/6 complex binds to centromeres and regions between converging transcribed genes, overlapping with cohesin localization (Bustard et al., 2012; Jeppsson et al., 2014a; Lindroos et al., 2006). Smc5/6 recruitment to chromatin is dependent on cohesin and Eco1-mediated cohesion.

Smc5/6 was shown to be associated with topologically stressed DNA (Jeppsson et al., 2014a; Kegel et al., 2011). The topological stress arises in the chromosomes when the DNA is unwound for replication. The replicating DNA causes positive supercoil formation ahead of the fork. The cells either deal with positive supercoil by creating a transient nick by type II topoisomerase TopII, passing the strand through the nick to relieve the topological stress and re-ligating the nick, or by allowing fork rotation to remove the stress ahead. However, this latter process creates sister chromatid intertwinings (SCIs) or precatenanes behind the fork. In case cells lack Top2 function, topological stress accumulates and Smc5/6 recruitment to chromosomes is enhanced. Furthermore, association of Smc5/6 preferentially to larger chromosomes also indicated a bias for topological stress. It was proposed that the Smc5/6 complex facilitates fork rotation, sequesters SCIs and thereby facilitates topological stress removal.

Not only are the Smc5/6 subunits essential for proliferation in yeast, they are also critical for DNA repair. Mutants of Smc5/6 complex are hypersensitive to all kinds of DNA damage such as UV radiation, Hydroxyurea (HU), Camptothecin (CPT), Methyl methanesulfonate (MMS) and Mytomycin C (MMC) (Onoda et al., 2004). The DNA damage sensitivity of

Smc5/6 mutants is also tested on other organisms such as DT40 cells, *Drosophila melanogaster*, *C. elegans* and human cells. However, the mutants of Smc5/6 are able to activate the checkpoint to WT levels indicating that the defect is due to its inability to repair the DNA and not due to faulty checkpoint response (Harvey et al., 2004; Torres-Rosell et al., 2007a). Smc5/6 was shown previously to play a role in the homologous recombination (HR) pathway, however the HR machinery is not essential in *S. cerevisiae* but the Smc5/6 complex is. This indicates an additional HR independent role for Smc5/6. Smc5/6 is shown to be associated with regions predisposed to fragility and DSB formation in yeast and human studies. Smc5/6 is important, but not essential, for the Cohesin binding to DSBs and preserving the broken ends (De Piccoli et al., 2006; Lindroos et al., 2006; Potts and Yu, 2005). Apart from the connection between Smc5/6 and Cohesion at DSBs, the two protein complexes are related to several other cellular functions. Along with several yeast studies, a human cell study also showed that Smc5/6 depletion shows abnormal curly chromosomes that indicate a cohesion defect. These cells also show anaphase bridges leading to chromosome loss and missegregation. The aberrant mitosis is also accompanied by Condensin defect and defective Topoisomerase IIα distribution (Gallego-Paez et al., 2014). This may indicate a role for Smc5/6 in removing Cohesin, along with Top2, during DNA segregation to prevent mitotic catastrophe. Smc5/6 is shown to prevent accumulation of sister chromatid junctions (SCJs) upon treatment with DNA damaging agents (Branzei et al., 2006). The accumulation of unresolved SCJs can be observed in Smc5/6 mutants and depletion strains (Bermúdez-López et al., 2010; Sollier et al., 2009). Smc5/6 is important for removal of SCJs generated either by Shu1- and Mms2- dependent processes or Mph1 activity (Choi et al., 2010; Xue et al., 2014).

Apart from its role in DNA repair and HR, Smc5/6 is also known to play a role at stalled RFs. Recombination at damaged replication forks is controlled by the Sgs1-Top3-Rmi1 (STR) complex and Ubc9/Mms21-mediated SUMOylation, relying on the Smc5/6 complex (Branzei et al., 2006; Sollier et al., 2009). There are at least two pathways evolved by cells to prevent accumulation of recombination structures during fork stalling or damaged templates, orchestrated by the replication checkpoint and Smc5/6 complex-mediated SUMOylation, respectively (Branzei et al., 2006; Lopes et al., 2001). In addition, Smc5/6 prevents accumulation of recombination intermediates at stalled RFs (Bustard et al., 2012; Menolfi et al., 2015). Together these studies point at a role of Smc5/6 in regulating replication and recombination at stalled forks.

Smc5/6 is also shown to suppress gross chromosomal rearrangements (GCRs). Several mutants of the Smc5/6 complex were shown to increase the GCR rate in a *S. cerevisiae* study (Hwang et al., 2008). The GCRs were dependent on functional break induced repair by

Rad52/Rad51. The breaks formed were repaired by recombination-based mechanisms mainly the homology dependent repair events including repetitive sequences such as Ty elements, ARS and tRNA genes (Hwang et al., 2008).

The reported functions of Smc5/6 in unperturbed conditions suggest a role for the complex during replication of rDNA regions and other NPSs. Several studies have shown that Smc5/6 is important for rDNA and telomere segregation. Smc5/6 mutants show anaphase bridges and lagging chromosomes, particularly rDNA missegregation. Smc5/6 was shown to regulate recombination at rDNA regions (Peng et al., 2018; Torres-Rosell et al., 2007a; Torres-Rosell et al., 2005; Torres-Rosell et al., 2007b). Smc5/6 mutants also showed defect in telomere clustering and even telomere segregation defects (Torres-Rosell et al., 2005; Zhao and Blobel, 2005). Smc5/6 is important in ALT cancer cell lines for telomere maintenance. ALT cancer cell lines are a subset of cancer cells that do not express telomerase and depend on the alternative lengthening of telomeres (ALT) pathway. In the ALT cells, knock down of *MMS21*, *SMC5* or *SMC6* leads to reduction in recombination at telomeres and reduction in telomere size leading to cell senescence (Potts and Yu, 2007). Recent studies in DT40 avian cells also linked roles of Smc5/6 during Fanconi Anemia pathway. This study uncovered roles of Smc5/6 upon inter-strand cross links formation to avoid formation of anaphase bridges and genomic instability (Rossi et al., 2020). Another recent study using human cell lines showed that depletion of Smc5/6 components caused errors during mitosis. The complex was also shown to be essential for maintenance of repeat regions in human cells as well. Depletion of Smc5/6 complex during interphase was observed to be harmful for the dividing cells (Venegas et al., 2020).

Together, these reports show an important role for the Smc5/6 complex in dealing with RF pausing in unperturbed conditions. We are interested in further understanding how Smc5/6 complex carries out its role and to identify protein complexes that cooperate with Smc5/6 in this process.

1.4.1.4 The Smc5/6 complex and human diseases

Smc5/6 mutants are associated with several developmental syndromes and even cancer predisposition. Smc5/6 plays a role in embryonic development and mutants of Smc5/6 in mouse are embryonic lethal (Ju et al., 2013). A few mutants of Smc5/6 are identified and associated with human pathologies. A 2014 clinical study identified missense mutation in NSMCE2 (Mms21) in two patients. The mutation led to reduction in NSMCE2 expression and was associated with primordial dwarfism, diabetes with extreme insulin resistance, and gonadal failure. The patient cells showed increased anaphase bridges, micronuclei formation and delayed replication completion. The phenotypes were reverted *in vitro* by expressing

WT *NSMCE2* allele in patient cells but not by expressing SUMO ligase defective allele of *NSMCE2*. This study showed a role for Smc5/6 complex in DNA repair particularly through the NSMCE2 SUMO ligase activity (Payne et al., 2014). Two independent studies in 2015 indicated a role for Smc5/6 complex in preventing cancer and aging in mice. (Jacome et al., 2015) showed that the mutant of NSMCE2 (Mms21) with defective SUMO ligase activity leads to symptoms similar to Bloom's syndrome including defective recombination and formation of micronuclei. The NSMCE2 mutation was aggravated by BLM (Sgs1) regarding hypersensitivity and segregation defects. This indicated a role for Smc5/6 complex in DNA repair, protection from cancer and preventing aging in parallel with the BTR (STR in yeast) complex. Another lab (Saunus et al., 2015) conducted a genome and transcriptome study to understand the factors contributing to brain metastases (BM). They conducted analysis of DNA copy-number, exome and RNA sequencing to understand the variation in genome and transcriptome of 36 BM patients. They identified mutations in *SMC5* as key factor in the process of BM. Another clinical study in 2016 observed a *NSMCE3* (Nse3) missense mutation in a new syndrome leading to a destabilized Smc5/6 complex (van der Crabben et al., 2016). The destabilized complex rendered cells sensitive to replication stress and DNA damage, increased chromosomal rearrangements and micronuclei and HR defects. The patients also showed autosomal recessive chromosome breakage syndrome. The effects included faulty function of T and B cells and acute respiratory distress in early stages of life. Four children from two independent families were identified with the mutations and associated chromosome breakage syndrome with severe lung disease during childhood (van der Crabben et al., 2016).

In 2018 three independent studies connected the Smc5/6 complex with suppression of various viral infections. (Abdul et al., 2018) identified Smc5/6 complex as an antiviral restriction factor against hepatitis B virus (HBV). HBV is associated with cancer and liver diseases in humans. This study showed that degradation of Smc5/6 by viral HBx proteins lies behind the infection. The evolution of Smc5/6 and viral proteins indicate a virus-host evolutionary competition and thus Smc5/6 is an anti-viral factor against the HBx proteins allowing cells to defend against HBV infection. (Bentley et al., 2018) explore the virus-host protein interactions for the human papillomavirus (HPV) E2 protein and Smc5/6 complex. HPV infection can lead to serious illness including anogenital carcinoma, cervical cancer, head and neck oropharyngeal squamous cell carcinoma etc. The authors identified interaction between E2 and the core components of Smc5/6 complex, Smc5 and Smc6. Furthermore, the Smc5/6 complex is not essential for the transcriptional activation or viral DNA replication or amplification by HPV E2 protein. The study indicated a possible role for Smc5/6 during integration of viral DNA in human genome by homology mediated

pathways. (Xu et al., 2018) observed interaction between Smc5/6 and PJA1 which is a RING-H2 E3 ubiquitin ligase involved in restriction of viral DNA replication. They showed that Smc5/6 and PJA1 facilitate binding of the Smc5/6 complex to viral DNA. This is an efficient defense mechanism against DNA viruses like HBV, HSV1. Together Smc5/6, PJA1 and topoisomerases eliminate viral and episomal DNA to protect cells against viral infections.

As dysfunction in Smc5/6 complex is thus implicated in several human diseases, the study of the Smc5/6 complex may provide a better understanding of the processes. Possibly the basic understanding of Smc5/6 complex can lead to therapeutic use against the above-mentioned conditions of developmental syndromes, viral infections and cancer metastasis.

1.4.2 The STR complex

1.4.2.1 Details of the STR complex

The STR complex is composed of Sgs1-Top3-Rmi1 in *S. cerevisiae* and BLM-TOP3α-RMI1-RMI2 in higher eukaryotes. The interaction between Type IA topoisomerase and RecQ helicase is conserved from bacteria to humans (Harmon et al., 1999; Johnson et al., 2000; Wu et al., 2000). The catenation and decatenation by *E. coli* Top3 are stimulated by RecQ and even in human cells DNA strand passage by TOP3α is activated by BLM indicating a role for complex formation in the promotion of the helicase-topoisomerase activity (Harmon et al., 1999; Oakley and Hickson, 2002).

A genetic study in yeast identified the Sgs1 helicase mutations as slow growth suppressor of Top3. Sgs1 and Top3 physical interaction was later detected by (Gangloff et al., 1994). More recently a RecQ mediated genome instability factor, named Rmi1 (human orthologs RMI1-RMI2, also known as NCE4), was identified to be associated with the Sgs1-Top3 complex. Similar to Top3, *SGS1* deletion also suppresses the growth defects of *rmi1Δ* (Chang et al., 2005; Mullen et al., 2005). As mentioned above, these three proteins interact physically and form the Sgs1-Top3-Rmi1 (STR) complex.

Sgs1 is a large 1447 amino acid protein. Its helicase activity is encoded in the 400-1268 residues (Bennett et al., 1998). Several other domains, including the 200 amino acids in the C-terminus and the N-terminus interacting with Top3 are necessary for its function *in vivo*. Interestingly, expression of Sgs1 in *sgs1 top3* background recreates the growth defects of *top3*, while expression of Sgs1 without the C-terminus does not, indicating its function depends on C-terminal residues (Gangloff et al., 1994). On the other hand, the region of 1-107aa in the N-terminus of Sgs1 is essential for its *in vivo* function and interaction with Top3 (Bennett et al., 2000). *In vivo* pulldown experiments also show that Rmi1-Top3 can form a stable complex without Sgs1, while interaction of Sgs1 with either Top3 or Rmi1 depends

on their interaction (Mullen et al., 2005). Sgs1-V29E point mutant abolished the interaction between Sgs1-Top3 (Bennett and Wang, 2001). Missense mutations in both N and C terminus of Top3 abolished its interaction with Sgs1, indicating role of both N and C terminus in the complex formation (Onodera et al., 2002).

Sgs1 is an ATP dependent RecQ DNA helicase. Sgs1 binds preferentially to branched DNA structures (ssDNA/dsDNA junction with 3' overhang) and unwinds in 3' to 5' direction (Bennett et al., 1999; Bennett et al., 1998). Human cells have five RecQ helicases while yeast cells only have Sgs1. Among the human RecQ helicases, Sgs1 is most homologous to BLM (Chu and Hickson, 2009). Top3 is a type IA topoisomerase. It is known to create a single stranded nick in a ssDNA region and remove the topological constrain from the chromatid (Dekker et al., 2002; Kim and Wang, 1992). Rmi1 possesses a structure specific DNA binding ability. It is essential for the stability of the complex and thus an important component of the complex (Chang et al., 2005). Rmi1 binds to Sgs1 and Top3 through a conserved OB-fold core. The OB-fold domain is centrally located and mutations in this region abolishes its interactions with Sgs1 and Top3 (Kennedy et al., 2015; Wang et al., 2010).

1.4.2.2 Known roles of the STR complex

Mutants of the STR complex show hyperrecombination during both mitosis and meiosis, increased crossover events and DNA damage including chromosome translocations and rearrangements. These phenotypes indicate functions for the STR complex in the regulation of DNA replication and recombination (Gangloff et al., 1994; Mankouri and Hickson, 2006).

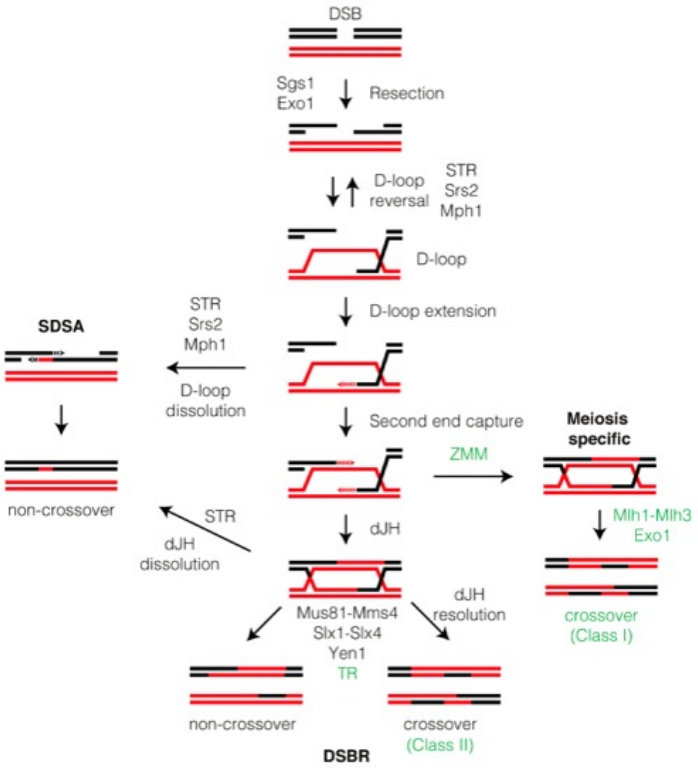

Fig 1.4: The STR complex and other factors in DSB repair pathway (adapted from (San-Segundo and Clemente-Blanco, 2020))

The roles of STR and individual components are well studied in the homologous recombination pathway. Sgs1 plays a role in early HR pathway of DSB repair to facilitate resection of DSBs. Together with endonuclease Dna2, Sgs1 unwinds the DSB and the exonuclease removes the unwounded ssDNA to create DNA overhangs for homology search (Gravel et al., 2008; Mimitou and Symington, 2008; Zhu et al., 2008). In bacteria, RecQ together with RecJ, and in human cells BLM together with DNA2 or EXO1, carries out the same function (Handa et al., 2009; Nimonkar et al., 2011; Nimonkar et al., 2008). Once the single stranded overhang is created, homology search is initiated in the sister chromatid. Strand invasion creates D-loops that are early structures before double holiday junctions (dHJs). The STR complex (together with Mph1 and in parallel with Srs2 helicase) plays a role in displacing D-loops thereby promoting non-crossover outcome (Fasching et al., 2015; Piazza et al., 2019). D-loops that are not dissolved by Srs2/Mph1-STR are extended to form dHJs. The dHJs are dissolved by the STR complex. Sgs1 helicase unwinds the homologous regions of the dHJ and type IA topoisomerase Top3 removes the interlinking to separate the two sister chromatids. This prevents crossover product formation (Bzymek et al., 2010; Cejka et al., 2010; Plank et al., 2006; Wu and Hickson, 2003). Alternatively, the dHJs can be cleaved by endonucleases to create crossover or non-crossover products. Structure

specific endonucleases Mus81/Mms4 and Slx1-Slx4 play roles parallel to the STR complex for dHJ processing (Fricke and Brill, 2003; Kaliraman et al., 2001; Mullen et al., 2001).
Apart from the DSB repair, the STR complex also plays roles at damaged forks. Mutants of the STR complex show accumulation of recombination intermediates during lesion bypass. The DNA damage tolerance mechanisms involving template switch depend on the STR complex for removing the intermediates formed. Without the STR complex, cells accumulate these intermediates and face problems while segregating chromatin (Bernstein et al., 2009; Liberi et al., 2005a). Homologs of the STR complex in bacteria and human cells were observed to be important for removal of anaphase bridges, convergent RFs and successful segregation of DNA (Chan et al., 2009; Suski and Marians, 2008).
In 2006 (Branzei et al., 2006) suggested STR complex to be involved in the recombination repair. Furthermore, Smc5/6 and STR are shown to depend on each other for their role during DNA recombination and repair. Several studies (Bermúdez-López et al., 2016; Bonner et al., 2016) confirmed this suggestion and linked function of the STR complex and its SUMOylation by the Smc5/6 complex. STR and Smc5/6 complexes interact upon DNA damage. Smc5/6 modifies the STR complex that interacts with Smc5/6 also with the help of SUMO interacting motifs (SIMs) found in Sgs1. The modified STR facilitates the removal of recombination intermediates formed upon DNA damage. One of the studies claimed that functions of Sgs1 independent of the STR complex are not affected by SUMOylation or lack of it, while the other showed that Exo1 dependent resection by Sgs1 is dependent on its SUMOylation by Smc5/6. While at NPSs, Smc5/6 was shown to play a crucial role (Menolfi et al., 2015), the structures formed there could resemble recombination and replication like structures and thus similar cooperation between Smc5/6 and STR can be expected. Thus, we started to investigate the role of the STR complex along with Smc5/6 at NPSs.

1.4.2.3 The STR complex and human diseases

Sgs1 is a member of RecQ family of helicases. Human cells contain five RecQ helicases and mutations in three of them are associated with known genetic disorders. Mutations in the RecQ helicase BLM are associated with Bloom's syndrome (BS), mutations in WRN are associated with Werner's syndrome (WS) and mutations in RECQ4 are associated with Rothmund-Thomson Syndrome (RTS). BS is an autosomal recessive disorder, characteristics of BS include growth defects, immunodeficiency and elevated risk of cancer. BS patients show increased chromosomal aberrations (Langlois et al., 1989). WS on the other hand is a rare genetic disorder characterized by premature aging with patients showing characteristics of aging at a very young age, high somatic mutations and chromosomal mis-segregation (Fukuchi et al., 1989; Scappaticci et al., 1982). Several mutations of RecQ4 are

characterized and linked to RTS which is an autosomal recessive syndrome. RTS is characterized by facial erythema, blisters, edema, early aging, increased cancer susceptibility, photosensitivity and poikilodermatous skin (Ahn et al., 2019; Kitao et al., 1999; Vennos and James, 1995; Yadav et al., 2019). All the syndromes are associated with increased recombination rates. Yeast studies also showed association between Sgs1 deletion and aging (Sinclair et al., 1997). Cells with deletion of *SGS1* showed 40% average lifespan compared to the WT cells, the cells showed premature sterility and telomere silencing defects that indicate aging of the cells.

Human Top3A is associated with mitochondrial DNA where it is required for successful decatenation and segregation of mitochondrial DNA. Mutants of Top3 showed defects in mitochondrial DNA segregation and result in a human mitochondrial disease (Nicholls et al., 2018). Furthermore, Top3 mutations are also associated with Juvenile myoclonic epilepsy (JME) characterized with seizers, cognitive and behavioral abnormalities. A patient study recognized a deletion in Top3B as one of the causes for JME (Daghsni et al., 2018). Top3B deletion was also associated with another syndrome called DiGeorge/Shprintzen/velocardiofacial syndrome with characteristic cognitive and behavioral abnormalities and facial dysmorphism. This and several other studies have connected mutation/deletions in Top3B and learning disabilities, autism and neurodevelopmental disorders (Butler et al., 2015; Iossifov et al., 2012; Kaufman et al., 2016; Stoll et al., 2013; Tan et al., 2011).

Most of the mutants of the human BTR complex or other RecQ helicases are causing risk of cancer and early aging in the patients. This indicates that the BTR complex in humans and the STR complex in yeast inhibit aging and genome instability in dividing cells. In this project we plan to understand the role of the STR complex and to see the relation between its roles upon DNA damage and during unperturbed replication.

1.4.3 Top2

1.4.3.1 DNA Topoisomerases

Replicating DNA often entangles and supercoils when helicases unwind the DNA template. Various topological constraints restrict the replicating DNA (Postow et al., 2001; Schvartzman et al., 2013). Unwinding of DNA creates positive supercoils ahead of the fork and/or precatenanes behind. If these are not resolved, cells enter mitosis with physically linked sister chromatids and can have mis-segregation and chromosome loss (Postow et al., 2004). DNA topoisomerases play major role in maintaining the DNA topology. These are highly conserved enzymes that control catenation, DNA supercoiling, precatenation and

knotting. The activity of DNA topoisomerases is essential for cell survival (Bermejo et al., 2007; Liu and Wang, 1987).

DNA topology is altered during both replication and transcription. Movement of both replication fork and transcription bubble creates positive supercoils ahead of them. Both replication and transcription machinery can rotate along DNA double helix creating precatenanes (Harada et al., 2001; Reyes-Lamothe et al., 2008). Precatenanes are intertwinings of replicated DNA that moves the torsional stress backwards. The positive supercoil and torsional stress accumulated around replication and transcription machinery is the substrate for DNA topoisomerases. Apart from progression of replication, termination of replication also causes topological stress. The DNA topoisomerases are thus important for replication fork fusion and termination (Wang, 2002b).

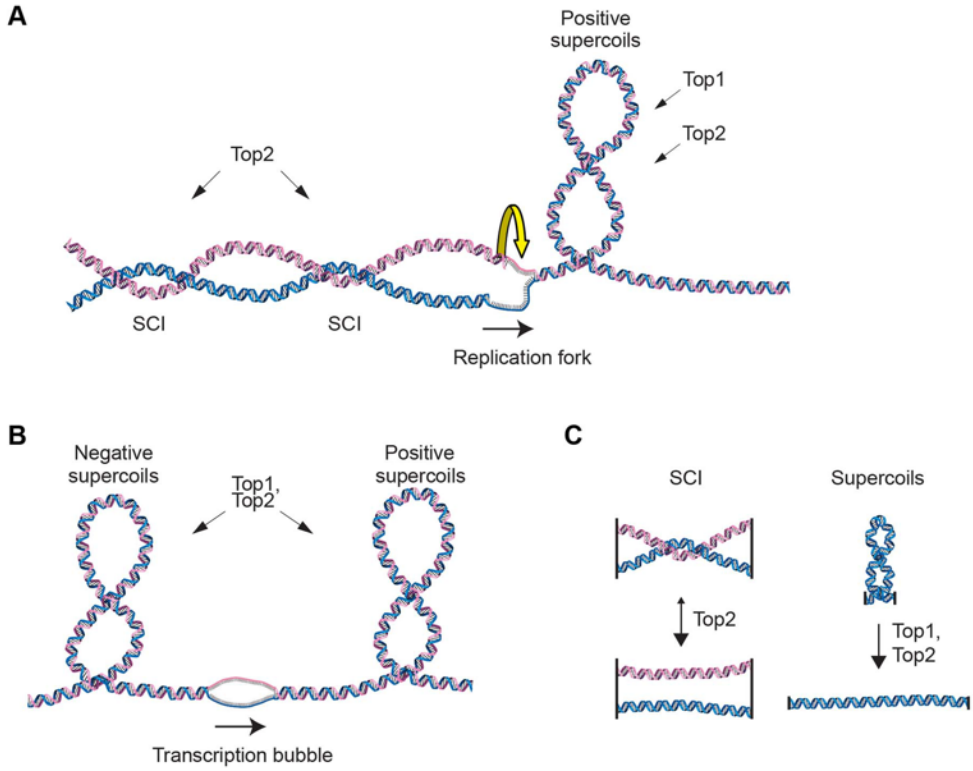

Fig1.5: Summary of DNA topology and topoisomerase action adapted from (Jeppsson et al., 2014b)

There are two classes of DNA topoisomerases type I and type II topoisomerases. Type I topoisomerases create a transient single stranded nick that allows unwinding of the two strands to relieve supercoil. While Type II topoisomerases create a transient double stranded nick that allows ATP dependent passage of the intact strand though the break thus removing the DNA entanglements (Nitiss, 1998). The two groups of topoisomerases are further classified into four subgroups: IA, IB, IIA, IIB. The topoisomerases of the same subfamily have low sequence homology but they are structurally and functionally similar (Champoux, 2001).

Type IA enzymes create a transient single stranded break in a ssDNA region and catalyze the strand passage while holding the two DNA end created by the break forming an enzyme-bridge. This category of enzymes has activity restricted to positively supercoiled DNA and not negatively supercoiled DNA. Top3 is the *S. cerevisiae* type IA topoisomerase (Dekker et al., 2002; Kim and Wang, 1992). Type IB enzymes create the transient single strand nick in a dsDNA region and the mechanism of action is similar to type IA. Type IB topoisomerases can remove both positive and negative supercoil from DNA. Top1 is the *S. cerevisiae* type IB topoisomerase (Champoux, 2001). Type IIA topoisomerases have the capacity to create a double stranded break and pass the intact DNA strand through to reduce torsional stress and relieve excessive winding or positive supercoiled DNA. Top2 is the *S. cerevisiae* type IIA topoisomerase. Type IIB topoisomerases share the activities with type IIA, but this subgroup of topoisomerases is found only in archaea or plants (Bergerat et al., 1997; Bergerat et al., 1994).

1.4.3.2 Bacterial Topoisomerases

During replication, bacterial genome also accumulates DNA supercoiling that needs to be eliminated. Bacterial topoisomerases maintain genome structure and allow interaction between protein-DNA, transcription and replication. Bacterial genome is circular, replication of such circular genome faces similar topological problems as eukaryotic replication. Such topological impediments need to be resolved by topoisomerases (Champoux, 2001). In particular, the most commonly studied bacterial model organism E. coli possesses four known topoisomerases- Topo I, DNA gyrase/ Topo II, Topo III and Topo IV (Wang, 2002a). Topo I and III are type I topoisomerases while Topo II (gyrase) and Topo IV are type II topoisomerases. The functions of topoisomerases are conserved from bacteria to higher eukaryotes even though the genomic complexity increases exponentially.

Replication of circular DNA created positive super helical stress that is predominantly removed by Type II topoisomerases. Bacterial Topo III (but not Topo I) was also observed to be able to compensate for the absence of gyrase (Hiasa and Marians, 1994). The ability of Topo III to remove positive topological intertwinings during replication suggested that it could support replication elongation to facilitate successful DNA duplication. This was interesting comparison between Topo II (gyrase) and Topo III. On the other hand, bacterial Topo II was not able to remove catenated DNA which was primarily resolved by Topo II and Topo IV (Nurse et al., 2003). Thus, roles of Topoisomerases are overlapping in bacteria and absence of one topoisomerase can be compensated by other.

1.4.3.3 Top2 and its known functions

Top2 is a type II topoisomerase. Top2 is essential for cell growth and the cells lacking Top2 show chromosome loss, breakage and non-disjunction along with higher recombination events and entangled chromosomes. The functions of Top2 depend on the formation of microtubules. Thus, Top2 is active post S phase (Holm et al., 1989). Top2 is known to be on chromatin in S phase and localizes at centromeres during metaphase (Bachant et al., 2002; Bermejo et al., 2007). Top2 also facilitates fork fusion in *S. cerevisiae* to carry out replication termination (Fachinetti et al., 2010). Replication based positive supercoils are removed by both Top2 and Top1, while SCIs generated by fork rotation are removed by Top2 alone (Bermejo et al., 2007; DiNardo et al., 1984; Holm et al., 1989; Kim and Wang, 1992). Top2 is required for replication through CFSs that overlap with NPSs. Top2 along with Rad52, Sgs1, Srs2, Mus81/Mms4 are required for Condensin and Mec1 dependent formation of breaks at CFSs and expression of CFS (Hashash et al., 2012). This indicates a putative role for Top2 along with Smc5/6 in NPS replication.

A plasmid-based study in 2016 showed that Top1 and Top2 were co-purified with the Smc5/6 complex and the proteins showed in vitro activity to relax negative and positive supercoiled plasmid DNA. It was observed that Smc5/6 directly stimulates Top2 mediated plasmid catenation in an ATP-hydrolysis dependent manner, thus connecting Smc5/6 activity and topological stress management (Kanno et al., 2015). Other studies also connected Smc5/6 and Top2 function. The Top2 mutant *top2-4* did not perturb replication of DNA but caused increased formation of SCIs. In the *top2-4* background, Smc6 binding sites increased by 92% while restoration of Top2 function in G2/M phase allows reduction in Smc5/6 accumulation on chromosomes, indicating a trigger for Smc5/6 binding by SCI accumulation. This study predicted a role for Smc5/6 in assisting fork rotation in absence of Top2 function (Jeppsson et al., 2014a; Kegel et al., 2011). A human cell study observed physical interaction between Smc5/6 and Top2. A Smc5/6 mutant with defective NSMCE2 function was sensitive to long-term Top2 poisoning. They predicted that the endogenous recombination structures formed due to Top2A during early replication were resolved by Smc5/6 (Verver et al., 2016). Another recent yeast study linked Top1 and Top2 topoisomerases to programmed RFBs. They observed physical interaction between Top1-Top2 and Tof1. They predicted that the topoisomerases are attached to replisome for unperturbed S-phase progression. They observed that deletion of Top1 or Top2 alone reduced the RF pausing while deleting both Top1 Top2 completely abolished fork pausing to the level of *tof1* mutants. This indicated a role for Top1-Top2 in replication fork pausing and progress through NPSs such as rDNA regions (Shyian et al., 2020). This interaction could be simply due to the presence of Top1/Top2 at regions of topological stress ahead of

the RF due to Fob1 mediated RF block. However, the role of Top2 in RF pausing is interesting as Top2 also acts on precatenanes forming behind RFs. Tof1 plays a role to prevent fork rotation (Schalbetter et al., 2015). Another possibility is that Tof1/Csm3 act together with Top2 to activate RF barriers and prevent excessive topological stress. Top2 could be part of one of the mechanisms to prevent fragility at rDNA regions from excessive replication-transcription collision (Larcher and Pasero, 2020).

The studies so far indicate a well-documented interdependence of Top2, RF pausing and Smc5/6 complex, making Top2 a putative factor for NPS maintenance. We test this hypothesis in this thesis.

1.4.3.4 Top2 and human diseases

Topoisomerases are important factors during replication and cell division and therefore are indispensable for normal cell growth. Cancer cells are often rapidly dividing. A prostate cancer (PC) study identified TOP2A upregulation in both primary and metastasized PC. Furthermore, the upregulation at mRNA and protein levels was directly linked to aggressive primary and metastasized cancer, thereby suggesting TOP2A as a driving oncogene. The study predicted the use of Top2 as a biomarker for identifying possible aggressive tumor occurrences (Labbé et al., 2017). Another 2019 study identified patient mutations from two independent families in TOP2B that caused B cell immunodeficiency syndrome. Upon expression of mutant variant of Top2 in yeast and mouse models the authors observed the mutation had a partial dominant negative phenotype. They observed defective B cell survival, proliferation and development along with defective antibody secretion. This study linked TOP2B activity with B cell formation and function (Broderick et al., 2019). Another recent work showed links between Top2 mediated DNA breaks and susceptibility to cancer in ATM mutants. The breaks formed by TOP2 are repaired by TDP2 and ATM independently. Ataxia-Telangiectasia (A-T) is a cancer-prone syndrome caused by ATM loss. *atm*$^{-/-}$ mice show increased cancer predisposition upon *TDP2* loss, with the phenotype of *atm* and *tdp2* mutants being partially rescued by *TOP2* loss. Top2 was localized at DSBs in each background indicating a possible role for Top2 in inducing malignancy in A-T patients (Álvarez-Quilón et al., 2020).

1.4.4 PCNA and modifiers of PCNA

1.4.4.1 DNA damage tolerance (DDT) pathways

When replicating cells encounter DNA damage, the replication machinery can stall and activate fork remodeling pathway or restart downstream the lesion leaving a gap. Post-replicative repair (PRR) pathways, conserved from yeast to mammals, have emerged as

important in these fork restart pathways. PRR is also known as DNA damage tolerance (DDT), as the main role is not of canonical repair, but rather of replication through the lesions to mediate lesion tolerance. DDT can be mediated via recombination (often error free in outcome) or translesion synthesis (TLS) polymerases (occasionally or often error prone in outcome). TLS polymerases have low fidelity and can place wrong nucleotides while replicating past lesions. On the other hand, the recombination pathway often uses the undamaged sister chromatid as a template, thus making this choice error free save there are repeats or other secondary structures that can lead to deletions and amplifications. Genetically, two recombination-based pathways of DDT have been defined, template switch (TS) and the salvage pathway (Branzei, 2011; Branzei and Foiani, 2010; Branzei and Szakal, 2016).

The error free pathway will create recombination-like X-shaped intermediates transiently, which need to be resolved in order to facilitate normal chromosome segregation. The cells depend on Sgs1 and Top3 to resolve these intermediates (Branzei et al., 2008a; Liberi et al., 2005a). Smc5/6 mediated SUMOylation plays a role in the process of eliminating recombination intermediates by Sgs1-Top3 as *mms21-sp* and *mms21-CH* mutants accumulate recombination intermediates in a similar manner to Sgs1-Top3 mutants (Branzei et al., 2006). The process of DDT is often post replicative as it was recently visualized (Wong et al., 2020). Several lines of evidence substantiate this notion. First, DDT can take place even when the expression of factors involved in DDT (both error free and error prone branches) are restricted to G2/M phase with the help of the Clb2 promoter and degrons or restrictive expression (Daigaku et al., 2010; Karras and Jentsch, 2010). Another structural study using electron microscopy analysis showed this process to be associated with gap fillings and dHJ intermediates rather than with fork reversal mechanisms (Giannattasio et al., 2014b). Thus, DDT mechanisms are important for replication completion and single stranded DNA management while cells are replicating through a damaged template.

1.4.4.2 Regulation of DDT via PCNA modifications

One regulator of DDT pathway selection is via post translational modifications of the proliferating cell nuclear antigen (PCNA). PCNA is a homo-trimeric clamp that encircles DNA and facilitates replication. PCNA can be both ubiquitylated and SUMOylated. Upon DNA damage, PCNA is mono or polyubiquitylated at a highly conserved Lysine K164. The mono-ubiquitylation of PCNA depends on Rad6/Rad18, where Rad6 is an E2 ubiquitin conjugating enzyme and Rad18 is an E3 Ubiquitin ligase. The polyubiquitylation of PCNA at Lysine K63 depends on Ubc13-Mms2/Rad5, where Ubc13-Mms2 is a E2 Ubiquitin conjugating enzyme and Rad5 is an E3 Ubiquitin ligase. PCNA can also be SUMOylated at

two Lysine residues K164 and K127. The SUMOylation of PCNA is regulated by E2 SUMO conjugate Ubc9 and the E3 SUMO ligase Siz1 and to a lesser extent, Siz2 (Hoege et al., 2002; Lee and Myung, 2008).

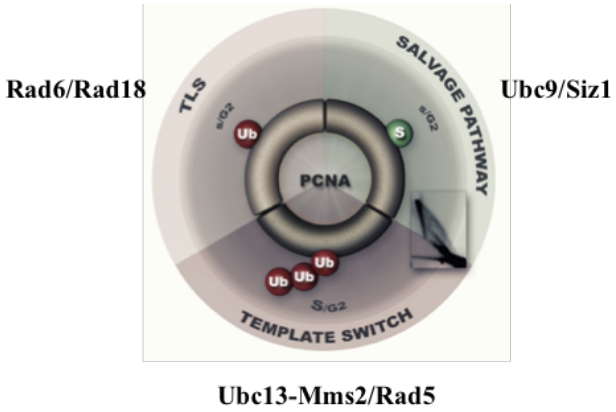

Fig1.6: Summary of PCNA modifications related to branches of DDT (adapted from (Branzei and Szakal, 2016))

Monoubiquitylation of PCNA promotes translesion synthesis pathway dependent on TLS polymerases Rev1, Rev3 and Rev7 in yeast (Kannouche et al., 2004; Stelter and Ulrich, 2003; Waters et al., 2009). In mammals the TLS polymerases include REV1, POLH (POLη), POLI (POLι), POLK (POLκ), POLN (POLν), POLQ (POLθ) and POLζ (with catalytic subunit REV3 and accessory subunit REV7) and PRIMPOL (Bianchi et al., 2013; García-Gómez et al., 2013; Mourón et al., 2013; Yang and Gao, 2018). These polymerases can replace the replicative polymerases and allocate wrong nucleotides across lesions. If PCNA is polyubiquitylated, the TS pathway is activated. The recombination and PCNA polyubiquitylation are thought to cooperate during TS to mediate damage bypass. This is preferred pathway in S-phase for DDT. Apart from ubiquitylation, PCNA can also be SUMOylated. SUMOylation of PCNA triggers template switching but prevents other types of HR that are deemed toxic. The salvage pathway is primarily acting post S-phase and it takes care of DNA lesions that escaped damage tolerance during replication. The toxicity, if any, of the salvage pathway is poorly understood, as both TS and salvage pathway fall under the error free DDT branch and depend on SCJs (Branzei and Szakal, 2016; Gonzalez-Huici et al., 2014; Karras et al., 2013; Papouli et al., 2005; Pfander et al., 2005).

1.4.4.3 PCNA/DDT and human diseases

PCNA is a sliding clamp playing roles in cell proliferation and DDT. One of the properties of cancer cells is their faster proliferation. This makes PCNA a putative target for cancer therapy as targeting PCNA can affect the aggressive proliferation of cancer cells both at primary and metastasized locations. PCNA could also be used as a diagnostic tool and for

cancer therapeutics (Stoimenov and Helleday, 2009; Visakorpi, 1992; Wang, 2014). Not only PCNA, but various factors modifying PCNA, are also considered as putative targets for cancer therapy. The modifiers of PCNA activate a specific branch of DDT and thus allow tolerance of lesions. Targeting PCNA modifiers limits cancer cells from using a specific branch of DDT and weakens their response to DNA damage. In combination with chemotherapy, targeting DDT factors could lead to even a better response. Furthermore, mutations in DDT pathway are rendering cells to be sensitive to DNA damage and thus predisposed to cancer. Therefore, identifying mutations in DDT factors could help us detect individuals at higher risk to cancer in a similar manner to BRCA1/2 (Gallo and Brown, 2019; Somasagara et al., 2017; Vuorela et al., 2011; Zou et al., 2018). Apart from putative role in cancer progression, PCNA and DDT also plays a crucial role in preventing aging. As cells are exposed to various endogenous and exogenous DNA damaging factors, the ability to effectively deal with DNA damage postpones aging of the cells. Thus, DDT is a major factor for prevention of aging and allowing healthy cell growth while dealing with DNA damage (Castells-Roca et al., 2015; Pilzecker et al., 2019). TLS polymerases are also linked to several human disease. REV3 is linked autosomal dominantly to a developmental disorder Möbius Syndrome. Patients of Möbius Syndrome show defective eye movement and facial paralysis. The mouse models with heterozygous Rev3 also show symptoms similar to Möbius Syndrome (Tomas-Roca et al., 2015; Verzijl et al., 2003). REV7 was linked to Fanconi Anemia (FA). A bi-allelic mutation of REV7 was identified and implicated in FA development. FA is a disease related to inter-strand crosslinking (ICL) defects. The patients show bone marrow failure that develops into anemia, fertility defects, congenital defects and higher susceptibility to cancer. Apart from its role dependent on REV3, REV7 also plays a role in preventing DNA end resection to promote non-homologous end joining. Since REV3 mutants do not show FA function, the role of REV7 in FA susceptibility could be due to defects in promoting end joining and DSB repair. However, ICL repair does not involve non-homologous end joining thus hinting towards role of TLS pathway in FA susceptibility (Bluteau et al., 2016; Boersma et al., 2015; Xu et al., 2015). We are interested in understanding the roles for PCNA and DDT in NPS replication and topological stress management. Understanding the cellular roles of these factors will help us to design ways to use them in therapeutics and as biomarkers.

Chapter2

Materials and Methods

2.1 Yeast strains, media and buffers

2.1.1 Yeast strains

Yeast strains used in this study were derivative of *Saccharomyces cerevisiae* (W303 strain), the genotypes as shown in Table1:

Table 2.1: List of strains used

Strain name	genotype	Source
FY1296	*Mat A ade2-1 trp1-1 leu2-3 112 his3-11 15 ura3 can1-100 Rad5+ (W303)*	Lab collection
FY1646	*Mat alpha ade2-1 trp1-1 leu2-3 112 his3-11 15 ura3 can1-100 Rad5+ (W303)*	Lab collection
FY1060	*W303 Mat A sgs1Δ::HIS3MX6*	Lab collection
FY1326	*W303 Mat A pol30-K164R*	Lab collection
FY1332	*W303 Mat A smc6-P4-13MYC::KANMX4*	Lab collection
FY1432	*W303 Mat A smc6-56-13MYC::KANMX4*	Lab collection
FY1686	*W303 Mat A top2-4 hmo1Δ::HIS3*	Lab collection
FY1738	*W303 MAT A fob1Δ:: HISMX6*	Lab collection
FY1739	*W303 MAT A Rrm3-10FLAG::KANMX*	Lab collection
FY1746	*W303 MAT A sgs1-K621R::KANMX*	Lab collection
FY1787	*W303 MAT A rad5-Q1106D::KANMX*	Lab collection
FY1938	*W303 Mat A irc5Δ::TRP*	Lab collection
FY2029	*W303 MAT A pol30::POL30(TRP1) trp1Δ63::his3Δ5'-his3Δ3'(URA3)*	Lab collection
FY2030	*W303 MAT A pol30::POL30(TRP1) trp1Δ63::his3Δ5'-his3Δ3'(URA3) elg1Δ::KANMX4*	Lab collection
FY2031	*W303 MAT A pol30::pol30-D150E(TRP1) trp1Δ63::his3Δ5'-his3Δ3'(URA3) elg1Δ::KANMX4*	Lab collection
HY0628	*W303 Mat A siz1Δ::HPHMX4*	Lab collection
HY0922	*W303 Mat A mms2Δ::HPHMX4*	Lab collection
HY1729	*W303 Mat alpha mms4Δ::HPHMX4*	Lab collection
HY2004	*W303 Mat A elg1Δ::KANMX4*	Lab collection
HY2076	*W303 Mat A rad18Δ::HPHMX4*	Lab collection

HY2192	*W303 Mat A chl1Δ::KANMX4*	Lab collection
HY2680	*W303 Mat A elg1Δ::KANMX4 rad5Δ::HPHMX4*	Lab collection
HY2796	*W303 Mat A rad51Δ::LEU2*	Lab collection
HY2806	*W303 Mat A SMC6-6HIS-3FLAG::KANMX4*	Lab collection
HY2936	*W303 Mat A top2-4 G2::NATNT2-SMC6*	Lab collection
HY2942	*W303 Mat A top2-4 SMC6-6xHIS-3FLAG::KANMX4*	This study
HY3167	*W303 Mat A S::NATNT2-SMC6*	Lab collection
HY3293	*W303 Mat A pADH1-tc3-3xHA-Top3::NATMX4*	Lab collection
HY3362	*W303 Mat A top2-1*	Lab collection
HY3611	*W303 Mat A rmi1Δ::KANMX4*	Lab collection
HY3633	*W303 Mat A rad5Δ::HPHMX4 hmo1Δ::HIS3*	Lab collection
HY3661	*W303 Mat A hmo1Δ::HIS3*	Lab collection
HY3663	*W303 Mat alpha rad5Δ::HPHMX4*	Lab collection
HY3674	*W303 Mat A ura3-1::ADH1-OsTIR1-9MYC(URA3) top3::pADH1-tc3-3xHA-Top3(HPHMX4)-AID::NATMX4*	Lab collection
HY3701	*W303 Mat A top2-4 S::NATNT2-SMC6*	This study
HY3721	*W303 Mat A ura3-1::ADH1-OsTIR1-9Myc(URA3), sgs1::pADH1-tc3-3xHA(HPHMX4)-Sgs1-aid(KANMX)*	Lab collection
HY3805	*W303 Mat A Top2-10FLAG::KANMX4*	Lab collection
HY3807	*W303 Mat A TOP3-6HIS-10FLAG::KANMX4*	Lab collection
HY3882	*W303 Mat A sgs1::pADH1-tc3-3xHA-Sgs1 (NATMX)*	Lab collection
HY3974	*W303 Mat Alpha top2-4*	Lab collection
HY4071	*W303 Mat A rrm3Δ::HIS3MX6*	Lab collection
HY4421	*W303 Mat A S::NATNT2-SMC6 tof1Δ::KANMX*	Lab collection
HY4422	*W303 Mat A csm3Δ::HIS3MX6 S::NATNT2-SMC6*	Lab collection
FY4478	*W303 Mat A csm3Δ::HIS3MX6*	Lab collection
HY4674	*W303 Mat A ura3-1::ADH1-OsTIR1-9MYC(URA3) Top2-AID-9MYC::KANMX*	Lab collection
HY4898	*W303 Mat A S::NATNT2-Mms21*	Lab collection
HY4905	*W303 Mat A S::NATMX4-SMC6 ubc13Δ::HPHMX4*	Lab collection
HY4915	*W303 Mat A S::NATMX4-SMC6 rad5Δ::HPHMX4*	Lab collection
HY4968	*W303 Mat A rad5Δ::HPHMX4 siz1Δ::NATMX*	Lab collection
HY5373	*W303 Mat A S:: NATMX4-Nse1*	Lab collection
HY5375	*W303 Mat A S:: NATMX4-Nse5*	Lab collection

HY5377	*W303 Mat A G2::NATMX4-Nse1*	Lab collection
HY5569	*W303 Mat A rad52Δ:: HPHMX4*	Lab collection
HY5627	*W303 Mat A S::NATNT2-SMC6 top2-4 rad51Δ::LEU2*	Lab collection
HY5629	*W303 Mat A S::NATNT2-SMC6 top2-4 rad5Δ::HISMX6*	Lab collection
HY5857	*W303 Mat A S::NATNT2-SMC6 top2-4 tof1Δ::KANMX*	Lab collection
HY6522	*W303 Mat A top2-4 rad5Δ::HISMX6*	Lab collection
HY6524	*W303 Mat A top2-4 tof1Δ::KANMX*	Lab collection
HY6606	*W303 Mat A S::NATNT2-Mms21-PK9-HIS3MX6*	Lab collection
HY6670	*W303 Mat A S::NATNT2-SMC6 scc1-73*	Lab collection
HY7177	*W303 Mat A rrm3Δ::TRP1 sgs1Δ::KANMX4 fob1Δ::NATNT2*	Lab collection
HY7609	*W303 Mat A pADH1-tc3-3xHA-Top3::NATMX4 Smc6-6xHIS-3FLAG::KANMX4*	This study
HY7717	*W303 Mat A SMC6-13myc::TRP*	This study
HY7936	*W303 Mat A smc6-P4-13myc::KANMX TOP3-6HIS-10FLAG::KANMX4*	This study
HY8025	*W303 Mat A leu2::GPD1-OsTIR::LEU Smc6-AID-9MYC::HPHMX*	This study
HY8031	*W303 Mat A S::NATNT2-SMC6 TOP3-6HIS-10FLAG::KANMX4*	This study
HY8110	*W303 Mat A leu2::GPD1-OsTIR::LEU Smc6-AID-9MYC::HPHMX TOP3-6HIS-10FLAG::KANMX4*	This study
HY8112	*W303 Mat A Rmi1-6HIS-10FLAG::KANMX4*	This study
HY8455	*W303 Mat alpha srs2Δ::HIS3MX6*	Lab collection
HY8735	*W303 Mat A top2-4 Rmi1-10FLAG::KANMX4*	This study
HY8737	*W303 Mat A top2-4 TOP3-6xHIS-10FLAG::KANMX4*	This study
HY8767	*W303 Mat alpha mph1Δ::HPHMX4*	Lab collection
HY8851	*W303 Mat A Rmi1-10FLAG::KANMX4, leu2::GPD1-OsTIR::LEU Smc6-AID-9myc::HPHMX*	This study
HY8945	*W303 Mat A Rmi1-10FLAG::KANMX4 smc6-P4-13myc::KANMX4*	This study
HY8947	*W303 Mat A pADH1-tc3-3xHA-Top3::NATMX4 S::NATNT2-SMC6*	This study
HY9015	*W303 Mat A sgs1Δ::HIS, SMC6-6xHIS-3FLAG::KANMX4*	This study

HY9056	*W303 Mat A Top2-10FLAG::KANMX4 smc6-56-13MYC::KANMX4*	This study
HY9058	*W303 Mat A Top2-10FLAG::KANMX4 smc6-P4-13MYC::KANMX4*	This study
HY9060	*W303 Mat A Top2-10FLAG::KANMX4 leu2::GPD1-OsTIR::LEU Smc6-AID-9myc::HPHMX*	This study
HY9102	*W303 Mat A sgs1Δ::HIS Top3-10FLAG::KANMX4*	This study
HY9104	*W303 Mat A rmi1Δ::KANMX Top3-10FLAG::KANMX4*	This study
HY9105	*W303 Mat A csm3Δ::HIS3MX6 top2-4 S::NATNT2-SMC6*	This study
HY9273	*W303 Mat A csm3Δ::HIS3MX6 top2-4*	This study
HY9342	*W303 Mat A sgs1-K621R::KANMX, Top3-10FLAG::KANMX4*	This study
HY9390	*W303 Mat A Smc6-56-Sup-13MYC::KANMX*	This study
HY9410	*W303 Mat A mms21-C200A/H202A::HIS3 Top3-10FLAG::KANMX4*	This study
HY9457	*W303 Mat A irc5Δ::TRP top2-4*	This study
HY9688	*W303 Mat A sgs1::pADH1-tc3-3xHA-Sgs1 (HPHMX4) rad5Δ::URA3*	Lab collection
HY9700	*W303 Mat A top2-4 scc1-73 Top3-10FLAG::KANMX4*	This study
HY9879	*W303 Mat alpha rad54Δ:: KanMX4*	Lab collection
HY10014	*W303 Mat A smc6-56-13MYC::KANMX pADH1-tc3-3xHA-Top3::NATMX4*	This study
HY10047	*W303 Mat A smc6-56-sup-13MYC::KANMX pADH1-tc3-3xHA-Top3::NATMX4*	This study
HY10146	*W303 Mat A sgs1::pADH1-tc3-3xHA-Sgs1 (HPHMX4) smc6-56-Sup-13MYC::KAN*	This study
HY10149	*W303 Mat A sgs1::pADH1-tc3-3xHA-Sgs1 (HPHMX4) smc6-56-13MYC::KAN*	This study
HY10229	*W303 Mat alpha rad18Δ::HPHMX4 top2-4*	This study
HY10230	*W303 Mat alpha mms2Δ::HPHMX4 top2-4*	This study
HY10231	*W303 Mat alpha rad5Δ::HPHMX4 top2-1*	This study
HY10356	*W303 Mat A sgs1::pADH1-tc3-3xHA-Sgs1 (HPHMX4) top2-4*	This study

HY10448	*W303 Mat A sgs1Δ::natMX4 Smc6-56-Sup-13MYC::KANMX*	This study
HY10488	*W303 Mat A chl1Δ::KanMX4 smc6-56-sup-13myc::KANMX4*	This study
HY10490	*W303 Mat A mus81Δ::NATMX4 Smc6-56-13MYC::KANMX4*	This study
HY10491	*W303 Mat A mus81Δ::NATMX4 Smc6-56-Sup-13MYC::KANMX4*	This study
HY10492	*W303 Mat A mms4Δ::HPHMX4 Smc6-56-13MYC::KANMX4*	This study
HY10493	*W303 Mat A mms4Δ::HPHMX4 Smc6-56-Sup-13MYC::KANMX4*	This study
HY10494	*W303 Mat A mph1Δ::HPHMX4 Smc6-56-13MYC::KANMX4*	This study
HY10496	*W303 Mat A mph1Δ::HPHMX4 Smc6-56-Sup-13MYC::KANMX4*	This study
HY10543	*W303 Mat A mms21-C200A/H202A-13Myc::HIS3*	Lab collection
HY10633	*W303 Mat A srs2Δ::HIS3MX6 Smc6-56-Sup-13MYC::KANMX4*	This study
HY10658	*W303 Mat A top2-4 sgs1Δ::HIS3MX6*	This study
HY10660	*W303 Mat A top2-4 ura3-1::ADH1-OsTIR1-9MYC(URA3) top3::pADH1-tc3-3xHA-Top3(HPHMX4)-AID::NATMX4*	This study
HY10661	*W303 Mat A top2-4 smc6-56-13MYC::KANMX4*	This study
HY10793	*W303 Mat A top2-4 rmi1Δ::KANMX4*	This study

2.1.2 Media and buffers

2.1.2.1 Media for *E. coli*

LB

1% Bactotryptone

0.5% Yeast extract

1% NaCl

pH 7.25

LB Agar (LB + 2% Agar)

LB Amp (LB + 50 μg/ml ampicillin)

2.1.2.2 Media for *S. cerevisiae*

YP

1% Yeast extract

2% bactopeptone

pH 5.4

YP Agar (YP + 2% Agar)

YPD (YP + 2% Glucose)

YP Raf (YP + 2% Raffinose)

YP Gal (YP + 2% Raffinose +2% Galactose)

SC

0.67% yeast nitrogen base (YNB, DIFCO w/o AA)

2% glucose

amino acids (as per requirement)

SC Agar (SC + 2% Agar)

Dropout media (SC without said amino acid)

VB sporulation media

$NaAc.3H_2O$ 1.36%,

KCl 0.19%

NaCl 0.12% ,

$MgSO_4.7H_2O$ 0.074%

(+ 1.5% agar)

2.1.2.3 Buffers

2X Laemmli buffer:

4% SDS

20% glycerol

10% 2-mercaptoethanol

0.004% bromphenol blue

0.125 M Tris HCl

pH6.8

SDS-PAGE running buffer:
Glycine 2 M
Tris 0.25 M
SDS 0.02 M
pH 8.3

Transfer buffer:
1% glycine
0.02 M Tris base
20% methanol

SSC 20X buffer:
NaCl 3 M
Sodium Citrate 0.3 M
pH 7.5

TAE 50X:
Tris-acetate 0.04 M
EDTA 0.001 M

TBS 10X:
NaCl 1.5 M
Tris 0.5 M
pH 8.0

TE 1X:
Tris-HCl 10 mM
EDTA 1 mM
pH 7.4

2.2 Yeast Strain Construction

2.2.1 Bacterial Transformation:

50µl of fresh chemically competent *E. coli* (DH5alpha or TOP10) cells were thawed on ice prior to the addition of plasmid DNA. Cells were incubated with DNA on ice for 5' and then subjected to a heat shock for 60'' at 37° C. After the heat shock the cells were returned to

ice for 2'. Finally, 1ml of LB medium was added to the reaction tube. Cell suspension was incubated on a shaker at 37°C for 1hr before plating onto LB Amp plates. Plates were incubated overnight at 37°C.

2.2.2 Plasmid DNA isolation (Miniprep):

Single colonies were picked up from the LB Amp plates and inoculated overnight in 10 ml LB supplemented with 50µg/ml ampicillin. The cells were pelleted for 5' at 8000rpm and transformed into 1.5ml Eppendorf tubes. Minipreps were performed with Wizard Plus SV Minipreps DNA Purification System (Promega) following the manufacturer's instructions. Final elution of plasmid was made in 100µl ddH_2O. The concentration and quality of plasmid DNA was measured with nanodrop.

2.2.3 *Saccharomyces cerevisiae* transformation (LiAc/SS carrier DNA/PEG method)

S. cerevisiae mutants were created by Lithium Acetate-based transformation of yeast cells using PCR amplification of a gene deletion or tagging cassette (Gietz et al., 1995). The cassette contained a selectable marker flanked with approximately 40bp of homologous DNA to the upstream and downstream regions of genes of interest or C-terminus of gene of interest in case of tagging. The primers were designed according to (De Antoni and Gallwitz, 2000; Janke et al., 2004; Kötter et al., 2009; Longtine et al., 1998).

The cells in log phase, grown at 25°C were collected by pelleting at for 5' at 4000rpm and were resuspended in TE/LiAc (Lithium Acetate 0.1M; TE 1X) to the final concentration of $2x10^9$ cells/ml. Cells were then incubated at 28°C for 15'-20'. $1x10^8$ cells (50µl from the previous step) were mixed with 3-6µg of the transforming DNA cassette (about 5µl) and 5µl of denatured carrier DNA (salmon sperm DNA, Sigma) denatured beforehand at 95°C for 5'. The mix was incubated at 30°C for 20' followed by addition of 300 µl 40% PEG/LiAc and incubation at 28°C for 30'. 10% DMSO (36µl) was then added and cells were heat-shocked at 42°C for 15'. Following heat-shock, cells were kept at RT for 5' and then pelleted down and washed with YPD to remove traces of DMSO and PEG. Cells were resuspended in 3ml YPD and recovered for about 3 hrs at 25°C. Finally the cells were plated on selective plates (YPD+antibiotic or SC drop out media) and kept at 25°C. The colonies obtained after transformation were confirmed by PCR and Western blot (when required) before storing in glycerol stock.

2.3.4 Crosses

To combine different yeast mutants, we crossed haploid mutants with single mutation (or in some cases even several mutations) with opposite mating type (MatA or Mat alpha). We

started by growing MatA and Mat alpha strains separately, then mixed them on a YPD plate for 3-4 hrs to allow mating and selected diploid zygotes under the micromanipulator (Singer). Diploid colonies from single zygotes were grown for 2-3 days and then patched on VB sporulation plates to induce meiosis. After 3-5 days when sufficient number of tetrads were formed, we separated the 4 spores of tetrads using the micromanipulator on YPD plate and incubated at 25°C until colonies were formed from a single spore. We dissected about 10 tetrads per plates and 2-5 plates per cross based on the number of markers in order to get the desired combination. Genotypes of haploid colonies obtained from spores were checked by marker resistance and PCR (if required). To confirm we also checked the correct 2:2 segregation of markers and deduced genotype of dead spores in case of synthetic interactions.

2.3 Yeast growth, synchronization, conditional protein depletion and drug treatment:

2.3.1 Yeast cell growth:

The cells were grown at 25°C in YPD medium supplemented with Adenine (50µg/ml). When cells were synchronized with Nocodazole (Sigma), they were grown in YP+2% Glucose (not autoclaved) pH 7.4 and for α-factor (Sigma) arrest the cells were grown in YPD media.

2.3.2 G1 arrest:

Yeast cells of mating type α produce pheromone α-factor, which allows mating between the two Mat types. Mat A cells respond to the pheromone, they activate mating genes and show certain morphological trends including G1 arrest. We used the pheromone α-factor (Sigma) to synchronize the Mat A cells in G1 phase (O'Reilly et al., 2012).

Mat A cells were grown exponentially overnight, $0.8x10^7$ cells/ml were treated with 3-5 µg/ml of α-factor for 1hr 45' (usually 15-30 minutes more for mutants) with half the amount of α-factor added after 1hr. G1 arrest was checked under microscope and when >95% cells showed G1 morphology, FACS samples were collected for confirmation of arrest. Depending on the protocol, the cells were washed once with YP and then released in media containing drug or at a higher temperature.

2.3.3 G2/M arrest:

Nocodazole is a microtubule poison, that depolymerizes the microtubules. In response to this poison, the cells activate spindle assembly checkpoint and get arrested in pro-metaphase (G2/M phase with two buds of equal size). We used the nocodazole to synchronize cells loosely in G2/M phase (Mayer and Goin, 1988).

Cells were grown exponentially overnight, $0.8x10^7$ cells/ml were treated with 10-20µg/ml of Nocodazole (dissolved in DMSO, 1% DMSO in total) for 2hrs 15' (usually 15 minutes more for mutants). G2/M arrest was checked under microscope and when >95% cells showed G2/M morphology, FACS samples were collected for confirmation of arrest. Depending on the protocol, the cells were washed twice with YP+1%DMSO and then released in media containing drug or at a higher temperature.

2.3.4 MMS and HU treatment:

For acute treatment with Mehylmethane Sulphate (MMS), cells were treated with 0.033% MMS in YPD and samples were collected at the prescribed timepoints. For chronic treatment with MMS, the YPD Agar plates were prepared with indicated MMS concentration and cells were spotted on the plate.

For acute treatment with Hydroxyurea (HU), cells were treated with 200mM HU in YPD and samples were collected at the prescribed timepoints. For chronic treatment with HU, the YPD Agar plates were prepared with indicated HU concentration and cells were spotted on the plate.

2.3.5 Conditional depletion of proteins:

Temperature sensitive alleles were grown at 25°C as permissive conditions and shifted to 37°C to prevent the function of the mutant protein.

Tetracycline dependent depletion of mRNA (translational suppression) was performed by treating the cells with 0.6mM tetracycline (nzytech) during the arrest. Tetracycline was added again after release in fresh media and again after 2hrs for experiments with longer sample collection.

Auxin inducible degron (AID) tag was added to genes to achieve protein degradation upon Auxin (Iodoacetamide (IAA), Sigma) addition. The cells were treated with 0.2mg/ml of Auxin (stock 50mg/ml) during the arrest. Same amount of Auxin was added later in the fresh media during release. For more efficient depletion of proteins, tetracycline and AID tags were used together (Tc-protein-AID).

2.4 Protein based techniques:

2.4.1 TCA protein extraction:

The TCA protein extraction was performed as described in (Reid and Schatz, 1982). The cells were grown overnight, 10ml of exponentially growing cells (10^7 cells/ml) were pelleted. The cells were resuspended in 1ml TCA and transferred into 2ml Eppendorf tube and pelleted again. The cells were resuspended in 50µl TCA 20%, added an equal volume

of acid-washed glass beads (425-600µm, Sigma-Aldrich) and vortexed for 10' to break the cells. 100µl of TCA 5% TCA was added to the tube and the lysate was transferred to a new 1.5ml Eppendorf tube and centrifuges at 3000rpm for 10'. The pellet was resuspended in 100µl 2X Laemmly buffer, vortexed and neutralized with 50µl Tris base 1M. The protein was then boiled at 95°C for 5' and centrifuged for 10' at 3000 rpm at RT. The supernatant was collected in new tube and processed further with SDS-PAGE and Western blot.

2.4.2 SDS-PAGE and Western Blot

The proteins were separated on a Mini-PROTEAN precast polyacrylamide gel (bio-rad) 7.5% or 4-20% gradient gel based on the size of the protein of interest (Laemmli, 1970). The gel was run in SDS-PAGE running buffer at constant voltage of 120V. The gel was run until the loading dye was run out.

The proteins were transferred on Nitrocellulose membrane (Protran, Whatman 0.45 mm) in 1X transfer buffer in cold. The transfer was carried out at constant voltage of 100V for 1hr at 4°C. Following transfer, the membrane was washed once with water, stained with Ponceau solution (Ponceau S 1gr, acetic acid 50 ml, up to 1000 ml ddH_2O) to check the quality of transfer, stained membrane was cut based on the size of protein of interest and loading control. Ponceau solution was washed off with 1X TBST and membrane was inoculated for 1hr in 5% milk/1X TBST for blocking. After blocking with non-fat milk, the membrane was incubated with the primary antibody overnight. On the next day, the membrane was washed 10' with 1X TBST thrice before incubating with secondary antibody for 1hr. Following secondary antibody, the membrane was washed again thrice with 1X TBST and using ECL kit (Amersham) signal on the membrane is revealed. The membrane was then exposed to ChemiDoc (Bio-Rad, Molecular Imager ChemiDoc XRS+) and the image was acquired.

Table2.2: List of antibody and dilutions:

Tag/protein	Primary antibody	Company	Dilution
Flag	Anti-Flag M2 (F1804)	Sigma	1:5000
HA	Anti-HA (12CA5)	In house (IFOM)	1:3000
V5 (PK)	Anti-PK (SV5-Pk1)	Bio-Rad / AbD Serotec	1:5000
Myc	Anti-Myc (9E10)	In house (IFOM)	1:5000
Pgk1	Anti-Pgk1 (22C5)	Invitrogen	1:7000
Tubulin	Anti- α Tubulin	In house (IFOM)	1:7000
Secondary Mouse	Anti-mouse	In house (IFOM)	1:20000

2.5 DNA techniques

2.5.1 PCR and cassette preparation

For the preparation of cassettes of gene manipulation (deletion or tagging), we designed primers mapping in the region of interest (In case of deletion, mapping the beginning and end of the gene. For C-terminal tagging, mapping in the the beginning and end of the stop codon) followed by the primers for amplification of marker. For colony PCR, the colonies were boiled in 4µl NaOH (10mM) for 10' and continued with PCR reaction.

We set PCR with the following conditions:

PCR mix:	PCR reaction:
Plasmid DNA 1µl/ colony PCR 4µl	Initial denaturing 95°C, 2'
PCR mastermix 12.5µl	{Denaturing 95°C, 20''
Primer1 1.25µl	Annealing 50°C, 30''
Primer2 1.25µl	Extension 65°C, 2' (approx. 1'/kb)} X 30 cycles
ddH_2O upto 25µl	Final Extension 65°C, 4'

The PCR was checked in 1% agarose gel stained with GelRed (Biotium) and size was compared with 1kb ladder (NEB).

2.5.2 DNA sequencing

For confirmation of point mutations and tags, we sequenced the PCR products. For sequencing, the concentration of PCR product was estimated on a gel and it was diluted to 50ng/µl. The PCR product was then sent to Cogentech facility at IFOM for sequencing. The data was aligned with the WT sequence in SnapGene and mutation was confirmed.

2.6 Yeast techniques

2.6.1 FACS (Fluorescence Activated Cell Sorting) Analysis:

FACS analysis was done with a modified protocol from (Haase and Reed, 2002). We started with 1-2 x10^7 cells for FACS analysis. Cells were collected in 2ml Eppendorf tube and fixed with 70% ethanol. The cells washed once with Tris-HCl 50mM pH 7.5, followed by treatment with 2mg/ml RNAse A (Sigma) in Tris-HCl 50mM pH 7.5 for 3hrs to overnight at 37°C. The cells were then washed and resuspended in Proteinase K (Roche) 1mg/ml for 30' at 50°C. The cells were pelleted and resuspended in 500µl Tris-HCl 50mM pH 7.5 and stored at 4°C until acquisition. For acquisition, 1ml of Tris-HCl 50mM pH 7.5 solution containing 1µl SytoxGreen (1µM final concentration) was mixed with 100µl cells from the previous step in a FACS tube. The cells were sonicated for 6'' and acquired with Becton Dickinson FACSCalibur FL1H fluorescence.

2.6.2 Spot Assays and Genetic interactions:

For spot assays we harvested 0.5 OD (around 1 x10^7) cells from the overnight culture in the first lane. We made serial 1:7 dilutions for 5 lanes. Cells were spotted on YPD and YPD+MMS/HU/CPT plates and incubated at indicated temperatures for 2-4 days. The images of spot assay were acquired on the 2nd and 3rd day of spotting. Each spot assay is repeated twice with different spores with same genotype to confirm the observed interactions.

To investigate genetic interactions between the mutants, we crossed the strains on the plate for 4 hours, picked zygotes, sporulated the diploids and dissected 10 tetrads per plate for several plates. Once the tetrads were grown we checked the genetic background by checking markers present in each spore and then marked them according to their genotype. We deduced the genotype of the dead spores based on other spores.

2.6.3 Chromatin Immunoprecipitation (ChIP) on chip and qPCR:

Chromatin immunoprecipitation is a technique used to identify the interplay between proteins and DNA. Various proteins are bound to chromatin and regulate its accurate replication, condensation and maintenance. With techniques like ChIP-on-chip and ChIP-qPCR we can get a genome-wide or locus specific picture of association of protein of interest and DNA. ChIP-on-chip experiments are performed only once but we compare different components of the complex to confirm the localization. ChIP-qPCR experiments are repeated thrice, the mean and standard error bars are plotted for the three biological repeats. In this technique, we cross-link DNA-protein, isolate protein of interest (usually with a tag) and then purify DNA isolated with the protein. This purified DNA can then either be analyzed for genome-wide association on an Affymetrix microarray (*S. cerevisiae* Tiling 1.0R, P/N 900645) or can be analyzed by a locus specific quantitative PCR (qPCR). The first type of analysis gives us a more general picture at a 300bp resolution while the second method gives us more quantitative data for a single locus. ChIP-on-chip and ChIP-qPCR analysis were carried out as described in (Bermejo et al., 2009c), employing anti-Flag monoclonal antibody M2 (Sigma) and anti-myc monoclonal antibody 9E10. ChIP experiment were performed after Nocodazole 20µg/ml treatment, to analyze chromatin enrichment of a given protein in G2/M phase. For both methods, comparison was made between input samples and IP samples, where the total protein was estimated with input fraction while the fraction of this total protein bound to chromatin was isolated in IP fraction. Analysis of the data was performed using TAS (Affymetrix) and MAT software. The schematic representation of ChIP protocol modified from (Katou et al., 2006).

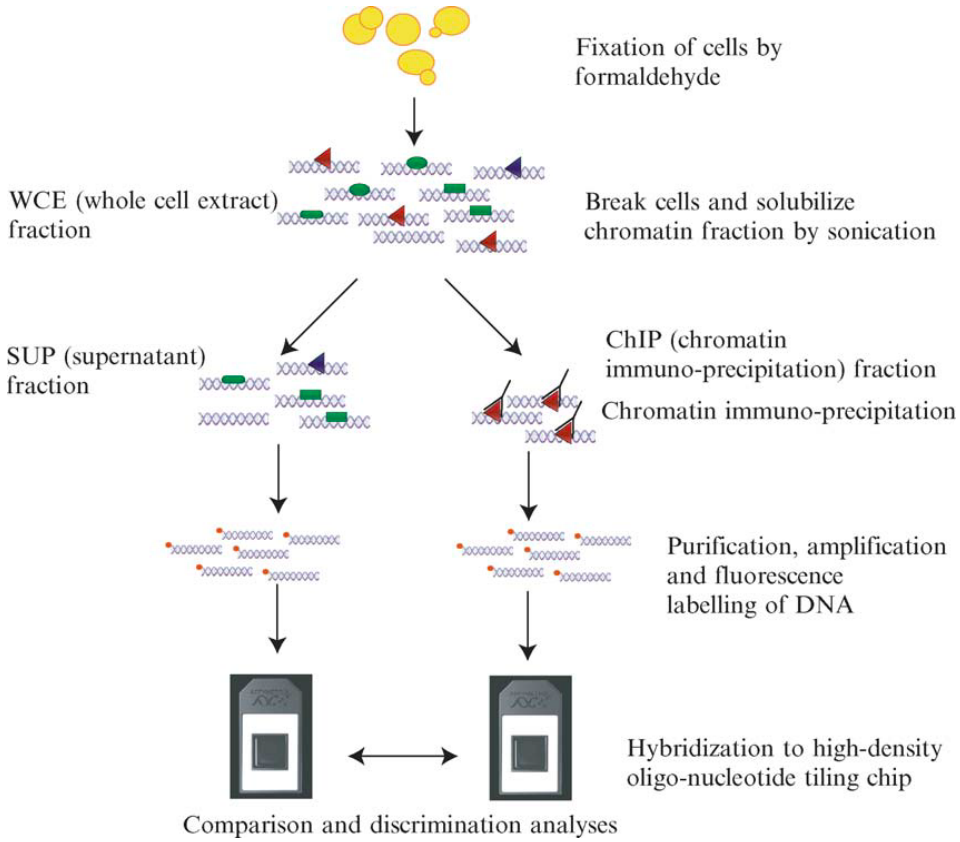

Fig2.1: Schematic representation of ChIP-on-chip protocol

Solutions:

PBS: 137 mM NaCl, 10 mM PO_4 ph 7.4, 2.7 mM KCl (filtered 0.2 µM)

TBS: 20 mM Tris-HCl pH 7.5, 150 mM NaCl (filtered 0.2 µM)

TE: 10 mM Tris-HCl pH 8.0, 1 mM EDTA (filtered 0.2 µM)

3M Sodium Acetate

5M NaCl stock

25 mM CoCl2

PBS/BSA: 1x Phosphate Buffered Saline containing 5 mg/ml Bovine Serum Albumin (filtered 0.2 µM)

Lysis Buffer: Hepes-KOH pH 7.5 50 mM, NaCl 140 mM, EDTA 1 mM, Triton-X100 1%, Na-deoxycholate 0.1% (autoclaved)

Wash Buffer: Tris-HCl pH 8.0 10 mM, LiCl 250 mM, NP-40 0.5%, Na-deoxycholate 0.5%, EDTA 1 mM (autoclaved)

Elution Buffer: Tris-HCl pH 8.0 50 mM, EDTA 10 mM, SDS 1%

TE -1% SDS: Tris-HCl pH 8.0 10 mM, EDTA 1 mM, SDS 1%

100% ice cold Ethanol

80% ice cold Ethanol

70% ice cold Ethanol

10X One-Phor-All-Buffer: Tris-Acetate pH7.5 100 mM, Mg-Acetate 100 mM, K-Acetate 500mM

Proteinase K: Stock 50 mg/ml in 50% Glycerol; stored at -20˚C

RNase A: Stock 10 mg/ml; Prepared as in protocol from SIGMA ALDRICH; stored at -20˚C

Protein A Magnetic beads preparation:

For 100 ml yeast culture:

We transferred 60µl Magnetic beads (ProteinA, Invitrogen) in 1.7ml pre-lubricated tube. Washed the beads twice with 0.5ml cold PBS/BSA by gently mixing and putting back on the magnetic grid. After the washes, beads were finally resuspended in 60µl PBS/BSA and 20µg of antibody of interest was added to the tube. This beads-antibody mix was incubated overnight in a rotating wheel overnight at 4°C.

Before use of the antibody coupled beads, they were washed twice with cold PBS/BSA and resuspended in 60µl lysis buffer. 15µl of antibody coupled beads were added to each tube containing 400µl lysate.

Chromatin extracts preparation and immunoprecipitation

100ml cells were grown, arrested and collected as described before. 50ml cells were transferred in 50ml falcon tube containing 1% final concentration (1.350 ml of a 37% solution) of Formaldehyde (Sigma). Cells were incubated at RT for 15'-30' and then quenched with 2ml Glycine 2.5M. They were immediately put on the ice until further processing. To remove excess of formaldehyde and glycine, cells were washed three times with 20ml cold TBS 1X. After washes, cells were resuspended in 400µl Lysis buffer supplemented with Antiproteolytic cocktail (Complete, Roche) and transferred in 2ml lysis tubes. To each tube about 1ml zirconium beads were added. Cells were broken with multi-beads shocker at 4°C with following conditions: speed: 6,5 m/sec., 20 sec/cycle, 4-6 cycles. The breakage of the cells was confirmed by observing under the phase contrast microscope and breakage cycles were extended until more than 90% of the cells were lysed. After the lysis, lysis tubes were punctured with a hypodermic syringe needle (27G1/2) and fixed into fresh 1.5ml tubes. Lysate was recovered by centrifugation at 800rcf for 5' at 4°C. After the lysate was recovered, we discarded the lysis tubes and centrifuged the Eppendorf tubes at 13000rcf for 1' at 4°C. The supernatant contains the chromatin unbound proteins, 5µl of supernatant was collected for western blot in a tube containing 5µl 2X Laemmli buffer and stored at -20°C until western blot analysis. Rest of the supernatant was discarded and the pellet (that contained chromatin bound proteins) was resuspended in 450µl supplemented lysis buffer. Chromatin fraction was sheared with 5 cycles of sonication for 15 sec at 1.5

tune 20% intensity. After each cycle of sonication, samples were centrifuged at 2300g for 1' at 4°C. After sonication, the size of sheared chromatin can be assessed by running the extract on a 1.2% TAE agarose gel. We expected to see a smear of DNA fragment between 100-1000bp, if not additional sonication cycles can be performed. Once the sonication was successful, samples were centrifuged at 16000rcf for 5' at 4°C. The supernatant of this step contained fragments of DNA and DNA bound proteins. 5µl of supernatant was collected for western blot in a tube containing 5µl 2X Laemmli buffer and stored at -20°C until western blot analysis. 10µl of supernatant was collected for input reaction in tube containing 190µl of TE-1% SDS, the input tubes were incubated overnight at 65°C to reverse crosslinking. Rest of the supernatant is collected in a 1.7ml pre-lubricated tube and 15µl of antibody coupled beads were added to the tube. The lysate and beads were incubated overnight on a rotating wheel to facilitate proper antibody-tag binding.

Beads washing and crosslink reversal:

Beads were extensively washed to remove the unbound proteins and DNA. For each wash, tubes were placed on the magnetic grid, once all the beads were collected at the wall of the tube clear liquid was removed with vacuum pump. The beads were then mixed with wash solution and resuspended gently by inverting several times. The washes were performed in the following order:

- 2x with 1 ml of cold Lysis Buffer (without anti proteolytic tablet).
- 2x with 1 ml of cold Lysis Buffer supplemented with 360 mM NaCl
- 2x with 1 ml of cold Wash Buffer.
- 1x with 1 ml of cold TE pH 8.

After final wash, tubes were centrifuged at 800g for 1' at 4°C. Remaining TE solution was removed with vacuum pump and the beads were resuspended in 40µl Elution Buffer. For efficient elution, the tubes were incubated at 65°C for 10' with 1200rpm mix in a thermomixer. The tubes were then centrifuged at 16000rcf for 1' at RT and were placed on the magnetic grid. The IP fraction from this step contained DNA bound proteins eluted with the antibody. 5µl of the IP fraction was collected for western blot in a tube containing 5µl 2X Laemmli buffer and stored at -20°C until western blot analysis. Remaining IP fraction was added to a fresh tube containing 4 volumes of TE-1%SDS (140µl when western blot samples were collected, 160µl otherwise). The tubes were incubated at 65°C overnight for reverse crosslinking.

The samples collected for western blot were boiled at 95°C for 30' (or more) and processed further. For the western blot samples of ChIP we expected to observe strong band of protein

of interest in the IP fraction and weaker or no bands in chromatin unbound and flow-through fractions.

DNA purification:

After overnight incubation, we consolidated input and IP samples by pulse spin. To make the volumes even, we added 25µl TE to tubes with less volume due to western blot samples. Then to each tube 89.5µl TE, 3µl glycogen (20mg/ml roche) and 7.5µl ProteinaseK (50mg/ml) was added. The tubes were incubated at 37°C for 2hrs-overnight. Following proteinaseK treatment, 12µl NaCl 5M was added to each tube and we purified DNA by two extractions with equal volume (300 µl) phenol/chlorophorm/isoamylalcohol (25:24:1), pH 8.0 at RT and once with equal volume of chloroform to remove traces of phenol from the samples. The IP and input samples were then precipitated with 2 volumes of cold 100% ethanol (600µl) at -20°C for 3hrs-overnight.

After precipitation of DNA, samples were pelleted at 16000rcf for 15' at 4°C, washed once with cold 80% ethanol and pelleted again at 16000rcf for 15' at 4°C, following the wash samples were dried for 5' at RT to remove traces of ethanol and were resuspended in 30 µl of TE containing 10 µg of RNase A. The samples were treated with RNAse A at 37°C for 1hr. After RNAse treatment, samples were cleaned with Qiagen PCR purification kit according to manufacturer's protocol. The elution was done twice with 50µl elution buffer. At this stage, the two samples for IPs were pooled together to have one tube for each IP and each input. We added 100µl elution buffer to input samples to adjust volumes. We precipitated the DNA with 10µl of 3M Sodium Acetate, 4µl of glycogen (20mg/ml) and 2.5 volumes of cold 100% ethanol (535µl) and incubated the samples at -20°C for at least 3hrs-overnight. The precipitated DNA was centrifuged and washed as previously with cold 70% ethanol. After wash, the tubes were dried for 5' to remove traces of ethanol and resuspended in 10µl ddH_2O for ChIP-on-chip or 50µl ddH_2O for ChIP-qPCR. Depending on the experiment, the ChIP DNA was processed differently from this step onwards.

ChIP-qPCR reaction:

The IP DNA obtained from ChIP was diluted 1:5 and input DNA was diluted 1:10. The diluted DNA was used to set up qPCR reaction as follows:

qPCR mix:	PCR reaction:
DNA 5µl	Initial denaturing 95°C, 5'
qPCR mastermix 12.5µl	{Denaturing 95°C, 10''
Primer1 1.25µl	Annealing 60°C, 30'' Single acquisition} X 40 cycles

Primer2 1.25µl ddH_2O upto 25µl	Melting 95°C, 1'' 37°C, 1'' 95°C Continuous acquisition Cool 37°C 1''

The list of qPCR primers for various genomic loci is as below:

Table 2.3: List of oligos for qPCR and 2D probes

Oligo	purpose	Sequence
TER302CF	q-PCR primer at TER302	GGGTAGACGAAACTATA TACGCAAT
TER302CR	q-PCR primer at TER302	TGCCCTCCTCCTTGTCAATA
TER603AF	q-PCR primer at TER603	ATGGGGGTTGAACATTGTGT
TER603AR	q-PCR primer at TER603	TCGCATATAAGCAAGTGGTTT
TER1004FF	q-PCR primer at TER1004	CCATCTTGTTGTCCATGTCC
TER1004FR	q-PCR primer at TER1004	CGCATGGGATTTTGCTATC
ARS305F	q-PCR primer at ARS305	TCAGAGCCTTCTTTGGAGCT
ARS305R	q-PCR primer at ARS305	TCACACCGGACAGTACATGA
ARS1F	q-PCR primer at ARS1	TGGTGTTGATGTAAGCGGAG
ARS1R	q-PCR primer at ARS1	AAAGTCAACCCCCTGCGATG

After the qPCR reaction, the data was processed in an excel sheet to calculate ΔΔCt and %input bound to DNA. The results were plotted as a bar graph for representation. The qPCR was repeated twice for each sample (technican replicates). The ChIP-qPCR experiments were repeated three times to get three biological replicates of each experiment. The p-value was calculated based on students' t-test to compare various mutants.

ChIP-on-chip sample processing:

DNA amplification:

Amplification step was performed using WGA2 GenomePlex Complete Genome Amplification (WGA) Kit to get sufficient amount of DNA for hybridization. We followed manufacturer's instructions from the Library Preparation step. We prepared library preparation mix with 2µl of 1X Library preparation Buffer, 1µl of Library stabilization solution in each tube and placed the samples in thermal cycler at 95°C for 2 minutes. The sampled were then cooled on ice, consolidated by centrifugation, and returned to ice before

addition of 1µl Library Preparation Enzyme, vortexed thoroughly and centrifuged briefly. The samples were then placed in a thermal cycler and incubated as follows:

16°C for 20 minutes

24°C for 20 minutes

37°C for 20 minutes

75°C for 5 minutes

4°C hold

We then removed samples from thermal cycler and centrifuged briefly. Samples were amplified further or stored at -20°C for upto 3 days.

For further amplification of samples following master-mix was prepared:

Nuclease-free water:	48.5 µl
10X Amplification Master Mix:	7.5 µl
Reaction from previous step:	14.0 µl
WGA DNA Polymerase:	5.0 µl

This mix was vortxed to mix, centrifuged and kept in thermocycler for following amplification conditions:

Initial Denaturation: 95° C for 3 minutes

Performed 14 cycles as follows:

Denature:	94° C for 15 seconds
Anneal/Extend:	65° C for 5 minutes
Final hold	4°C

After completion of amplification, 1.9µl of each reaction was loaded in 1.2% agarose gel. We expected to observe smear ranging from 100 to 1000bp. IP and input samples were cleaned with Qiagen PCR purification kit according to manufacturer's protocol. The elution was done twice with 50µl elution buffer each time. We precipitated the DNA with 5µl of 3M Sodium Acetate, 2µl of glycogen (20 mg/ml) and 267.5µl cold 100% ethanol and incubated the samples at -20°C for at least 3hrs-overnight. The precipitated DNA was centrifuged and washed as previously with 1ml cold 80% ethanol. After wash, the tubes were dried for 5' to remove traces of ethanol and resuspended in 42µl ddH_2O. 1.5µl of samples were used to measure the DNA concentration with nanodrop (at 260 nm). The minimum concentration for proceeding with hybridization was 100mg/ml. If the concentration was lower, we performed 2 more rounds of amplification before hybridization of samples. To prevent excessive background in the experiment, we avoided performing more than 20 cycles of amplification.

DNAse digestion:

The amplified ChIP DNA was further digested with DNase in order to get fragments of smaller size to be easier for recognition with microarray. The DNase mix was prepared as follows (for 13 samples):

ddH2O	14.8 µl
10X One-Phor-All-Buffer plus	2 µl
25mM CoCl2	1.2 µl
DNase I (1U/µl)	2 µl

We prepared the following reaction mix using mix of previous step:

10X One-Phor-All-Buffer plus	4.85 µl
25mM CoCl2	2.9 µl
DNase I reaction mix	1.5 µl
DNA (5-10 µg) + ddH2O (IP/input) samples	40.75 µl

Samples were incubated at 37° C for 30'' and then transferred to 95°C for 15'.

DNA labelling:

From previous step, samples were collected by quick spin and transferred into a new 1.5ml Eppendorf tube. To these tubes, 5µl of TdT reaction buffer, 1µl Biotin-N11-ddATP and 1µl terminal transferase (400U/µl) was added. This was followed by pulse spin and samples were incubated at 37° C for 1hr.

Hybridization and analysis of the data:

Hybridization, washing, staining, and scanning were performed according to the manufacturer's instructions (Affymetrix). Primary data analyses were carried out using the Affymetrix microarray Suite version 5.0 software to obtain hybridization intensity, fold change value, fold change p-value and detection of p-value for each locus.

Evaluation of the significance of protein cluster distributions within the different genomic areas and protein-binding correlations was performed by confrontation to the model of the null hypothesis distribution generated by a Montecarlo-like simulation. The significance of the overlap between proteins clusters was evaluated as in (Bermejo et al., 2009a), (Gonzalez-Huici et al., 2014).

2.6.4 Pulse Field Gel Electrophoresis (PFGE) and digested plugs

Pulse Field Gel Electrophoresis (PFGE) is a technique that allows separation of large fragments of DNA (upto millions of base pairs) based on their size by applying an alternating current in a zig-zag manner. This technique can be efficiently used to separate yeast

chromosomes, allowing us to observe formation of breaks on a particular chromosome. The program for running PFGE can be fine-tuned further to exclusively separate large chromosomes or small chromosomes. After the run, we probe for chromosome of our interest (e.g. Chr. XII for rDNA) and observe the smear that indicates break on the chromosome (Birren et al., 1989a; Birren et al., 1989b; Lai et al., 1989).

Similar technique can also be used in a more modified way, by digesting genomic DNA after preparation of plugs. In this case a simple one-dimensional electrophoresis is enough to separate DNA fragments. The breaks in our region of interest can be visualized by probing for that region after southern blot (Sasaki and Kobayashi, 2017).

Solutions and Buffers

0PG Buffer: 28.85ml of 1M Na_2HPO_4, 21.15ml of 1M NaH_2PO_4, 450ml ddH_2O autoclaved (0PG buffer: 0.1M Phosphate buffer pH 7)

1PG Buffer: 20ml Tris-HCl 1M pH 6.8, 50ml EDTA 0.5M pH 8, make up to 500ml with ddH_2O autoclaved (40mM Tris-HCl pH 6.8, 50mM EDTA)

2PG Buffer: 250ml 0PG Buffer, 50ml EDTA 0.5M pH 8, make up to 500ml with ddH_2O autoclaved (50mM Phosphate buffer with 50mM EDTA)

3PG Buffer: 50ml Tris-HCl 1M pH 6.8, 200ml EDTA 0.5M pH 8, 5g Sarkosyl, 2mg/ml Proteinase K (Proteinase K added fresh before using the buffer) make up to 500ml with ddH_2O autoclaved. (100mM Tris-HCl pH=6.8, 200mM EDTA, 1% w/v Sarkosyl, 2mg/ml Proteinase K)

4PG Buffer: 25ml Tris-HCl 1M pH 7.5 make up to 500ml with ddH_2O autoclaved. Add 1:100 RNaseA from 10mg/ml stock (fresh before use) (50mM Tris-HCl pH 7.5 with 0.1mg/ml of RNaseA)

1.5% Agarose Mix- Agarose certified from Biorad for PFGE: 10ml 2PG Buffer + 0.15g Agarose

Plugs digestion: 2PG Buffer, 10mM DTT, 0.5 mg/ml Zymoliase 100T USB.

To prepare 100ml of 2PG buffer, DTT and Zymoliase (*add 50mg of Zymoliase 100T USB), 0.155g DTT.

*Zymolase can be reduced to 0.25mg/ml depending on its activity. It is important that the yeast cell wall is completely digested.

DNA isolation in agarose plugs

We started with 50 ml of 1.5-2 x 10^7 cells/ml and added 0.5ml of 10% Sodium Azide (Sodium Azide stock solution was prepared in autoclaved ddH_2O water; the stock solution is filtered) to get a final concentration of 0.1%. It was immediately put in ice and left until

all the time points were collected. The minimum time for Sodium Azide fixation was 30'. Cells were then centrifuged in a 50 ml falcon tube at 4000 rpm for 5' at 4°C, washed once with 10ml cold 1PG Buffer, resuspended in 1.5ml of cold 1PG Buffer without zymoliase and DTT and transferred in 2ml Eppendorf tube. This was followed by three washes with cold 1.5ml of 1PG Buffer. After final wash, we removed all liquid with a gel loading tip and left the 2ml Eppendorf tubes with the washed cellular pellets in ice.

For preparation of plugs we pre-warmed 1.5ml Eppendorf tubes at 55°C in a thermomixer. We prepared a mix of 1.5% w/v of PFGE certified agarose (Biorad) in 10ml of 2PG buffer in a 50ml falcon tube and completely dissolved the agarose in the mix using a microwave oven. (Agarose mix should reach the boiling temperature and agarose particles must be completely dissolved). We then prepared 1ml aliquots of the melted agarose mix in the pre-warmed 1.5ml eppendorf tubes and kept them at 55°C in the thermomixer the way that the agarose did not get solid. The plugs molds were prepared by sealing their bottom sides with a piece of tape, we labelled on the tape of each plug mold the name of the corresponding sample. Cellular pellets were resuspended in 300µl of 2PG Buffer without Zymoliase and DDT. The tubes with resuspended cellular pellets were put in a second thermomixer pre-warmed at 40°C. Once the cell suspension reached 37-40°C, we added 300µl of the previously prepared agarose mix to a tube containing 300ul of the cell suspension, which was kept at 40°C in the thermomixer, mixed for 6 times by carefully pipetting up and down without forming bubbles. Filled plug molds with 90µl cells/agarose mix per plug (for 50ml starting culture, we expected to get 10 plugs). We avoided forming bubbles while filling the molds and while mixing culture and agarose. Filled molds were then transferred to 4°C fridge undisturbed for 30' in order to allow blocks to solidify. We then ejected plugs with gel loading tip or yellow tip in a 50ml falcon tube containing 5ml plug digestion solution i.e. 2PG Buffer containing zymoliase and DTT (calculated about 0.5ml per plug). (All plugs were put inside the liquid. Any plug left outside the liquid overnight was discarded.). The plugs were left at 37°C O/N. The next day we gently removed the solution keeping the plugs in the tube with the help of a spatula, without damaging the plugs and resuspended the plugs in 5ml 3PG Buffer (again, calculated 0.5ml for each plug). Incubated at 42°C for ON. After proteinaseK treatment, we discarded 3PG Buffer, resuspended plugs in 5ml of 4PG Buffer without RNaseA, kept at RT for 30 minutes. We repeated this twice to wash away proteinaseK. We then added 500µl RNaseA (10mg/ml) to 50ml 4PG Buffer. Discarded 4PG Buffer from the plugs and resuspended them in 5ml of 4PG Buffer with RNaseA. Kept at 37°C for ON. Affter RNaseA treatment, we washed thrice with 5ml of 4PG buffer, to wash away RNaseA completely. After washes, we stored plugs in 1PG buffer at 4°C in cryo-vials tubes with not less than 0.5ml of 1PG buffer/plug. Preparedd 0.6% gel containing 1: 20,000

EtBr. Loaded half of the plug in the gel and run a normal agarose gel to check the quality of plug preparation. The image was taken with chemi-doc to analyse the amount of DNA in the plugs. The plugs were then ready for PFGE or digested plugs (1D gel electrophoresis).

PFGE running:

We filled the PFGE apparatus with 3L of 0.5X TBE solution prepared from the kitchen. Closed the lid and started cooling the apparatus. The gel was made with 1% Agarose with TBE 0.5X not autoclaved (15ml 5X TBE not autoclaved + 135ml MilliRX autoclaved water). We made the gel while keeping 5ml aside for sealing the plugs in place. The gel was left at RT for 1hr to solidify. Plugs needed to be equilibrated with 4PG buffer before loading (as 1PG buffer contains EDTA). We washed one plug per sample for one loading, four washes for 30 mins with 5ml 4PG for each plug. The plugs were ready, they were cut with scalpel and half of each plug was loaded in the gel. Remaining half was kept in 4PG buffer at 4°C to be loaded if the first run was not good quality. We sealed the plugs at position by 5ml of agarose kept at 65°C. Allowed the agarose to cool down, removed excess agarose from the well with the help of tissue paper.

Once the gel was ready, we checked the temperature of the running apparatus, oriented the gel in the apparatus and placed the electrodes in correct orientation. Aligned the clamp of the electrode in correspondence to the position of the wells (wells being on one specific side of the gel). Plastic tray with the clamps was slowly place it inside the PFGE chamber. We did not switch off liquid circulation while putting the gel in the apparatus in order to maintain the temperature of the apparatus. We left the gel in the apparatus for 15' to cool down. After the gel was cooled, we started the running with desired protocol. (To visualize the small chromosomes, we used 165V, 24hrs, 60s pulse, for rDNA we used). Once the run was completed, we incubated the gel for 1 hour with EtBr (1:20,000 EtBr in 1L 0.5X TBE), destain for 15 minutes with 1L 0.5X TBE and capture image to see proper running of samples. This was followed with Southern blot.

Digested plugs

The plugs were cut half, washed four times for 30 mins with 5ml 4PG for each plug. The plugs were then incubated with 0.5ml digestion mix containing restriction enzyme of our interest and buffers. After overnight digestion, plugs were washed with 5ml 4PG buffer and loaded in a normal agarose gel (0.7%) in 1X TBE and run for 20-22hrs. The run was checked by EtBr staining and once it was confirmed the gel was processed for Southern blot.

2.6.5 2D gel electrophoresis

When replication origin is fired, replication fork progresses bidirectionally. The fork progression continues until it meets replication fork arising from adjacent active origin travelling in the opposite direction. The replication structures thus formed are of different sizes and shapes. If we analyze the origin of replication, ideally, we shall observe replication bubbles of varying sizes and shapes. If we analyze a region away from the replication origin that is replicated passively, we might observe single replication fork (Y shaped) of various sizes and shapes or two forks approaching each other (double Y) of various sizes and shapes. The structures thus formed during replication are of differing sizes and shapes. Apart from this, if replication is perturbed or is stalled, we might also observe stalled replication forks or recombination intermediates of different shape. 2D gel electrophoresis experiments are repeated at least twice and often with different mutants or different depletion systems to confirm the phenotypes observed.

We can analyze the population of structures formed at a particular locus during replication and repair by Neutral-neutral two-dimensional agarose gel electrophoresis (2D-gel electrophoresis). With this technique we can separate nascent branched DNA molecules based on mass and shape (Bell and Byers, 1983a; Bell and Byers, 1983b; Brewer and Fangman, 1987). In this method, we first cross link the DNA with psoralen to preserve the replication/recombination structures and prevent branch migration. Then we extract DNA from cells using CTAB method. CTAB method preserves the cross-linked branched molecules of DNA. The extracted DNA is digested with the restriction enzymes flanking region of our interest. This way we get the fragments of genomic DNA containing our region of interest as smear of a particular size plus replicated DNA of this region (which is up to two-fold larger than the expected size). The digested genomic DNA is then run on first-dimension gel where it is separated based on its size. The low percentage first dimension gel is run at low voltage in an EtBr free gel to separate the DNA solely on the size. Then we separate each sample lane containing the smear of region of our interest from this gel and run it in the second-dimension gel. The second-dimension gel is optimized to separate the DNA fragments based on their shape. The gel used is of higher agarose percentage, run at higher voltage with EtBr (in both gel and running buffer). After run, we follow it with southern blotting to visualize the separated replication/recombination structures.

The migration of DNA fragments of various sizes and shapes is depicted below:

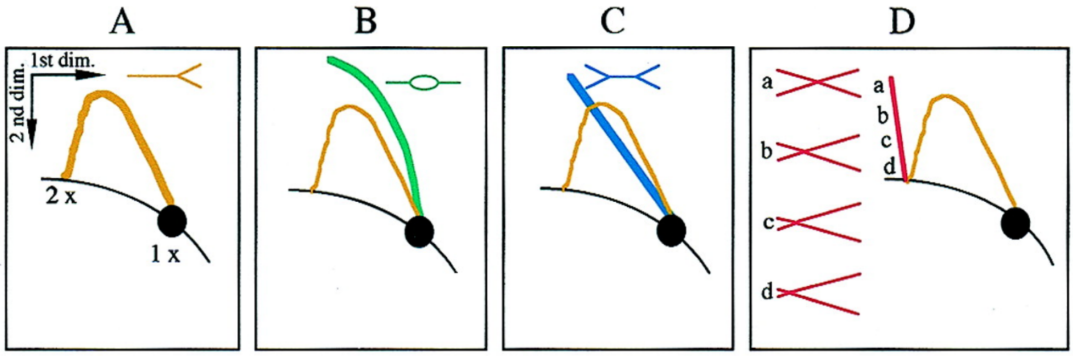

Fig 2.2 depicts the patterns of migration for various replication and recombination intermediates. Adapted from (Lucas and Hyrien, 2000).

Based on the region under observation, we see slightly different pattern of 2D gels. Here, we mainly focused on two types of regions, the early replication origins where we observe replication bubble, single replication fork forming a Y shape along with recombination intermediates that formed X shape due to the link between two DNA strands (X-molecules) forming commonly following 2D pattern:

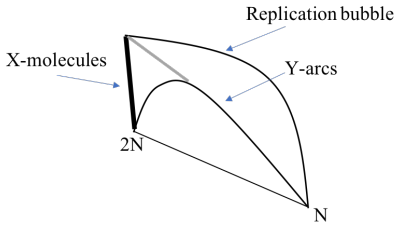

Fig 2.3 depicts the patterns of migration for various replication and recombination intermediates at an early origin of replication.

We also observed termination regions (TERs) where two replication forks approach, giving us replications forks in Y form or double Y or more variable termination signal and recombination intermediates (X-molecules). These regions commonly form the following 2D pattern:

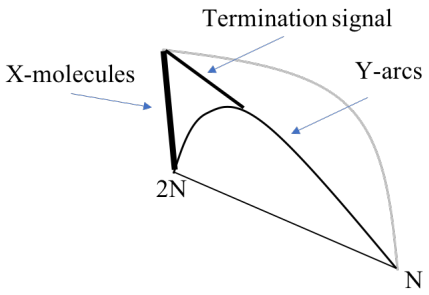

Fig2.4 depicts the patterns of migration for various replication and recombination intermediates at a termination site (define by (Fachinetti et al., 2010)).

The protocol for 2D is previously describes in (Branzei et al., 2006), (Liberi et al., 2005a), (Lopes et al., 2003).

Material:

Sodium Azide 10%

Spheroplasting buffer: 1M sorbitol, 100mM EDTA pH 8.0, 0.1% β-mercapto ethanol, 100U zymoliase/ml (made the same day) Zymolase (from Biolab) was kept in liquid at –20°C and defrosted prior to use.

Table 2.4: Composition of spheroblasting buffer

	for 30 mL	for 45 mL	for 60 mL
1M Sorbitol	15 mL	22,5 mL	30 mL
100 mM EDTA	6 mL	9 mL	12 mL
Zymoliase	3mL	4,5 mL	6 mL
H_20	6 mL	9 mL	12 mL
β-mercapto EtOH	30 µL	45 µL	60 µL

Solution I: 2% w/v CTAB (cetyl-trimethyl-ammonium-bromide), 1.4M NaCl, 100mM Tris HCl pH 7.6, 25mM EDTA PH 8.0 (freshly filtered)

RNase A (10mg/ml) treated according to Maniatis.

Proteinase K (20mg/ml)

Chloroform/isoamylalcohol 24:1

Corex glass tubes

Solution II: 1% CTAB, 50mM Tris HCl pH 7.6, 10mM EDTA (filtered before use)

Solution III: 1.4M NaCl, 10mM Tris HCl pH 7.6, 1mM EDTA

Isopropanol

70% EtOH

10mM Tris HCl pH 8.0

Psoralen solution: 0.2 mg/ml Trioxalen (Sigma) in 100% Ethanol, kept in the dark. Dissolved by stirring overnight at 4°C. Stored at -20°C.

6 well plates (FALCON)

UV stratalinker (Stratagene), 365 nm and 265 nm UV bulbs

CTAB DNA extraction:

1. Around 2-4*10^9 cells (200ml of 1-2*10^7) were collected for each sample. We added 1/100 volume of Sodium Azide 10% and cooled down the cells immediately on ice.

The cells were then centrifuged at 5000 rpm for 5 min at 4ºC, washed in 20ml cold ddH_20, transferred and re-centrifuged in a 50ml Falcon tubes.

2. For Psoralen crosslinking, the cells were suspended in 5 ml cold ddH_2O and then transferred in the wells of a 6-well plate (a strain/time point-1 well). To each well we added 300 µl of tri-methylpsoralen solution (0.2 mg/ml in EtOH 100%; stored at -20ºC, mix at 4ºC before use).
3. Psoralen was mixed with 5ml pipette making sure no cells were stuck to the bottom or sides of the 6 well plate.
4. Cells were then covered with aluminium foil and incubated for 5' on ice before transferring under the UV lamp, and irradiating for 10'. After the UV exposure, we added again 300 µl psoralen and repeated the 5' incubation on ice, in the dark, and then 10' irradiation. This was repeated 2 more times to perform 4 rounds of psoralen crosslinking in total.
5. After finishing the psoralen crosslinking, we transferred the cells to Falcon tubes and washed each well with 5ml cold MilliQ, and transferred that cell suspension to the Falcon tubes. The cells were centrifuged at 5000rpm for 5 min at 4ºC and kept the pellet on ice.
6. For spheroblast preparation, we resuspended the cell pellet by vortexing in 5ml spheroplasting buffer and incubated the cells at 30ºC for 45'-60'. The tubes were inverted several times during incubation. Once the speroblasts were ready, they were centrifuged at 4000rpm for 10' at RT.
7. We then removed the spheroblasting buffer and washed cells with 10ml ddH_20 without disturbing the pellet at RT. Then the pellet was resuspended in 2ml ddH_20 and resuspended by vortexing.
8. To this tube, we added 2.5ml *Solution I* and 200µl RNase (10mg/ml). Incubated 15'-30' at 50ºC.
9. After RNase treatment, we added 200µl ProteinaseK (20mg/ml) and incubated for 1.5hrs at 50ºC. The tubes were inverted several times during incubation. We then added 100µl *Proteinase K* and incubated overnight at 30ºC.
10. The samples were centrifuged for 10' at 4300 rpm: both the pellet and the Supernatant were processed separately. The pellet was kept aside for further extraction (step 15).
11. The supernatant was transferred carefully in a 15ml Falcon tube containing 2.5ml of Chloroform/isoamylalcohol 24:1 at RT, mixed several times and centrifuged at 4300rpm for 5' at RT.

12. The clear upper phase containing the DNA was carefully transferred to a 30ml Corex glass tube. A white protein layer was formed between the two phases, which was carefully avoided while transfer.
13. To the corex tube we added 10ml (2 volumes) of Solution II, covered with parafilm and inverted several times to mix.
14. The corex tube was centrifuged at 8500rpm for 10' at RT in a swing out rotor and discarded the supernatant. To this we added 2.5ml Solution III and waited until processing of pellet.
15. Meanwhile, the pellet of step 10 was resuspended in 2ml Solution III, mixed vigorously and incubated at 50ºC for 30'-60'. We waited until the solution was homogeneous.
16. The solution was transferred carefully into a 15ml Falcon tube containing 1ml of Chloroform/isoamylalcohol 24:1 at RT, mixed vigorously and centrifuged at 4300rpm for 10' at RT. The clear upper phase containing the DNA was carefully transferred to the Corex glass tube from step 14.
17. The tubes were centrifuged at 8500 rpm for 10' at RT in a swing out rotor and discarded the supernatant. We precipitated the DNA by adding 1 volume of isopropanol (RT), gently mixed the sample to ensure proper DNA precipitation. Centrifuged the DNA at 8500rpm for 10' at RT in a swing out rotor.
18. We discarded the supernatant and briefly washed the pellet with 1ml 70% EtOH (RT). Centrifuged at 8500 rpm for 1', removed as much ethanol as possible using a pipette, dried for approx. 2', and dissolved the pellet in 250 µl 10mM Tris HCl pH 8.0.
19. After mixing the samples for 60' we collected samples with quick spin and transferred DNA in an Eppendorf tube with cut tip.
20. The quality of DNA was checked by nanodrop and running an agarose gel. The DNA was ready for gel electrophoresis.

Digestion of DNA

1. We digested 10µg of DNA in 150µl reaction volume, added from 15µl 10X BSA to a final concentration of 1X, to this we added 6µl, incubated for 30' and then added 5µl more. Mixed carefully with a yellow tip.
2. The samples were digested for 5hrs to overnight at 37ºC.
3. After digestion, we added 1/8V (19µl) KAc 2.5M pH=6 (autoclave) and 1V (169µl) of Isopropanol and inverted the tubes. The DNA was precipitated by centrifugation at 14000rpm for 10' at RT. Washed once with 0.5ml 75% ethanol and resuspended in 20µl TE 1X autoclaved.

4. The samples are left to resuspend from 1hr to overnight at RT.

Electrophoresis:

First Dimension:

1. 0.35% agarose gel was prepared with low melting agarose in 300ml 1X TBE. The gel was poured at 4ºC and was allowed to solidify.
2. After the gel was solidified, it was placed in the running tank, with 1X TBE.
3. To 20µl digested DNA dissolved in 1X TE, 5µl loading dye 20X was added. The samples were loaded in the alternate wells.
4. Gel was run at 50V at RT for about 18-20hrs.

Second Dimension:

1. After the run of first dimension gel, the gel is soaked in 1L 1X TBE + 30µl EtBr 10mg/ml in a tray, for about 30'. After the staining, the gel was cut to get DNA fragments of 3.5kb to 12kb in a 9.5cm gel slice. Then the lanes are cut separately to get each sample in one slice of gel.

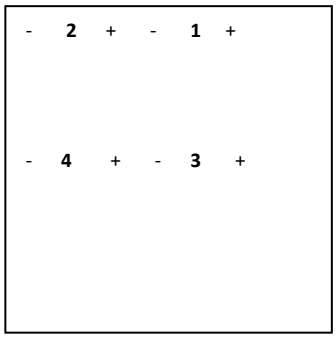

2. The slices are arranged as in drawing, + indicates the higher MW.
3. After arranging thr slices, we poured the second gel: 0.9% in 500 mL 1X TBE with 4.5g of agarose and EtBr 15µl, the gel was let to solidify at RT for about 30'.
4. We prepared 2L 1X TBE with 60µl EtBr and added to the gel running tank.
5. Once the was solidified, it was moved to the tank and run at 180V for 7hrs at 4ºC.
6. After running the upper 2 gels were separated from lower 2 gels leaving 1cm under the slices from first dimension (total about 10cm slices).
7. These gels were now ready for the southern blot.

Southern Blot:

1. The slices of gel were transferred into plastic trays and washed thrice as follows:
    - HCl 0,25N 1 x 15'
    - Denaturing solution 1 x 20'
    - Blot#2 1 x 20'
2. The genescreen membrane was equilibriated with 10X SSC buffer.

3. The southern blot was built with 3M papers, gel slices, genescreen membrane, 3M papers, paper towels and weight on the top to facilitate capillary action. 10X SSC buffer was used for overnight transfer.

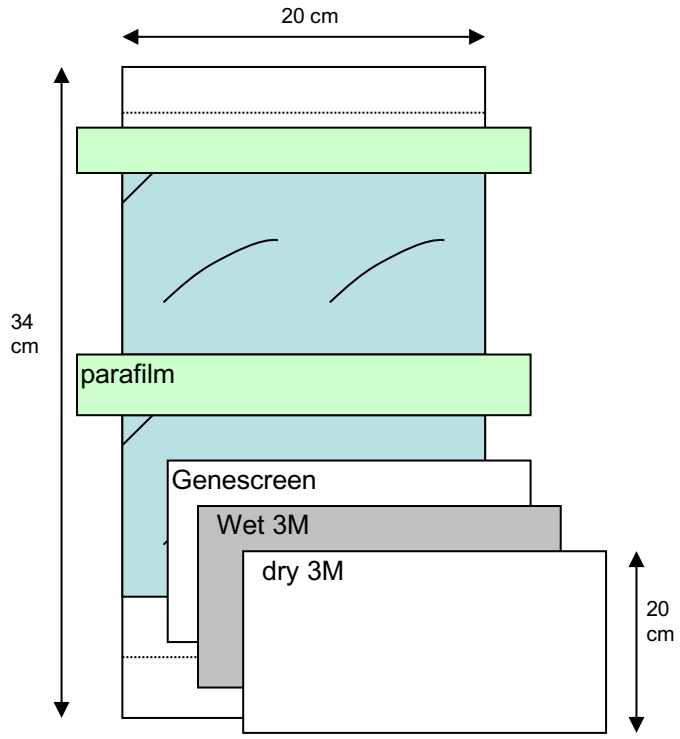

Fig 2.5: Setting of a southern blot

4. The membrane was dried for 30' RT after the transfer, then crosslinked with UV, using the program autocrosslinking of the Stratalinker once.
5. The filters can be stored at this stage before hybridization.

Hybridization of filters:

Table 2.5 Oligoes for amplification of 2D gel electrophoresis probes:

Oligo	purpose	Sequence
TER302Fw	amplification of termination probe (2D)	GAAGGTTCAACATCAATTGATTG ATTCTGCCGCCATGATC
TER302Rv	amplification of termination probe (2D)	GCTTCCCTAGAACCTTCTTATGTT TTACATGCGCTGGGTA
ARS305FW	amplification of ARS305 probe	GTTCCGAAACAGGACACTTAGC
ARS305RV	amplification of ARS305 probe	ATCCAGGAGGGACTCAATGTAG

1. Hybridization of filters were done in glass tubes in the hybridization oven. The tubes and Perfecthyb plus solution (Sigma) were prewarmed at 65ºC.
2. The filters were washed once with 10X SSC and then placed in the tubes and mixed with 30ml Perfecthyb plus solution (Sigma) and warmed for about 1hr.
3. Radioactive probe was prepared as follows:
    a. 50 ng of DNA
    b. 30.4 ml H_20

    Boiled for 10' and kept on ice immediately
    c. 10 µl Buffer
    d. 2 µl BSA
    e. 0.7 µl of dATP, dTTP, dGTP solutions
    f. 3-5 units of Klenow DNA polymerase
    g. 5µl α^{32}P dCTP 6000 Ci/mmole)
4. Radioactive probe was incubated at 65ºC for 1hr.
5. Labelled DNA was cleaned with G50 columns (1st centrifuged 3000 rpm 1', changed tube, added reaction, waited 1-2' and centrifuged again)
6. The labelling was checked with Geiger counter.
7. The labelled DNA was boiled for 10' and then placed on ice. In the tube containing filters, labelled probe and 200µl ssDNA were added. The filters were incubated at 65ºC on rotation overnight with probe.
8. The next day, the filters were washed with wash solution I and wash solutionII

Washing solution I (at 65°C)		Washing Solution II (at 42°C)	
SSC 2x	50ml SSC 20x	SSC 0,1x	5ml SSC 20x
SDS 1%	25ml SDS 20%	SDS 0,1%	5ml SDS 20%
	Final volume 500ml H_2O		Final volume 1000ml H_2O

9. Washes were conducted as follows:

1. 50ml *Wash Sol. I* at 65°C in tube	10' in at 65°C, rolling
2. 450ml *Wash Sol. I* at 65°C in plastic dish	15' with agitation at 65°C
3. 500ml *Wash Sol. II* at 42°C	15' with agitation at 42°C
4. 500ml *Wash Sol. II* a 42°C	15' with agitation at 42°C

10. After the washes, the filters were dried and put in the cassette in Saran wrap, exposed to a film or phosphoimmager. The filters were exposed overnight for origins of replication and 2-3 days for termination regions.

11. After sufficient incubation, the image was captured with Typhoon scanner (GE healthcare).

2.7 Suppressor Screen:

The natural suppressor screen was carried out for *smc6-56* cells which are temperature sensitive and are dead at 37°C (Onoda et al., 2004). We used this temperature sensitivity of *smc6* mutants to our advantage. We carried out a natural suppressor screen of *smc6-56* mutants.

2.7.1 Natural Suppressor screen

The *smc6-56* cells were grown overnight at 25°C and about 5 OD of log phase cells were pelleted and spread on a YPD agar plate. The plates were then incubated at 37°C for several days. The colonies that obtained after few days contained mutations that allowed *smc6-56* cells to grow at higher temperatures. We picked up 8 colonies randomly for further analysis. The cells were then back-crossed with *smc6-56* to identify monoallelic mutants among these. We found that 5 out of 8 suppressor colonies were monoallelic. These 5 were further characterized to identify the mutation responsible for suppression.

We sequenced Smc6 and other known suppressors of Smc6 sensitivities before proceeding with whole genome sequencing. We identified intragenic suppressor mutation in Smc6 sequence for all 5 suppressors. This mutation was further validated.

The suppressor screen is summarized in the figure below:

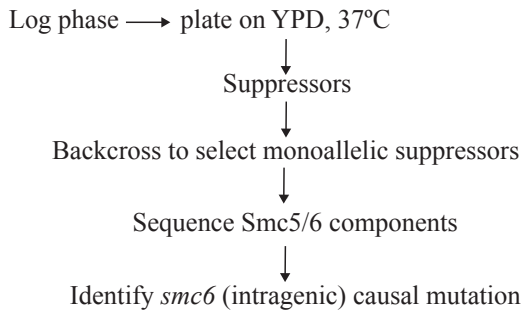

Fig2.6: Schematic representation of suppressor screen.

2.7.2 Validation of suppressor mutation

The suppressor mutation was validated by two methods:

First, we back-crossed the suppressor and checked for 2:2 segregation of its temperature and DNA damage sensitivity. This indicated the monoallelic nature of the suppressor mutation.

Second, we created a deletion of *SMC6* in WT diploid (*smc6*/*SMC6* background) and transformed de-novo created cassette containing *smc6-56* and suppressor mutation. The diploid transformants were selected for markers of *smc6-56-sup*, dissected to get haploid

smc6-56-sup (de-novo). The haploids were then sequenced to confirm the presence of *smc6-56* mutations and suppressor mutation. This de-novo suppressor was tested for temperature and DNA damage sensitivity to confirm that the rescue indeed happened because of the suppressor point mutation.

Smc5/6 and STR complexes colocalize genome-wide and at NPSs

Smc5/6 complex was shown to safeguard replication through NPSs (Menolfi et al., 2015). Smc5/6 complex does not possess a known catalytic activity (such as nuclease, helicase, topoisomerase) to act on the recombination intermediates forming at NPSs. We therefore hypothesized that Smc5/6 might functionally interact with resolvases, such as the STR complex, to finely regulate the balance between replication and recombination at NPSs, allowing successful replication of these regions and preventing genome instability. To understand the interplay between Smc5/6 and STR at NPSs, we examined the localization of STR components to NPSs and genetic interactions with known contributors of NPS integrity.

3.1 Smc5/6 and STR are linked to each other genetically and localize at NPSs

3.1.1 Mutants of Smc5/6 and STR complexes show synthetic lethality with *RRM3* deletion

To understand whether STR plays a role at NPSs, we checked genetic interactions with Rrm3 mutations. Rrm3 is a helicase that facilitates replication fork passage through NPSs and is implicated in replication through programmed replication blocks at rDNA region (Azvolinsky et al., 2009a; Ivessa et al., 2003; Mohanty et al., 2006). rDNA repeats are covering about 8-12% of yeast genome and are one of the major contributors of replication fork pausing and fragility. Saccharomyces Genome Database (SGD) reports several genetic interactions of *RRM3* (Fig3.1).

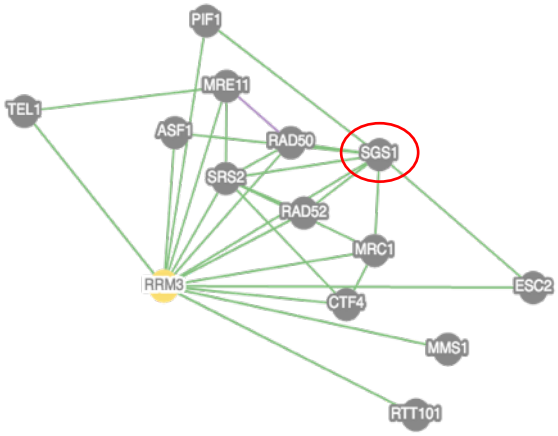

Fig3.1: Reported genetic interactions for *RRM3* (Saccharomyces Genome Database).

Of these, the synthetic lethality between *RRM3* and *SGS1* deletions, reported by several independent studies (Ooi et al., 2003; Schmidt and Kolodner, 2004; Tong et al., 2001; Torres et al., 2004), was of interest to us. We started off by reproducing the synthetic lethality

between *SGS1* and *RRM3* and also between *SMC6* and *RRM3* reported previously by our lab (Menolfi et al., 2015) (Fig3.2).

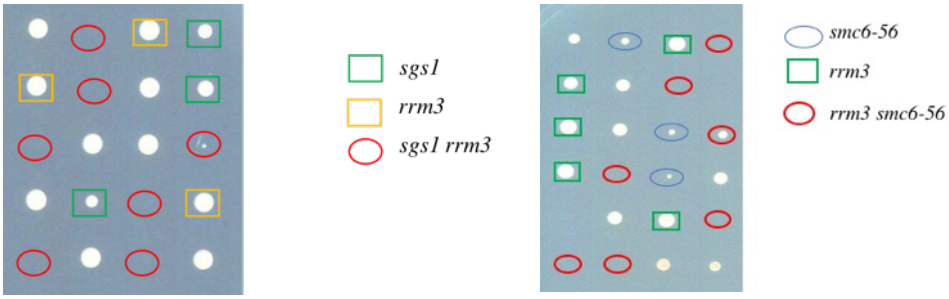

Fig3.2: Synthetic lethality between *sgs1/smc6-56* and *rrm3* observed by tetrad analysis.

We reproduced those results. The *sgs1 rrm3* lethality could be caused by defects in NPS replication. Our lab has previously reported that Smc5/6 mutations (*S-smc6* allele) shows synthetic lethality with *RRM3* deletion, which is rescued by *FOB1*, *TOF1*, and *CSM3* deletions that facilitate pausing at programmed replication barriers (Menolfi et al., 2015). The synthetic lethality between *SMC5/6* and *RRM3* deletions could thus arise because of problems in rDNA replication including extensive pausing and breaks (Torres-Rosell et al., 2007a). Consistent with our previous results, we also observed synthetic lethality between *smc6-56* (point mutant of Smc6) and *rrm3Δ* (Fig3.2).

We thus asked if STR lethality with *RRM3* deletion was similarly rescued by removing factors of programmed replication block at rDNA (Fig3.3).

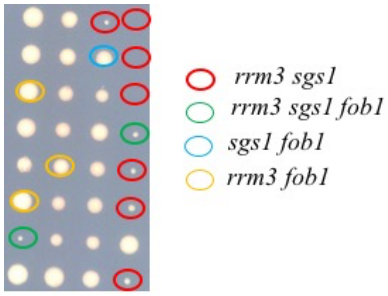

Fig3.3: Synthetic lethality/sickness between *sgs1* and *rrm3* was not rescued by *fob1* as observed by tetrad analysis.

We observed no rescue of *sgs1Δ rrm3Δ* synthetic lethality by *fob1Δ*. Deletion of *TOF1* and *CSM3* are synthetic lethal with *sgs1Δ* therefore we did not test the corresponding triple mutants. We concluded that the synthetic interactions between *RRM3* and *SGS1* did not solely depend on rDNA. The synthetic lethality was dependent on Rad51 and it was previously reported that deleting *RAD51* can rescue *sgs1Δ rrm3Δ* synthetic interaction (Torres et al., 2004). Unlike Smc5/6, synthetic lethality between *SGS1* and *RRM3* was mainly due to Rad51-dependent recombination and not primarily due to rDNA defects.

3.1.2 Mutants of Smc5/6 and STR complexes show synthetic lethality

Similar to what we observed with *RRM3* deletion, we also observed synthetic lethality between mutants of Smc5/6 and STR. This was already reported by our lab using cell cycle restricted alleles in previous studies (Menolfi et al., 2015).

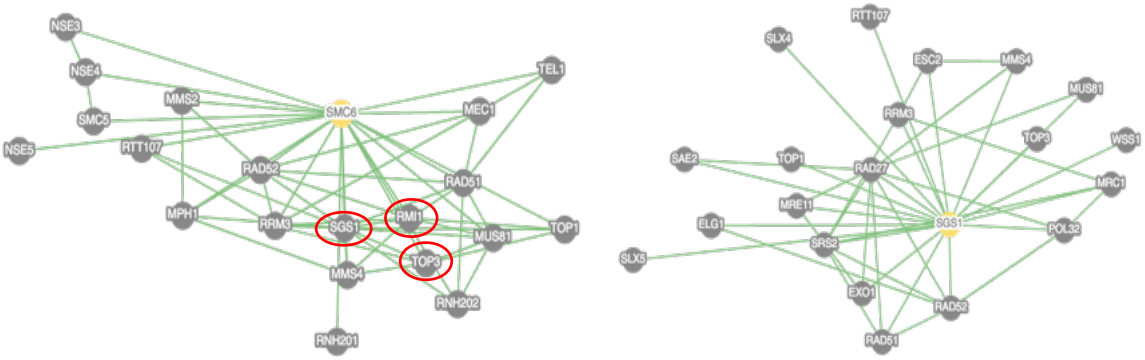

Fig3.4: Reported interactions for *SMC6* and *SGS1* on SGD.

We first checked SGD for reported genetic interactions of *SGS1* and *SMC6*. We found the reported interactions only one way, likely due to the essential nature of SMC5/6 complex components (Fig3.4). We then checked the genetic interactions between several mutants and cell cycle restricted alleles of Smc5/6 and *SGS1* deletion.

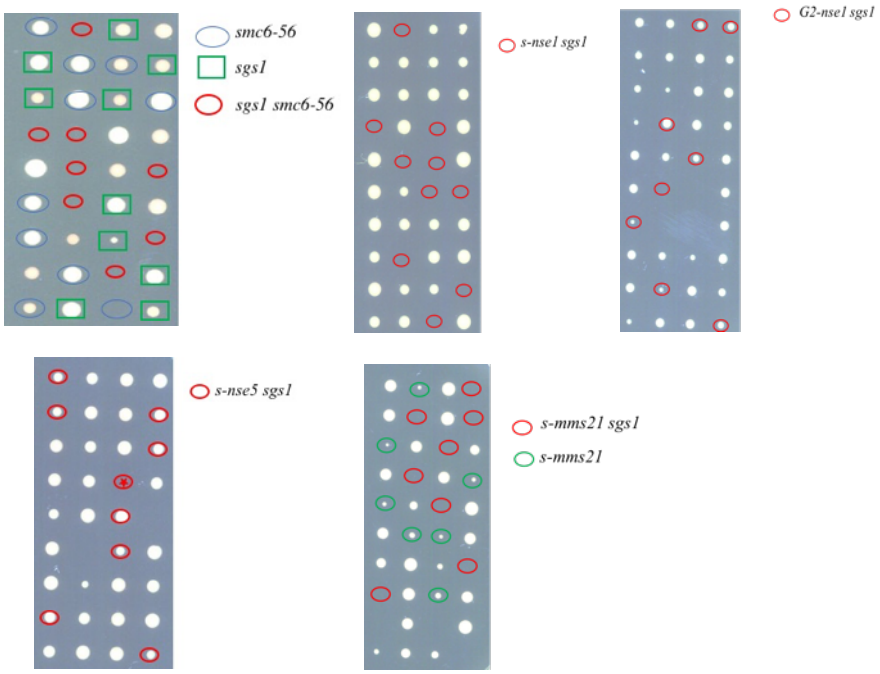

Fig3.5: Genetic interactions between Smc5/6 variants and *SGS1* observed by tetrad analysis.

We observed synthetic lethality for mutants of Smc6 (*smc6-56*), most of the S-phase restricted alleles (except *S-nse5*) but not for G2-phase restricted alleles.

In 2016 it was reported by two independent studies that Smc5/6 SUMOylates components of the STR complex upon DNA damage and regulates the function of STR (Bermúdez-López et al., 2016; Bonner et al., 2016) as previously suggested (Branzei et al., 2006). We examined whether the observed genetic interaction could be due to defects in modification of the STR complex. We therefore checked the genetic interaction between *mms21-CH* (point mutants of *MMS21* which lacks the SUMO ligase activity (Takahashi et al., 2008)) and *sgs1*, and also between *smc6-56* and *sgs1-KR* (point mutant of *SGS1* with defective SUMOylation but intact Smc5/6 interaction through SIM domains, (Bermúdez-López et al., 2016)). We observed the double mutants were not lethal, although we found mild slow-growth between *mms21-CH* and *SGS1* deletion (Fig3.6).

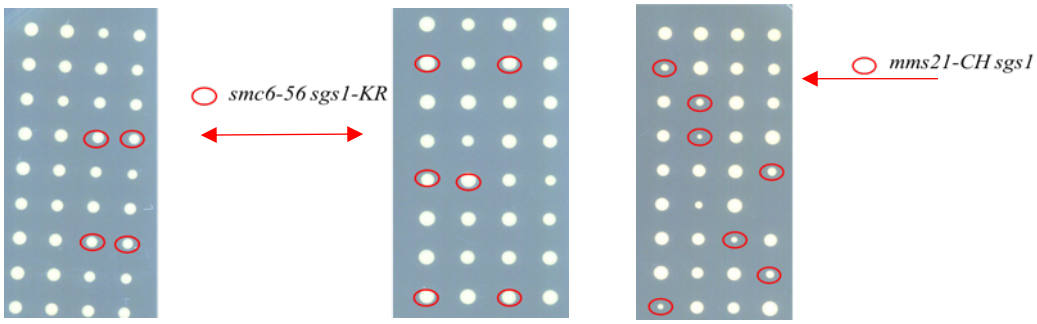

Fig3.6: Genetic interactions between *SMC5/6* and *SGS1* mutants observed by tetrad analysis.

We conclude that since the physical interaction between Smc5/6 and STR complexes was prominent only upon treatment with DNA damage and it was too weak to be observed in unperturbed cell cycle (Bermúdez-López et al., 2016; Bonner et al., 2016), the potential regulatory roles of STR SUMOylation are not essential for replication and recombination regulation through NPSs.

3.1.3 Smc5/6, STR and Rrm3 colocalize genome-wide and are present at NPSs

After examining the genetic interactions between protein complexes of our interest, we proceeded to check their localization on chromatin. We checked the genome-wide localization of endogenous Smc6 (tagged C-terminally with the 3Flag tag), Top3 and Rmi1 (tagged C-terminally with the 10Flag tag) in unperturbed G2/M phase (when NPSs are replicated) and compared their clusters with the ChIP-on-chip profile of Rrm3-3Flag. ChIP-on-chip is a non-quantitative method to analyse the genome-wide binding pattern of the protein of interest. This method does not tell us any information about the amount of protein at different loci.

We also conducted statistical analysis to calculate the overlap between each profile and NPSs such as TERs, tRNA and CENs (Fig3.7). The ChIP of Sgs1 with different tags and in

different crosslink conditions did not work well, potentially because the interaction between protein and chromatin is weak and transient.

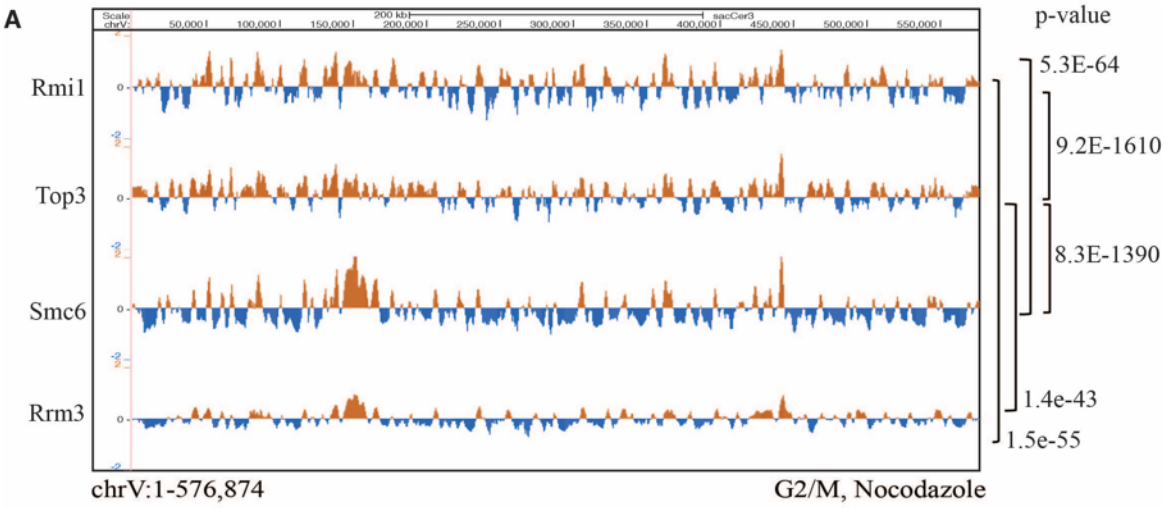

B

tRNAs

Protein	Increase	p-value
Smc6	3.03	3.6E-1010
Top3	2.15	1.9E-53
Rmi1	2.49	1.6E-69
Rrm3	2.77	2.6E-57

CENs

Protein	overlap with CENs	Increase	p-value
Smc6	16 (100%)	4.07	1.4E-12
Top3	16 (100%)	2.60	6.6E-08
Rmi1	16 (100%)	3.09	2.9E-09
Rrm3	16 (100%)	4.19	7.3E-13

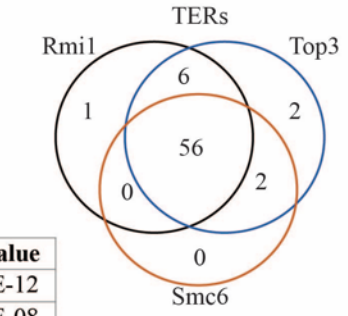

Fig3.7: Genome-wide colocalization of Smc5/6, STR and Rrm3: A) ChIP-on-chip profiles of Smc6, Top3, Rmi1 and Rrm3 indicate a statistically significant overlap between the genome-wide protein profiles in unperturbed G2/M phase. ChrV shown here as a representative image. B) The statistical analysis indicated overlap between Smc6, Top3, Rmi1 and Rrm3 profiles and tRNA and CENs. C) Manual analysis indicates overlap between TERs and Smc6, Top3, Rmi1 and Rrm3 profiles.

We first observed that each of Smc6, Top3 and Rmi1 profiles overlap with the profile of Rrm3 with statistical significance ($p<0.001$). Furthermore, the peaks of Smc6, Top3 and Rmi1 overlapped with each other with statistical significance. This indicated that both STR and Smc5/6 complexes were present at many genomic loci together. We further carried out statistical analysis to measure the overlap between tRNA genes and centromeres (CENs). We observed that both STR and Smc5/6 complexes, as well as Rrm3, showed significant fold increase with tRNA and CENs (subgroups of NPSs). This fold increase was compared to a value generated by expected random overlap between the sets of peaks. The statistical comparison between this overlap gave us a significant p-value for each protein profile

compared to both tRNA and CENs. We manually compared the peaks of each profile and TERs described by (Fachinetti et al., 2010). We observed that 56 out of 71 TERs (79% TERs) were occupied with all three proteins, while some TERs were occupied only by Top3 or Rmi1. This showed that similar to other subgroups of NPSs, the majority of TERs were bound by Smc5/6 and STR complexes. We conclude from ChIP-on-chip profiles that Smc5/6 and STR complexes co-localize with each other and with Rrm3, and are present at different types of NPSs.

3.1.4 Quantification of Smc5/6 and STR at NPSs

In order to validate the ChIP-on-chip profiles and to have a quantitative estimation of Smc5/6 and STR enrichments at NPSs, we carried out ChIP-qPCR experiments at three TERs (TER302, TER603 and TER1004) with cells having untagged or Flag-tagged Smc5/6 and STR in unperturbed G2/M phase. We conducted three independent biological replicates, plotted the average and standard error of the biological replicates.

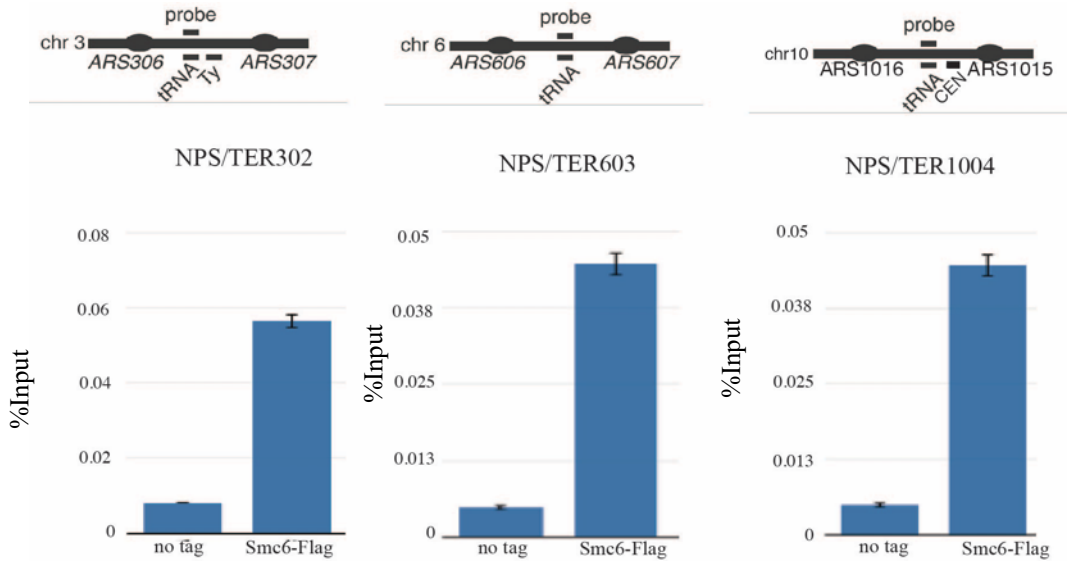

Fig 3.8: Quantification of Smc6 at NPSs in unperturbed G2/M-synchronized cells (N=3)

We observe that Smc6-Flag is enriched at all three NPSs (TERs) on chromosome 3, 6 and 10, quantified by ChIP-qPCR in unperturbed G2/M phase of cell cycle compared to the no tag control. We thus validated the ChIP-on-chip profiles and quantified the enrichment as percentage of input protein present on the chromatin at that locus (i.e. normalized with input values and converted to percentage).

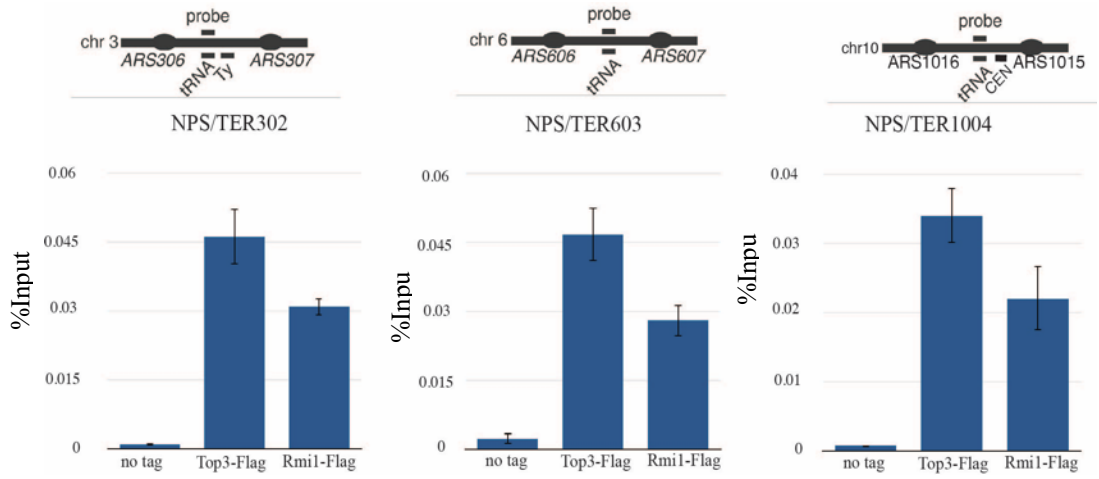

Fig3.9: Quantification of Top3 and Rmi1 at NPSs in unperturbed G2/M-synchronized cells (N=3)

We observe that similar to Smc6-Flag, Top3-Flag and Rmi1-Flag are also enriched at NPSs (TERs) on chromosome 3, 6 and 10, quantified by ChIP-qPCR in unperturbed G2/M phase of cell cycle compared to the no tag control. We thus validated the ChIP-on-chip profiles and quantified the enrichment as percentage of input protein present on the chromatin at that locus. We thus conclude that both Smc5/6 and STR complexes are present at NPSs in G2/M phase when these regions are being replicated or after their replication is complete. In order to understand the roles of STR and Smc5/6 at NPSs we decided to use mutants and depletion strains and investigate specific effects on NPSs.

3.1.5 Mutants of *SMC6* are defective in binding to NPSs

We started by checking point mutants of Smc6 available in the lab. The *smc6-56* mutant carries three mutations in the coiled-coil domain, while *smc6-P4* carries a single mutation close to ATpase domain (fig3.10).

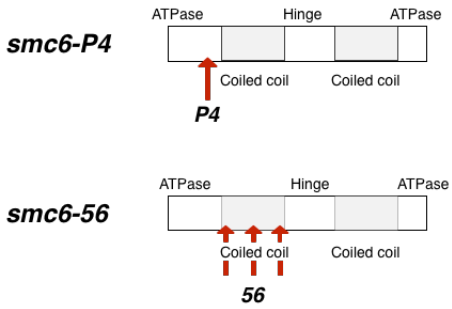

Fig3.10: Schematic representation of mutations of *smc6-P4* and *smc6-56*

These mutants are previously characterized by (Onoda et al., 2004; Peng and Feng, 2016) for temperature sensitivity (*smc6-56* only) and DNA damage sensitivity. In (Menolfi et al., 2015), our lab showed that these mutants accumulate recombination intermediates at NPSs

(TERs). We therefore wanted to see whether the mutant proteins showed any phenotype for NPS binding.

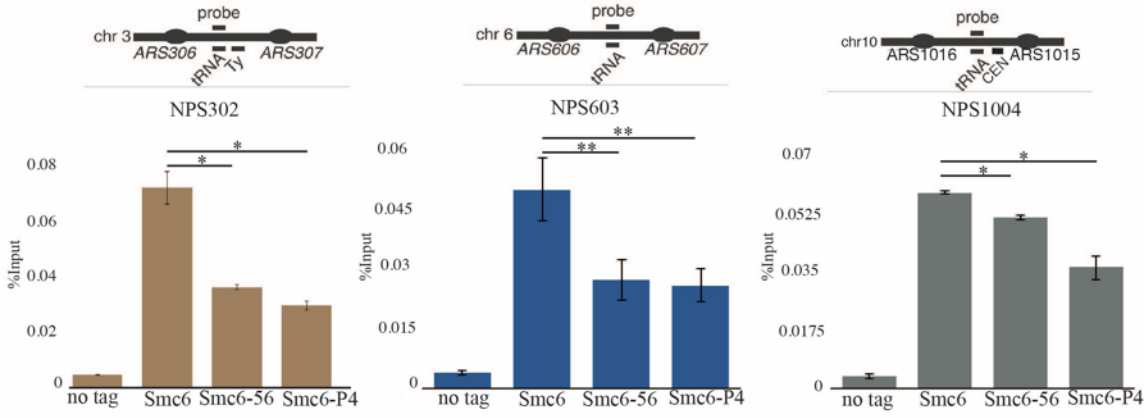

Fig3.11: Quantification of Smc6 and its variants at NPSs in unperturbed G2/M-synchronized cells (N=3)

We observed that compared to WT Smc6, the mutants were defective in binding or enrichment at NPSs. The amount of protein accumulated at all the NPSs we checked (TER302, TER603, TER1004) was significantly less that the WT Smc6 (Fig3.11). We therefore concluded that the recombination defect observed at NPSs is associated with reduced retainment of Smc5/6 at NPSs in these mutants. We observe different phenomena by ChIP-qPCR and ChIP-on-chip methods. Here we observe the amount of Smc6 and its variants at genomic regions of our interests (TERs here) while in ChIP-on-chip we get a genome-wide picture of protein binding profiles.

3.1.6 Smc6-56 variant is defective in binding to stalled forks

It is already reported that Smc5/6 complex is recruited to stalled replication forks (RFs) and regulates their maintenance (Bustard et al., 2012). We wanted to confirm this by ChIP-qPCR and observe the effect of mutations on recruitment of the complex to stalled forks. For this, we arrested cells in G1 with α factor, released them in high HU concentration (200 mM) to stall replication and checked by qPCR the recruitment of Smc6 and its variants to early replication origins (ARS305, ARS1) where fork stalling is expected to occur.

We observed that, as previously reported, Smc6-myc was recruited to stalled RFs upon HU treatment at early origins. We also observed that Smc6-56-myc but not Smc6-P4-myc was recruited with less efficiency to the stalled forks. We conclude that Smc5/6 is enriched at stalled RFs. However, *smc6-56*, a variant of Smc6 fails to bind efficiently to stalled RFs (Fig3.12).

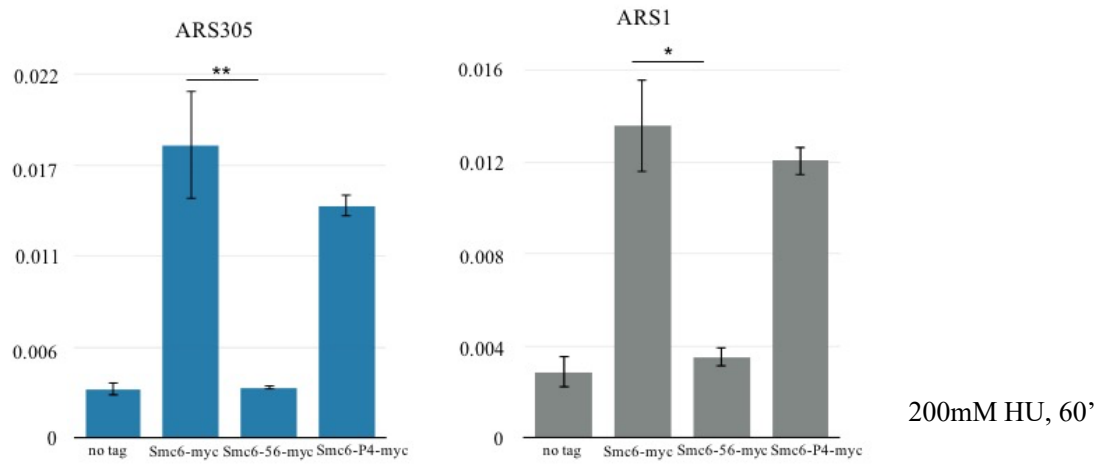

Fig3.12: Enrichment of Smc6 and its variants at stalled forks upon HU treatment (200mM HU, N=3)

3.2 Mutation in the Smc5/6 complex reduces the amount of Top3 (but not Rmi1) at NPSs, but not vice-versa

3.2.1 The genome-wide localization of Top3 is not affected by dysfunction/depletion of Smc5/6

After we observed that Smc6 point mutants were defective in localization to NPSs, we checked whether these mutants had any impact on the recruitment of the STR complex to NPSs. We examined the genome-wide localization of Top3 in *smc6* mutants, cell cycle restricted variants and upon Smc6 depletion. We used the *S-smc6* background where the promoter of *SMC6* was changed to *pCLB6* in order to largely restrict the expression of *SMC6* in the S-phase of cell cycle (Menolfi et al., 2015). As previously reported, there is leaky expression and retention of protein in G2/M, making it an imperfect depletion system (Fig3.13). We also used Smc6-AID where Smc6 is tagged with Auxin inducible degron (AID) tag. Upon auxin addition, Smc6 protein is degraded by the proteasome (Fig3.13). Along with depletion strains, we also used a point mutant of Smc6, *smc6-P4*, with a single mutation close to the ATPase domain. Smc6-P4 is a mutant protein expressed at normal expression levels (Fig3.10).

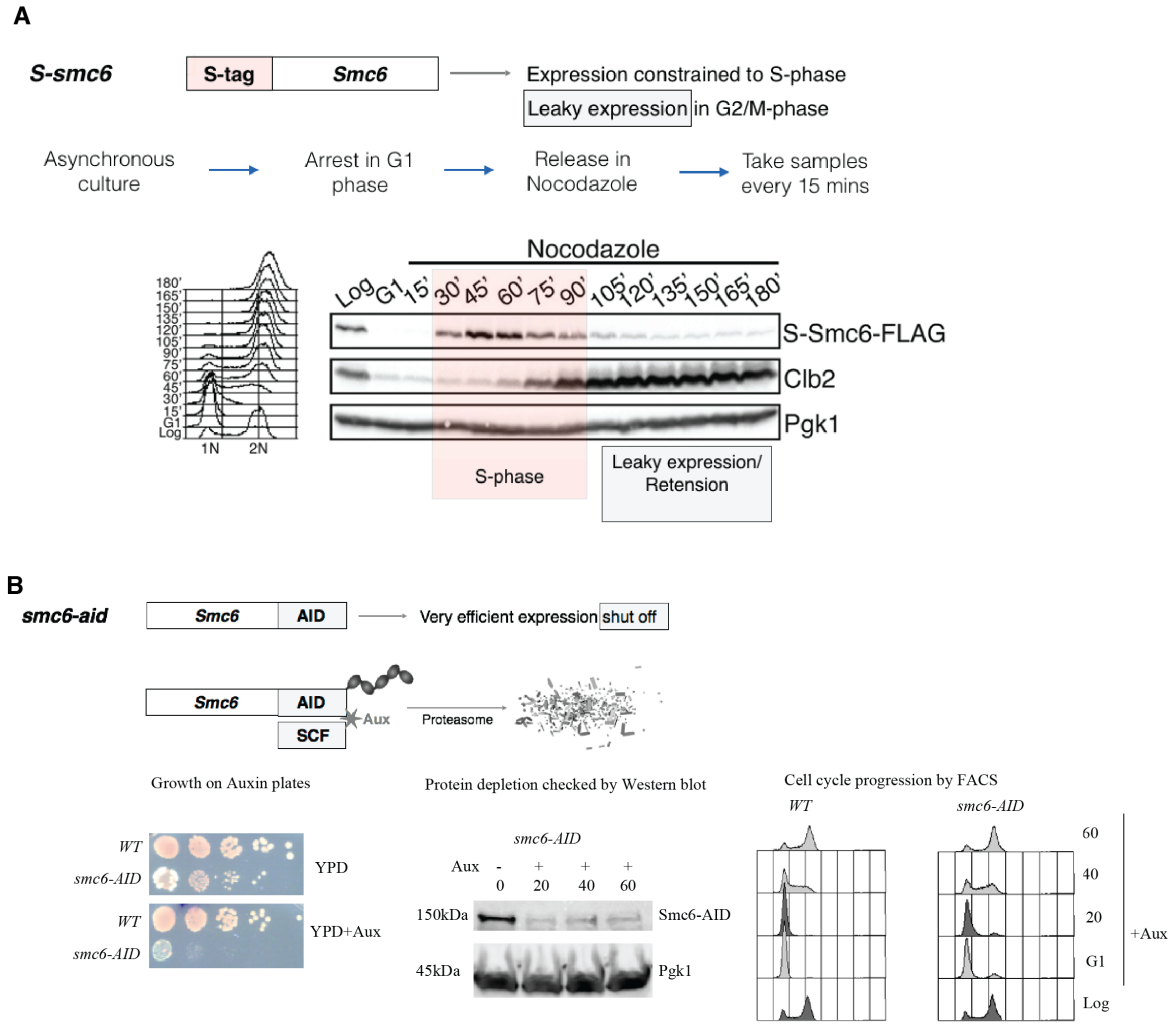

Fig3.13: Schematic representation of various alleles of *SMC6*. A) Schematic of *S-smc6* expression and degradation. Incomplete protein degradation of S-Smc6 observed by western blot. B) Schematic of *smc6-aid* depletion. Depletion of Smc6-AID upon auxin addition checked by grown on auxin plate and western blot. The effect of Smc6-AID depletion upon cell cycle progression checked by FACS analysis

In each of these backgrounds, we tagged Top3 with a Flag tag and conducted ChIP-on-chip analysis in cells arrested in G2/M with nocodazole. We observed statistically significant overlap between Top3 profiles in *smc6* mutants and WT. Thus, upon depletion of Smc6 after G1 arrest or restricting Smc6 expression to S phase, Top3 recruitment genome-wide remained intact. Even in the *smc6-P4* background where Smc6 localization to NPSs was defective, we observed no alteration in Top3 recruitment genome-wide. This indicated no significant role for Smc5/6 in the genome-wide recruitment of the STR complex in G2/M (Fig3.14). This also suggests that STR localizes to NPSs independently from Smc5/6.

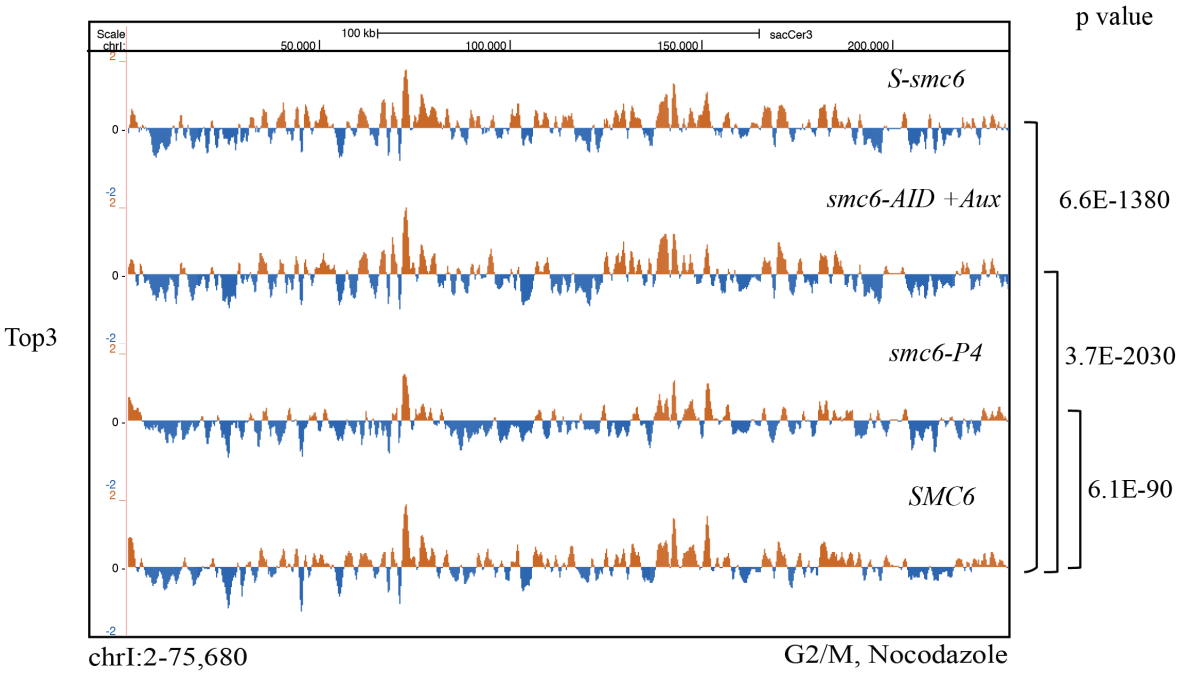

Fig3.14: Genome-wide localization of Top3 in G2/M-synchronized WT and *smc6* cells. ChIP-on-chip profiles of Top3-Flag from G2/M-synchronized WT as well as *smc6* mutant cells. ChrI is shown here as an example. The indicated p-values relate to the genome-wide overlap between the considered ChIP-on-chip protein clusters

3.2.2 The enrichment of Top3 (but not Rmi1) at NPSs is reduced upon Smc5/6 dysfunction, independently from SUMO ligase activity of the function

When we observed no genome-wide changes in the profiles of Top3 upon Smc6 mutation/depletion, we decided to look at NPSs specifically and evaluate further the amount of Top3 at NPSs (TERs in particular).

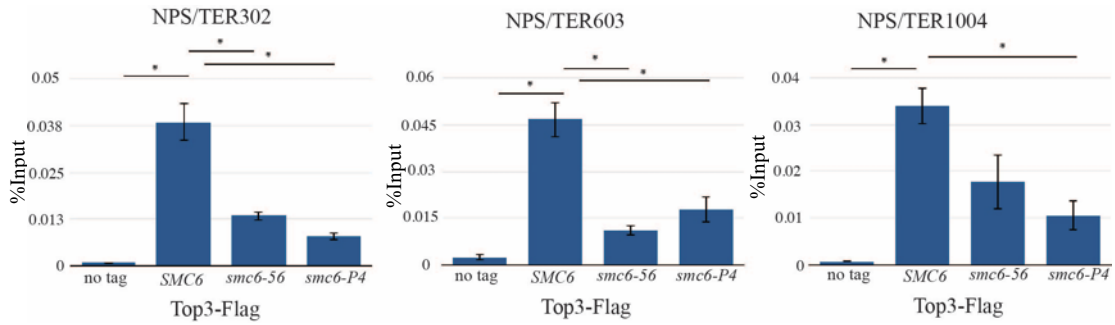

Fig3.15: Quantification of Top3 at NPSs in *SMC6* WT and *smc6* mutants. ChIP-qPCR analysis to quantify the Top3-Flag bound to NPSs in unperturbed G2/M cells (N=3)

We carried out a ChIP-qPCR experiment with the Top3-Flag in *SMC6* WT and *smc6* mutant backgrounds in G2/M arrested cells and at permissive temperature for *smc6-56*. We observe that the amount of Top3 bound to several NPSs (TER302, TER603 and TER1004 on

chromosome 3, 6 and 10 respectively) was significantly reduced ($p<0.05$) upon *smc5/6* dysfunction (Fig3.15). The ChIP-qPCR values were obtained from three biological replicates and were compared by students' unpaired t-test. This indicated that enrichment/retention of Top3 at NPSs was dependent on functional Smc5/6 complex.

Our results from genome-wide and locus specific techniques indicate that Top3 binding genome-wide is not perturbed by *SMC6* mutations, while the amount of Top3 at various loci of our interest is perturbed. The two techniques (ChIP-on-chip and ChIP-qPCR) observe different properties of tagged protein (Top3-Flag in this case). On one hand, ChIP-on-chip observes genome-wide binding of protein while ChIP-qPCR observes amount of the protein at a particular region chosen by set of primers for the qPCR (different TERs as shown in the graph). Contrasting results between the two techniques suggest a role for Smc5/6 in regulating amount of Top3 at NPSs but not its ability to bind to these regions and be recruited genome-wide.

We next wanted to examine whether we could generalize this for the STR complex. We therefore repeated similar experiment with Rmi1-Flag.

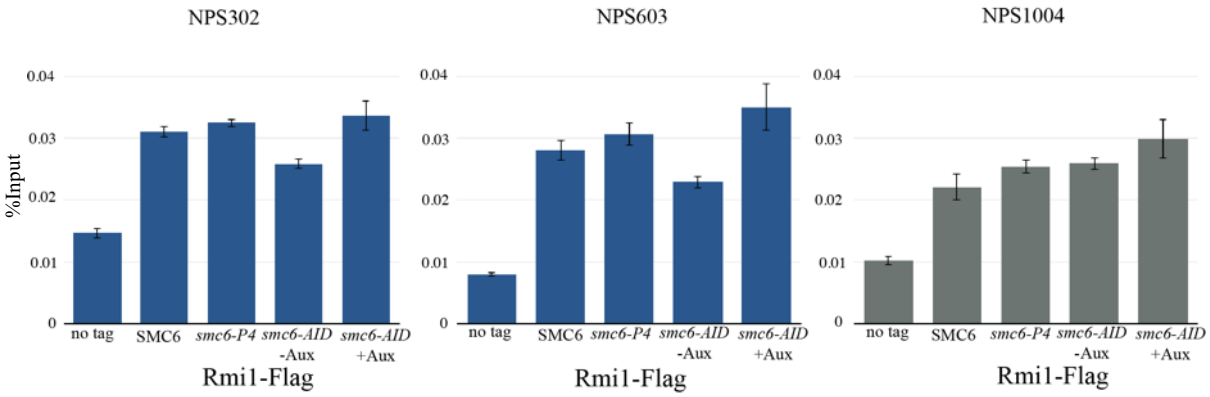

Fig3.16: Quantification of Rmi1 at NPSs in *SMC6* vs *smc6* mutants/depletion. ChIP-qPCR analysis to quantify the Rmi1-Flag bound to NPSs in unperturbed G2/M cells (N=3)

To our surprise, we observed that the binding of Rmi1 to NPSs was unaltered by *SMC6* mutation *smc6-P4* or Smc6 depletion. This could be due to the fact that Rmi1 possess a DNA binding domain, and therefore could bind and be retained to chromatin irrespective of the Smc5/6 complex. However, at this stage we cannot rule out that *smc6-P4* and the depletion were not penetrant enough to observe the defect on Rmi1.

We therefore conclude that the enrichment/retainment of Top3 to NPSs is dependent on the Smc5/6 function, but its recruitment genome-wide is not.

To understand the role of Smc5/6 in the retention of Top3 at NPSs, we decided to use a mutant of Smc5/6 defective in SUMO ligase activity (*mms21-CH*, with point mutation in SUMO ligase) and a mutant of Sgs1 with a defective SUMOylation (*sgs1-K621R*, mutated

Lysin to abolish SUMOylation). As previous studies indicated DNA damage dependent SUMOylation of STR by Smc5/6 leading to its recruitment and activity at damaged DNA substrate (Bermúdez-López et al., 2016; Bonner et al., 2016), we checked the effect of perturbed SUMOylation of Sgs1 and defective SUMO ligase mutant of Smc5/6 ChIP-qPCR. The previous two reports observed that SUMOylation of STR complex by Smc5/6 occurred mainly upon treatment with DNA damaging agents like MMS, the damage caused by NPSs or HU is different from the MMS treatment. However, we were still curious to see whether STR SUMOylation played any role in their recruitment to NPSs.

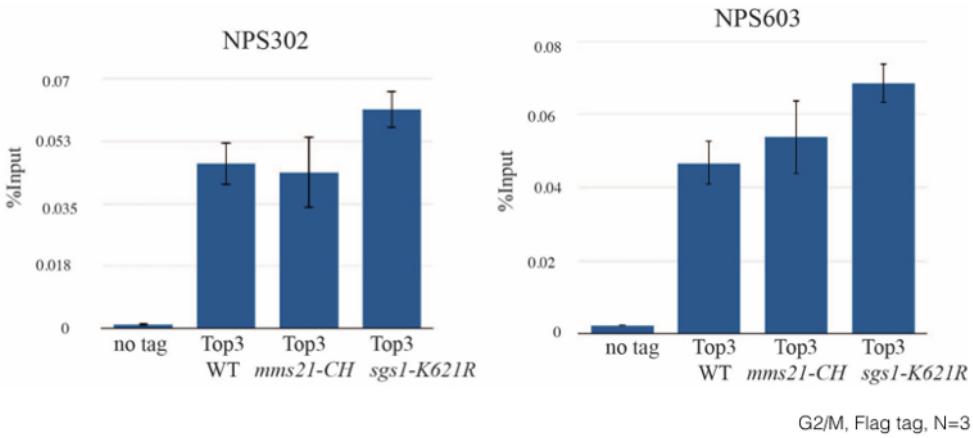

Fig3.17: Quantification of Top3 at NPSs in *MMS21 SGS1* vs *mms21-CH*, *sgs1-K621R* mutants. ChIP-qPCR analysis to quantify the Top3-Flag bound to NPSs in unperturbed G2/M cells (N=3)

We observed that the enrichment of Top3 at NPSs was not affected by SUMOylation defective *mms21-CH* or *sgs1-KR* (Fig3.17). This indicated that there is no substantial role for SUMOylation of STR by Smc5/6 in regulating its enrichment at NPSs. This agrees with the previous two studies suggesting SUMOylation being important upon MMS treatment but no in unperturbed or HU treated cells (Bermúdez-López et al., 2016; Bonner et al., 2016). Most probably, the Smc5/6 complex plays a structural role in this process.

3.2.3 Enrichment of Smc5/6 to NPSs is unaffected by STR deletion/depletion

As we observed effects of Smc5/6 dysfunction on Top3 enrichment, we next addressed whether the two protein complexes depend of each other for NPS association. We therefore characterized the effect of STR deletion (*sgs1Δ*) and depletion (*Tc-top3*) on Smc6-Flag recruitment to NPSs (TERs in particular) in G2/M phase.

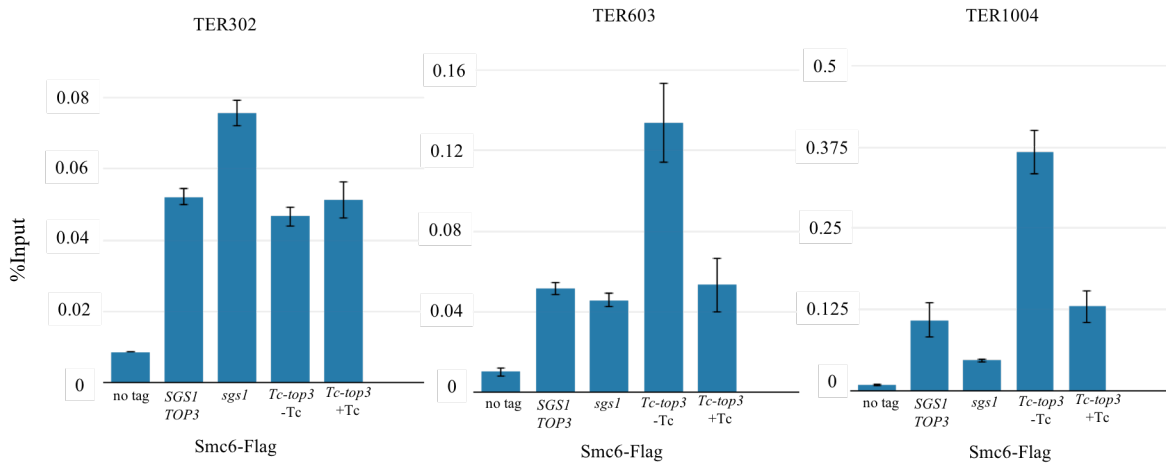

Fig3.18: Quantification of Smc6 at NPSs in *SGS1 TOP3* and *sgs1* or *top3* mutants. ChIP-qPCR analysis to quantify the Smc6-Flag bound to NPSs in unperturbed G2/M cells (N=3)

We observed no effect of STR deletion/depletion on Smc5/6 enrichment at NPSs, indicating that STR does not affect Smc5/6 recruitment to NPSs. This suggests that the two complexes are recruited to NPSs independently while having a putative collaborative role in their mutual retention.

We next checked whether the recruitment of Top3 at NPSs was dependent on STR complex formation. We checked by ChIP-qPCR the amount of Top3 at NPSs in WT cells (*SGS1 RMI1*) and compared it with *sgs1Δ* and *rmi1Δ* mutants.

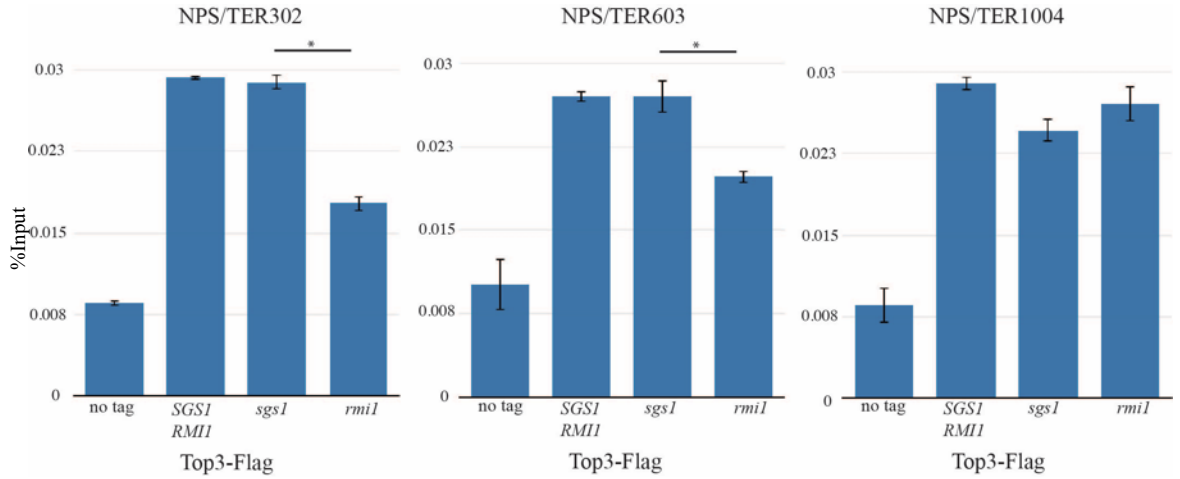

Fig3.19: Quantification of Top3 at NPSs in *SGS1 RMI1* and *sgs1, rmi1* mutants. ChIP-qPCR analysis to quantify the Top3-Flag bound to stalled forks upon HU treatment (200 mM HU, N=3)

We observe that the enrichment of Top3 to NPSs is unaffected by *sgs1Δ*, but significantly reduced at 2 out of 3 TERs checked in *rmi1Δ*. This could be due to the loss of DNA binding subunit of the STR complex. Thus, the enrichment of Top3 at NPSs is dependent on the structural role of Smc5/6 and DNA binding properties of the STR complex.

3.2.4 Top3 is enriched at stalled replication forks

Next, we wanted to confirm the binding of Top3 to stalled RFs. Therefore, we released G1 arrested cells in media containing HU to cause fork stalling and checked by ChIP-qPCR the recruitment of Top3 to early replicating origins (ARS305 and ARS1) in *SMC6* and *smc6* mutants.

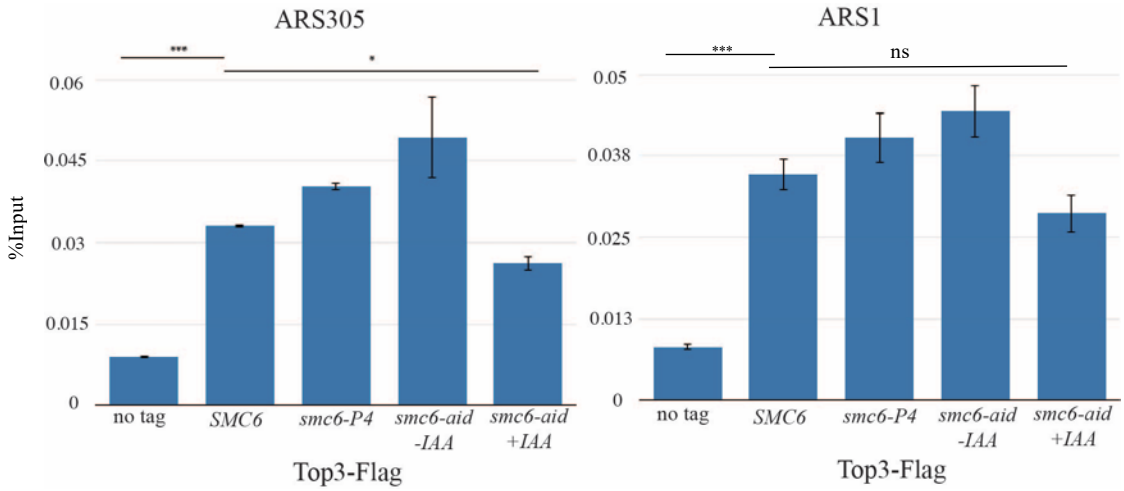

Fig3.20: Quantification of Top3 at stalled forks in *SMC6* and *smc6* mutants. ChIP-qPCR analysis to quantify the Top3-Flag bound to stalled forks upon HU treatment (200 mM HU, N=3)

We observed that Top3 was recruited to the stalled RFs at ARS305 and ARS1 upon HU treatment. The enrichment at ARS305 was reduced significantly by depleting Smc6 (upon auxin addition). The same was observed for ARS1, but the decrease in Top3 recruitment was not significant by t-test. This could be due to the larger error bars in the ARS1 qPCR values. In line with our previous observation that *smc6-P4* did not show a defect in binding to stalled RFs (Fig3.12), we also observed normal Top3 recruitment to stalled RFs in the *smc6-P4* background. The *smc6-56 TOP3-FLAG* strain was slow growing and we failed to arrest it in G1 phase to conduct this experiment. In conclusion, we observe reduction of Top3 binding to stalled RFs when Smc6 is depleted.

3.2.5 Overexpression of STR complex does not rescue *smc6-56* phenotypes

As we observed reduced Top3 recruitment to NPSs and stalled forks in *smc6-56* background, we examined the effects of increasing the amount of STR in *smc6-56* cells in regard to temperature sensitivity. We therefore used *GAL* promoter to overexpress Top3/Top3-YF (dominant negative allele of Top3) and Sgs1 from a high copy vector (Mankouri and Hickson, 2006) in WT and *smc6-56* cells at permissive and higher temperatures.

We observed that STR overexpression did not rescue the temperature sensitivity of *smc6-56*. The overexpression of Sgs1 or Top3YF was even harmful for cells at permissive

temperatures. The temperature sensitivity of *smc6-56* remained unaltered even upon overexpression of *TOP3* or *SGS1* (Fig3.21). This indicates that regulation of Top3 binding at NPSs by Smc5/6 is independent of abundance of STR but possibly depends on Smc5/6 function in creating a suitable substrate for Top3.

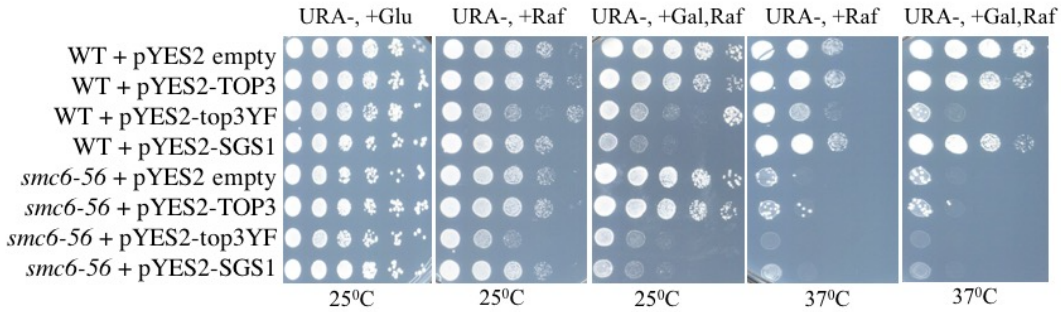

Fig3.21: Ectopic over-expression of *TOP3* and *SGS1* in WT and *smc6-56* cells. The effect of STR overexpression was observed by spot assay at permissive and restrictive temperatures. Glucose plates were used to shut off Gal promoter and as negative control

To conclude, we observed that Smc5/6 and STR complexes localize to NPSs largely independently of each other. The retention of Top3 is positively influenced by Smc5/6 at NPSs and stalled forks, but independently of the SUMO ligase activity of Smc5/6. We hypothesize a structural role of the Smc5/6 protein complex in facilitating Top3 retention.

Chapter 4

Smc5/6 and STR complexes regulate replication, recombination and fragility at NPSs

In the previous chapter we observed that both Smc5/6 and STR complexes were present at NPSs. To understand their role at NPSs, we used mutants of Smc5/6 and/or depletion/deletion of Sgs1/Top3 and checked for phenotypes at NPSs and stalled forks. We took two approaches to observe their effect on recombination and fragility at NPSs. First, we checked the accumulation of recombination intermediates at specific loci (one NPS and one early origin, in HU treated cells) by 2D gel electrophoresis, then we compared by PFGE the size of chromosome 12 which contains rDNA repeats in *S. cerevisiae*. In these approaches, we observed the effect of Smc5/6 and STR dysfunction on DNA replication-associated recombination in general and at rDNA in particular.

4.1 Smc5/6 and STR mutation/depletion causes accumulation of recombination intermediates at NPSs and at stalled forks

In order to understand the effect of STR on recombination at NPSs, we used a technique commonly used in our lab to observe replication and recombination intermediates: 2D gel electrophoresis. We treated the cells with HU to slow down replication and facilitate visualization of transient and scarce recombination intermediates. We used the *smc6* mutant *smc6-56* as control, as it was previously shown by our lab that *smc6-56* and *smc6-P4* accumulate recombination intermediates at NPSs (Menolfi et al., 2015), and WT strain as a negative control. In addition, we used deletion/depletion of Sgs1, Top3 and depletion of Smc6 to check effect of Smc5/6 or STR dysfunction on recombination at NPSs. The cell cycle progression was confirmed by FACS analysis and protein depletion was visualized by western blot. The temperature for the experiment was permissive (28ºC) for *smc6-56* cells.
We checked two genomic regions regarding recombination intermediate accumulation. First, we checked NPS/TER302, as a representative NPS located in a late replicating region. Another region was ARS305, an early replicating origin where we can observe stalled forks from early timepoints. We already know that Smc5/6 and STR complexes are enriched at these regions in unperturbed cell cycle (NPSs) (Fig3.8, Fig3.9) or upon HU treatment (Fig3.12, Fig3.20).

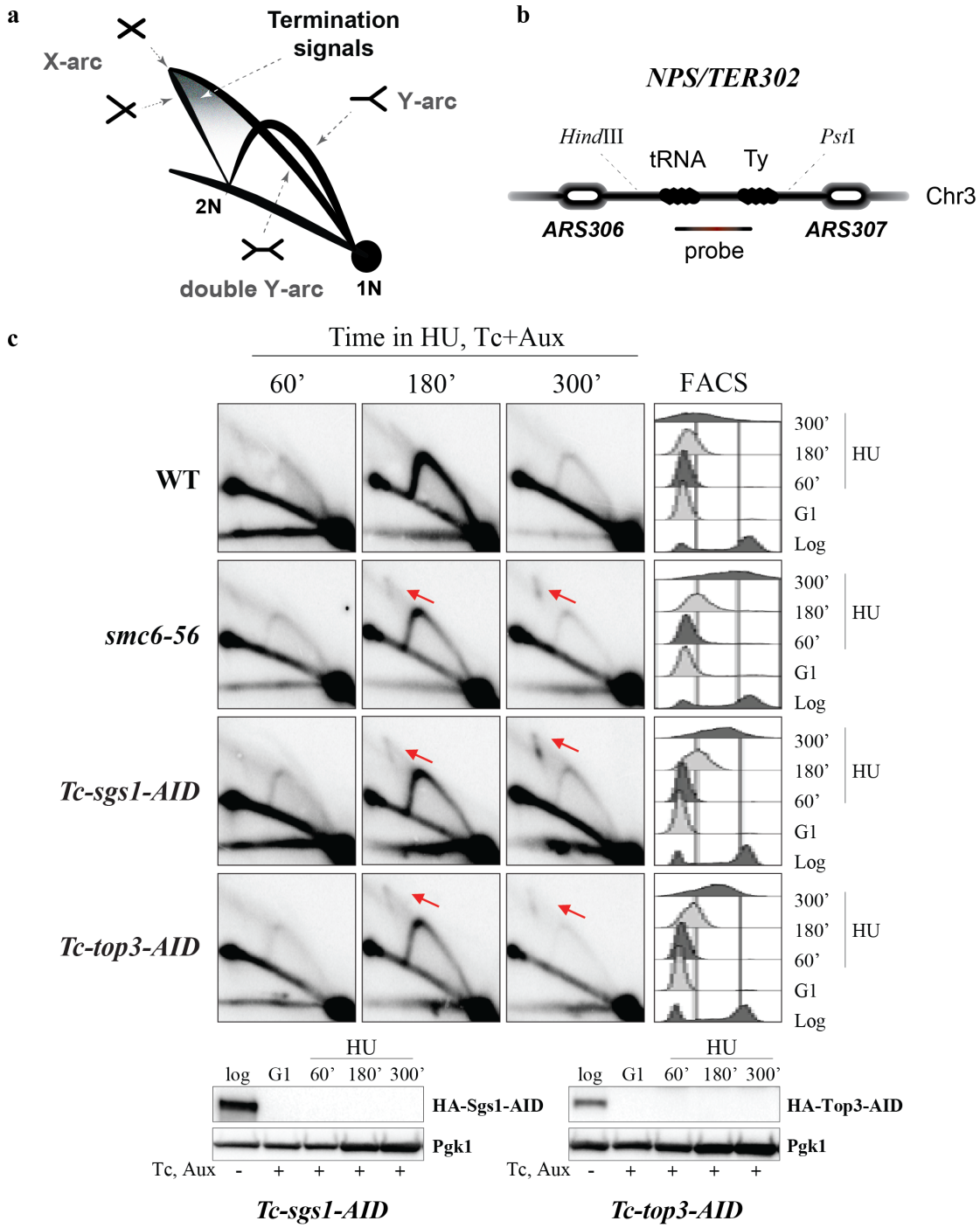

Fig4.1: Accumulation of recombination intermediates at stalled replication forks in STR and Smc5/6 mutants. A) Schematic representation of replication intermediates observed by 2D gel electrophoresis at termination regions. B) Schematic representation of the NPS302/TER302 region analysed by 2D gels. C) Visualization of recombination intermediates (as indicated by red arrows) by 2D gel electrophoresis from cells of the indicated genotype. The cells were synchronized in G1 phase and released in media containing 200 mM HU. Cells were collected at the indicated time-points. Sgs1 and Top3 were depleted with Auxin and Tetracycline. X-molecules accumulate as a spike indicated by an arrow. Cell progression confirmed by FACS analysis and protein depletion confirmed by western blot

We observe the 2D gel pattern as depicted in Fig 4.1A, we observe in the WT double-Y arc due to replication forks approaching each other and the intensity of arc reduces as the replication is completed. In line with previous reports, we do not observe recombination intermediates for the WT strain. For *smc6-56*, the replication arc remains similar to the WT, but there is accumulation of recombination intermediates that persist even after 5 hours of release from G1. *Tc-top3-aid* and *Tc-sgs1-aid* strains show accumulation of recombination intermediates similar to *smc6-56* (Fig4.1). We conclude that Smc5/6 and STR mutants show recombination intermediate accumulation at NPS TER302. These recombination intermediates are persistent even after 300' after release from G1, when most replication is complete as deduced by flow cytometry analysis. This indicates that Smc5/6 and STR complexes are involved in the processing of these recombination intermediates.

Further, we wanted to check what happens at an early replication origin upon fork stalling. For early replicating origins, we observe the 2D gel pattern as described in Fig4.2A. In WT sample, replication bubble and Y arc gradually disappear at later time-points as the replication fork passes through this region. Smc5/6 and STR mutants accumulate recombination intermediates even at late time-points (Fig4.2).

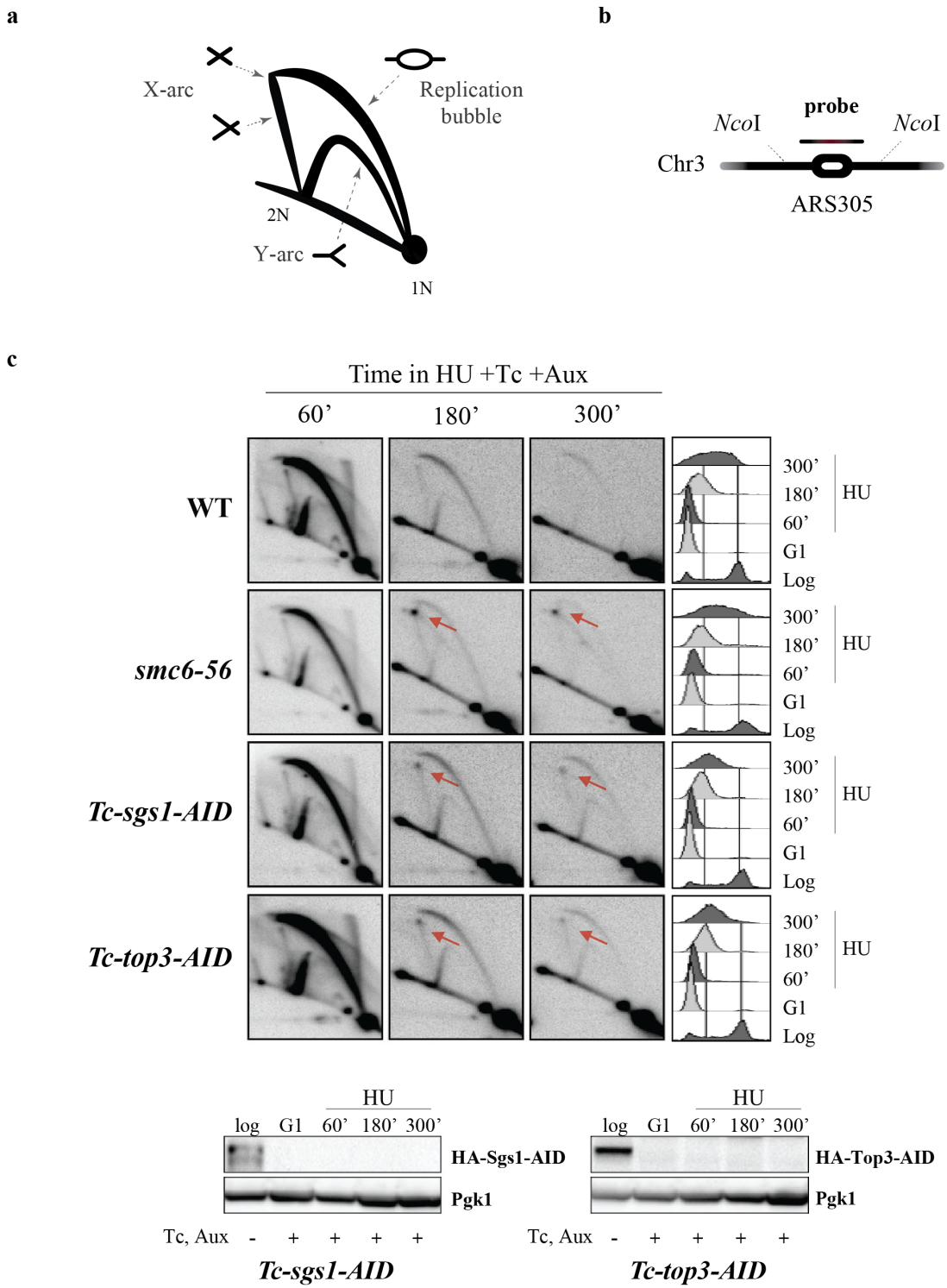

Fig4.2: Accumulation of recombination intermediates at ARS305 observed by 2D electrophoresis. A) Schematic representation of replication intermediates observed by 2D gel electrophoresis at an early replication origin. B) Schematic representation of region analysed with 2D gels, ARS305 an early replicating origin. C) Visualization of recombination intermediates (as indicated by red arrows) by 2D gel electrophoresis from cells of the indicated genotype. The cells were synchronized in G1 phase and released in media containing 200 mM HU. Cells were collected at indicated time-points. Sgs1 and Top3 were depleted with Auxin and Tetracycline. X-molecules accumulate as a spike indicated by

an arrow. Cell progression confirmed by FACS analysis and protein depletion confirmed by western blot

Based on this result, we conclude that Smc5/6 and STR play similar roles in counteracting accumulation of recombination structures at stalled forks. Taken together, our results indicate that Smc5/6 and STR localize to stalled RFs and NPSs to avert recombination intermediate accumulation.

4.2 Smc5/6 and STR mutation/depletion cause rDNA fragility

It is reported that both Smc5/6 and STR play roles in rDNA replication (Mundbjerg et al., 2015; Torres-Rosell et al., 2005). Without these complexes, there is variation in rDNA copy number due to aberrant recombination events. Smc5/6 also plays a role in successful rDNA segregation (Torres-Rosell et al., 2005).

The budding yeast nucleolus is a hub of rDNA arrays that can exceed 1Mb size, with the size varying depending on the number of rDNA repeats. There are 100-200 units of about 9.1 kb rDNA repeats on chromosome 12 making it the largest chromosome (Petes, 1979). Therefore, we use the program of PFGE running for large chromosome separation. We observe the chromosomes separated in Pulse Field gel by staining with EtBr and then we probe for rDNA after southern blot and observe only the chromosome 12. With this technique we investigated changes in rDNA repeats upon Smc5/6 and STR dysfunction.

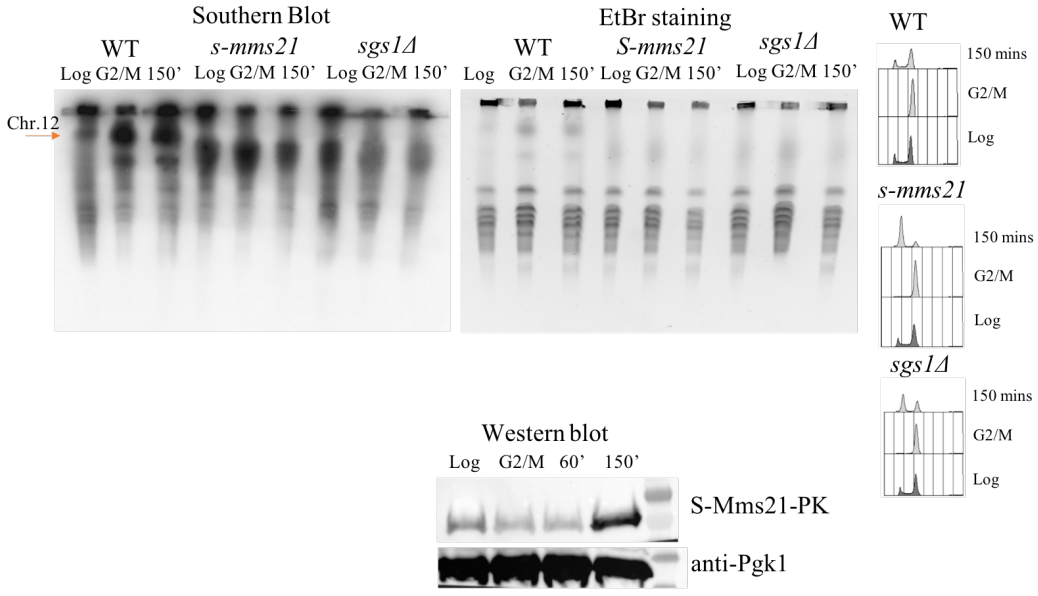

Fig4.3: Changes in size chromosome 12 (containing rDNA repeats) in *S-mms21* and *sgs1* mutants observed by PFGE. PFGE probed for chromosome 12 and EtBr stained. The samples were collected after G2/M arrest at indicated timepoints. Cell cycle progression and Mms21 expression checked by FACS and WB

For this experiment we arrested cells in G2/M and released them in media containing alpha factor to arrest the cells in the next G1 phase. Along with WT as negative control, we used *S-mms21* and *sgs1Δ*. *S-mms21* is a strain in which Mms21 expression is restricted to S phase (similar to *S-smc6* previously used). Without Mms21, not only does the complex not have SUMO ligase activity but also the stability of the complex, outside of S phase, is majorly disturbed.

We observed that *smc5/6* and *sgs1* mutants shows defects in chromosome 12 size. The size of the chromosome containing rDNA repeats is reduced compared to the WT strain. Interestingly, this decrease in size is observed at all timepoints. This is probably due to the alterations happening during growth of mutant cells and not the outcome of a single cell cycle (fig4.3). We conclude that the Smc5/6 and STR mutants have unstable rDNA copies that are constantly undergoing recombination and there are frequent variations in the copy numbers even without external stress.

Thus, Smc5/6 and STR counteract excessive recombination and prevent structural changes at rDNA. These complexes play important roles in preventing replication fork reversal and recombination genome-wide upon HU treatment. They may also be crucial for the recovery of replication forks upon prolonged stalling. To understand the interplay between Smc5/6 and STR complexes better, we conducted a genetic screen for *smc6* mutant and followed its effects at NPSs.

Chapter 5

Suppressor screen for *smc6-56* temperature sensitivity

In order to understand the function of Smc5/6 and possibly the interplay between Smc5/6 and STR, we decided to conduct a natural suppressor screen for temperature sensitivity of the *smc6-56* mutant, manifested at 37ºC. Our aim was to suppress the defects of Smc5/6 and then see if the suppressor affects the synthetic lethality between Smc5/6 and STR dysfunction or other aspects of STR functionality that may be regulated by Smc5/6.

5.1 Spontaneous suppressor screen

5.1.1 Scheme of suppressor screen

We started by culturing *smc6-56* cells at 25ºC overnight. OD5 (about 10^8 cells total) of this culture was then plated on the YPD plates and grown at 37ºC, in parallel OD0.5 (about 10^7 cells total) of cells were plated on YPD and grown at 25ºC as control. After several days, we saw colonies appearing on the plate at 37ºC. These were the suppressors that accumulated one or more mutations that allowed them to bypass the temperature sensitivity of *smc6-56*. We then confirmed the *smc6-56* mutations, and grew the suppressors at 37ºC to confirm suppression of temperature sensitivity. We picked 8 colonies for further analysis.

The colonies thus picked up were back-crossed with the *smc6-56* parent strain. This was done in order to select the suppressors arising from a single mutation. If suppressor was indeed due to single mutation, we expected to observe 2:2 segregation of the suppression phenotype. By doing this, we selected for 5 out 8 suppressors that were monoallelic for further validation. We decided to first sequence *SMC6* and *SMC5* before proceeding to whole genome sequencing. We identified mutation in *SMC6*, which was further validated for being responsible of the phenotype, by creating the identified mutation de-novo (fig5.1).

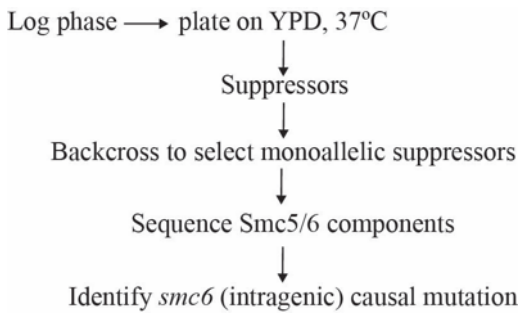

Fig5.1: Scheme of natural suppressor screen

5.1.2 Suppressors identified were monoallelic and rescued the temperature sensitivity to WT level

Once the suppressors were obtained from the screen at 37°C, they were checked for monoallelic nature and then for suppression of temperature sensitivity. We found five out of eight suppressors to be monoallelic and confirmed their ability to suppress *smc6-56* temperature sensitivity. We checked by serial dilution and spotting on a YPD plate at non-permissive temperature and observed complete rescue of temperature sensitivity (Fig5.2).

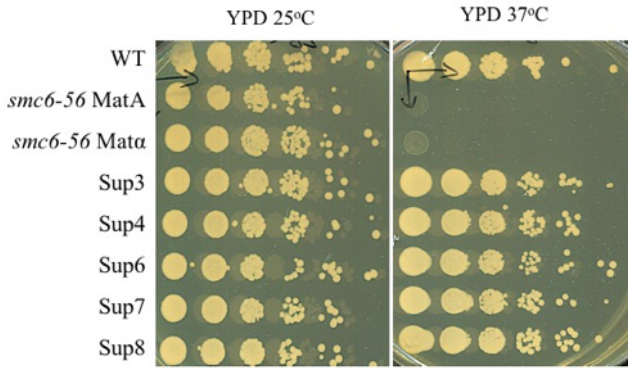

Fig5.2: Rescue of temperature sensitivity by *smc6-56-sup*. The Suppression of temperature sensitivity was confirmed by spot assay at 37°C, the image was taken after 2 days of spotting

5.1.3 Identification of suppressor mutation

Once we confirmed the monoallelic nature of suppressors, we were interested in the nature of suppressor mutations. We therefore sequenced the Smc5/6 components and known suppressors of Smc6 phenotypes (*MPH1*, *RAD51*) in each of the monoallelic suppressors.

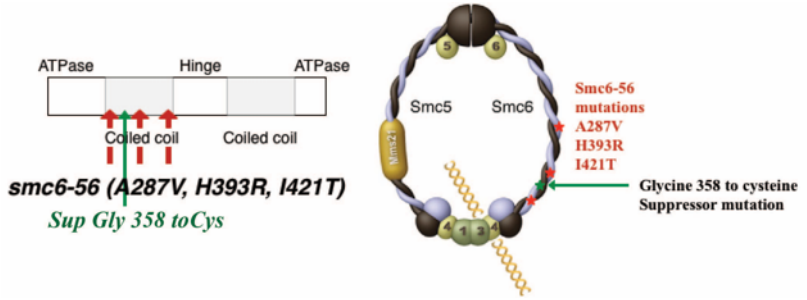

Fig5.3: Identification of the suppressor mutation in Smc6 coiled-coil. The suppressor mutation marked in green among the *smc6-56* mutations in red, in the coiled-coil domain of *SMC6* gene

All the monoallelic suppressors contained the same mutation in the *SMC6* gene (Fig5.3). We identified an intragenic mutation in *SMC6*, between the three mutations of *smc6-56*. The mutation was changing the Glycine 358 to Cysteine. Observing the Smc5/6 structure, we hypothesized that *smc6-56* mutations may change orientation the coiled-coil structure of Smc6 towards altered ring or inefficient ATPase head domain. In case of Suppressor, the suppressor mutation (on top of *smc6-56* mutations) may change the orientation of Smc6

coiled-coil to establish a more functional Smc5/6 ring and/or ATPase. We also hypothesized that the new Cys residue may establish Cys-Cys covalent bonds, which might be responsible for new changes in the Smc5-Smc6 interaction.

5.1.4 Suppression of DNA damage sensitivity

Once we had identified the suppressor mutation, we checked whether the suppressor *smc6-56-sup* alleviated the DNA damage sensitivity of *smc6-56*. We checked by spot assay the sensitivity of *smc6-56* and *smc6-56-sup* to MMS, HU and CPT.

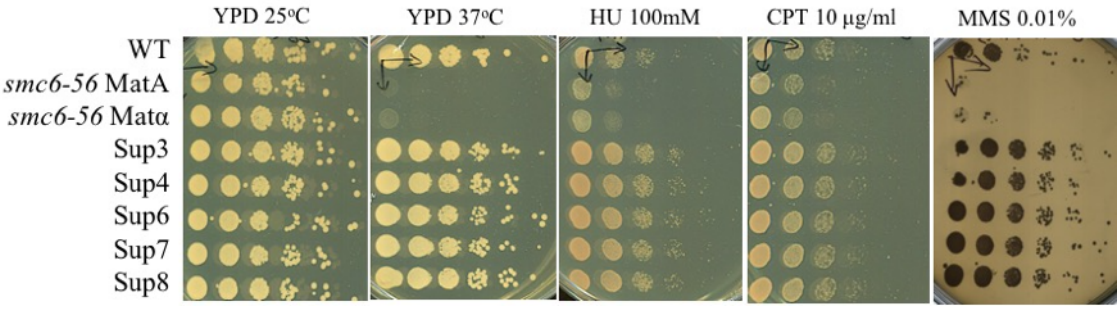

Fig5.4: Rescue of DNA damage sensitivity by *smc6-56-sup*

The Suppression of DNA damage sensitivity was confirmed by spot assay on indicated concentrations of HU MMS and CPT, the image was taken after 2 days of spotting.

We observed that the *smc6-56-sup* completely rescued the sensitivity of *smc6-56* to different types of DNA damages caused by HU-induced fork stalling, MMS damage or topoisomerase 1 poisoning (CPT). Such a complete rescue of sensitivities indicated that the suppressor mutation could indeed regain a functional Smc5/6 complex.

5.2 Validation of suppressor

For validation of the suppressors we took two approaches. First, we back-crossed the suppressors and checked several spores for 2:2 segregation of temperature and DNA damage sensitivity. We then re-created the suppressor mutation in the *smc6-56* background and checked the suppression of temperature sensitivity by the *de-novo* suppressor.

For the first validation, we back-crossed all five suppressors (genetically identical) to *smc6-56* parent strain and separated four spores of ten tetrads for each cross. We grew ten tetrads of back-crossed suppressor and two tetrads from a control *smc6-56* X *smc6-56* cross. We then spotted the spores on plates of YPD and YPD+MMS, grew them either at 25°C or 37°C. Only one of the back-cross is shown for reference (Fig5.5).

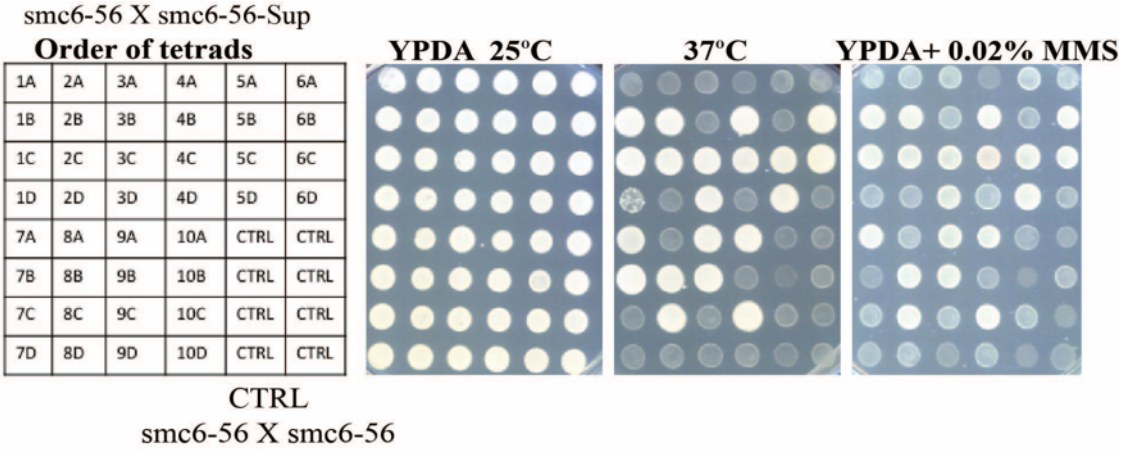

Fig5.5: Validation of *smc6-56-sup* by back-crossing. The spores were spotted in indicated order on the indicated plates and image was taken after two days

We observed that the temperature and DNA damage sensitivity of *smc6-56* was segregated 2:2 in the suppressor mutations. This was similar to the experiment conducted for confirming the mono-allelic nature of suppressor mutations. In that experiment, we only checked suppression of temperature sensitivity for a few tetrads. We now checked ten tetrads for each monoallelic suppressor (which are still genetically identical) and we also confirmed the 2:2 segregation of the DNA damage sensitivity. This further confirmed the monoallelic nature of the suppressor.

We next proceeded to validate that this mutation was indeed the source of suppression.

To validate that, we created a cassette by PCR with *smc6-56::KANMX* as template and with primers containing *smc6-56-sup* mutation. The cassette thus contained three mutations of *smc6-56* and the mutation corresponding to *smc6-56-sup*. This cassette was then transformed into a WT strain first. When we transformed into *SMC6* WT strain, due to the long homology between *SMC6* and *smc6-56-sup*, only C-terminus with selection marker got integrated and we selected for many *SMC6::KANMX* colonies. We therefore decided to transform *smc6-56-sup::KANMX* in a diploid *SMC6/smc6Δ* and dissect to get haploid of *smc6-56-sup*. Once we obtained colonies negative for marker of *smc6Δ* and positive for *smc6-56-sup*, we dissected the diploids and selected for haploid with *smc6-56-sup*. We further confirmed the transformants by sequencing. This *de novo* suppressor was then used for spot assay.

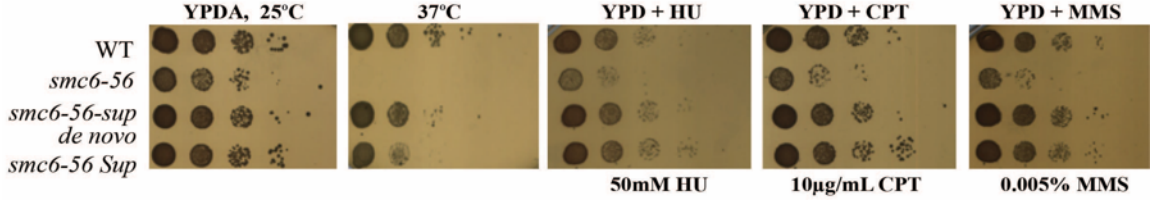

Fig5.6: Validation of *smc6-56-sup* by *de novo* creation of suppressor mutation. The suppressor was confirmed by spot assay on the indicated plates and image was taken after two days

We observed that the suppressor with de novo *smc6-56-sup* mutations was able to rescue the temperature and DNA damage sensitivity of *smc6-56*. This meant that having a single mutation more than the *smc6-56* mutations rescued the temperature and DNA damage sensitivity of *smc6-56*, validating that the suppressor mutation was indeed responsible for the suppression of temperature and DNA damage sensitivity. After successful validation of the suppressor mutation, we compared various phenotypes of *smc6-56* and *smc6-56-sup* at NPSs.

5.3 Suppressor mutation rescued the effect of *smc6-56* mutations on the NPS localization, NPS recombination and various genetic interactions

5.3.1 Suppressor mutation partially rescues the defect of *smc6-56* NPS localization

After obtaining the suppressor of *smc6-56* temperature sensitivity we checked the phenotypes of *smc6-56-sup* allele at NPSs. First, we checked by ChIP-qPCR whether the Smc6-56-sup can localize to NPSs as efficiently as the WT protein in unperturbed G2/M phase.

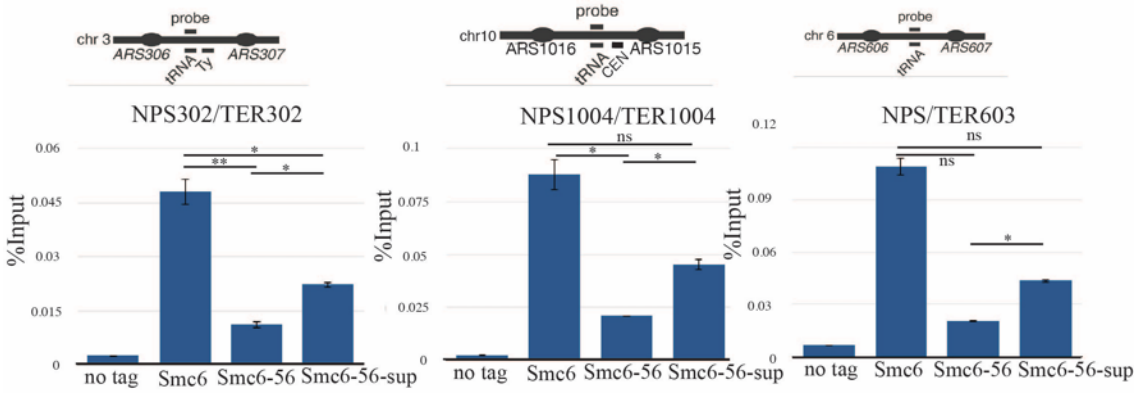

Fig5.7: Quantification of Smc6 and its variants at NPSs in unperturbed G2/M-synchronized cells (N=3)

We observed that the suppressor mutation partially rescues the enrichment of Smc6 at NPSs, but the rescue is not to the WT level (Fig5.7). The enrichment of Smc6-56-sup-myc at NPSs is better than Smc6-56-myc but not as good as Smc6-myc WT protein. This indicates that even though there is improvement with the structure of Smc5/6 complex, the suppressor allele is still encoding a mutant protein which is still having defective phenotypes compared to the WT. Next, we checked the effect of *smc6-56-sup* allele on the recruitment of Top3 to NPSs.

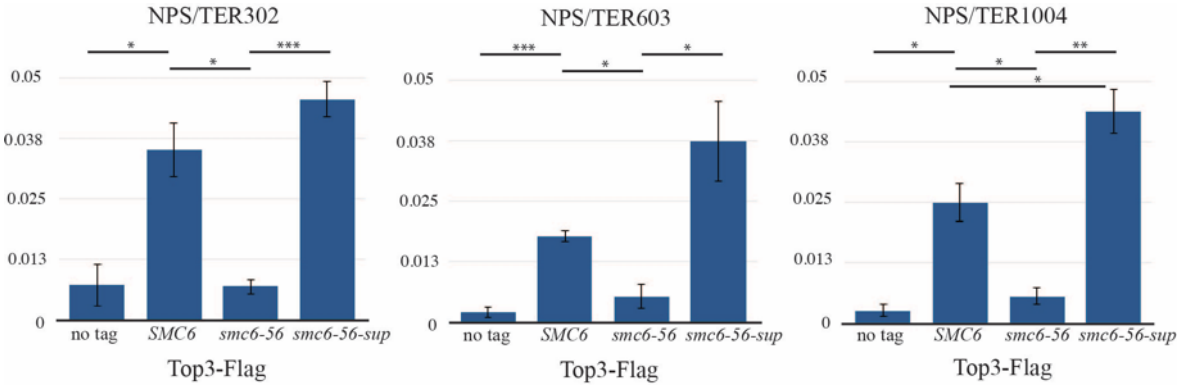

Fig5.8: Quantification of Top3 at NPSs in WT vs *smc6* background in unperturbed G2/M-synchronized cells (N=3)

We observed complete rescue of Top3 recruitment to NPSs (Fig5.8). This indicated that the partial recovery of Smc6-56-Sup at NPSs leads to complete rescue of Top3 recruitment. This suggests a direct role of Smc5/6 complex in recruitment of the STR complex at NPSs. We then wanted to see whether the rescue of Top3 recruitment is also associated with rescue of the recombination phenotype.

5.3.2 Suppressor mutation completely rescues the recombination defect of *smc6-56*

In the previous result (4.1), we observed that *smc6-56* accumulated recombination intermediates at NPSs which were observed by 2D gel electrophoresis. After obtaining suppressor of *smc6-56* temperature sensitivity, we were curious to see whether the suppressor recued the recombination intermediates at NPSs and stalled forks upon HU treatment.

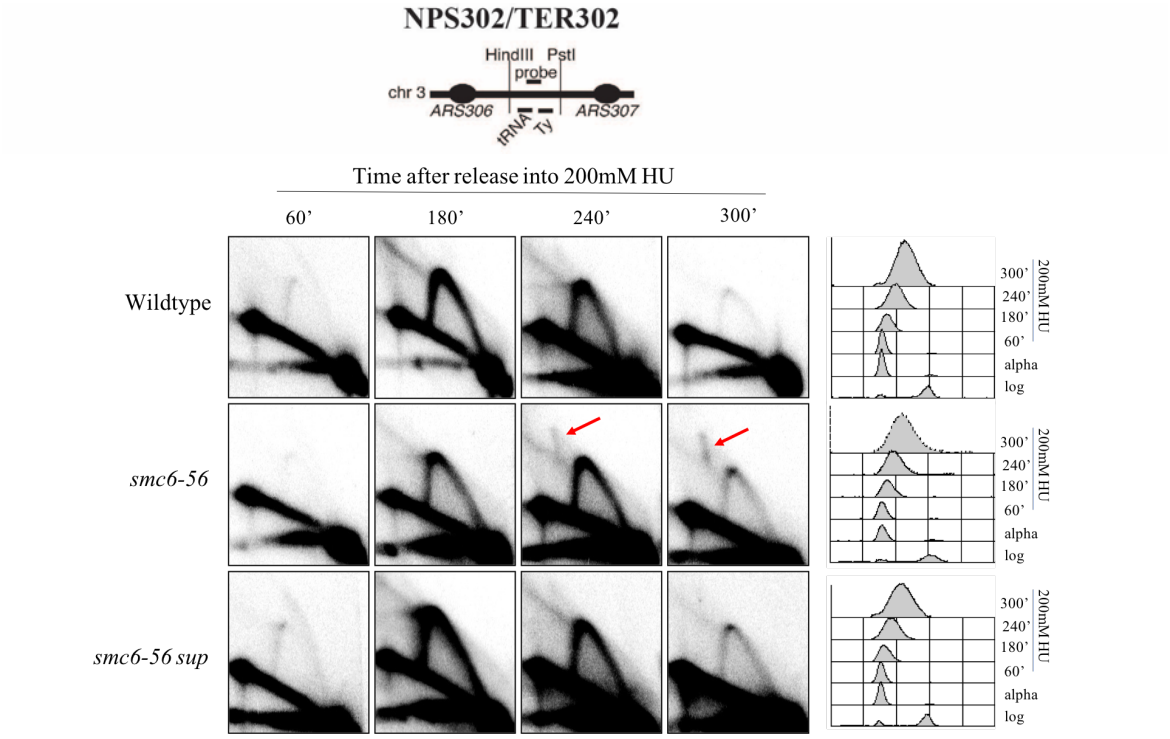

Fig5.9: Accumulation of recombination intermediates at TER302 as observed by 2D electrophoresis. Schematic representation of TER302. Visualization of recombination intermediates (as indicated by red arrows) by 2D gel electrophoresis from cells of the indicated genotype. The cells were synchronized in G1 phase and released in media containing 200 mM HU. Cells were collected at indicated time-points

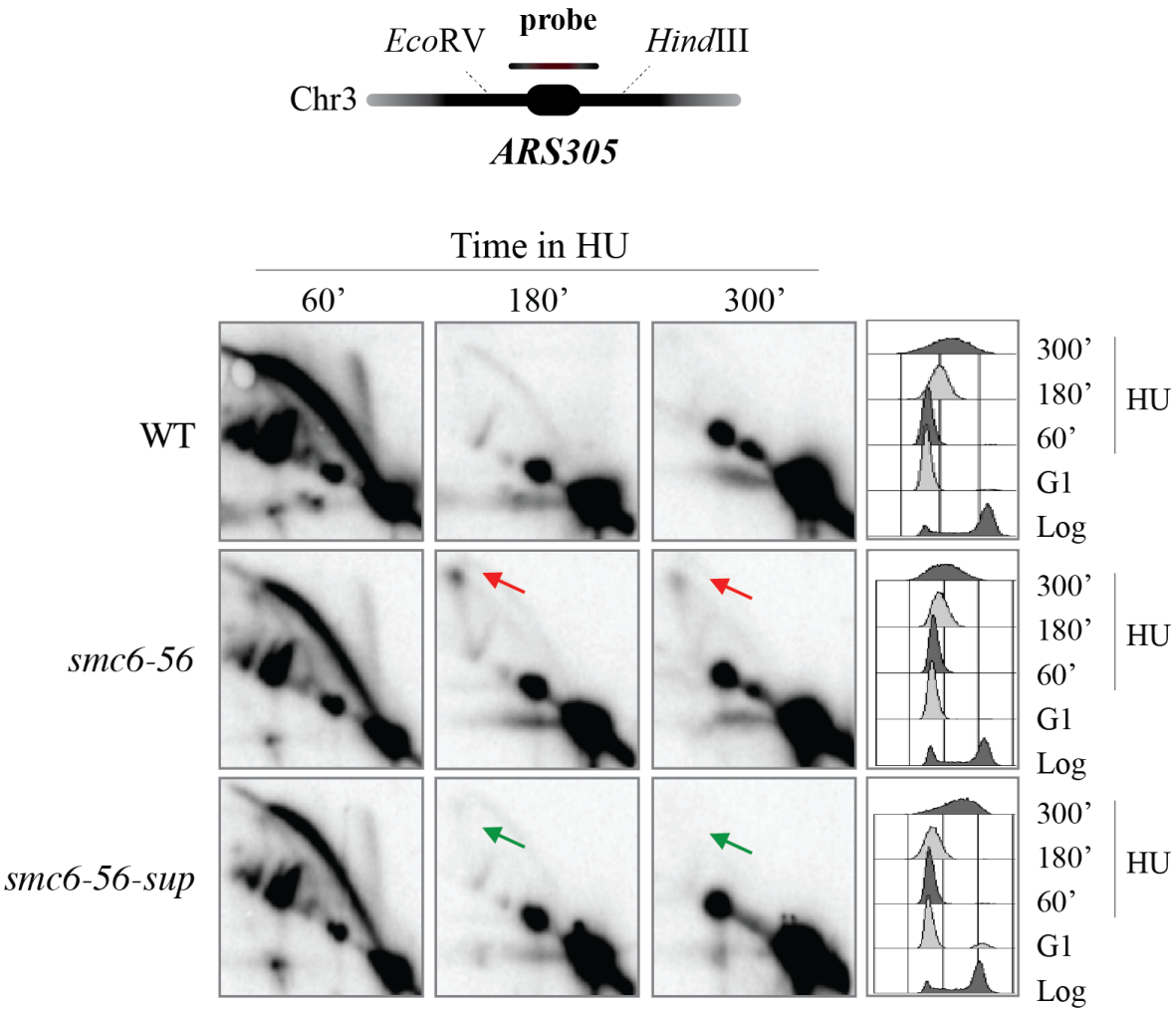

Fig5.10: Accumulation of recombination intermediates at ARS305 as observed by 2D electrophoresis. Schematic representation of ARS305. Visualization of recombination intermediates (as indicated by red arrows) by 2D gel electrophoresis from cells of the indicated genotype. The cells were synchronized in G1 phase and released in media containing 200 mM HU. Cells were collected at indicated time-points

We observed that at stalled RFs, both at TERs and ARSs, the suppressor completely rescued the accumulation of recombination intermediates. The *smc6-56* accumulated recombination intermediates at later timepoints at NPS as we expected, while the suppressor showed no accumulation (Fig5.9). Also, at ARS305, we observed accumulation of recombination intermediates at early timepoints for *smc6-56*, which was completely rescued by the suppressor mutation (Fig5.10). The result at NPSs indicated that even though there were lower levels of Smc6 variant at NPSs (Fig5.7), this was sufficient both to recruit the STR complex and to rescue the accumulation of recombination intermediates.

5.3.3 Suppressor mutation rescues genetic interactions of *smc6-56* with STR and Rrm3

We next checked whether *smc6-56-sup* showed genetic interaction with *rrm3Δ*. We expected to see a rescue of *rrm3Δ smc6-56* synthetic lethality, and this was indeed the case (Fig5.11). The genetic interaction between *sgs1Δ* and *smc6-56* was also rescued (Fig.5.12).

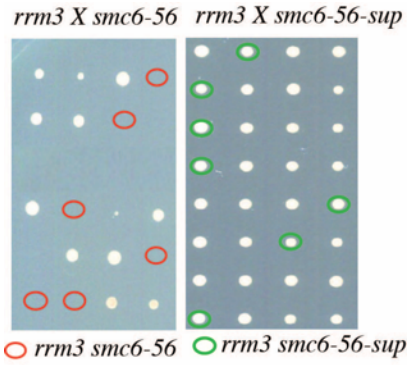

Fig5.11: Synthetic lethality between *smc6-56* and *rrm3Δ* rescued by suppressor mutation as observed by tetrad analysis

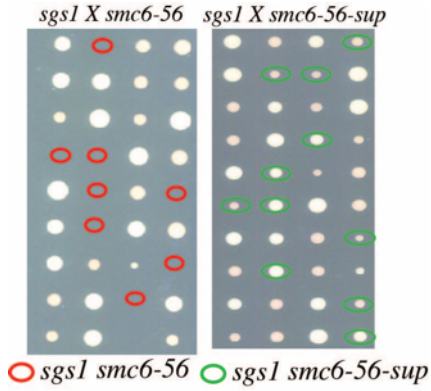

Fig5.12: Synthetic lethality between *smc6-56* and *sgs1Δ* rescued by suppressor mutation as observed by tetrad analysis

In 2013, a yeast study has shown that the DNA damage sensitivity of *smc5/6* mutants can be rescued by *mph1Δ* through hyperactivation of the Mec1 checkpoint. The recombination intermediate accumulation in absence of Smc5/6 function is dependent on Mph1 helicase (Chen et al., 2013). We next asked whether the genetic interaction between *smc5/6* and STR mutants could be due to excessive recombination genome-wide and thus be rescued by *mph1Δ*.We observed that the synthetic lethality between *smc5/6* and STR mutations was independent of role of *mph1Δ*. Furthermore, this synthetic interaction was rescued by suppressor mutation in presence or absence of Mph1. This indicated that the synthetic interaction was not due to the formation of Mph1 mediated aberrant recombination intermediated in absence of Smc5/6 or there were back-up pathways such that could counteract Mph1 activity.

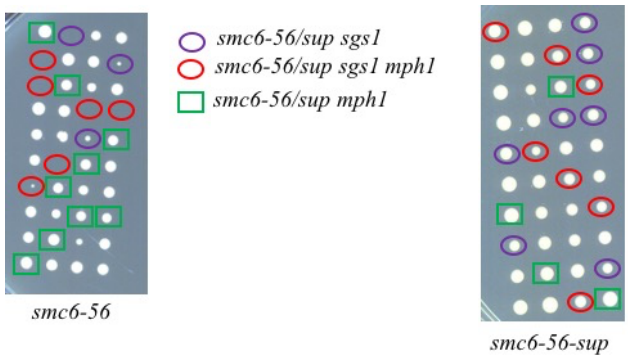

Fig5.13: Synthetic lethality between *smc6-56* and *sgs1Δ* is not rescued by *mph1Δ*, moreover the rescue of said synthetic lethality by the *smc6-56-sup* does not depend on *MPH1* as observed by tetrad analysis

Even after observing the rescue of genetic interactions in absence of *MPH1*, we were curious to see the effect of *MPH1* deletion on the recruitment of Top3 to NPSs upon *smc6-56* mutation. We expected a role for Mph1 helicase upon *smc5/6* dysfunction failing to create the suitable substrates for STR action. We addressed this by ChIP-qPCR.

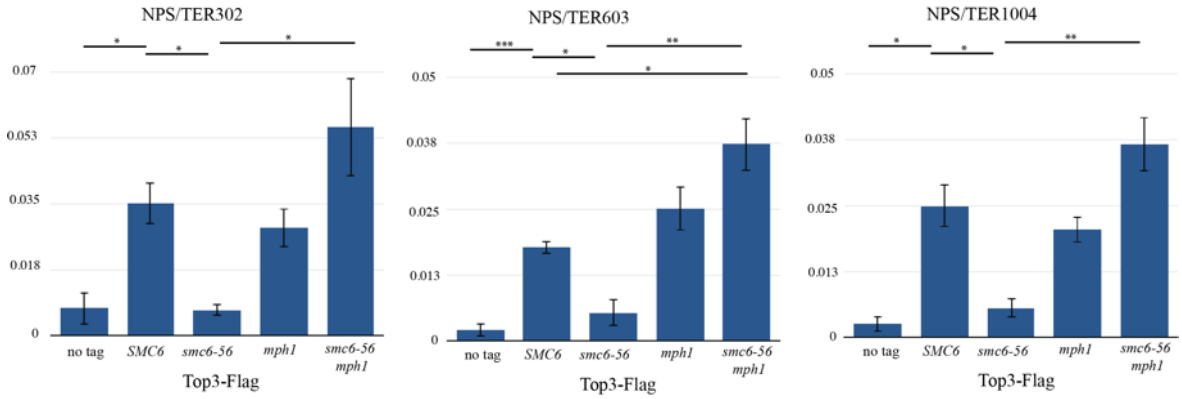

Fig5.14: Quantification of Top3 at NPSs in WT vs *smc6/mph1* background in unperturbed G2/M-synchronized cells (N=3)

We observed that deletion of *MPH1* alone did not affect the recruitment of Top3 to NPSs while deletion of *MPH1* in combination with *smc6-56* led to the rescue of Top3 recruitment to NPSs. This suggested a role for Smc5/6 in preventing Mph1 action at NPSs to create aberrant structures that are not processed by the STR complex. In the absence of Smc5/6 full activity, Mph1 can reverse forks and this may prevent STR from accumulating to NPSs. While without both Smc5/6 and counteracting Mph1 action, STR complex can directly accumulate to the NPSs. This gave us better understanding of the Smc5/6 mediated regulation of the STR complex.

We decided to study in more details the genetic interactions between *smc6-56*/*smc6-56-sup* with various factors implicated in the recombination pathway to understand the reasons for

synthetic lethality between *smc6-56* and *sgs1*. Another reason to study the genetic interactions between Smc5/6 and other factors involved in DNA repair was to see whether the suppressor shows any notable phenotypes differently from the WT Smc5/6 complex.

5.3.4 Genetic interactions between *smc6-56-sup* and dHJ resolvases

Smc5/6 and STR mutants accumulate recombination intermediates at NPSs/stalled forks. We asked whether factors that affect Rad51 filament formation, D-loop disruption or dHJ dissolution or resolution are affected by Smc5/6 dysfunction and the suppressor mutation. Specifically, we checked the genetic interactions of Smc5/6 (*smc6-56* and *smc6-56-sup*) with helicases (Sgs1, Chl1, Srs2, Mph1) and nucleases (Mus81, Mms4). We already observed genetic interactions between Smc5/6 and the STR complex. We crossed to get diploids of Smc5/6 mutants and mutants of above-mentioned factors, dissected the sporulated diploids to get double mutants. Segregated tetrads were then checked for presence of markers and we identified (and/or deduced from dead spores) the genotypes of each spore. We observed one new genetic interaction with Srs2 and confirmed the previously known genetic interaction between Smc5/6 and Mus81/Mms4 (Menolfi et al., 2015). We began the analysis by checking genetic interactions between Mus81/Mms4 and Smc5/6. Previous work from our lab showed that *mus81Δ/mms4Δ* is synthetic sick with *S-smc6* (Menolfi et al., 2015). We checked the combination of *mus81Δ/mms4Δ* with *smc6-56*.

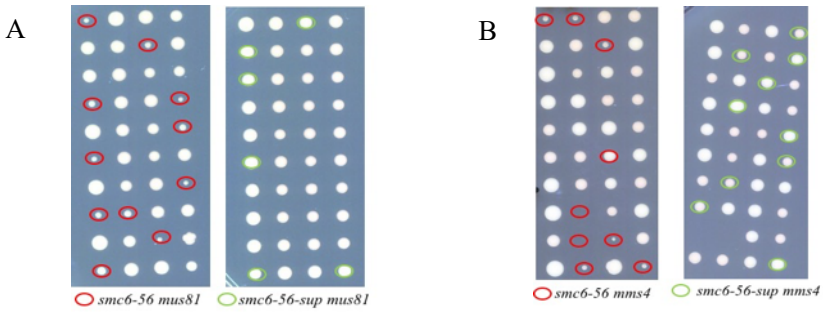

Fig5.15: Synthetic sickness between *smc6-56* and *mus81Δ/mms4Δ* rescued by suppressor mutation as observed by tetrad analysis in (A) for *mus81Δ* and (B) for *mms4Δ*

We observed that combination of *mus81Δ smc6-56* and *mms4Δ smc6-56* showed proliferation defects. This synthetic sickness was not observed for *smc6-56-sup*. Of note, there is synthetic lethality between *sgs1Δ* and *mus81Δ/mms4Δ*, the Mus81/Mms4 pathway acts as a backup pathway for the STR complex in resolving recombination structures. The Mus81/Mms4 pathway is known to be activated in G2/M phase to remove the recombination intermediates that are persistent and are not processed by the STR complex (Ashton et al., 2011; Szakal and Branzei, 2013a). We observed that *smc6-56* showed synthetic interactions with several pathways of recombination intermediates processing but *smc6-56-sup* did not

(Fig5.12, Fig5.15). Keeping in mind that *smc6-56* accumulated recombination intermediates at stalled forks while *smc6-56-sup* did not, we hypothesize that the recombination function of Smc5/6 influences both STR and the Mus81/Mms4 complex at different stages of recombination intermediates formation and/or processing.

Next, we checked the genetic interaction between *smc6-56* and *chl1Δ*. Chl1 is a DNA helicase with roles in inter-strand cross-link repair (ICL) and rDNA stability (Daee et al., 2012; Das and Sinha, 2005). The human homolog of *CHL1* is *DDX11*, known to play a crucial role in replication through DNA secondary and tertiary structures, such as G-quadruplex, hairpin loops, etc. Mutations in human ortholog are linked to Warsaw breakage syndrome that resembles at cellular level Fanconi anemia (Guo et al., 2015; van der Lelij et al., 2010). We further checked whether the double mutants of *smc6-56* and *chl1Δ* showed genetic interactions. We observed no genetic interactions between *smc6-56* and *chl1Δ* (Fig5.16).

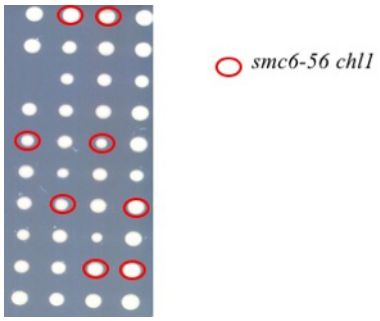

Fig5.16: *smc6-56* and *chl1Δ* do not show synthetic lethality/sickness

Another genetic interaction we were interested in testing was between *smc6-56* and *srs2Δ*. *srs2Δ sgs1Δ* double mutant shows G2/M arrest most likely due to improper recombination events, the double mutant also shows rDNA circles and premature aging (McVey et al., 2001).

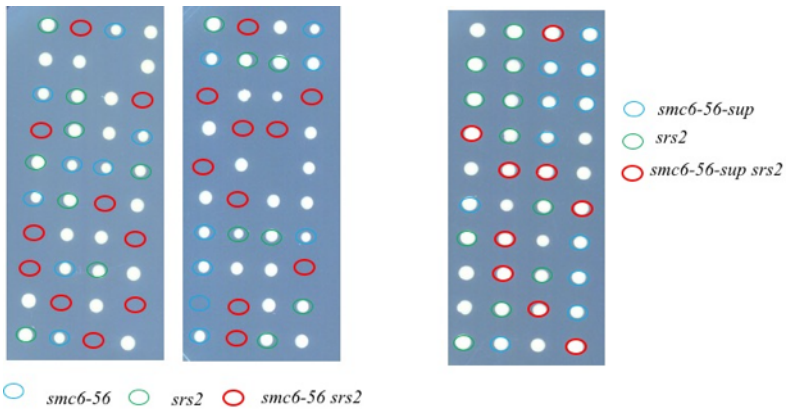

Fig5.17: Synthetic lethality between *smc6-56* and *srs2Δ* rescued by suppressor mutation as observed by tetrad analysis

We observed that similar to *sgs1Δ*, *srs2Δ smc6-56* showed synthetic lethality, which was rescued by the suppressor mutation (Fig5.17).

We decided to check the DNA damage sensitivity of suppressor in combination with several other factors to check the difference between WT and *smc6-56-sup*. We started off by checking the DNA damage sensitivity of STR deletion/depletion strains in combination with *smc6-56-sup*. We began with MMS, HU and CPT sensitivity that cause a chronic replication stress.

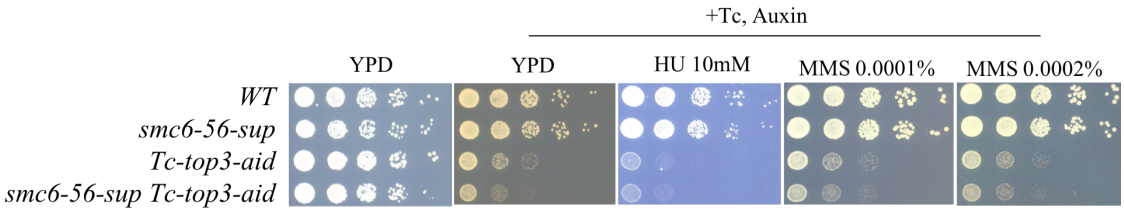

Fig5.18: Genetic interactions between Smc5/6 and STR observed by spot assay. The cells were serially diluted and spotted on the plates of indicated concentration of DNA damaging agents and images taken on 2nd day

We observed that compared to *Tc-top3-aid*, *smc6-56-sup Tc-top3-aid* was not more sensitive to DNA damage. The double mutant was showing same sensitivity as the single mutant, but had aggravated growth defects, making exact conclusions on epistasis difficult (Fig5.18).

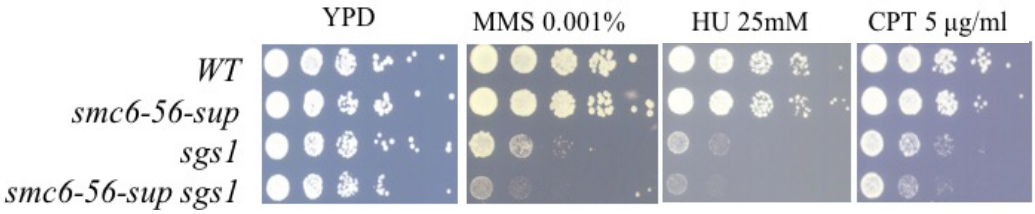

Fig5.19: Genetic interactions between Smc5/6 and STR observed by spot assay. The cells were serially diluted and spotted on the plates of indicated concentration of DNA damaging agents. Images were taken on the 2nd day

We observed that *smc6-56-sup* was showing additivity with *sgs1Δ* for DNA damage sensitivity. Alone *smc6-56-sup* was not sensitive but the combination of *smc6-56-sup sgs1Δ* was more sensitive than the single mutant *sgs1Δ* (Fig5.19). This supported the notion that *smc6-56-sup* was not able to form a fully WT Smc5/6 complex. We further wanted to see whether the aggravated DNA damage sensitivity of *smc6-56-sup sgs1Δ* depended on Rad51 mediated recombination intermediates accumulating in double mutant. We conducted a spot assay to address this question.

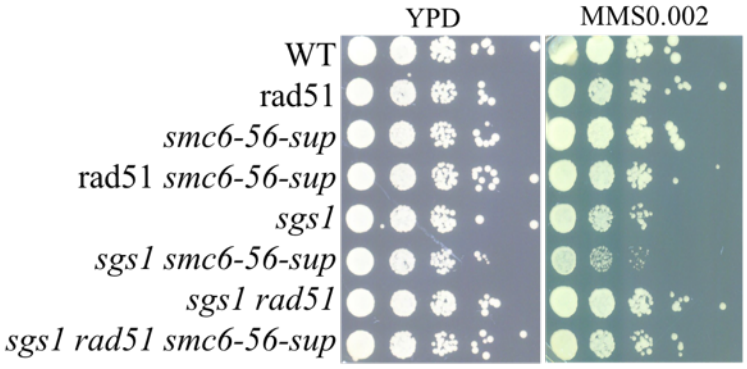

Fig5.20: Genetic interactions between Smc5/6 and STR rescued by *rad51Δ* as observed by spot assay. The cells were serially diluted and spotted on the plates of indicated concentration of DNA damaging agents. Images were taken on the 3rd day

We observed that the aggravated MMS sensitivity of *smc6-56-sup sgs1Δ* was indeed due to the unresolved recombination intermediates and deletion of *RAD51* was able to partially rescue the DNA damage sensitivity. We further checked the effect of *smc6-56-sup* on DNA damage sensitivity of *sgs1-SIM* and *sgs1-KR* mutants to see contribution of STR SUMOylation in the synthetic interactions between Smc5/6 and STR complexes. We also checked the effect of *smc6-56-sup* mutation on DNA damage sensitivity of mus81*Δ*/mms4*Δ* by spot assay.

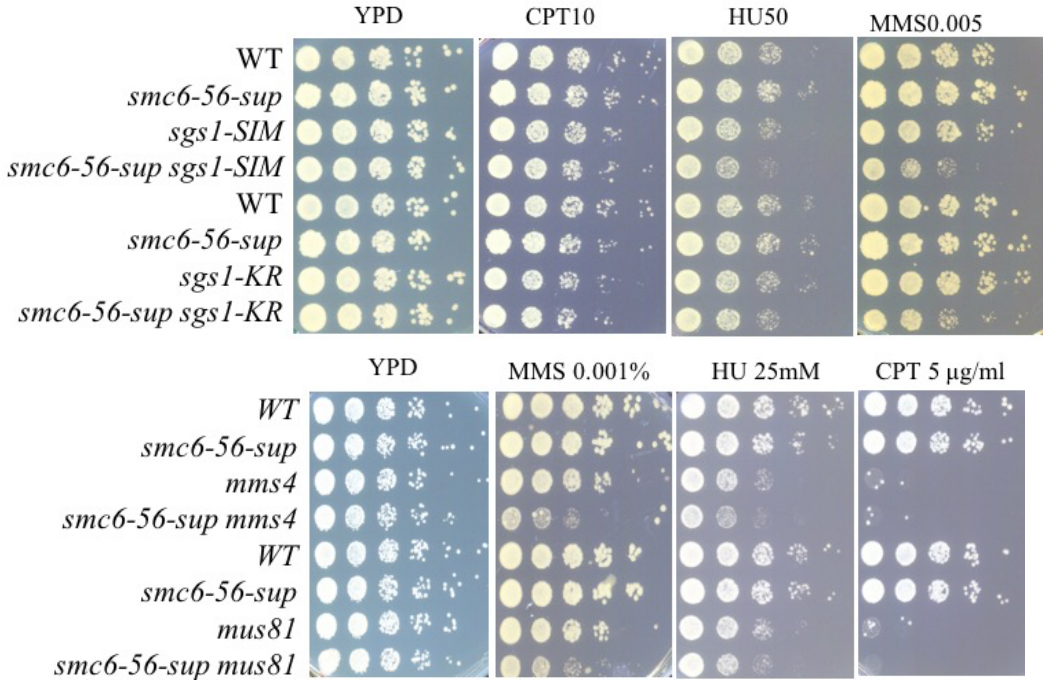

Fig5.21: Genetic interactions between *smc6-56-sup* and sgs1/*mus81Δ/mms4Δ* observed by spot assay. The cells were serially diluted and spotted on the plates of indicated concentration of DNA damaging agents and images were taken on 2nd day

Similar to *sgs1Δ*, we observed additivity between *smc6-56-sup* and *sgs1-SIM/mus81Δ/mms4Δ* DNA damage sensitivity while additivity between *smc6-56-sup* and *sgs1-KR* was observed only on MMS plates. This indicated that the successful rescue of the *smc6-56* phenotypes by suppressor mutation required functional Sgs1 and Mus81 DNA repair pathways. While rescue of HU or CPT sensitivity does not critically depend on SUMOylation of Sgs1, rescue of MMS sensitivity of *smc6-56-sup* does depend on the SUMOylation of the STR complex by Smc5/6. The genetic study also suggested a role for SUMO interaction property of Sgs1 in recruitment of STR complex to stalled replication forks (aggravated HU sensitivity of *smc6-56-sup* by *sgs1-SIM* mutant).

We next checked genetic interactions (in terms of DNA damage sensitivity) between *mph1Δ*, *chl1Δ* and *srs2Δ*.

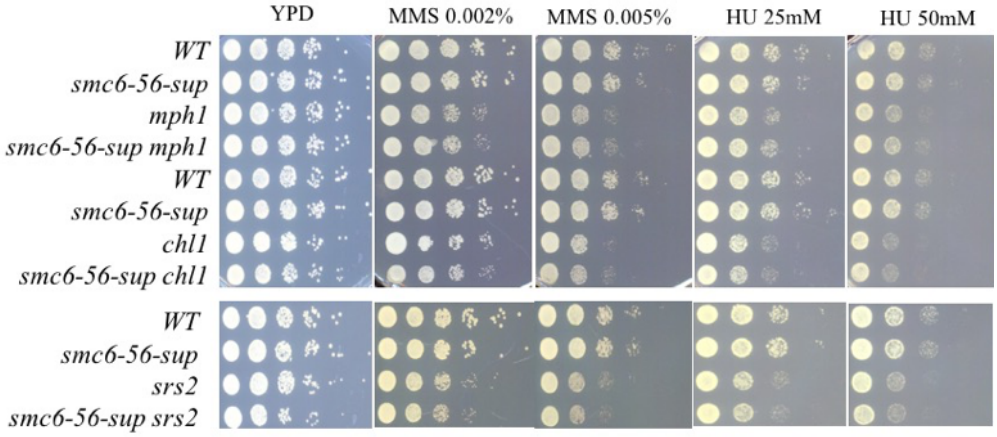

Fig5.22: Genetic interactions between *smc6-56-sup* and *mph1Δ/chl1Δ/srs2Δ* observed by spot assay. The cells were serially diluted and spotted on the plates of indicated concentration of DNA damaging agents and images taken on 2nd day

We observed no additive DNA damage sensitivity for *smc6-56-sup* in combination with *chl1Δ*, *mph1Δ* or *srs2Δ*. The genetic analysis so far suggested that for proliferation, *smc6-56* needs functional Srs2, Mus81/Mms4 and STR. To overcome DNA damage sensitivity, *smc6-56-sup* needs a functional STR complex and Mus81/Mms4, but not Srs2. Neither DNA damage sensitivity of *smc6-56-sup* nor proliferation of *smc6-56* is affected by *chl1Δ* and *mph1Δ* in any way.

5.4 *smc6-56-sup* and *sgs1* shows additive accumulation of recombination intermediates at NPSs

We previously observed that the DNA damage sensitivity of *smc6-56-sup* depended on Sgs1 function. We hypothesized that the sensitivity of the double mutant could be due to excessive accumulation of recombination intermediates at stalled RFs genome-wide upon HU treatment. To test this, we conducted 2D gel electrophoresis experiment with *Tc-sgs1* in

combination with *smc6-56* and *smc6-56-sup* with relevant single mutants. We checked both TER302 and ARS305 to see the effect at stalled RFs.

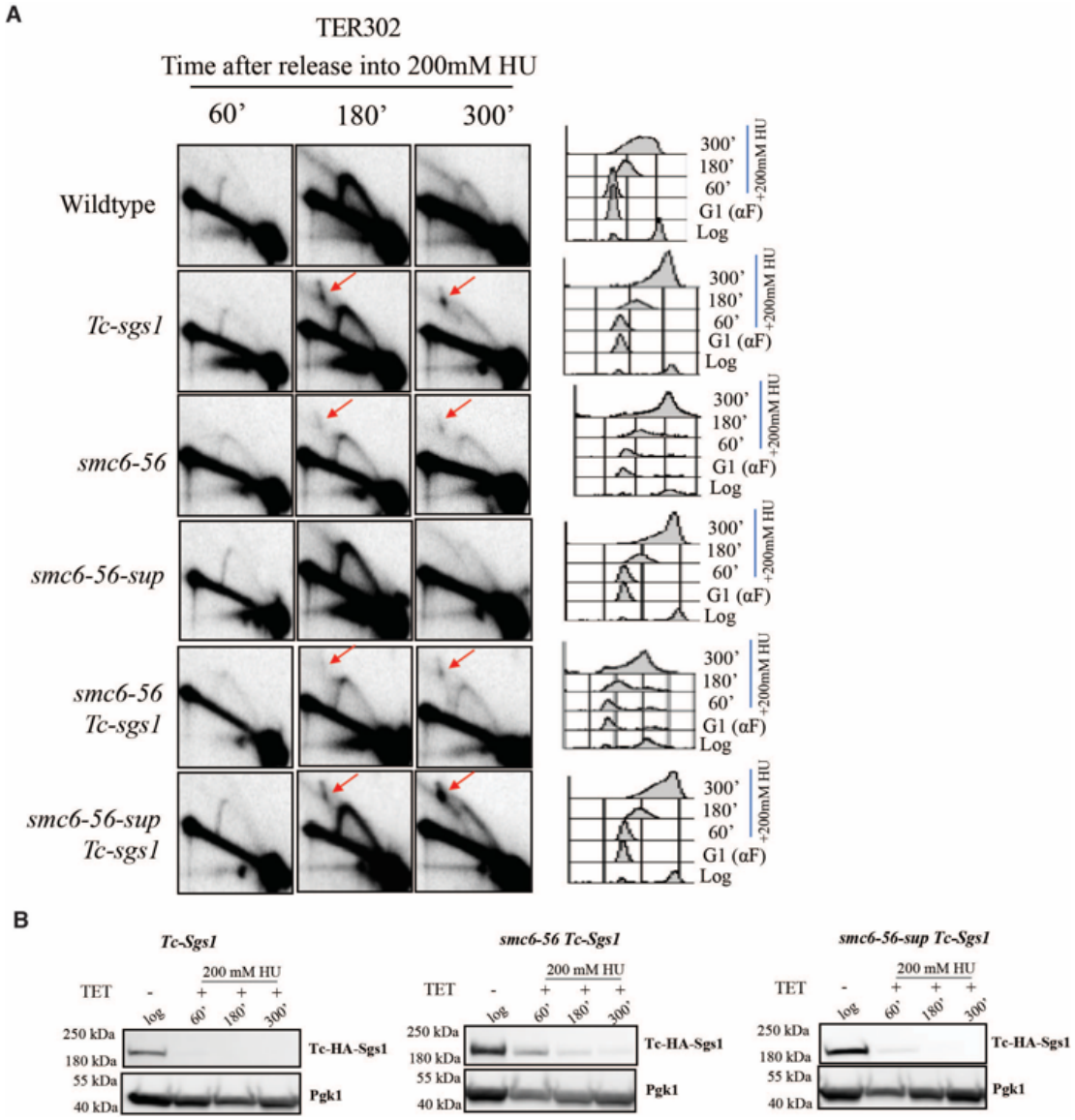

Fig5.23: Accumulation of recombination intermediates at TER302 observed by 2D gel electrophoresis. A) Schematic representation of replication intermediates observed by 2D gel electrophoresis at termination regions. B) Schematic representation of the NPS302/TER302 region analysed by 2D gels. C) Visualization of recombination intermediates by 2D gel electrophoresis from cells of the indicated genotype. The cells were synchronized in G1 phase and released in media containing 200 mM HU. Cells were collected at the indicated time-points. Sgs1 was depleted with Tetracycline. X-molecules accumulate as a spike indicated by an arrow. Cell progression confirmed by FACS analysis and protein depletion confirmed by western blot

We observed at TER302, as expected *Tc-sgs1* and *smc6-56* accumulated recombination intermediates while *smc6-56-sup* did not accumulate. The combination of *smc6-56 Tc-sgs1* accumulate recombination intermediates to the level of *sgs1* while the combination of *smc6-*

56-sup Tc-sgs1 accumulated recombination intermediates more than each of the single mutants (fig5.23).

At ARS305, we observed that, in line with our previous results, *Tc-sgs1* and *smc6-56* accumulated recombination intermediates while *smc6-56-sup* did not. The combination of *smc6-56 Tc-sgs1* accumulated even more recombination intermediates than single mutants. Interestingly, even at ARS305, *Tc-sgs1 smc6-56-sup* accumulated more recombination intermediates than the single mutants (fig5.24).

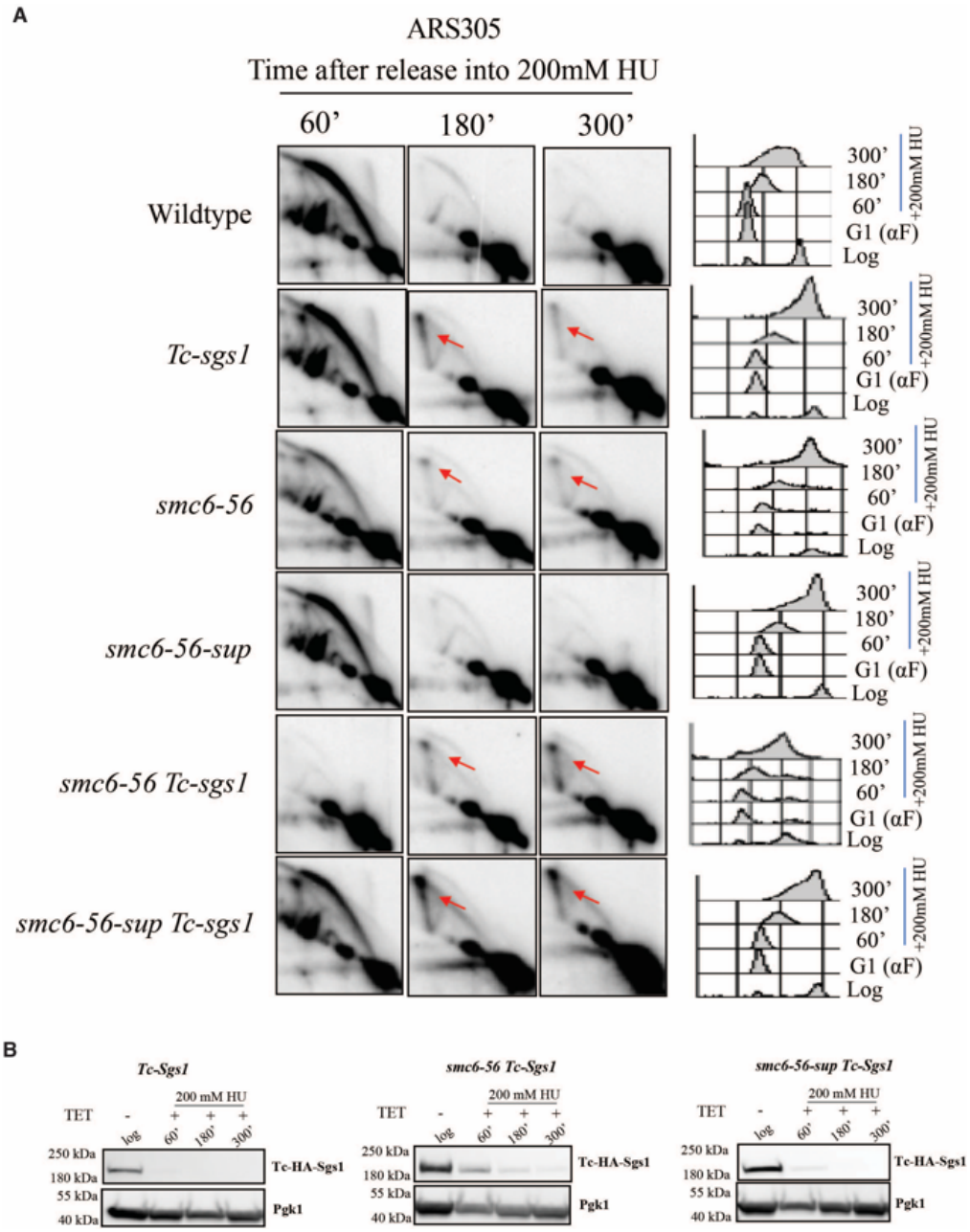

Fig5.24: Accumulation of recombination intermediates at ARS305 observed by 2D gel electrophoresis. A) Visualization of recombination intermediates by 2D gel electrophoresis at an early replicating origin from cells of the indicated genotype. The cells were synchronized in G1 phase and released in media containing 200mM HU. Cells were collected at indicated time-points. B) Sgs1 protein depletion was confirmed by western blot

Although the observation that *smc6-56-sup Tc-sgs1* accumulated more recombination intermediates than single mutants was interesting, we also observed that *Tc-sgs1* depletion was incomplete in the *smc6-56* background. To exclude the possibility of the aggravated recombination intermediate accumulation in *smc6-56-sup Tc-sgs1* is due to its ability to degrade Sgs1 better, we decided to repeat the experiment with *sgs1Δ* strains. Since *smc6-56 sgs1Δ* was lethal, we skipped this combination.

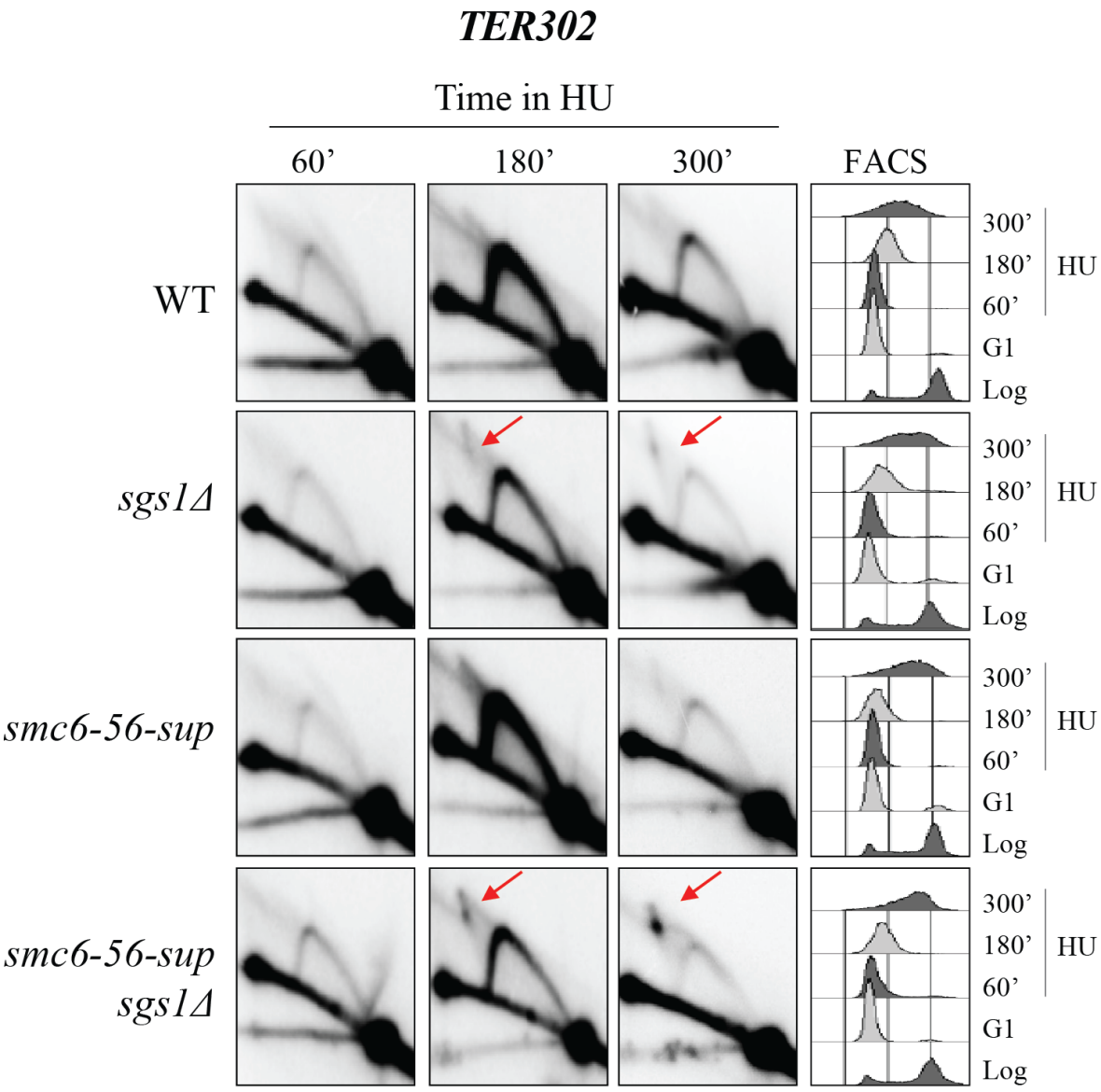

Fig5.25: Accumulation of recombination intermediates at TER302 observed by 2D gel electrophoresis. Visualization of recombination intermediates (as indicated by red arrows) by 2D gel electrophoresis from cells of the indicated genotype. The cells were synchronized in G1 phase and released in media containing 200mM HU. Cells were collected at indicated time-points

We observed that consistent with our previous results, even upon *SGS1* deletion, *smc6-56-sup sgs1Δ* accumulated more recombination intermediates that *sgs1Δ* alone both at TER302 and ARS305. This supported our hypothesis that upon HU treatment, *sgs1Δ smc6-56-sup*

accumulates excessive recombination intermediates and therefore shows additive sensitivity upon chronic HU treatment (Fig5.25, Fig5.26 and Fig5.19).

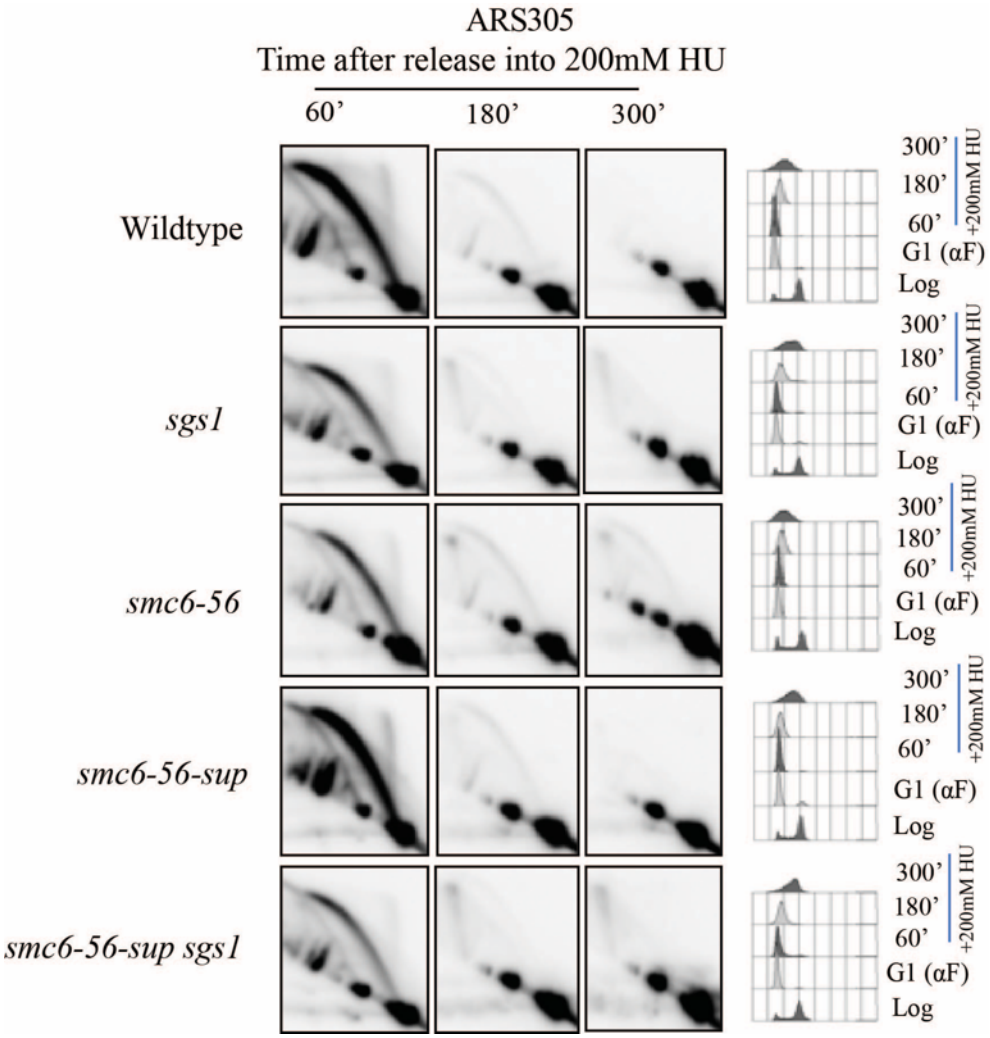

Fig5.26: Accumulation of recombination intermediates at ARS305 observed by 2D gel electrophoresis. Visualization of recombination intermediates by 2D gel electrophoresis at an early replicating origin from cells of the indicated genotype. The cells were synchronized in G1 phase and released in media containing 200 mM HU. Cells were collected at indicated time-points

We further argued that the Mus81/Mms4 pathway may be contributing to the observed aggravation in *smc6-56-sup sgs1 cells*. We therefore compared the effect of Mms4 depletion on the recombination intermediates accumulated at stalled forks at TER302 upon prolonged HU treatment and compared it with *sgs1Δ* background.

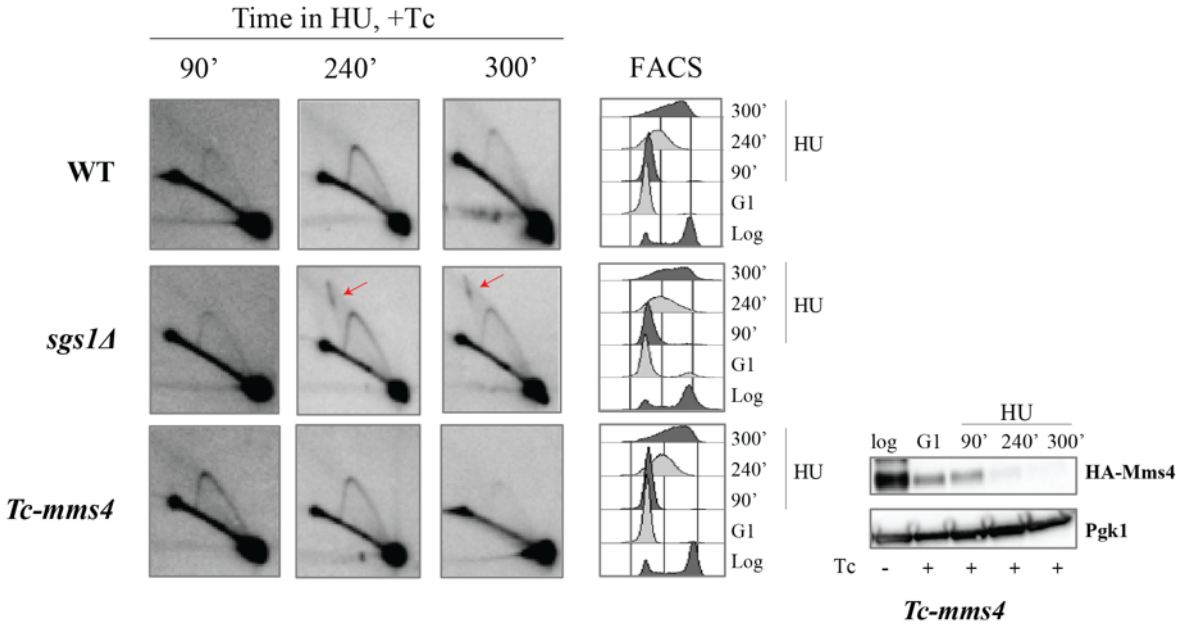

Fig5.27: Accumulation of recombination intermediates at TER302 observed by 2D gel electrophoresis. Visualization of recombination intermediates (as indicated by red arrows) by 2D gel electrophoresis at a NPS from cells of the indicated genotype. The cells were synchronized in G1 phase and released in media containing 200mM HU. Cells were collected at indicated time-points

Differently from the STR complex, depletion of Mms4 did not accumulate recombination intermediates at TER302. This suggested that in presence of STR complex, Mus81/Mms4 did not majorly contribute to the recombination intermediate resolution at NPSs. We further wanted to investigate whether Smc5/6 affects the recruitment of Mus81/Mms4 to NPSs. We checked it by ChIP-qPCR in unperturbed G2/M phase.

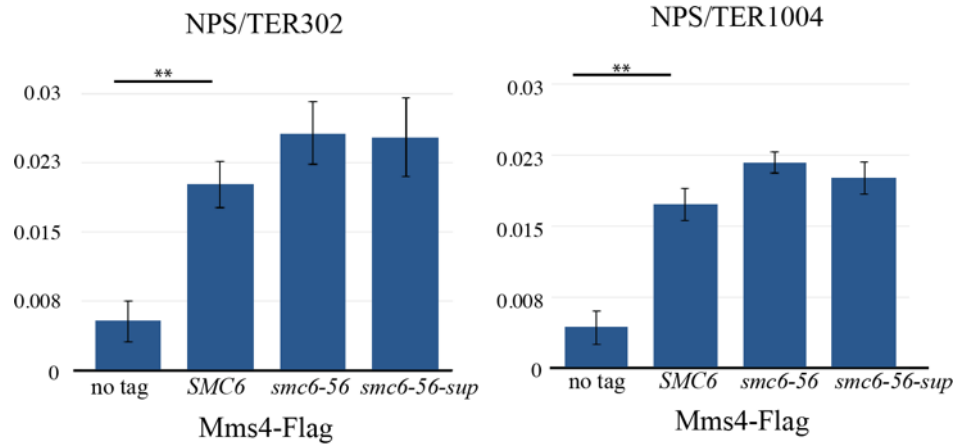

Fig5.28: Quantification of Mms4 at NPSs in WT vs *smc6-56/sup* background in unperturbed G2/M-synchronized cells (N=3)

We observed that Mms4 was present at NPSs in unperturbed G2/M phase but the recruitment of Mms4 to NPSs was not affected by *smc6-56* and *smc6-56-sup* mutations.

To summarize our findings so far, we obtained a natural suppressor of *smc6-56* temperature sensitivity which rescued several phenotypes and genetic interactions of *smc6-56*. Moreover, we observed that to rescue the *smc6-56* phenotypes at stalled forks (and DNA damage sensitivity), the suppressor needed functional Sgs1 and Mus81-Mms4. Taken together, our suppressor allowed us to uncover that Smc5/6 coordinates multiple resolvases to facilitate NPS replication.

Chapter 6

Smc5/6 and STR respond similarly to topological stress

Replication of NPSs is a complex process with a fine balance between replication and recombination. Another feature of NPSs is the topological stress accumulating at these regions. Top2 is known to bind to these regions and relieve the topological structures (Fachinetti et al., 2010). Our next objective was to understand the interaction between the two topoisomerases Top2 and Top3 and their contribution to NPS maintenance along with the Smc5/6 complex.

6.1 *SMC5/6* and *STR* show genetic interactions with *TOP2*

6.1.1 *smc5/6* and *top2* mutants show additive temperature sensitivity

We used a temperature sensitive *top2* mutant for checking its genetic interactions with Smc5/6 complex as *TOP2* is essential for cell viability. We combined *top2-4* mutant with *S-smc6* and *G2-smc6* to see whether there is genetic interaction between *TOP2* and *SMC5/6*. We also used *smc6-56* to see whether we observe an additive effect of *smc5/6* and *top2* dysfunction. We checked the effect on temperature sensitivity by spot assay. We chose temperatures 30°C as the effect was seen more prominently at this temperature.

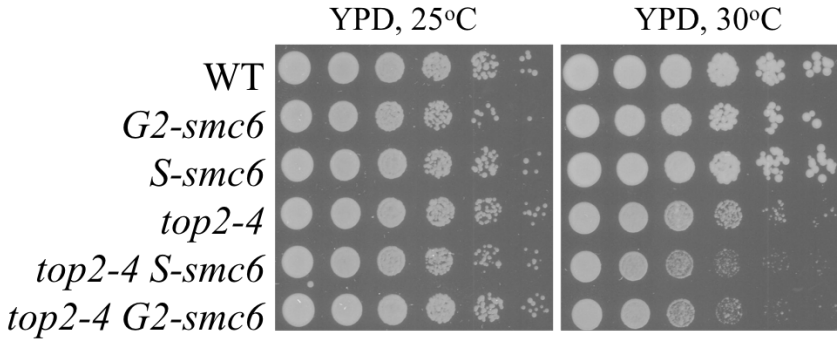

Fig6.1: Additive temperature sensitivity between *S-smc6*/*G2-smc6* and *top2-4* observed by spot assay

We observed that combination of *top2-4 S-smc6* was more temperature sensitive than *top2-4* alone (fig6.1). *G2-smc6* when combined with *top2-4* also showed aggravated temperature sensitivity, similarly with *S-smc6*. This indicated that Smc5/6 is important for cells to survive upon mutation in *top2*. In other way, without a functional Smc5/6 complex, cells required functional Top2 for survival.

We then asked if a similar genetic interaction with *top2*, is observed using the *smc6-56* mutant. *smc6-56* itself is temperature sensitive but the temperature sensitivity is prominently

seen only at 37°C or higher temperatures. At 30°C, *smc6-56* does not show temperature sensitivity or growth defects.

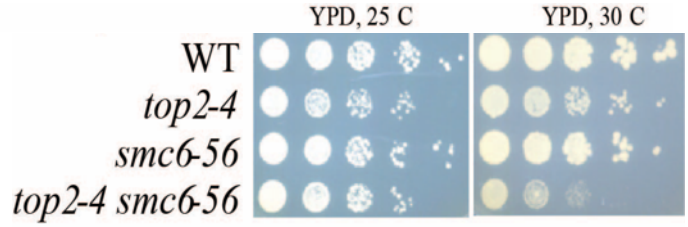

Fig6.2: Additive temperature sensitivity between *smc6-56* and *top2-4* observed by spot assay

We observed that even at permissive temperature for *smc6-56*, combination with *top2-4* resulted in reduced fitness (Fig6.2). The genetic interaction between Smc5/6 and Top2 was observed for both cell cycle restricted alleles and *smc6-56*. Thus, Smc5/6 and Top2 complement each other.

6.1.2 *sgs1/top3/rmi1* and *top2* mutants show additive temperature sensitivity

In previous chapter, we discussed genetic interactions between Smc5/6 and the STR complex. We further observed genetic interaction between Smc5/6 and Top2. We were now curious to see the role of STR complex in the absence of functional Top2. To address this, we checked the effect of *SGS1* deletion on *top2-4* temperature sensitivity.

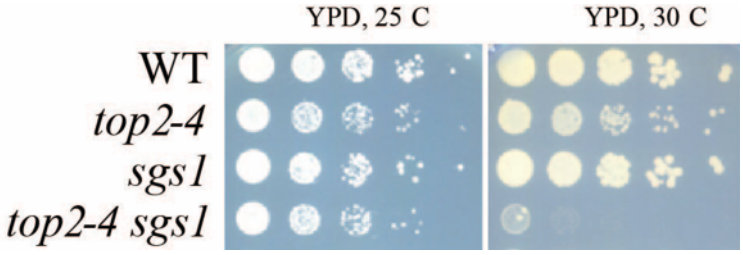

Fig6.3: Additive temperature sensitivity between *sgs1Δ* and *top2-4* observed by spot assay

We observed that similar to *smc5/6* mutants, *sgs1Δ* lowered the *top2-4* non-permissive temperature (Fig6.3). We further examined whether other components of the STR complex showed similar phenotypes. We investigated the effect of conditional depletion of Top3 (*Tc-top3*) on *top2-4* temperature sensitivity, as deletion of Top3 made cells extremely sick and prone to accumulation of random suppressor mutations. We also checked the effect of *RMI1* deletion on *top2-4* temperature sensitivity.

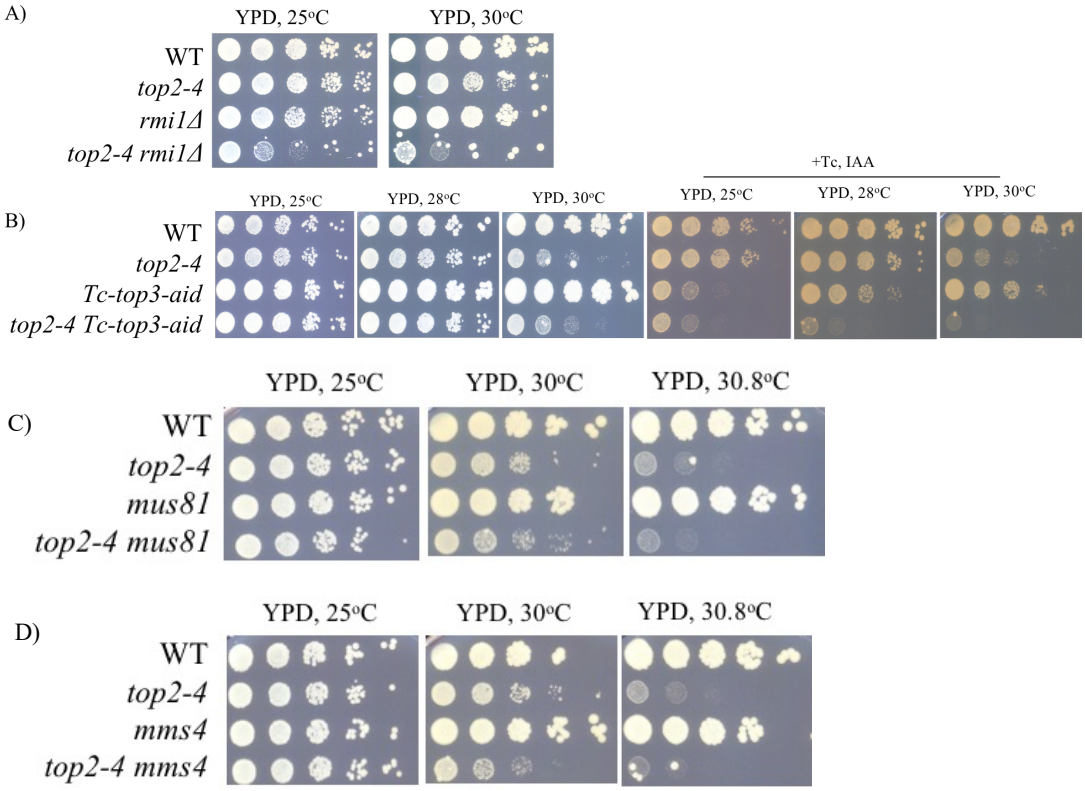

Fig6.4: Additive temperature sensitivity between *rmi1Δ, Tc-top3, mms4Δ*, *mus81Δ* and *top2-4* observed by spot assay

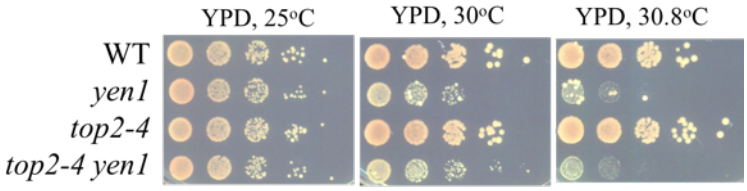

Fig6.5: No additive temperature sensitivity between *yen1Δ* and *top2-4* as observed by spot assay

We observed that similar to *sgs1Δ*, deletion of *RMI1* also caused aggravated temperature sensitivity of *top2-4*. This effect was also seen with conditional depletion of Top3. Deletion of *MMS4* but not *MUS81* aggravated the temperature sensitivity of *top2-4*, indicating this might not be due to the endonuclease activity of Mus81, but potentially other interactors. We also checked the effect of deletion of *YEN1* on *top2-4*, Yen1 acts as a HJ resolvase similar to Mus81/Mms4. We observed no additive sensitivity between *yen1* and *top2-4*. This suggested a role for Mms4 independent of the structure specific endonuclease/resolvase complex.

We further checked the effect of *sgs1-SIM* (with a mutation in the SUMO interacting motif) and *sgs1-KR* (defective in SUMOylation) on *top2-4* temperature sensitivity in order to understand the effect of Sgs1 SUMoylation by Smc5/6 complex on its role in *top2-4* background.

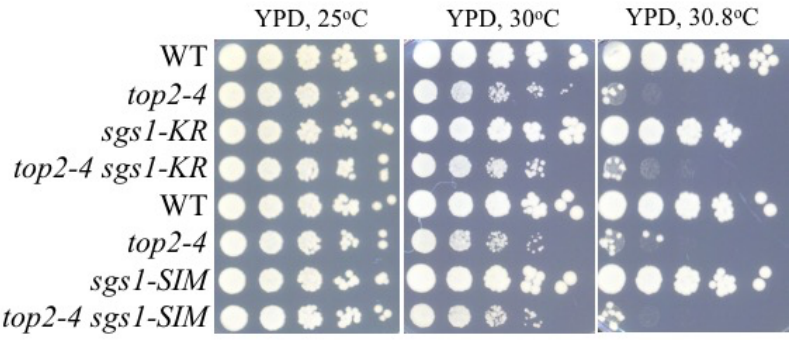

Fig6.6: No additive temperature sensitivity between *sgs1-SIM, sgs1-KR* and *top2-4* as observed by spot assay

We observed that SUMO defective or SUMO interaction defective Sgs1 mutants do not aggravate the temperature sensitivity of *top2-4*. This indicated that the role of Sgs1 at topologically constrained regions upon *top2-4* mutation was independent of SUMOylation or its interaction with Smc5/6 facilitated by the SIM motif of Sgs1. We concluded that similarly to Smc5/6, the STR complex also plays a role in maintaining cell viability when Top2 function is impaired however the role was independent of SUMOylation. We now wanted to further understand the interaction between Top2 and Smc5/6 (and STR) at NPSs in unperturbed cell cycle. We decided to see the various mutant phenotypes genome-wide and at NPSs.

6.2 Genome-wide effects of STR/Smc5/6 and Top2 dysfunction

6.2.1 The genome-wide distribution of Smc5/6 and Top3 increases upon Top2 dysfunction

It is reported that the genome-wide coverage of Smc5/6 increases upon *top2* mutation (Jeppsson et al., 2014a). We started off by confirming this observation. We checked the overlaps and genome coverage of Smc6 profile in WT vs *top2-4* backgrounds.

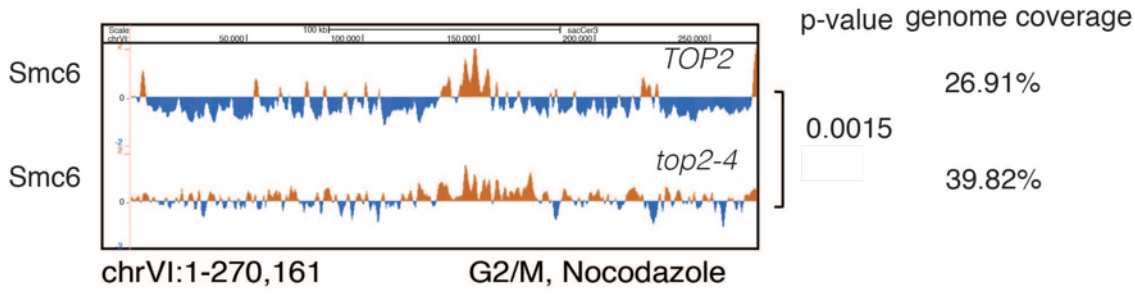

Fig6.7: Genome-wide localization of Smc6 in WT and *top2-4*: ChIP-on-chip profiles of Smc6 indicate increase in genome coverage of protein profiles in *top2-4* background in unperturbed G2/M phase. chrVI shown here as a representative image

We observed that similar to previous reports (Kegel et al., 2011), the genome coverage of Smc6 increased upon Top2 dysfunction. The ChIP was performed at permissive

temperatures. Notably, even in these conditions, Smc6 responded to increased topological stress possibly at NPSs by increase in its genome coverage.

We now wanted to check whether the same is observed for the STR complex. We began by checking the Top3 genome-wide profile in unperturbed G2/M phase in WT and *top2-4* background. We compared the profiles with Smc6 profile and also checked localization of these two proteins at NPSs in the *top2-4* background.

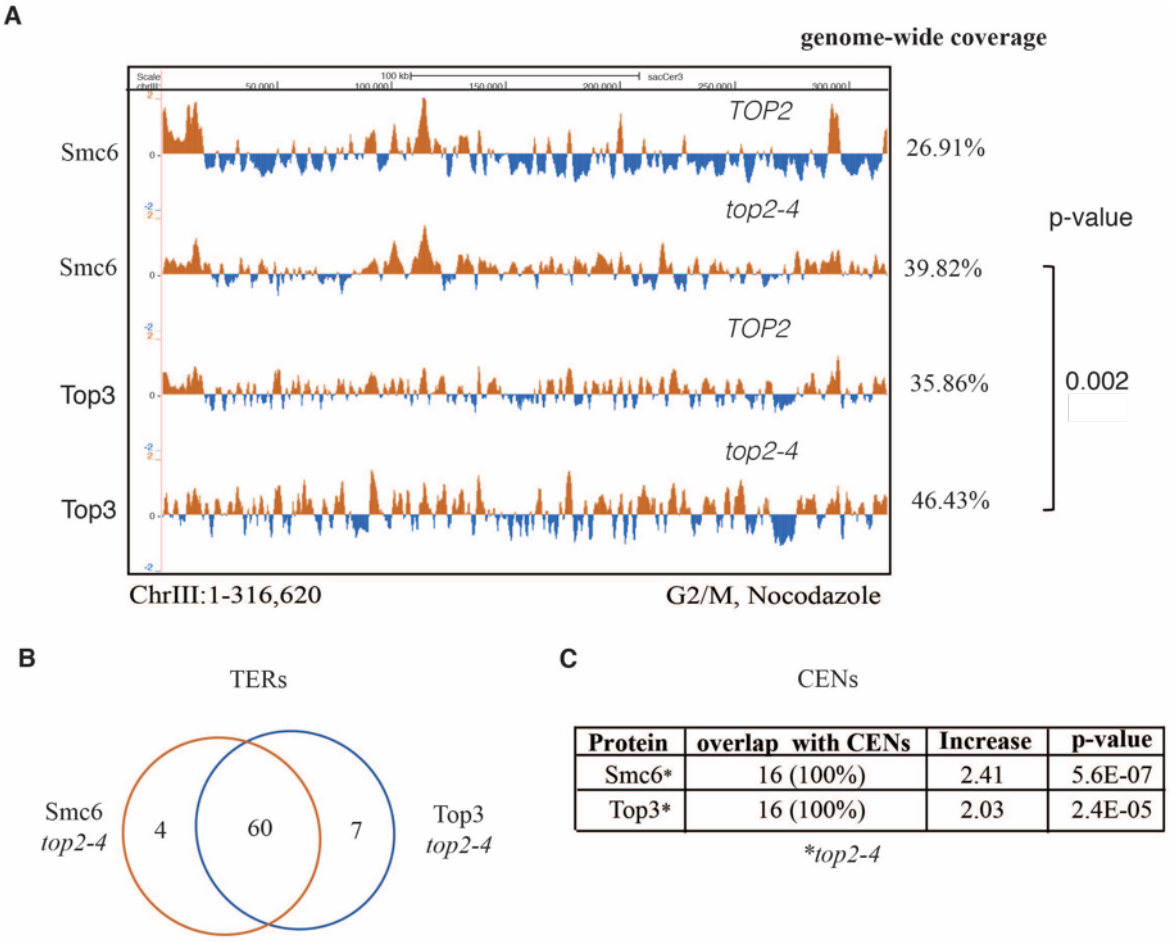

Protein	overlap with CENs	Increase	p-value
Smc6*	16 (100%)	2.41	5.6E-07
Top3*	16 (100%)	2.03	2.4E-05

**top2-4*

Fig6.8: Genome-wide localization of Smc6 and Top3 in *top2-4*: A) ChIP-on-chip profiles of Smc6 and Top3 indicate increase in genome coverage of protein profiles in unperturbed G2/M phase. Chr III shown here as a representative image. B) Manual analysis indicates overlap between TERs and Smc6 and Top3 profiles. C) The statistical analysis indicated overlap between Smc6 and Top3 profiles CENs

We observed that similar to Smc6, Top3 genome coverage increases by more than 10% upon Top2 dysfunction. We observed that Smc6 and Top3 are enriched at NPSs such as TERs and CENs. The profiles of Smc6 and Top3 overlap with each other in *top2-4*. This indicated that even though the topological stress induces more recruitment of Smc6 and Top3 to the genome, they are still present at similar loci and possibly act together at NPSs and other locations upon aggravated topological stress. To examine if this may be extended to the

whole STR complex or is specific to Top3, we decided to check the effect of *top2-4* mutation on genome-wide localization of Rmi1 by ChIP-on-chip.

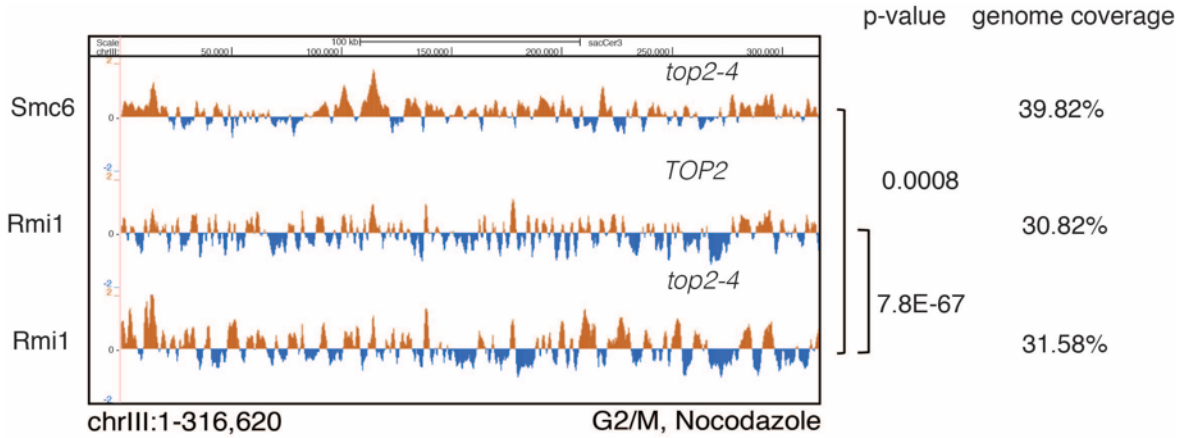

Fig6.9: Genome-wide localization of Smc6 and Rmi1 in WT and *top2-4*: ChIP-on-chip profiles of Rmi1 indicates only minimal increase in genome coverage of protein profile in *top2-4* background in unperturbed G2/M phase. Chr III shown here as a representative image

Unlike Top3 and Smc6, Rmi1 showed no increase in genome-wide coverage upon *top2-4* mutation. This could be due to two possible reasons. Rmi1 binds to DNA through its DNA binding domain and aggravated topological stress does not change its DNA binding capacity. Another possibility is that mutation in Top2 increases the genome-wide topological stress which triggers increased Top3 action and it has not particular effect on the role of STR complex. This could be similar to the observations made in bacterial studies where Topo III could compensate for gyrase (Topo II) deletion and process the topological stress (Hiasa and Marians, 1994). We decided to check more phenotypes of Smc5/6 and STR complex to understand the contributions of Smc5/6 and STR (or Top3 alone) upon aggravated topological stress.

6.2.2 The enrichment of Smc6 and Top3 at NPSs is not affected by *top2-4* mutation

Once we saw an effect on genome-wide overlap of Smc6 and Top3 upon Top2 dysfunction, we asked whether this meant there having less Smc6 or Top3 at NPSs in order to compensate for the broader distribution. We checked this by ChIP-qPCR at two TERs in unperturbed G2/M phase.

We observed that at NPSs there was no quantitative difference in the enrichment of either Smc6 or Top3 (Fig6.10). This indicated that the protein complexes were present at NPSs to WT levels but were also present at other locations of increased topological stress. To understand how was the increased genome-coverage taking place, we quantified and compared the amounts of Smc6, Top3 and Rmi1 levels from WT and *top2-4* strains.

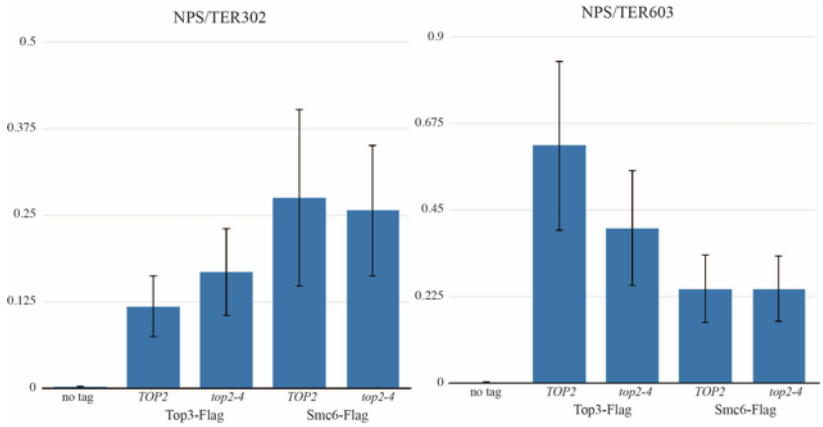

Fig6.10: Quantification of Smc6 and Top3 at NPSs in *TOP2* vs *top2-4*. ChIP-qPCR analysis to quantify the Smc6-Flag and Top3-Flag bound to NPSs in unperturbed G2/M cells (N=3)

6.2.3 Top3, but not Smc6 and Rmi1 levels, increase upon Top2 mutation

To understand the effect of Top2 dysfunction on Smc5/6 and STR protein levels, we performed a crude experiment. We quantified the amounts of the tagged proteins from western blot and normalized them on a loading control (Pgk1) in three independent biological replicates. These three experiments were then taken for statistical analysis by students' t-test and the data was plotted as bar graph of mean and standard error as error bars.

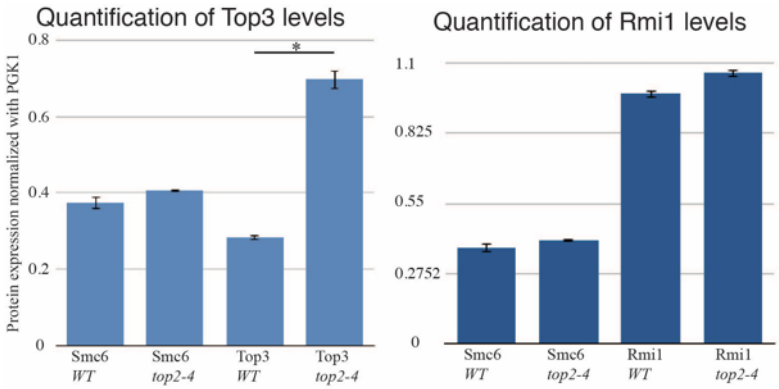

Fig6.11: Comparison of amount of Smc6/Top3/Rmi1 in WT vs *top2-4*. The amount quantified from a western blot and plotted as mean and standard error (N=3).

We observed that Smc6 level was not affected by *top2-4* mutation. However, the amount of Top3 was increased upon *top2-4* mutation. This was not true for the whole STR complex, as the amount of Rmi1 was not affected by *top2-4*.

This indicated that Top3 was compensating for the dysfunction in Top2 while this may not be a general phenomenon associated with the STR complex. As we have observed already that Top3 and Sgs1 could show different phenotypes in combination with Smc5/6 complex,

we associated this response of Top3 to topological stress as a function of Top3 alone and not of the STR complex. Moreover, as human TOP3A was reported to play a role in mitochondria, independent of the BTR complex (Nicholls et al., 2018), it is possible that the observed increase in Top3 levels may not be relevant for nuclear processes. Chromatin fractionation of Top3 levels in WT and *top2-4* may bring more light on this question.

6.2.4 Genome-wide localization of Top2 was not affected by Smc5/6 dysfunction or mutation

Since we observed that Top2 dysfunction affects Smc5/6 localization genome-wide, we were curious to see whether Smc5/6 can affect Top2 recruitment genome-wide. We checked this by ChIP-on-chip analysis of Top2 in *smc6-56*/*smc6-P4* mutant backgrounds, upon *SMC6* depletion (*smc6-aid* +AUX) and compared it with SMC6 background.

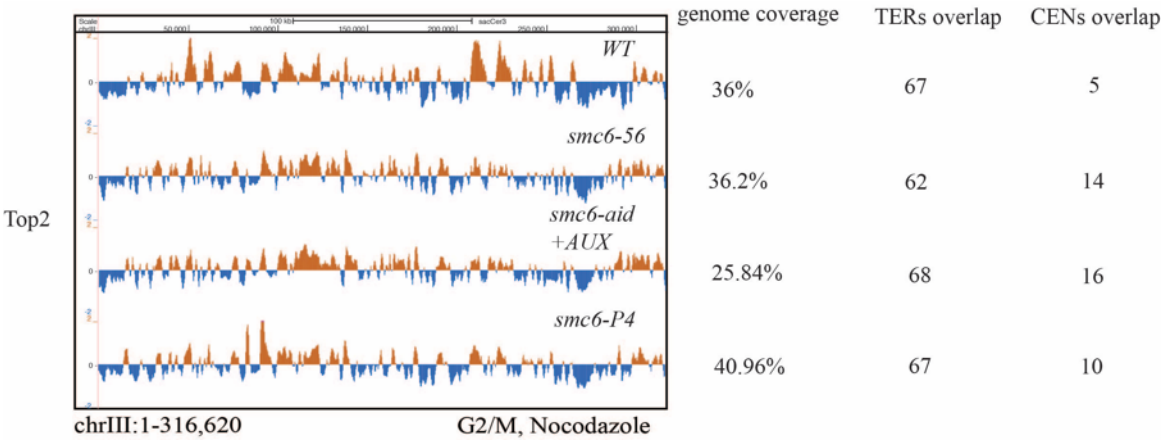

Fig6.12: Genome-wide localization of Top2 in *SMC6* vs *smc6* backgrounds: ChIP-on-chip profiles of Top2-Flag indicate increase in genome coverage of protein profiles in unperturbed G2/M phase. Chr III shown here as a representative image. The genome coverage and TER/CEN overlap shown next to each profile

We observed that the localization of Top2 is not affected by dysfunction or depletion of Smc6 (Fig6.12). The genome coverage was variable in different mutants but there was no common trend making it difficult to conclude. We observed that the localization to TERs was not affected by Smc6 mutation/depletion while localization to CENs was increased upon Smc6 mutation/depletion. This indicated that, at least at CENs, absence of Smc5/6 causes topological stress that needs to be compensated by Top2. However, there was no general trend for the NPSs and for genome coverage.

6.3 Overexpression of STR or Top2 or deletion of Rad51/Rad5 did not rescue the aggravation of temperature sensitivity

6.3.1 Overexpression of Top3/Sgs1 did not rescue the temperature sensitivity of *top2-4*

We previously observed that Top3 levels are increased in *top2-4* cells even at permissive temperature. We examined if *TOP3* overexpression may benefit proliferation in *top2-4* cells. We therefore checked whether the *top2-4* temperature sensitivity is rescued by overexpression of *TOP3* or *SGS1* by using a plasmid-based construct of *pGAL-TOP3* or *pGAL-SGS1*. The construct was completely shut down in presence of glucose, was mildly active in presence of raffinose and was overexpressed in presence of raffinose and galactose. We used WT cells as control along with *top2-4* cells. We used overexpression of *TOP3* dominant negative (*top3-YF*) mutant as well as WT *TOP3* (Mankouri and Hickson, 2006).

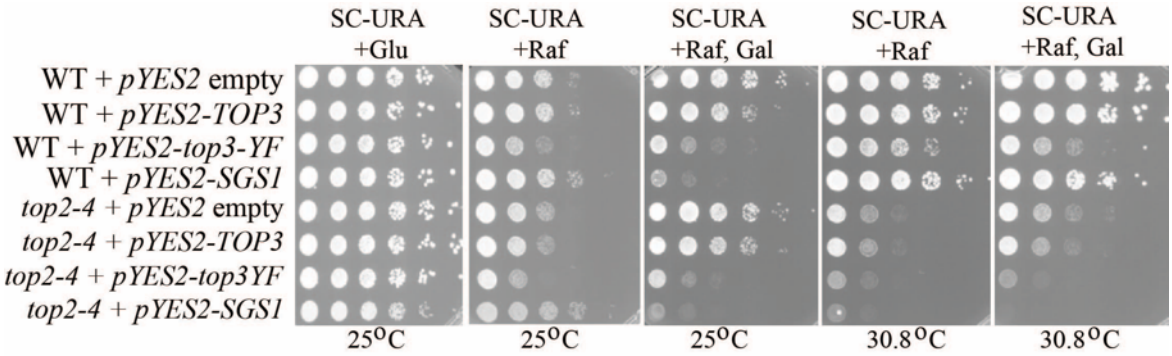

Fig6.13: Effect of overexpression of *TOP3* and *SGS1* on WT and *top2-4* observed by spot assay

We observed that *TOP3* overexpression in WT cells did not cause lethality but overexpression of *SGS1* and *TOP3-YF* did (as previously reported (Mankouri and Hickson, 2006)). Interestingly, overexpression of *SGS1* at higher temperature in WT cells was not lethal. However, *top2-4* cells did not show any growth benefit from overexpression of either Top3 or Sgs1. In contrast to WT, high levels of Sgs1 killed *top2-4* cells at higher temperatures. This indicated that excess Sgs1 at high temperature was toxic only in the presence of dysfunctional Top2. Furthermore, overexpression of Top3 did not rescue the temperature sensitivity of *top2-4* cells either, indicating that our hypothesis must be rejected. Although there are higher levels of Top3 in *top2-4* cells, overexpression of *TOP3* is not sufficient to suppress the lethality of *top2-4* at higher temperatures.

6.3.2 Overexpression of chlorella virus Top2 (cvTop2) does not rescue the temperature sensitivity of *smc6-56*

Another hypothesis that we wanted to test was whether excess *TOP2* activity can rescue the temperature sensitivity of *smc6-56*. We suspected that Smc5/6 may create a substrate for Top2. During replication, unwinding of dsDNA can accumulate positive supercoil ahead of fork and precatenanes behind the fork (Postow et al., 2001; Schvartzman and Stasiak, 2004). Chlorella virus codes for Top2 (cvTop2) that is shown to untangle both positive and negative supercoiled plasmid DNA in vitro (Lavrukhin et al., 2000). We received a plasmid-based construct for *pGAL-cvTOP2*, where upon Galactose addition cvTop2 is overexpressed (D'Ambrosio et al., 2008). We used WT and *smc6-56* strains to integrate the construct at *URA3* locus. After constructing the stable strains, we performed spot assay at permissive and high temperature.

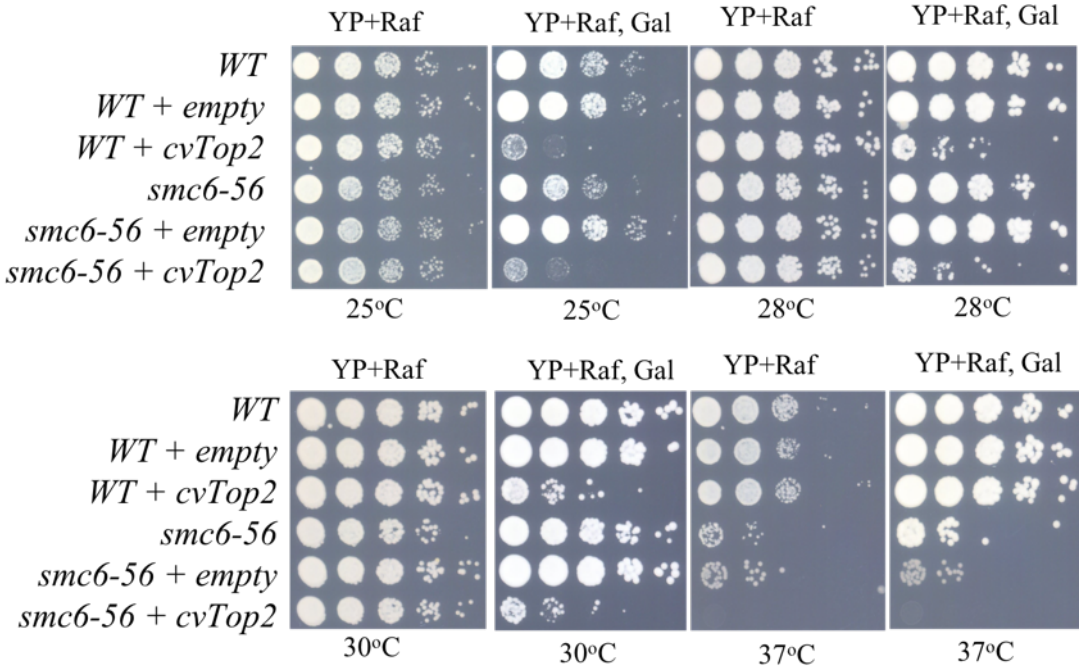

Fig6.14: Effect of overexpression of cvTop2 on the temperature sensitivity of *smc6-56* checked by spot assay

We observed that overexpression of *cvTOP2* caused lethality in the WT cells and hence did not rescue *smc6-56* phenotype. Possibly the more suitable experiment with this construct would be to check the segregation defects by microscope and allow only transient overexpression of *cvTOP2*.

6.3.3 Genetic interaction between *smc5/6*, *str* and *top2-4* is independent of recombination pathways

To understand whether the interaction observed between Smc5/6, STR and Top2 were dependent on recombination events or of a different nature, we checked the effect of Rad51 and Rad5 inactivation. We combined first *S-smc6 top2-4* with *rad5Δ* and *rad51Δ* and checked by spot assay.

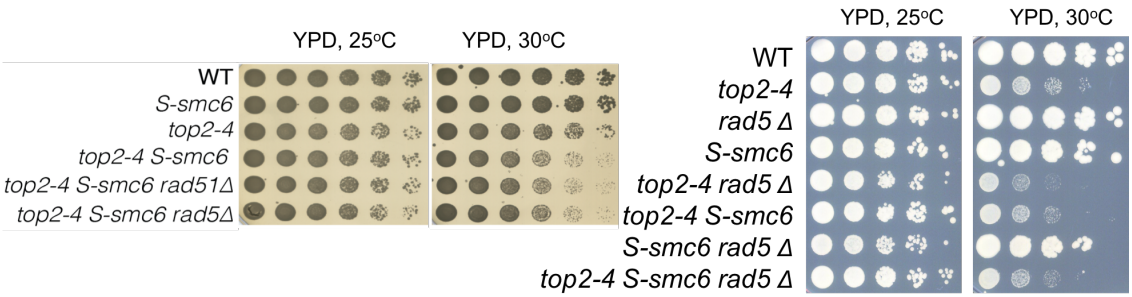

Fig6.15: Additive temperature sensitivity between *S-smc6* and *top2-4* was not rescued by *rad51Δ/rad5Δ* as observed by spot assay

We did not observe rescue of *top2-4 S-smc6* aggravated sensitivity by either *rad5Δ* or *rad51Δ*, indicating that that the aggravation of *top2-4* temperature sensitivity by *S-smc6* was not dependent on Rad5/Rad51 mediated recombination events. The same was observed for the *top2-4* combination with *Tc-sgs1* (Fig. 6.14). Notably, *rad5Δ* lowered the permissive temperature of *top2-4*, suggesting a role for Rad5 in managing the topological stress accumulating in *top2-4*, a topic that will be addressed in the next chapter.

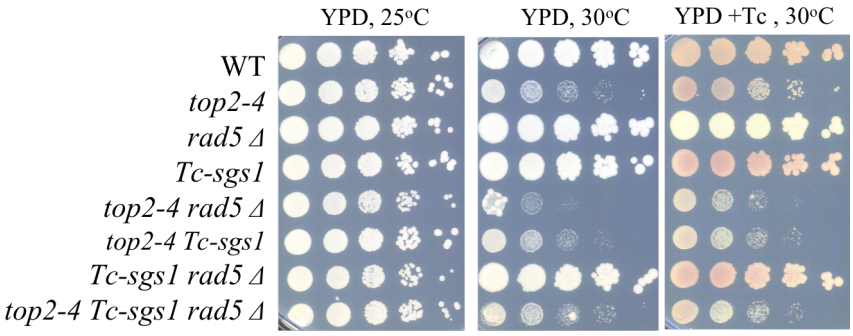

Fig6.16: Additive temperature sensitivity between *Tc-sgs1* and *top2-4* was not rescued by *rad5Δ* as observed by spot assay

In conclusion, we observed that Smc5/6 and Top3 respond to topological stress caused by *top2-4* mutation in similar manner as they both bind to DNA more abundantly. Both Smc5/6 and STR are important for survival of *top2-4* cells at higher temperature. The role is mainly Rad51 independent. We conclude that Smc5/6 and STR along with Top2 play a role in relieving topological stress at NPSs.

Interestingly, we also observed that *rad5Δ* alone aggravated the temperature sensitivity of *top2-4* more strongly that *S-smc6* or *Tc-sgs1*. We decided to investigate more along this direction and to understand the roles of Rad5 to cope with aggravated topological stress in the *top2-4* background.

Chapter 7

Cells depend on PCNA modifications while dealing with aggravated topological stress in *top2-4* mutant

When we observed that the aggravated temperature sensitivity of *top2-4 S-smc6* was not rescued by rad5*Δ*, we also observed that temperature sensitivity of *top2-4* cells was aggravated by *RAD5* deletion. We checked whether this was also observed for other factors that cooperate with Rad5 in DDT. We also examined how *top2-4* cells progressed through cell cycle in combination of various mutations to understand the reason behind synthetic sickness at high temperature. We observed that several PCNA modifiers, recombination factors and proteins of the DDT pathway aggravate the *top2-4* temperature sensitivity.

7.1 Deletion of several DDT factors and PCNA modifiers aggravated *top2-4* temperature sensitivity

We first confirmed the observation for additive temperature sensitivity between *top2-4* and *rad5Δ*. Once this was confirmed (Fig 7.1), we asked if the effect was due to defective PCNA modification. The aggravated temperature sensitivity could be due to failure of template switch due to defective PCNA polyubiquitination (affected by *MMS2* and *UBC13* mutations) or to other processes primed by PCNA monoubiquitylation (affected by *RAD18* deletion) and SUMOylation (reduced by *SIZ1* deletion). To address this, we checked the effect of deletion of *RAD18*, *MMS2*, *UBC13* and *SIZ1* on *top2-4* temperature sensitivity.

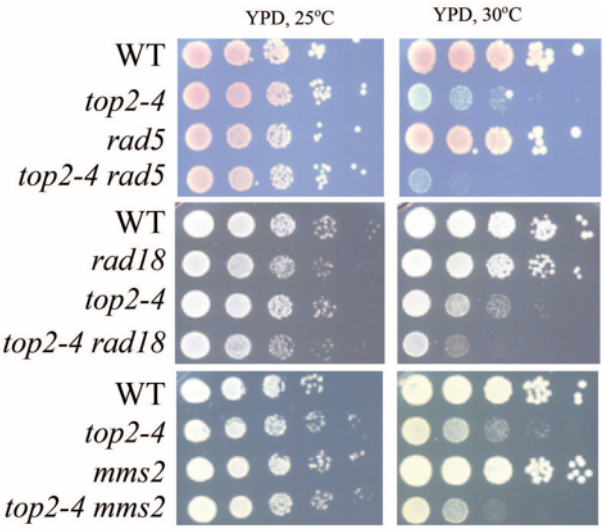

Fig7.1: Additive temperature sensitivity between *rad5Δ/rad18Δ/mms2Δ* and *top2-4* was observed by spot assay

We observed that similar to *rad5Δ*, *rad18Δ* and *mms2Δ* also showed aggravation of *top2-4* temperature sensitivity (Fig7.1). Rad18 is involved in PCNA monoubiquitylation. Mms2 along with Rad5 is part of PCNA polyubiquitination machinery. This indicated that PCNA

monoubiquitination is important for dealing with increased topological stress upon *top2-4* mutation. We confirm the relatively weak effect of *MMS2* deletion, we further checked the effect of *UBC13* deletion on *top2-4* in combination with *S-smc6* sensitivity.

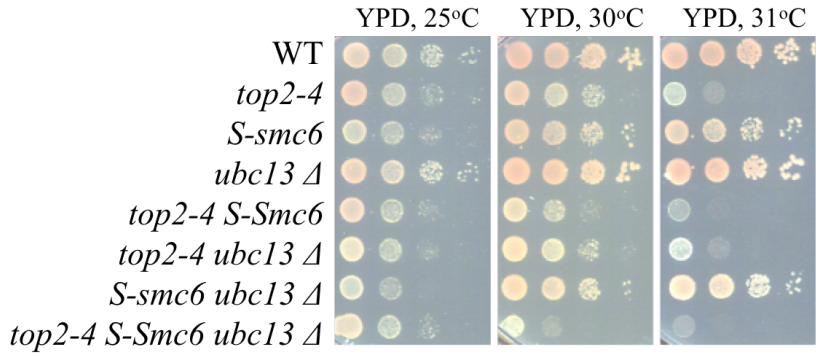

Fig7.2: Additive temperature sensitivity between *ubc13Δ* and *top2-4* was observed only when combined with *S-smc6* as observed by spot assay

We observed that *ubc13Δ top2-4* did not show increased temperature sensitivity than *top2-4* alone, *S-smc6 top2-4* was more sensitive than *top2-4* as observed previously. The triple mutant *top2-4 S-smc6 ubc13Δ* was more temperature sensitive than each of the double mutants and much more sensitive than *top2-4*. Possibly due to limitations in our technique, the effect of *UBC13* deletion was observed only in the *top2-4 S-smc6* background and will need further validation. Thus, there is a milder phenotype of *ubc13Δ* and *mms2Δ* compared to *rad5Δ* or *rad18Δ*. Next, we checked whether the helicase activity of Rad5 plays a role in aggravating *top2-4* sensitivity. We = combined helicase dead *rad5-Q1106D* (Choi et al., 2015) with *top2-4* and checked its effect on temperature sensitivity of *top2-4*.

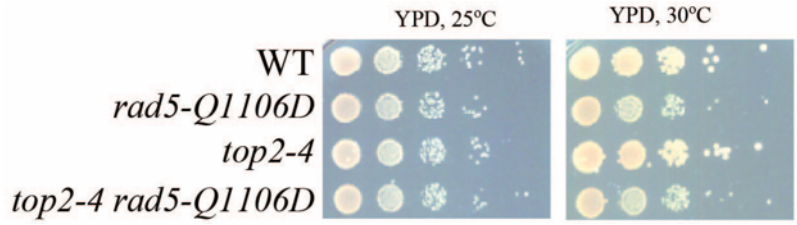

Fig7.3: No additive temperature sensitivity between *rad5-Q1106D* and *top2-4* was observed by spot assay

We observed no additive temperature sensitivity between *rad5-Q1106D* (helicase dead mutant) and *top2-4*. To roughly address whether PCNA SUMOylation may also contribute to mitigate topological stress, we checked the effect of *SIZ1* deletion on *top2-4* temperature sensitivity. To address whether the two pathways were acting in parallel with each other, we also combined *siz1Δ* with *rad5Δ* in combination with *top2-4* mutation.

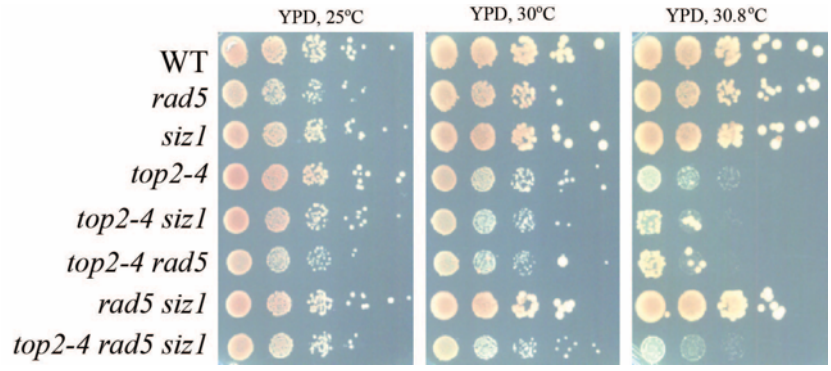

Fig7.4: Additive temperature sensitivity between *rad5Δ/siz1Δ* and *top2-4* was observed by spot assay, while the triple mutant rescued the sensitivity of double mutants

We observed that similar to *rad5Δ*, deletion of *SIZ1* aggravated the temperature sensitivity of *top2-4*. Interestingly, the triple mutant of *top2-4 rad5Δ siz1Δ* was as sensitive as *top2-4*. The effect of deletion of either *RAD5* or *SIZ1* was neutralized by not having both pathways. Because the strongest effects are observed with *rad18* and *rad5* that affect TLS in part via PCNA monoubiquitylation, we proceeded to address the role of impairing PCNA modifications with SUMO and ubiquitin at K164. Therefore, we used a PCNA mutant with defective ubiquitination *pol30-K164R* (Hoege et al., 2002). Moreover, to understand its role in parallel with the Smc5/6 complex, we made combinations of double and triple mutants for *S-smc6*, *pol30-K164R* and *top2-4*.

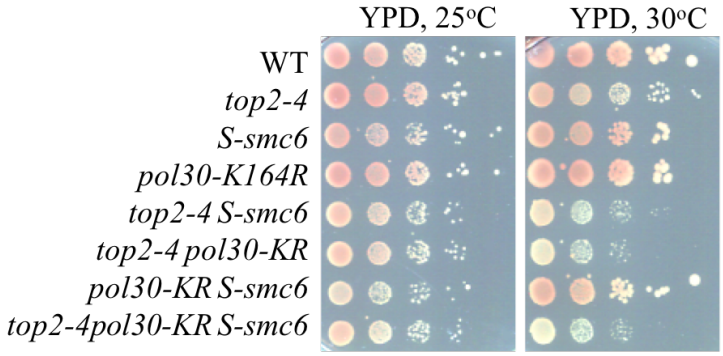

Fig7.5: Additive temperature sensitivity between *S-smc6/pol30-K164R* and *top2-4* was observed by spot assay, while the triple mutant showed same sensitivity as double mutants

We observed that similar to *S-smc6*, *pol30-K164R* also aggravated the temperature sensitivity of *top2-4*. The triple mutant however was as sensitive as the two double mutants. Another question regarding our results in this chapter so far was whether these observations are specific for *top2-4* mutant alone or they can also be observed with other *TOP2* mutants. We checked this by combining *top2-1* mutant with deletion of *RAD5*, *RAD18* and combining

top2-aid (conditional depletion strain) with deletion of *RAD5*. We checked the effect by temperature sensitivity for each combination.

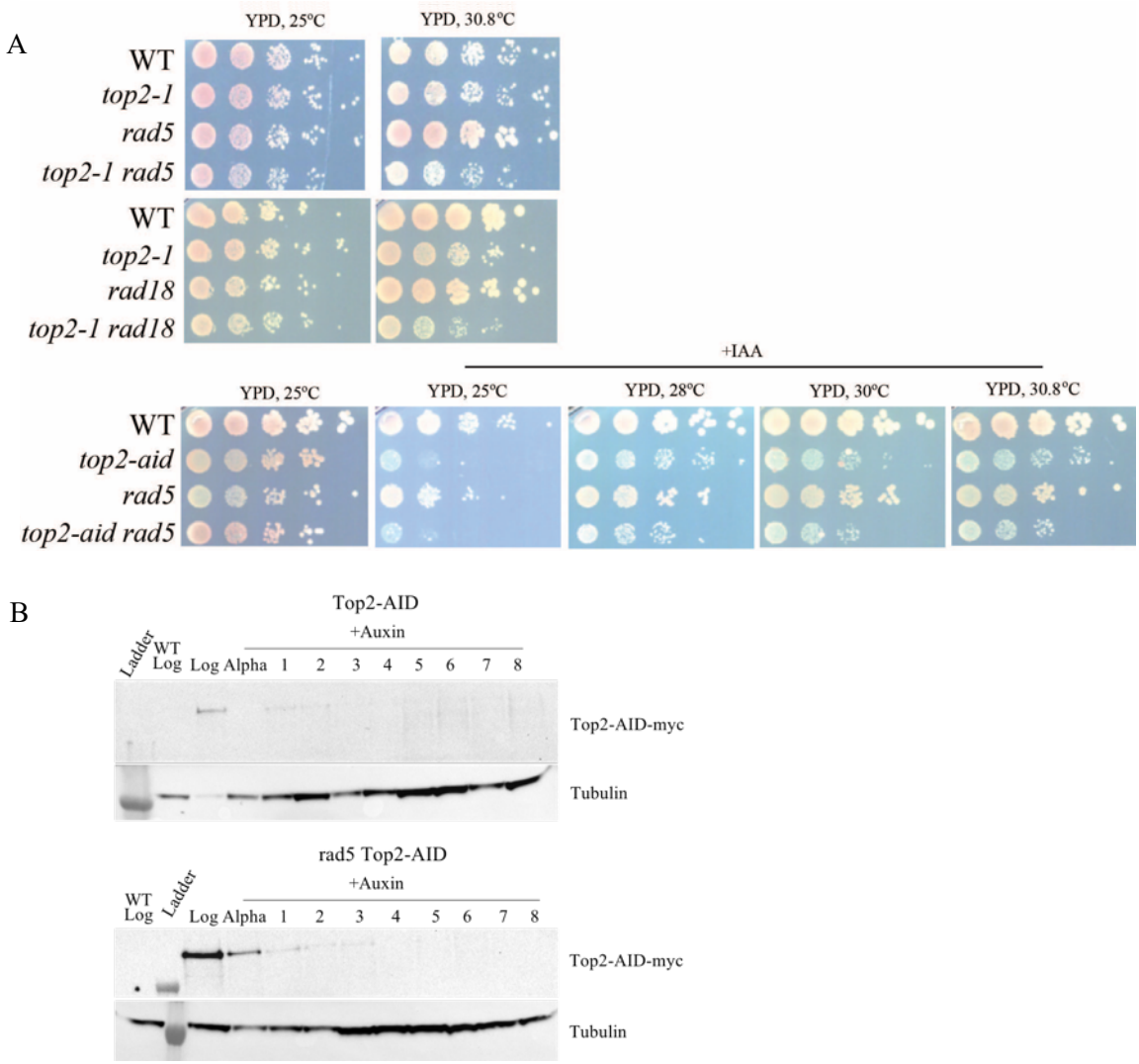

Fig7.6: A) Additive temperature sensitivity between *rad5Δ/rad18Δ* and *top2-1*, *rad5Δ* and *top2-aid* was observed by spot assay B) Long term depletion of Top2 checked by western blot

We observed that similar to *top2-4*, *top2-1* also showed mild aggravation of temperature sensitivity upon combination with *rad5Δ/rad18Δ*. *top2-1* alone was not temperature sensitive as *top2-4* at 30.8C, but we still observed mild additive sensitivity upon combining with *rad5Δ* and *rad18Δ*. Checking the growth at higher temperatures, but lower than the non-permissive temperature of 37ºC, would have been useful. We decided to use *top2-4* for further experiments. For *top2-aid*, we observed additive sensitivity on Auxin plates only at high temperature. We observed that at 25ºC, there was not additivity observed (we also checked lower auxin concentration to be sure). At higher temperature (28ºC, 30ºC and 30.8ºC), we observed the additive sensitivity between *TOP2* depletion and *RAD5* deletion. Since *TOP2* is an essential gene, we expected to see stronger lethality on Auxin plates, but

most probably the depletion of protein was leaky causing cells to survive on Auxin plates. We confirmed this by western blot, we observed residual amounts of Top2 in up to three hours and the depletion was slow and not perfect. We decided to continue with *top2-4* strain alone for further experiments.

7.2 PCNA modifications and stability are essential for proliferation in *top2-4* cells

In order to understand whether the modifications of PCNA conferred any benefit to its stability on chromatin and thus allowed better growth in *top2-4* cells, we decided to check the effect of deletion of *ELG1* on *top2-4* temperature sensitivity. Elg1 is part of the replication factor C-like complex (RLC). Elg1-RLC is known to unload the PCNA. Without Elg1 in G2/M phase, cells show increased genome instability due to retention of PCNA, while lack of Elg1 in S phase only mildly aggravates genome instability (Johnson et al., 2016). We decided to combine the deletion of *ELG1* with *top2-4* and *rad5* to check its effect on temperature sensitivity.

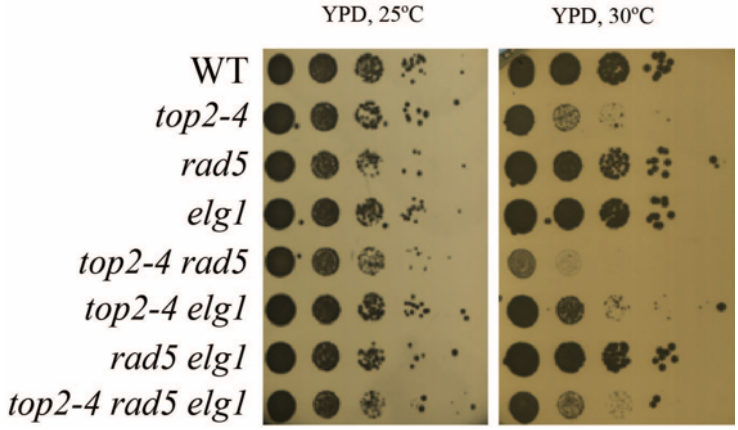

Fig7.7: Partial rescue of *top2-4* and *top2-4 rad5Δ* temperature sensitivity by *elg1Δ* as observed by spot assay

We observed that *top2-4* sensitivity was aggravated by *rad5Δ* as we have previously observed. Deletion of *ELG1* did not aggravate *top2-4* sensitivity, in fact it mildly rescued the temperature sensitivity of *top2-4*. Furthermore, *top2-4 rad5Δ* sensitivity was also partially rescued by *elg1Δ* (to *top2-4* levels). This indicated that PCNA is one of the limiting factors for *top2-4* and *top2-4 rad5Δ* growth.

In addition to deletion of *ELG1*, we used a mutant of PCNA previously established (Paul Solomon Devakumar et al., 2019) which forms weaker PCNA ring. Therefore, this *POL30* mutant is unstable on chromatin. We used strains with *POL30* replaced with a WT *POL30* allele or *POL30* replaced with mutant *pol30-DE* allele in combination with *top2-4* and *elg1Δ*. We checked the effect on temperature sensitivity by spot assay.

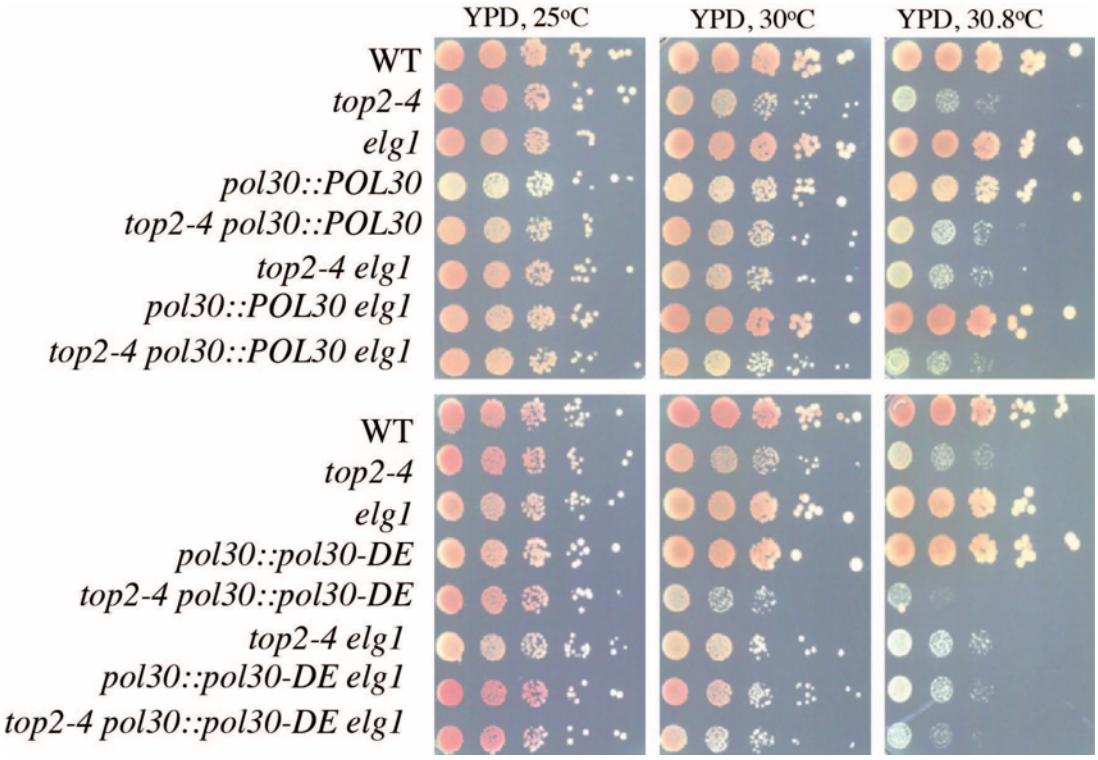

Fig7.8: Effect of destabilized PCNA on *top2-4* and *elg1Δ* observed by spot assay

We observed that similar to *pol30-K164R* mutant, *pol30-DE* also aggravated the temperature sensitivity of *top2-4*. While the *POL30* replaced with WT allele was not showing any effect on *top2-4* and *top2-4 elg1Δ*. We saw striking phenotypes for *pol30-DE*. We observed that deletion of *ELG1* mildly rescued temperature sensitivity of *top2-4* but it could not rescue *top2-4 pol30-DE* indicating that the rescue of *top2-4* was indeed relying on PCNA. We concluded that upon *top2-4* mutation, cells accumulate higher amounts of topological stress and the cells rely on PCNA dependent DNA damage tolerance pathways to maintain genome stability. In order to do so, cells need functional PCNA modification pathways and PCNA stability on chromatin.

We further wanted to dissect other recombination or repair factors involved in the process of maintaining genome stability in *top2-4* cells.

7.3 Several other factors of DDT contribute to survival of *top2-4* cells

We were curious to see which other factors contribute to the survival of *top2-4* cells at high temperature. We hypothesized that due to aggravated topological stress in *top2-4*, there could be incomplete replication that could be taken care by recombination dependent DDT pathways. In the absence of recombination dependent DDT, there could be unreplicated DNA that causes mis-segregation and chromosome loss leading to lethality. We therefore checked the factors involved in recombination pathways, helicases that respond to DNA damage as well as factors implicated in the cohesin cycle and contribute to DDT.

We started off by checking the effect of deletion of *IRC5* and mutant of *SCC1* on *top2-4* temperature sensitivity. Irc5 is one of the Snf2 family of DNA translocases that facilitates DDT and cohesion association with chromatin (Litwin et al., 2017). Cohesin is composed of the Smc1-Smc3 heterodimer that is bridged by Scc1 to form a ring that can entrap DNA to facilitate chromatin architecture and cohesion (Gligoris et al., 2014; Murayama and Uhlmann, 2015). We use a point mutant of Scc1 (S525N), *scc1-73* that is a temperature sensitive and shows reduction in Smc1/3 binding at higher temperature (Haering et al., 2004).

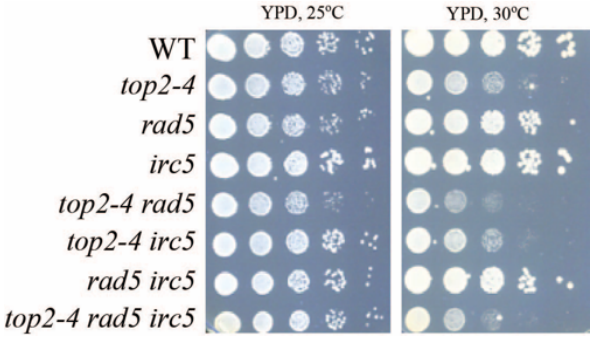

Fig7.9: No additive temperature sensitivity between *irc5Δ* and *top2-4* was observed by spot assay, *top2-4 rad5Δ irc5Δ* behaved like *top2-4*

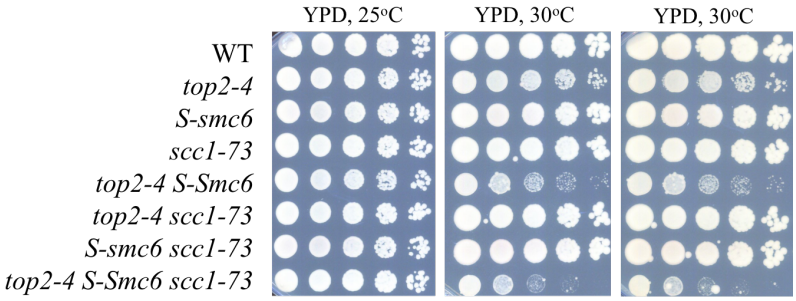

Fig7.10: Temperature sensitivity of *top2-4* was rescued by *scc1-73* only in presence of Smc6 in G2/M phase as observed by spot assay

We observed that deletion of *IRC5* did not show additive temperature sensitivity with *top2-4*, while the triple mutant of *rad5Δ irc5Δ top2-4* was as sensitive as *top2-4* (or *irc5Δ top2-4*), thus pointing out to a genetic interaction between Irc5 and Rad5 also in the context of

top2-4. To probe whether this may be related to defective cohesin, we also checked what happens to *top2-4 scc1-73* and in combination with *S-smc6*. We observed that *scc1-73* rescued the temperature sensitivity of *top2-4* to WT levels. But the combination of *top2-4 S-smc6 scc1-73* was more sensitive than *top2-4 S-smc6* indicating that the rescue of *top2-4* by *scc1-73* depended on Smc5/6 function.

In the absence of cohesin, Smc5/6 fails to load on the chromosomes. Even in *top2-4* cells, localization of Smc5/6 to chromosomes is dependent on cohesin. However, in *top2-4* background there were no increased recombination signal observed by 2D gels (Jeppsson et al., 2014a). The authors therefore proposed that cohesin protects SCIs from Top2 and allow their processing only by the Smc5/6 complex. In Scc1 mutants in *top2-4* cells although the SCIs are not protected anymore, Smc5/6 is still able to process the SCIs and thus there is rescue of temperature sensitivity. In the absence of both Smc5/6 and Top2 function, the SCIs are no longer processed. Thus, there is an increase in cell death at higher temperature. We wanted to investigate whether there were parallel pathways of processing aggravated topological stress.

Next, we checked the effect of deletion of *HMO1* on *top2-4* temperature sensitivity. Hmo1 is known to rescue the DNA damage sensitivity of *rad5Δ* (Gonzalez-Huici et al., 2014). Hmo1 is a HMG (high mobility group) family protein (Lu et al., 1996) . Hmo1 maintains the looping and compacting of DNA and facilitates transcription of RNA PolI dependent genes in particular at rDNA genes (Merz et al., 2008; Murugesapillai et al., 2014). Hmo1 is deleterious in *top2* mutants (Bermejo et al., 2009b). We were therefore curious to see the effect of deletion of *HMO1* on *top2-4 rad5Δ*

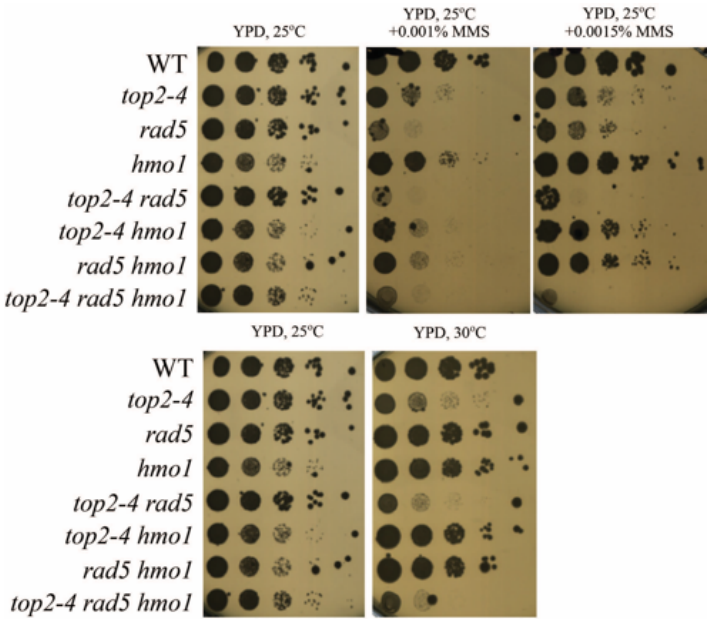

Fig7.11: Temperature sensitivity of *top2-4* and DNA damage sensitivity of *rad5Δ* was rescued by *hmo1Δ* as observed by spot assay

We observed that in consistency with previous reports, deletion of *HMO1* rescued the MMS sensitivity of *rad5Δ* (Gonzalez-Huici et al., 2014). We observed that *rad5Δ* aggravated MMS sensitivity of *top2-4* in a similar manner to temperature sensitivity. Interestingly, *hmo1Δ* could not rescue the *top2-4 rad5Δ* MMS sensitivity. We also observed that *top2-4* temperature sensitivity was rescued by *hmo1Δ* but again, it could not rescue *top2-4 rad5Δ* temperature sensitivity. This indicated that the rescue of *top2* mutant by *hmo1Δ* depended on the Rad5 function.

We then checked whether replication fork pausing caused problems in *top2-4* background. To address this, we used deletion of *FOB1*, *TOF1* and *CSM3* in combination with *top2-4* and *S-smc6*. Tof1 and Csm3 along with Mrc1 form the complex that allows repair of stalled forks upon DNA damage (Nedelcheva et al., 2005). Fob1 binds to rDNA RFB sites and facilitate fork pausing (Kobayashi and Horiuchi, 1996). Our lab had already shown that *smc6* mutants in combination with mutants of the STR complex are synthetic lethal due to excessive fork pausing and damage at rDNA regions. The synthetic lethality can thus be rescued by deletion of Fob1, Tof1 and Csm3 (Menolfi et al., 2015). We checked whether the same was also true for *S-smc6 top2-4* sensitivity.

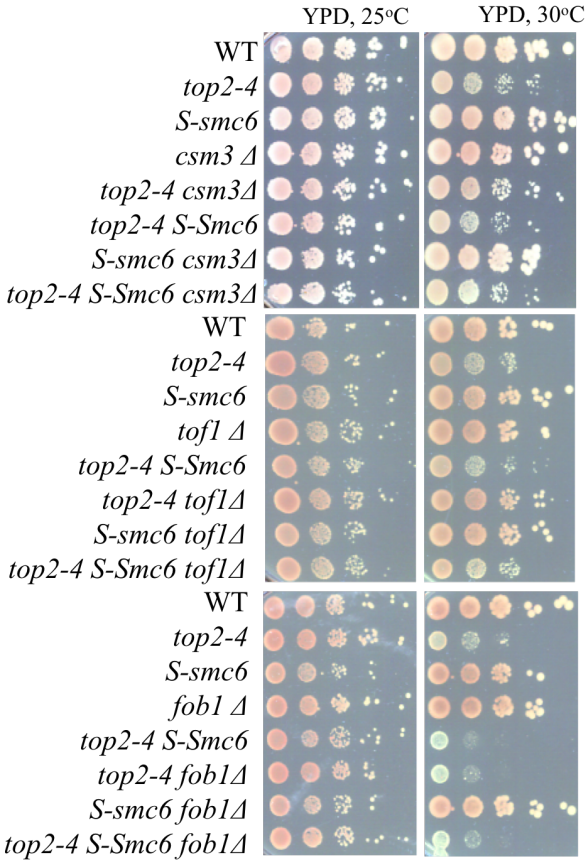

Fig7.12: Effect of *tof1Δ*/*fob1Δ*/*csm3Δ* on temperature sensitivity of *top2-4* and *S-smc6 top2-4* was observed by spot assay

We observed that deletion of *CSM3* did not increase the temperature sensitivity of *top2-4*, it mildly rescued the temperature sensitivity of both *top2-4* and *top2-4 S-smc6*. Deletion of *TOF1* rescued the *top2-4* temperature sensitivity completely, while it mildly rescued the temperature sensitivity of *top2-4 S-smc6*. Deletion of *FOB1* on the other hand did not rescue the temperature sensitivity of *top2-4* but it mildly rescued the sensitivity of *top2-4 S-smc6*. This result indicated a possibility that least partial contribution to the *top2-4 S-smc6* temperature sensitivity was due to excessive fork pausing at rDNA and other NPSs.

We further wanted to check the contribution of recombination dependent pathways on *top2-4* temperature sensitivity. We therefore checked the effect of deletion of *RAD52* and *RAD54* on *top2-4* temperature sensitivity.

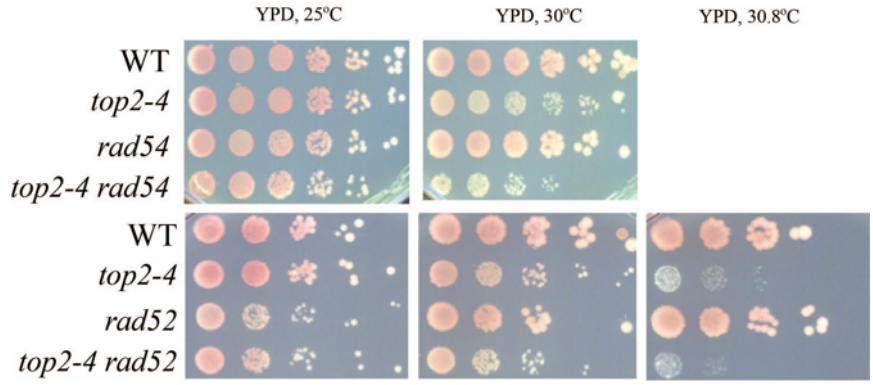

Fig7.13: Additive temperature sensitivity between *rad54Δ/rad52Δ* and *top2-4* was observed by spot assay

We observed that both mutants aggravated temperature sensitivity in *top2-4*. Thus, these pathways may act to mitigate topological stress due to Top2 dysfunction. In order to understand the dependence of topological stress generated by *top2-4* mutation on TLS polymerases, we combined deletion of all TLS polymerases with *top2-4* mutant and performed spot assay.

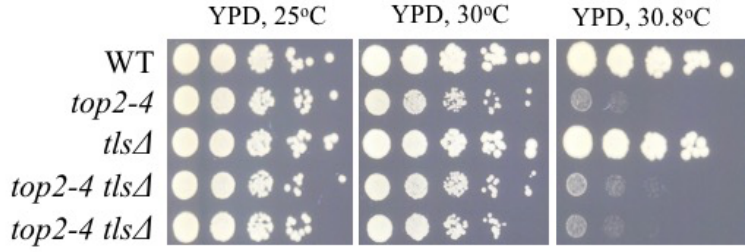

Fig7.14: Deletion of TLS polymerases did not aggravate the temperature sensitivity of *top2-4* as observed by spot assay

We observed that deletion of TLS polymerases did not aggravate *top2-4* temperature sensitivity. This indicated that the recombination dependent DDT pathways were responsible for handling the topological stress generated by *top2-4* mutant and TLS

polymerases had little to no contribution in the process. We further wanted to see the role of helicases Mph1 and Chl1 while dealing with increased topological stress in *top2-4* cells. We combined deletion of *MPH1* and *CHL1* with *top2-4* and performed spot assay.

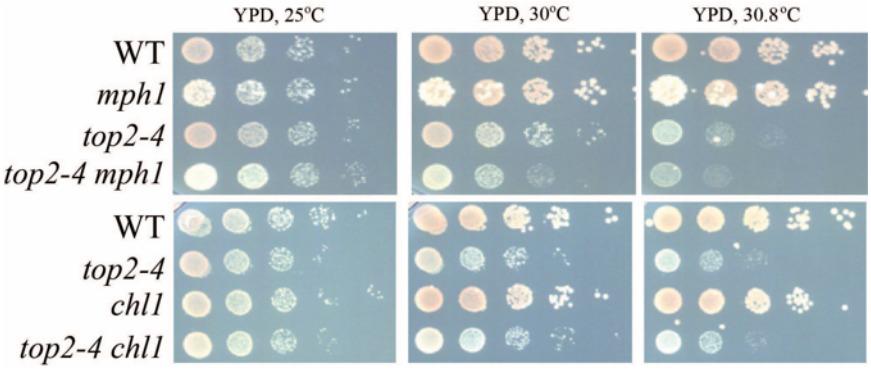

Fig7.15: No additive temperature sensitivity between *mph1Δ/chl1Δ* and *top2-4* was observed by spot assay

We observed that *top2-4* did not show additive temperature sensitivity upon deletion of *MPH1* or *CHL1* indicating that the helicases did not participate in the mechanisms of dealing with topological stress due to Top2 dysfunction.

7.4 *top2-4* cells arrest in mitosis in the absence of Rad5

In order to understand the mechanisms behind lethality of *top2-4* cells in combination with several other proteins, we checked their cell cycle progression by FACS analysis at higher temperature (30.8°C and 37°C). First, we checked long term progression for up to 6 hours after release from G1 phase at 30.8°C and 8 hours after release at 37°C. We compared the cell cycle profiles of *top2-4* and *top2-4 rad5Δ* with WT profile.

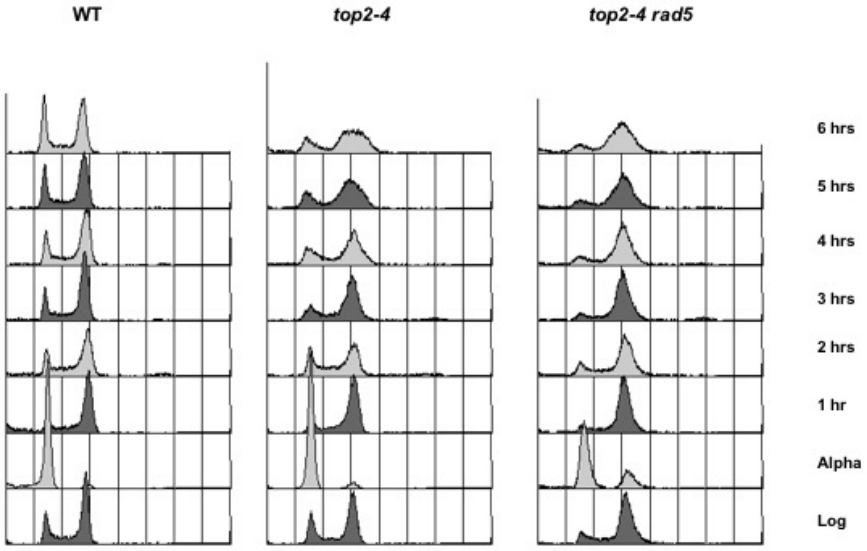

Fig7.16: Cell cycle progression of WT, *top2-4* and *top2-4 rad5* checked by FACS analysis at 30.8°C.

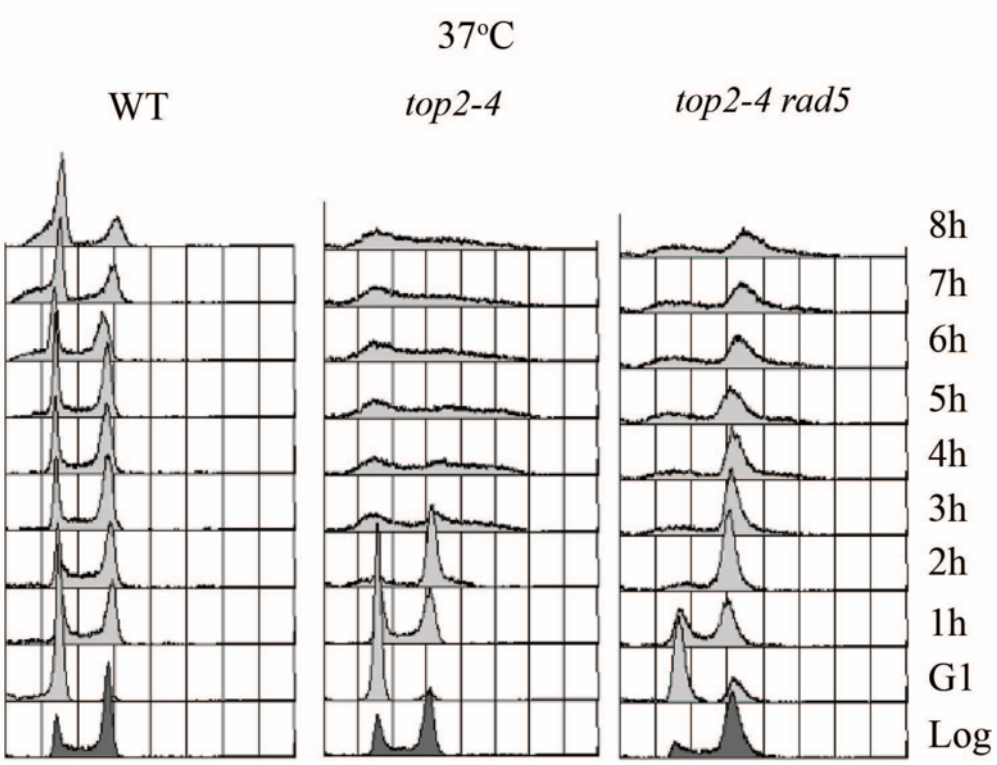

Fig7.17: Cell cycle progression of WT, *top2-4* and *top2-4 rad5* checked by FACS analysis at 37°C

We observed that at 30.8°C, within 1 hour after release from G1 WT cells progressed to G2/M phase and continued cycling thereafter. The mutant cells (both *top2-4* and *top2-4 rad5Δ*) reached G2/M phase in 1 hour, similar to WT, but they did not complete the cell cycle and remained in G2/M and mitosis even after 6 hours upon release. Differently from this, at 37°C, when WT cells were cycling faster, *top2-4* cells completed one cell cycle and remained in G1 and sub-G1phase 8 hours of release. Double mutants *top2-4 rad5* did not complete G2/M phase and majority of cells remained in mitosis. This indicated that there was an issue in completion of mitosis in *top2-4 rad5* cells that could be the cause of their lethality at high temperature. We further checked the progress of *top2-4 S-smc6*, *top2-4 pol30-K164R* and *top2-4 rad54Δ* in a similar setup at 30.8°C.

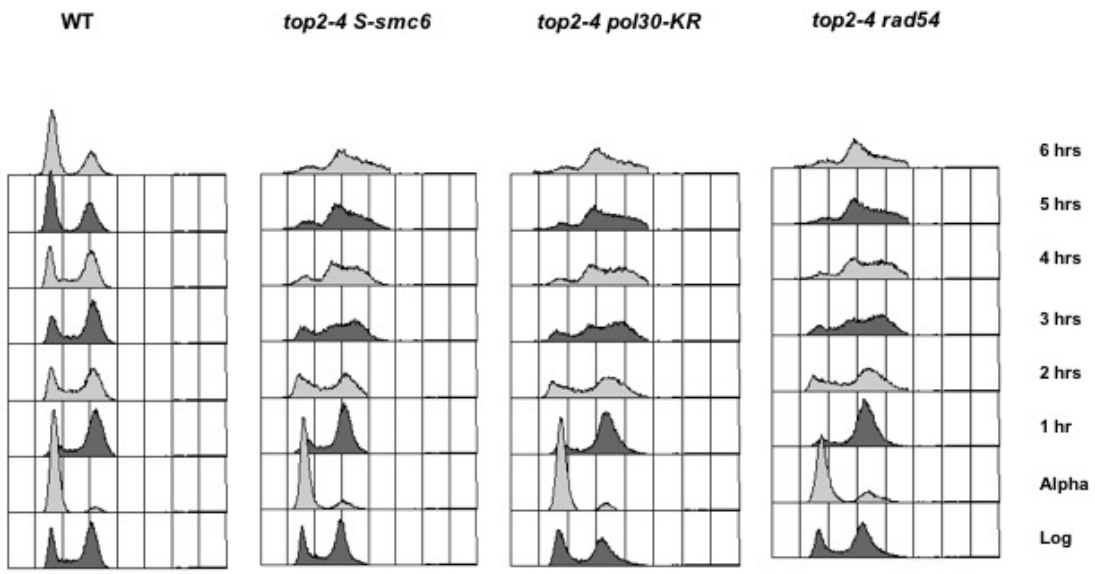

Fig7.18: Cell cycle progression of WT, *top2-4 S-smc6*, *top2-4 pol30-K164R* and *top2-4 rad54* cells checked by FACS analysis at 30.8ºC

As we had observed aggravation of *top2-4* temperature sensitivity by *sgs1Δ*, *mms4Δ* and *smc6-56*, we also checked the effect of these mutants on *top2-4* cell cycle progression in a similar manner.

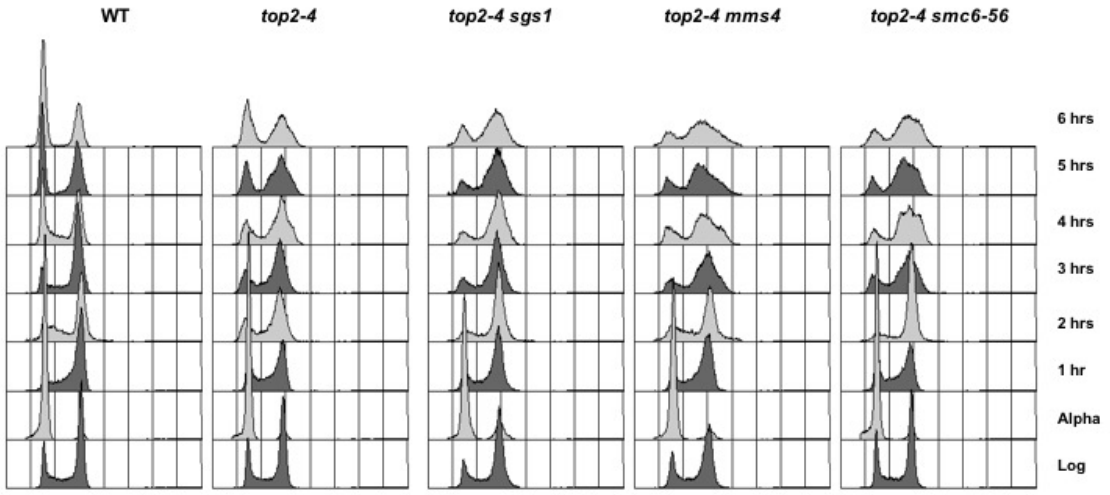

Fig7.19: Cell cycle progression of WT, *top2-4*, *top2-4 sgs1*, *top2-4 mms4* and *top2-4 smc6-56* cells checked by FACS analysis at 30.8ºC

We observed that similar to *top2-4 rad5Δ* cells, *top2-4 S-smc6*, *top2-4 pol30-K164R, top2-4 rad54Δ*, *top2-4 sgs1Δ*, *top2-4 mms4* and *top2-4 smc6-56* cells also progressed until G2/M phase and most of the cells remained in mitosis even 6 hours upon release from G1. Very small fraction of mutant cells entered the next G1 phase.

We particularly wanted to observe the release of cells from G2/M arrest. Therefore, we arrested WT and mutant cells with Nocodazole in G2/M phase and collected early timepoint samples. We checked cell cycle progression of *top2-4*, *top2-4 S-smc6* and *top2-4 rad5Δ* cells at 30.8°C for 120 min after G2/M release collecting FACS samples at various intervals. We compared the mutant cell cycle progression profiles with WT.

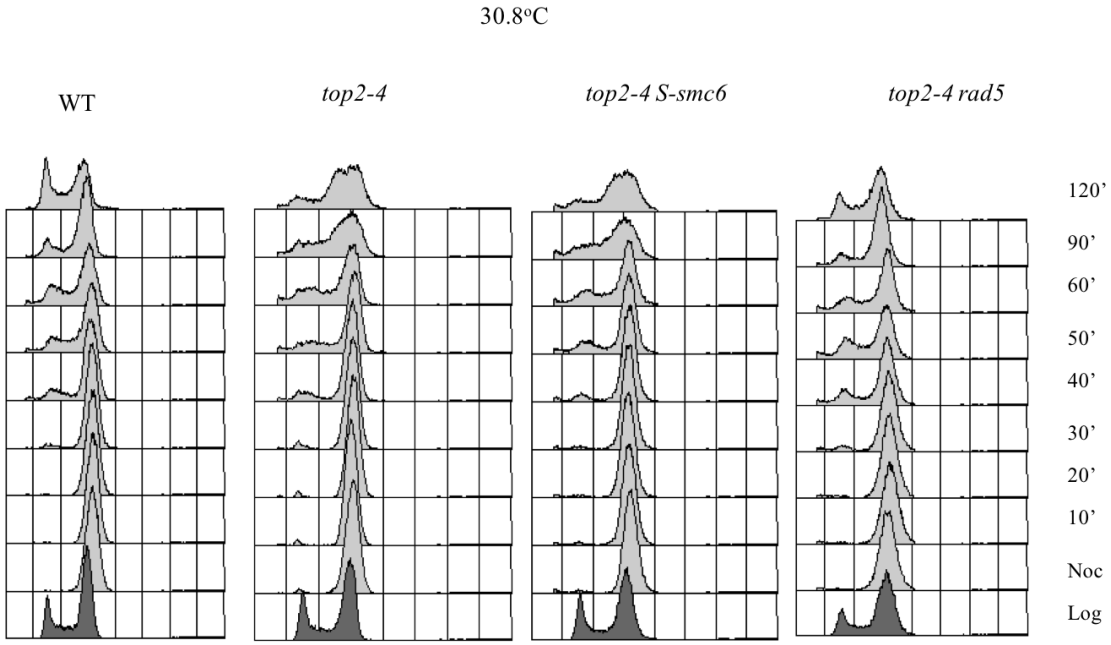

Fig7.20: Cell cycle progression of WT, *top2-4*, *top2-4 S-smc6*, and *top2-4 rad5Δ* cells checked by FACS analysis at 30.8°C

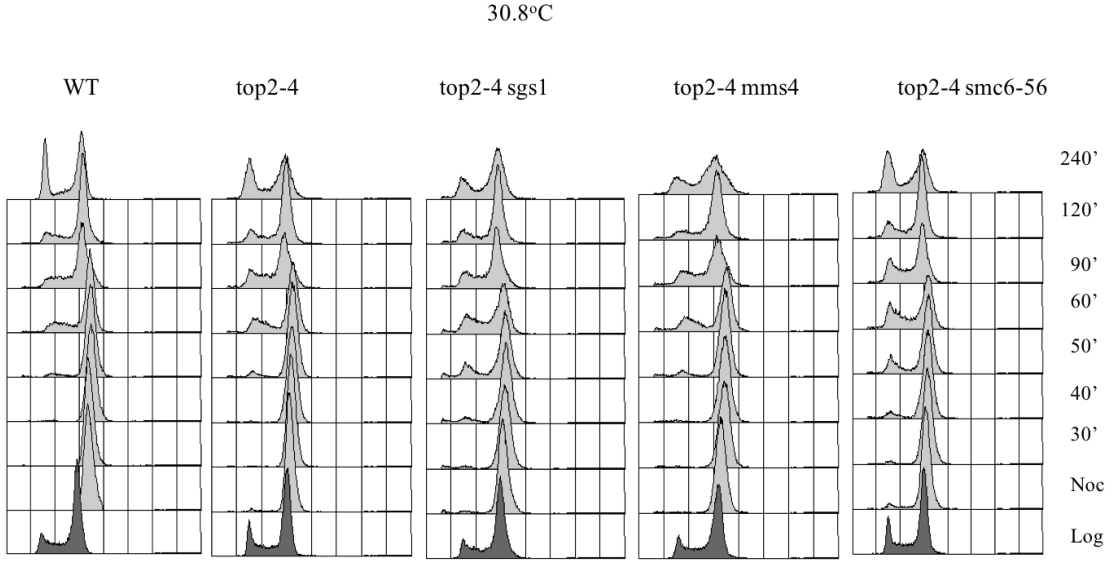

Fig7.21: Cell cycle progression of WT, *top2-4*, *top2-4 sgs1Δ*, top2-4 mms4*Δ* and *top2-4 smc6-56* cells checked by FACS analysis at 30.8°C

We observed that WT cells progressed through mitosis within 120' and we started to see a population of G1 cells. The mutants however were still in G2/M phase and the population of cells in G1 at 120 min was either negligible (*top2-4* and *top2-4 S-smc6*) or much lower compared to WT (*top2-4 rad5Δ*). This indicated that indeed the *top2-4* mutants alone and in

combination *smc5/6* and *rad5Δ* mutants were facing problems completing mitosis and starting the next cell cycle. We also observed reduction in the cells progressing in G1 phase for *top2-4 sgs1Δ* and *top2-4 mms4Δ* but not for *top2-4 smc6-56*. This result strengthened our hypothesis that *top2-4* cells depend on PCNA function or DDT pathways to complete replication and to successfully segregate chromosomes.

Thus, we conclude that along with the Smc5/6 function, PCNA modifications and stability is also important for cell viability of *top2* mutants. The cells rely on a recombination pathway resembling the one facilitating DDT to deal with aggravated topological stress at higher temperature. Without PCNA, DDT factors, Smc5/6 and STR, *top2-4* cells are not able to pass through mitosis and this severely affects their survival.

Chapter 8

Discussion and conclusions

Cells undergoing mitosis face several challenges, one of which being the successful completion of replication with high fidelity. NPSs contribute to this challenge due to their tendency to pause RFs that in turn cause DNA damage and fragility. Various features of NPSs such as tRNA genes, termination regions, Ty elements contribute to the fragility of these regions (Cheng et al., 2012; Song et al., 2014). However, the exact mechanisms of their successful replication and maintenance are not completely understood. The cells actively face risk of DNA damage while replicating these regions.

During replication helicases and topoisomerases actively facilitate replication through DNA-protein, DNA-RNA and DNA secondary structures along with regulating transcription and recombination at these fragile regions (Aguilera and Gómez-González, 2008; Azvolinsky et al., 2009b; Fachinetti et al., 2010; Lambert and Carr, 2005; Schalbetter et al., 2015). Along with the proteins actively participating in unperturbed replication of NPSs, checkpoint factors also stabilize replication fork at NPSs (Giannattasio and Branzei, 2017). Along with known factors such as Rrm3 and Top2, Smc5/6 complex is shown to be associated with early replication origins, stalled RFs, termination regions and NPSs (Lindroos et al., 2006; Menolfi et al., 2015). Components of the budding yeast Smc5/6 complex are essential for cell survival with this role being manifested during the G2/M phase of the cell cycle (Cheng et al., 2012; Menolfi et al., 2015). Here we investigated the factors collaborating with Smc5/6 complex for NPS replication and integrity.

8.1 Roles of Smc5/6 and STR in regulating recombination at NPSs

The known functions of Smc5/6 include its role in preventing chromosomal aberrations, complete or partial chromosome loss or rearrangements and chromsome segregation defects (Cheng et al., 2012). Both chromosome rearrangements and segregation defects observed for Smc5/6 mutants are potentially due to NPS instability, however the exact mechanisms of NPS maintenance by Smc5/6 are not clearly understood. Furthermore, the known catalytic activities of the Smc5/6 complex are limited to SUMOylation of multiple target proteins, DNA binding and likey loop extrusion (Marko et al., 2019; Pebernard et al., 2008; Zhao and Blobel, 2005). To play roles in DNA replication and recombination, Smc5/6 complex needs to be associated with chromosomal regions and likely with other proteins that may also be SUMOylated. Sgs1 of the STR complex is a known target of Mms21-Smc5/6 mediated SUMOylation, with this modification activating the STR function upon DNA damage

caused by MMS treatment (Bermúdez-López et al., 2016; Bonner et al., 2016). This complex is a helicase-topoisomerase complex and is known to play a role in dissolution of D-loops and dHJs during HR (Branzei et al., 2008b; Giannattasio et al., 2014a; Liberi et al., 2005b; Szakal and Branzei, 2013b). Considering the catalytic activities of the complex, STR complex appears to be an ideal collaborator for Smc5/6 complex also during NPS replication.

We confirmed the hypothesis with several experiments. Previously reported genetic interactions between *RRM3* and *SGS1* and between *SMC6* and *SGS1* were reproduced (Menolfi et al., 2015; Tong et al., 2001) indicating a role for the STR complex at NPSs and rDNA replication. Furthermore, Smc5/6 and STR complexes colocalized genome-wide and particularly at NPSs such as tRNA genes, TERs and CENs. While *smc6* partial loss of function mutants, such as *smc6-56* and *S-smc6*, are synthetic lethal with *sgs1Δ*, when we checked the genetic interaction between SUMO defective mutant of Mms21 (*mms21-CH*) with *sgs1Δ* and *sgs1* mutants that cannot be SUMOylated by Smc5/6 (*sgs1-KR*) with *smc6-56*, we did not observe synthetic lethality. This suggested that although the Smc5/6 complex modifies and regulates the action of STR complex only upon DNA damaging conditions (Bermúdez-López et al., 2016; Bonner et al., 2016), this modification is not critical in unperturbed G2/M phase. This observation was further supported by our ChIP-qPCR data, where dysfunction of Smc5/6 caused reduction in the Top3 retention at NPSs. However, mutant of Mms21 defective in SUMO ligase activity (*mms21-CH*) and mutant of Sgs1 that is not SUMOylated (*sgs1-KR*) did not show reduction in amount of Top3 at NPSs. Interestingly, combining *sgs1-SIM* mutant with *smc6-56-sup* aggravated its DNA damage sensitivity, suggesting that Smc5/6 possibly regulates other resolvases or factors that synergize with Sgs1 in dealing with replication stress. One possibility is that Top3 may play roles independent of Sgs1 in the process. If this role correlates with Top3 retention at NPSs, it will be worth to check the effect of *sgs1-SIM* mutation, alone and in combination with *smc6-56-sup*, on the recruitment of Top3-Flag to NPSs in the future. We then wondered whether increasing cellular Top3 amounts would rescue the defects of *smc5/6* mutants at NPSs. However, it was not the case. The possible explaination for this is that the activity of Smc5/6 and STR at NPSs could be due to the structural role of Smc5/6 to create substrates to be targetted by the STR complex. Smc5/6 complex was recently suggested to perform loop extrusion similar to other SMC protein complexes (Marko et al., 2019). The role of Smc5/6 during replication of NPSs could be through such topoloical entrapment of DNA and loop extrusion to identify the stalled replication forks and facilitate the creation of structures suitable for STR action. With its loop extrusion feature, Smc5/6 complex may

regulate Mph1 mediated fotk reversal. By localizing to NPSs, Smc5/6 may be preventing Mph1 to target the stalled or reversed forks (Chen et al., 2009), thus stabilizing the substrates for the STR complex. However, deletion of *MPH1* did not rescue the synthetic lethality between *smc6-56* and *sgs1Δ*. As in the absence of Smc5/6 and STR action the aberrant recombination intermediates accumulate, this result suggests that Mph1 is not singly responsible for the formation of intermediates that block cell division in *smc6-56 sgs1Δ*. Interestingly, however, Top3 recruitment to NPSs was rescued by deleting *MPH1* in *smc6-56*, suggesting potential competition between different resolvases in binding the substrate. However, deleting *MPH1* alone did not show an increase in amount of Top3 at NPSs, suggesting that it was only in the absence of Smc5/6 action that Mph1 affects Top3 recruitment. This clearly supported the hypothesis that the action of Mph1 was prevented by Smc5/6 complex to allow recruitment of Top3 (or the STR complex) at NPSs and carry out their role. This can be summarised as a model as shown in fig 8.1

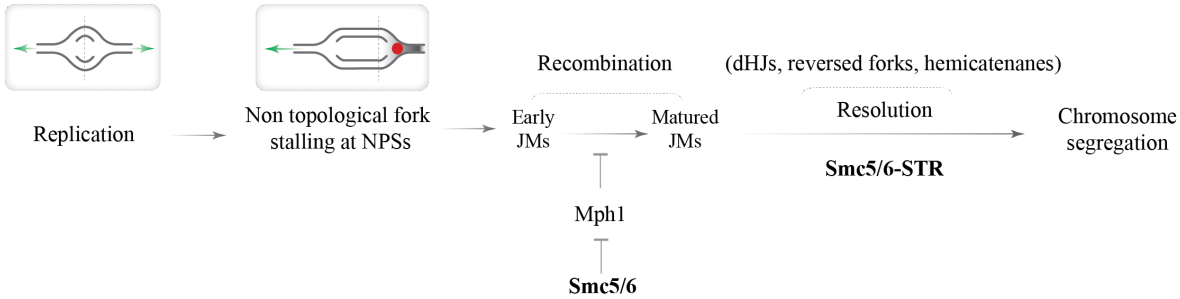

Fig8.1: Model of regulation of recombination at NPSs by Smc5/6 together with the STR complex

The model suggests Smc5/6 dependent recruitment of STR for processing of recombination intermediates at NPSs and stalled forks. The question that yet remains unanswered is whether Smc5/6 also contributes to limiting formation of recombination intermediates or only facilitates their resolution. We observed the role of Smc5/6 complex in resolution together with the STR complex. Sgs1 also contributes as a helicase at early stages of recombination, possibly preventing maturation of D-loops into dHJs. Our results suggest that Smc5/6 and STR perform both joint and independent roles at NPSs. We further tried to understand this interdependence between the two complexes in more details in order to shed light on the function of Smc5/6.

Similar to Smc5/6 (Menolfi et al., 2015), mutants of the STR complex accumulated recombination intermediates at NPSs, caused fragility at rDNA regions and showed higher percentages of 4-way junction DNA structures upon fork stalling (according to unpublished TEM data in the lab). The similarity between the phenotypes of mutants of both Smc5/6 and STR complex indicate their joint roles in NPS replication. While we were curious to

understand how the two complexes depend on eachother for their role at NPSs, we isolated an intragenic suppressor mutation in the *smc6-56* mutant that rescued many of its known defects. The *smc6-56-sup* mutant rescued the temperature and DNA damage sensivity observed for *smc6-56*. However, the suppressor only partially rescued the defect of Smc6-56-myc binding to NPSs. If indeed the NPS phenotype was solely dependent on Smc6 binding/retention to NPSs and recruiting Top3 (or STR complex), we would expect less Top3 at NPSs and accumulation of recombination intermediates at NPSs. The suppressor completely suppressed Top3 enrichment and accumulation of recombination intermediates by *smc6-56* at NPSs. This showed that low levels of Smc5/6 complex at NPSs in Smc5-Smc6-56-sup complex were enough to create substrates for Top3 and prevent accumulation of recombination intermediates. Most importantly, the improved binding of Top3 in *smc6-56-sup* indicates tight connections beteen Smc5/6 and Top3.

We also observed that the suppressor mutant contributes to replication stress resistance in manners complementary with other resolvases (Mus81/Mms4) or dissolvases (Sgs1). In combination with Srs2 or Mph1, there was no additivity observed. Early recombination intermediates such as D-loops can be resolved by helicases such as Srs2, Mph1 and Sgs1 while the mature dHJs are resolved by STR complex or Mus81/Mms4 (Branzei and Szakal, 2016; Giannattasio et al., 2014b; Sung and Klein, 2006; Wu and Hickson, 2003).
The increased replication stress in the double mutants is likely due to recombination, as *RAD51* deletion, alhough causing sensitivity on its own, could in part suppress the additivity between *smc6-56-sup* and *sgs1*mutations.
The lack of recombination intermediates accumulation in *smc6-56-sup* could be due to successful resolution of the intermediates by the STR complex or possibly via their resolution by the Mus81/Mms4 nuclease pathway. The latter possibility is less likely because Mms4 mutants do not accumulate recombination structures at NPSs, suggesting that Mus81 action is not a prominent pathway of resolution. However, it likely acts as a backup pathway to deal with unresolved recombination structures that escaped STR. On the other hand, the restoration of Top3 binding in *smc6-56-sup* enforces the idea of improved STR function. Yet, the additivity between *smc6-56-sup* and *sgs1* mutants, suggests that Smc5/6 wil play roles in regulating other resolvases, such as Mus81/Mms4 and/or helicases, such as Srs2 and Mph1. We further strengthened this hypothesis by observed additivity in recombination intermediates accumulation and delay in their processing at NPSs between *smc6-56-sup* and *sgs1Δ*. This observation indicated that Smc5/6 coordinates several resolvases at NPSs.

The additive recombination intermediates accumulation between *smc6-56-sup* and *sgs1Δ* hints also at the possibility that *smc6-56-sup* may cause deregulated activity of helicases such as Mph1. This in turn will create substrates such as reversed forks that are not resolved by STR, but require instead nucleases such as Mus81-Mms4. Alternatively, deregulation of Srs2 may cause more D-loops to mature into dHJs, which can be resolved by both STR and Mus81. In both these scenarios, the additivity between *smc6-56-sup* and *sgs1*, would imply a concomitant defect in Mus81-Mms4 resolution. This defect, however, is not associated with defective recruitment or retention of Mms4.

8.2 Roles of Smc5/6 and STR in regulating topological stress at NPSs

Previous reports have suggested a role for Top2 in regulating replication termination at TERs (Fachinetti et al., 2010). The function of Smc5/6 is crucial in the absence of Top2 (Jeppsson et al., 2014a). Similar to Smc5/6, we observed genetic interactions between STR mutants and Top2 dysfunction. Top3 mutants also show chromosome segregation defects that can be attributed to its role in decatenation of replicated DNA along with Top2 as proposed before (Gangloff et al., 1994; Kim and Wang, 1992). This suggests that Smc5/6 and STR complexes along with Top2 could be important for regulation of topologically constrained regions such as NPSs. If STR, like Smc5/6, also handles topological stress, we expected to observe growth defects of double mutants between *top2* and STR. This was indeed the case. The double mutant of *top2* and *top3/sgs1/rmi1* showed severe growth defects and the synthetic lethality was not rescued by *rad51* or *rad5* indicating that the lethality was independent of Rad51/Rad5 dependent recombination events. This suggested that the genetic interactions and phenotypes observed were mainly due to the topological structures formed and not due to roles of Smc5/6 and STR in recombination intermediates processing.

We also observed that similar to Smc6 (also reported by (Jeppsson et al., 2014a)), Top3 showed increased genome coverage upon *top2-4* mutation at permissive temperature, indicating that Top3 responds to aggravated topological stress. We also observed increase in amount of Top3 levels in *top2-4* mutants. However, increase in amounts of Top3 was not sufficient to rescue the defects of *top2-4* as this mutant was still temperature sensitive and artificial overexpression of Top3 did not rescue the temperature sensitivity of *top2-4* either. However, we observed STR independent roles for Top3 upon *top2* mutation. Mutation in *TOP2* only increased the expression of *TOP3* and not *RMI1*. The genetic interactions between other components of the STR complex with *top2-4* indicated a role for Top3 together with Sgs1 and Rmi1 in managing topological stress. Moreover, the cell cycle

progression experiments of *top2-4* and *top2-4 S-smc6/sgs1* showed that the cells were not able to complete the replication and were arrested in mitosis.
The role of Top3 in absence of Top2 could be to compensate for a missing topoisomerase. Top2 is typeII topoisomerase which creates transient dsDNA break and remove positive supercoiling, while Top3 can create only ssDNA nick and remove DNA intertwinings. There is a possibility that Top3 can remove the structures that are usually targetted by Top2 (similar to observations made in bacteria by (Hiasa and Marians, 1994)) by a two-step resolution or even two Top3 molecules can co-operate to create two ssDNA nick in parallel on two strands and remove the supercoiling. However, if such process was to happen in absence of Top2, the DNA strands must be held together in position before the whole process is completed and breaks are religated. Possibly, Smc5/6 complex and the STR complex may play a role in this process and facilitate the successful removal of positive supercoiling. This could be a plausible explaination for additive genetic interactions, genome coverage and increase in Top3 levels.

Previous studies showed a role for Smc5/6 complex in the absence of Top2 in the resolution of SCIs that could hinder chromosome resolution (Jeppsson et al., 2014a). We observe a role of STR complex along with Smc5/6 at these regions. Smc5/6 was proposed to promote fork rotation through its chromatin organisation at genomic regions with topological and other replication impedements (Kegel et al., 2011). In the absence of Top2 action, there might be increase in the topological impedements leading to excess Smc5/6 mediated fork rotation forming excessive precatenanes. STR complex possibly targets the precatenanes and allows succesfull resolution of chromosomes and completion of mitosis.

Together our results suggest a role for Smc5/6 and STR complexes together with Top2 to complete replication of topologically constrained regions and to successfully segregate chromosomes. The specific requirement of these proteins arise at specialized regions that are at higher risk of fragility such as NPSs and other topologically constrained regions.
This leads to the second part of our model which explains another set of impedements arising at NPSs, topological contraints and the role of Smc5/6-STR-Top2 at these regions (fig8.2).

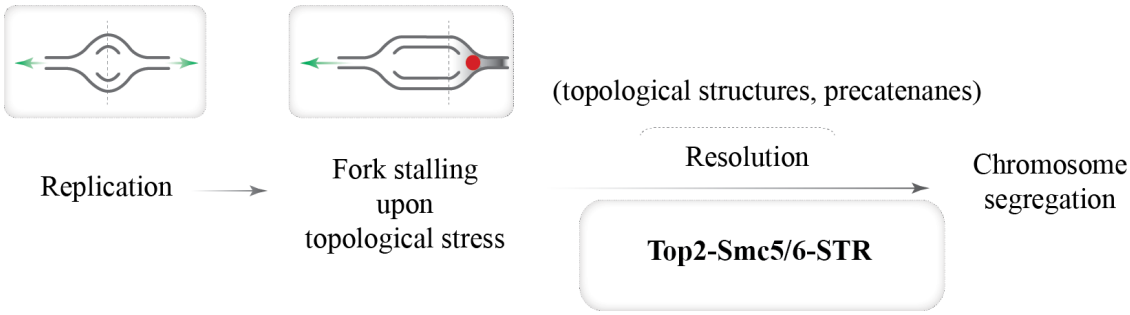

Fig8.2: Model of regulation of topological stress at NPSs by Top2 together with Smc5/6 and STR complexes

8.3 Roles of Top2 and PCNA modifiers in regulating topological stress

PCNA modifications are deciding factors for the choice of DNA damage tolerance pathways. PCNA can be monoubiquitylated, polyubiquitylated or SUMOylated in order to activate one of the three known DDT pathways (Branzei and Szakal, 2016). The regulation and role of PCNA upon DNA damage is well studied. PCNA plays crucial role at stalled RFs upon DNA lesions to rescue replication and prevent fork collapse (Branzei and Szakal, 2016; Gallo and Brown, 2019; Gallo et al., 2019). This suggests a role for PCNA also at NPS regions where occurrence of fork pausing is more frequent than in the rest of the genome. Upon Top2 dysfunction, topologically constrained regions become more at risk and may need special protection for replication completion and successful segregation. Our results suggested that PCNA, its modifications and other DDT factors play a role in this process.

We observed an additive genetic interaction between deletion of *RAD5* and *top2-4* mutation, but not between *RAD5* with mutation in helicase domain (rendering it impaired of helicase activity) and *top2-4*. This, along with the phenotypes of PCNA destabilization or PCNA stabilization via *elg1* mutation, and of other enzymes, such as *RAD18*, *MMS2* that affect PCNA ubiquitylation, indicated that the observed roles of Rad5 and Rad18 depend on PCNA. As we did not create a mutation in the HIRAN domain of *RAD5*, whether the observed function relies ssDNA binding remains unknown. These observations suggested reliance of *top2-4* mutants on PCNA dependent DDT pathways for their survival at high temperatures, indicating a role for DDT upon aggravated topological stress.

Once we observed that PCNA stability and modifications contribute to the survival of *top2-4* cells at higher temperature, we checked downstream proteins involved in recombination or mutagenesis. Deletion of recombination factors such as *RAD52* and *RAD54*, but not TLS

polymerases, aggravated the sensitivity of *top2-4* cells. This suggested that recombination dependent pathways were indeed responsible for survival of *top2-4* cells at higher temperature. One possible explanation for our data is that in the absence of Top2 function, cells are not able to replicate the topologically constrained regions. These regions are thus replicated later with the help of PCNA dependent DDT pathways to successfully complete replication and carry out proper chromosome segregation. The cell cycle profiles of the single and double mutants of *top2-4* and *rad5/rad54* agree with this hypothesis. We observed that the cells were arrested in G2/M phase unable to complete the first round of mitosis. We would like to confirm this observation by checking the effect of *top2-4* and other mutants on mitotic replication by BrdU pull down in the future. The results in this section suggest a back-up mechanism for Top2 dependent topological stress maintenance by PCNA and recombination dependent DDT factors as shown in fig8.3.

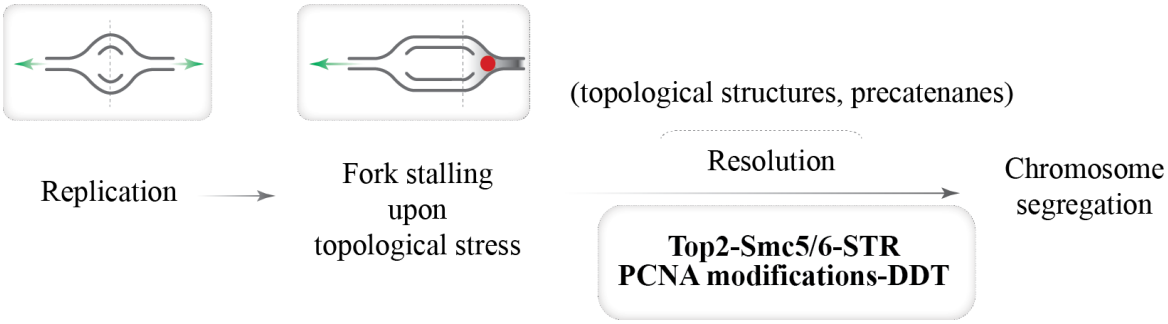

Fig8.3: Model of regulation of topological stress at NPSs by Top2 together with PCNA and DDT pathways

8.4 Cellular response to endogenous versus exogenous DNA damage

Cells are exposed to endogenous DNA damage during every cycle of replication. Our results suggest a role for the Smc5/6, STR, Top2 and DDT components in response to endogenous DNA damage at NPSs and topologically constrained regions. Smc5/6 and STR complexes are involved in controlling the fork rotation, precatenanes processing and control/processing of recombination intermediates. The backup pathway for Smc5/6 and STR function include the Mus81/Mms4 endonuclease complex, which is active during mitosis to resolve the recombination intermediates escaped from the STR action. Top2 together with PCNA dependent DDT pathways regulate the replication of topologically constrained regions that need special assistance during replication and if not replicated accurately, require post replicative tolerance pathways for replication completion.

When responding to exogenous DNA damage such as UV, MMS, HU or CPT treatment, cells do rely on similar mechanisms. However, we find differences in the regulation of the

pathways. We observe reliance of Smc5/6 on SUMOylation while dealing with STR activity upon external DNA damage which was not observed at NPSs in unperturbed replication (Bermúdez-López et al., 2016; Bonner et al., 2016). Topoisomerases and DDT mechanisms are active upon external damage but the TLS pathways were only observed to play a role upon external DNA damage (Bermejo et al., 2007; Branzei and Szakal, 2016).

Considering our observations, we can conclude that the factors involved in natural and artificial DNA damage are overlapping. The mechanisms of activation and regulation of these pathways are also similar. Upon external damage, the cells show aggravated response, leading to multiple parallel pathways getting activated, stronger regulation of proteins and inclusion of even mutagenic pathways for tolerance of stress. Observations made for NPSs resemble but are at a lower scale to what happens upon treatment with DNA damaging agents.

Upon either natural or artificial RF stalling, Smc5/6-STR-Top2 and backup proteins carry out essential function of replication completion and prevent accumulation of topological or recombination intermediates that can impede mitosis or lead to missegregation and aneuploidy. The defects in these pathways lead to errors in mitosis and cell death. Existence of several parallel pathways indicates an intricate network of control to make sure the replication is error free and completed successfully before mitosis.

8.5 Conclusions and future directions

In *S. cerevisiae*, Smc5/6 is essential in G2/M phase. Previous studies from our lab have shown a role for Smc5/6 in NPS replication and maintenance (Menolfi et al., 2015). Our new results show collaboration between other genome-caretakers and Smc5/6 at NPSs and topologically constrained regions. We observe that Smc5/6 and STR complexes play independent and interdependent roles at NPSs. We observe dual role for Sgs1 (or the STR complex) during recombination intermediates processing. Smc5/6 prevents excessive fork rotation to prevent precatenanes formation (Schalbetter et al., 2015), while Top3 (with Top1) may process the precatenanes for successful DNA segregation. On the other hand, Mph1, Sgs1 and Srs2 helicases can prevent conversion of early JMs to matured JMs by dissolution. At later stages, the STR complex (together with Mus81/Mms4 as back-up resolvases) can process the JMs and prevent accumulation of recombination intermediates. Smc5/6 orchestrates the contribution of all these pathways and ensures successful regulation of replication and recombination at NPSs. Our results suggest a scheme for replication and recombination at NPSs as described in fig8.4.

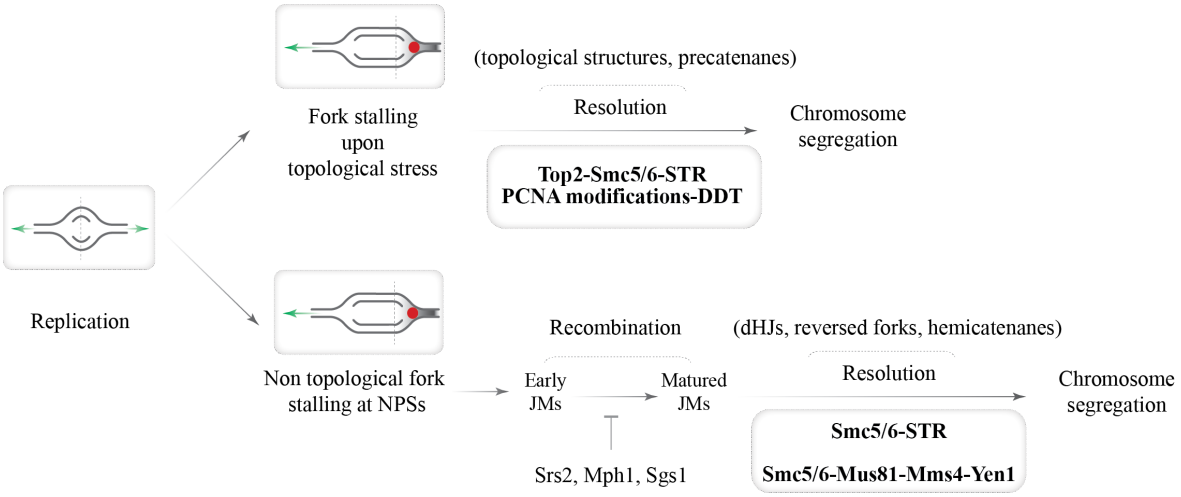

Fig8.4: Model depicting roles of Smc5/6, STR and other factors at NPSs

Apart from non-topological constraints, NPSs also accumulate topological stress during replication. Top2 is the best-known factor that takes care of topological stress at TERs and other NPSs (Fachinetti et al., 2010). Our results indicate a role for Smc5/6 and STR complex along with Top2 at such topologically constrained regions. Furthermore, in the absence of Top2, components of the DDT pathway become critical for cell survival. Our results indicate that upon Top2 dysfunction, DDT (along with PCNA modifications and stability) act as a backup pathway to deal with DNA damage caused by excessive topological stress. The recombination dependent pathways of DDT complete replication of such regions and allow successful DNA segregation in the absence of Top2 function. Interestingly, the process is independent of Rad51 function. Smc5/6 and STR also assist in this process, whereas robust presence of PCNA on chromosome and DDT factors involved in recombination pathways are critical.

Together, the results suggest a possible mechanism of NPS replication with two pathways to handle topological stress and non-topological replication impediments. While the topological stress is handled by Smc5/6 and STR complex together with Top2 and DDT factors, non-topological impediments can be handled by Smc5/6 complex with STR complex, Mus81/Mms4 and Yen1. The two pathways must overlap as regions like TERs and other NPSs are combinations of different types of impediments and largely accumulating topological stress. The two pathways must interact and compensate for each other in order to carry out successful NPS replication.

The first future direction for this project would be a deep structural and functional analysis of Smc6-56-sup. *smc6-56-sup* is an interesting mutant, with a new Cys358 instead of Glycine in *smc6-56*. This creates a possibility of sulphur bond formation and thus changing

the structure of Smc6 coiled coil and possibly the structure of Smc5/6. Smc5/6 can form a ring like structure, however recent studies of MukBEF and cohesin also suggest that SMC proteins can fold onto the elbow in the coiled coil domain (Bürmann et al., 2019). This suggests additional interactione between head and hinge domains. Considering that the structures of closely related *S. cerevisiae* and *S. pombe* show different regions of Nse5/6 association, there is a possibility that folding of the Smc5/6 core allows association of Nse5/6 subcomplex either to head domain or to hinge domain (Duan et al., 2009b; Pebernard et al., 2006). There is a possibility that the interactions between subcomplexes at hinge and head upon folding at the elbow within coiled-coil are defective due to the *smc6-56* mutations and this is corrected by suppressor mutation restoring the structure as well as interactions between the complex. However, this hypothesis needs to be tested further. Further work needs to be done in order to understand the exact structure of Smc5/Smc6-56-sup complex. The mutation in *smc6-56-sup* is strongly suppressing most of the *smc6-56* phenotypes, but is additive with mutations in Sgs1 and Mus81. A detailed study could maybe illuminate the exact mechanism of suppression and the reason behind partial suppression of Smc6-56-sup-myc binding to NPSs. Biochemical studies to understand the differences in interaction between Smc5/6 or Smc5/Smc6-56-sup complexes will shed light on the effect of suppressor mutation on the stability of complex, SUMO ligase activity, ATPase activity etc.

Next, it will be interesting to assess the effect of resolvases Slx1/Slx4 and Yen1 on the recombination accumulation phenotypes of *smc6-56*, *smc6-56-sup* and whether there are genetic interactions that can be translated into a phenotype in 2D gel electrophoresis. We would further like to understand the contribution of these factors in NPS replication. Our recent results indicate recruitment of Mms4 at NPSs is independent of Smc5/6 function, but depletion of Mms4 does not accumulate recombination intermediates at NPSs. This suggests a role for Mus81/Mms4 as backup of the STR complex. We would like to understand the regulation of the two protein complexes by Smc5/6 in more details.

We are also curious to see the localization of PCNA modifiers and DDT factors to understand their genome-wide recruitment, whether the recruitment is dependent on Smc5/6 or Top2 or other known factors. It would be interesting to see the genome-wide effect of *top2-4* mutation on Rad5 or other modifiers of PCNA. Mitotic arrest of cells with several mutant combinations of *top2-4* suggests a defect in mitotic DNA segregation or ongoing mitotic DNA replication. We would like to conduct BrdU analysis to understand the effect of *top2-4* alone and in combination with other factors on residual replication during mitosis. We are also interested in understanding the effect of defects in NPS replication on Cohesin

and Condensin. Most of the factors accumulating at NPSs are important for successful chromosome segregation and mitosis. We are thus curious to see the interaction of Condensin and Cohesin to this process. Future studies should add to the understanding of NPS replication and integrity.

References

Abdul, F., Filleton, F., Gerossier, L., Paturel, A., Hall, J., Strubin, M., and Etienne, L. (2018). Smc5/6 Antagonism by HBx Is an Evolutionarily Conserved Function of Hepatitis B Virus Infection in Mammals. J Virol *92*, e00769-00718.

Abe, T., Sugimura, K., Hosono, Y., Takami, Y., Akita, M., Yoshimura, A., Tada, S., Nakayama, T., Murofushi, H., Okumura, K.*, et al.* (2011). The histone chaperone facilitates chromatin transcription (FACT) protein maintains normal replication fork rates. J Biol Chem *286*, 30504-30512.

Abmayr, S.M., and Workman, J.L. (2012). Holding on through DNA replication: histone modification or modifier? Cell *150*, 875-877.

Adamus, M., Lelkes, E., Potesil, D., Ganji, S.R., Kolesar, P., Zabrady, K., Zdrahal, Z., and Palecek, J.J. (2020). Molecular Insights into the Architecture of the Human SMC5/6 Complex. J Mol Biol *432*, 3820-3837.

Admire, A., Shanks, L., Danzl, N., Wang, M., Weier, U., Stevens, W., Hunt, E., and Weinert, T. (2006). Cycles of chromosome instability are associated with a fragile site and are increased by defects in DNA replication and checkpoint controls in yeast. Genes Dev *20*, 159-173.

Aguilera, A., and Gómez-González, B. (2008). Genome instability: a mechanistic view of its causes and consequences. Nat Rev Genet *9*, 204-217.

Ahn, J.S., Osman, F., and Whitby, M.C. (2005). Replication fork blockage by RTS1 at an ectopic site promotes recombination in fission yeast. The EMBO journal *24*, 2011-2023.

Ahn, J.W., Inkeles, M., Hristov, A., and Eshaq, M. (2019). Histopathologic features of Rothmund-Thomson syndrome. JAAD Case Rep *5*, 726-728.

Almedawar, S., Colomina, N., Bermúdez-López, M., Pociño-Merino, I., and Torres-Rosell, J. (2012). A SUMO-dependent step during establishment of sister chromatid cohesion. Current biology : CB *22*, 1576-1581.

Alt, A., Dang, H.Q., Wells, O.S., Polo, L.M., Smith, M.A., McGregor, G.A., Welte, T., Lehmann, A.R., Pearl, L.H., Murray, J.M.*, et al.* (2017). Specialized interfaces of Smc5/6 control hinge stability and DNA association. Nat Commun *8*, 14011.

Álvarez-Quilón, A., Terrón-Bautista, J., Delgado-Sainz, I., Serrano-Benítez, A., Romero-Granados, R., Martínez-García, P.M., Jimeno-González, S., Bernal-Lozano, C., Quintero, C., García-Quintanilla, L.*, et al.* (2020). Endogenous topoisomerase II-mediated DNA breaks drive thymic cancer predisposition linked to ATM deficiency. Nat Commun *11*, 910-910.

Anderson, D.E., Losada, A., Erickson, H.P., and Hirano, T. (2002). Condensin and cohesin display different arm conformations with characteristic hinge angles. The Journal of cell biology *156*, 419-424.

Andrews, E.A., Palecek, J., Sergeant, J., Taylor, E., Lehmann, A.R., and Watts, F.Z. (2005). Nse2, a component of the Smc5-6 complex, is a SUMO ligase required for the response to DNA damage. Molecular and cellular biology *25*, 185-196.

Arcangioli, B., and de Lahondes, R. (2000). Fission yeast switches mating type by a replication-recombination coupled process. EMBO J *19*, 1389-1396.

Ashton, T.M., Mankouri, H.W., Heidenblut, A., McHugh, P.J., and Hickson, I.D. (2011). Pathways for Holliday junction processing during homologous recombination in Saccharomyces cerevisiae. Molecular and cellular biology *31*, 1921-1933.

Azvolinsky, A., Dunaway, S., Torres, J.Z., Bessler, J.B., and Zakian, V.A. (2006). The S. cerevisiae Rrm3p DNA helicase moves with the replication fork and affects replication of all yeast chromosomes. Genes Dev *20*, 3104-3116.

Azvolinsky, A., Giresi, P.G., Lieb, J.D., and Zakian, V.A. (2009a). Highly transcribed RNA polymerase II genes are impediments to replication fork progression in Saccharomyces cerevisiae. Mol Cell *34*, 722-734.
Azvolinsky, A., Giresi, P.G., Lieb, J.D., and Zakian, V.A. (2009b). Highly transcribed RNA polymerase II genes are impediments to replication fork progression in Saccharomyces cerevisiae. Molecular cell *34*, 722-734.
Bachant, J., Alcasabas, A., Blat, Y., Kleckner, N., and Elledge, S.J. (2002). The SUMO-1 isopeptidase Smt4 is linked to centromeric cohesion through SUMO-1 modification of DNA topoisomerase II. Molecular cell *9*, 1169-1182.
Bando, M., Katou, Y., Komata, M., Tanaka, H., Itoh, T., Sutani, T., and Shirahige, K. (2009). Csm3, Tof1, and Mrc1 form a heterotrimeric mediator complex that associates with DNA replication forks. The Journal of biological chemistry *284*, 34355-34365.
Bastia, D., Srivastava, P., Zaman, S., Choudhury, M., Mohanty, B.K., Bacal, J., Langston, L.D., Pasero, P., and O'Donnell, M.E. (2016). Phosphorylation of CMG helicase and Tof1 is required for programmed fork arrest. Proc Natl Acad Sci U S A *113*, E3639-3648.
Båvner, A., Matthews, J., Sanyal, S., Gustafsson, J.-A., and Treuter, E. (2005). EID3 is a novel EID family member and an inhibitor of CBP-dependent co-activation. Nucleic Acids Res *33*, 3561-3569.
Behlke-Steinert, S., Touat-Todeschini, L., Skoufias, D.A., and Margolis, R.L. (2009). SMC5 and MMS21 are required for chromosome cohesion and mitotic progression. Cell cycle (Georgetown, Tex.) *8*, 2211-2218.
Bell, L., and Byers, B. (1983a). Separation of branched from linear DNA by two-dimensional gel electrophoresis. Anal Biochem *130*, 527-535.
Bell, L.R., and Byers, B. (1983b). Homologous association of chromosomal DNA during yeast meiosis. Cold Spring Harb Symp Quant Biol *47 Pt 2*, 829-840.
Bennett, R.J., Keck, J.L., and Wang, J.C. (1999). Binding specificity determines polarity of DNA unwinding by the Sgs1 protein of S. cerevisiae. J Mol Biol *289*, 235-248.
Bennett, R.J., Noirot-Gros, M.F., and Wang, J.C. (2000). Interaction between yeast sgs1 helicase and DNA topoisomerase III. The Journal of biological chemistry *275*, 26898-26905.
Bennett, R.J., Sharp, J.A., and Wang, J.C. (1998). Purification and characterization of the Sgs1 DNA helicase activity of Saccharomyces cerevisiae. The Journal of biological chemistry *273*, 9644-9650.
Bennett, R.J., and Wang, J.C. (2001). Association of yeast DNA topoisomerase III and Sgs1 DNA helicase: studies of fusion proteins. Proceedings of the National Academy of Sciences of the United States of America *98*, 11108-11113.
Bentley, P., Tan, M.J.A., McBride, A.A., White, E.A., and Howley, P.M. (2018). The SMC5/6 Complex Interacts with the Papillomavirus E2 Protein and Influences Maintenance of Viral Episomal DNA. J Virol *92*, e00356-00318.
Bergerat, A., de Massy, B., Gadelle, D., Varoutas, P.C., Nicolas, A., and Forterre, P. (1997). An atypical topoisomerase II from Archaea with implications for meiotic recombination. Nature *386*, 414-417.
Bergerat, A., Gadelle, D., and Forterre, P. (1994). Purification of a DNA topoisomerase II from the hyperthermophilic archaeon Sulfolobus shibatae. A thermostable enzyme with both bacterial and eucaryal features. The Journal of biological chemistry *269*, 27663-27669.
Bergink, S., and Jentsch, S. (2009). Principles of ubiquitin and SUMO modifications in DNA repair. Nature *458*, 461-467.

Bermejo, R., Capra, T., Gonzalez-Huici, V., Fachinetti, D., Cocito, A., Natoli, G., Katou, Y., Mori, H., Kurokawa, K., Shirahige, K.*, et al.* (2009a). Genome-organizing factors Top2 and Hmo1 prevent chromosome fragility at sites of S phase transcription. Cell *138*, 870-884.
Bermejo, R., Capra, T., Gonzalez-Huici, V., Fachinetti, D., Cocito, A., Natoli, G., Katou, Y., Mori, H., Kurokawa, K., Shirahige, K.*, et al.* (2009b). Genome-organizing factors Top2 and Hmo1 prevent chromosome fragility at sites of S phase transcription. Cell *138*, 870-884.
Bermejo, R., Doksani, Y., Capra, T., Katou, Y.-M., Tanaka, H., Shirahige, K., and Foiani, M. (2007). Top1- and Top2-mediated topological transitions at replication forks ensure fork progression and stability and prevent DNA damage checkpoint activation. Genes & development *21*, 1921-1936.
Bermejo, R., Katou, Y.-M., Shirahige, K., and Foiani, M. (2009c). ChIP-on-chip analysis of DNA topoisomerases. Methods Mol Biol *582*, 103-118.
Bermúdez-López, M., Ceschia, A., de Piccoli, G., Colomina, N., Pasero, P., Aragón, L., and Torres-Rosell, J. (2010). The Smc5/6 complex is required for dissolution of DNA-mediated sister chromatid linkages. Nucleic Acids Res *38*, 6502-6512.
Bermúdez-López, M., Villoria, M.T., Esteras, M., Jarmuz, A., Torres-Rosell, J., Clemente-Blanco, A., and Aragon, L. (2016). Sgs1's roles in DNA end resection, HJ dissolution, and crossover suppression require a two-step SUMO regulation dependent on Smc5/6. Genes & development *30*, 1339-1356.
Bernstein, K.A., Shor, E., Sunjevaric, I., Fumasoni, M., Burgess, R.C., Foiani, M., Branzei, D., and Rothstein, R. (2009). Sgs1 function in the repair of DNA replication intermediates is separable from its role in homologous recombinational repair. The EMBO journal *28*, 915-925.
Bianchi, J., Rudd, S.G., Jozwiakowski, S.K., Bailey, L.J., Soura, V., Taylor, E., Stevanovic, I., Green, A.J., Stracker, T.H., Lindsay, H.D.*, et al.* (2013). PrimPol bypasses UV photoproducts during eukaryotic chromosomal DNA replication. Molecular cell *52*, 566-573.
Birren, B.W., Hood, L., and Lai, E. (1989a). Pulsed field gel electrophoresis: studies of DNA migration made with the programmable, autonomously-controlled electrode electrophoresis system. Electrophoresis *10*, 302-309.
Birren, B.W., Lai, E., Hood, L., and Simon, M.I. (1989b). Pulsed field gel electrophoresis techniques for separating 1- to 50-kilobase DNA fragments. Anal Biochem *177*, 282-286.
Bluteau, D., Masliah-Planchon, J., Clairmont, C., Rousseau, A., Ceccaldi, R., Dubois d'Enghien, C., Bluteau, O., Cuccuini, W., Gachet, S., Peffault de Latour, R.*, et al.* (2016). Biallelic inactivation of REV7 is associated with Fanconi anemia. J Clin Invest *126*, 3580-3584.
Boersma, V., Moatti, N., Segura-Bayona, S., Peuscher, M.H., van der Torre, J., Wevers, B.A., Orthwein, A., Durocher, D., and Jacobs, J.J.L. (2015). MAD2L2 controls DNA repair at telomeres and DNA breaks by inhibiting 5' end resection. Nature *521*, 537-540.
Bonner, J.N., Choi, K., Xue, X., Torres, N.P., Szakal, B., Wei, L., Wan, B., Arter, M., Matos, J., Sung, P.*, et al.* (2016). Smc5/6 Mediated Sumoylation of the Sgs1-Top3-Rmi1 Complex Promotes Removal of Recombination Intermediates. Cell reports *16*, 368-378.
Boule, J.B., Vega, L.R., and Zakian, V.A. (2005). The yeast Pif1p helicase removes telomerase from telomeric DNA. Nature *438*, 57-61.
Bourns, B.D., Alexander, M.K., Smith, A.M., and Zakian, V.A. (1998). Sir proteins, Rif proteins, and Cdc13p bind Saccharomyces telomeres in vivo. Mol Cell Biol *18*, 5600-5608.
Branzei, D. (2011). Ubiquitin family modifications and template switching. FEBS Lett *585*, 2810-2817.
Branzei, D., and Foiani, M. (2010). Maintaining genome stability at the replication fork. Nature reviews. Molecular cell biology *11*, 208-219.

Branzei, D., and Menolfi, D. (2016). G2/M chromosome transactions essentially relying on Smc5/6. Cell Cycle *15*, 611-612.
Branzei, D., Sollier, J., Liberi, G., Zhao, X., Maeda, D., Seki, M., Enomoto, T., Ohta, K., and Foiani, M. (2006). Ubc9- and mms21-mediated sumoylation counteracts recombinogenic events at damaged replication forks. Cell *127*, 509-522.
Branzei, D., and Szakal, B. (2016). DNA damage tolerance by recombination: Molecular pathways and DNA structures. DNA repair *44*, 68-75.
Branzei, D., Vanoli, F., and Foiani, M. (2008a). SUMOylation regulates Rad18-mediated template switch. Nature *456*, 915.
Branzei, D., Vanoli, F., and Foiani, M. (2008b). SUMOylation regulates Rad18-mediated template switch. Nature *456*, 915-920.
Brewer, B.J., and Fangman, W.L. (1987). The localization of replication origins on ARS plasmids in S. cerevisiae. Cell *51*, 463-471.
Brewer, B.J., and Fangman, W.L. (1988). A replication fork barrier at the 3' end of yeast ribosomal RNA genes. Cell *55*, 637-643.
Brill, S.J., DiNardo, S., Voelkel-Meiman, K., and Sternglanz, R. (1987). Need for DNA topoisomerase activity as a swivel for DNA replication for transcription of ribosomal RNA. Nature *326*, 414-416.
Broderick, L., Yost, S., Li, D., McGeough, M.D., Booshehri, L.M., Guaderrama, M., Brydges, S.D., Kucharova, K., Patel, N.C., Harr, M.*, et al.* (2019). Mutations in topoisomerase IIβ result in a B cell immunodeficiency. Nat Commun *10*, 3644-3644.
Bürmann, F., Lee, B.G., Than, T., Sinn, L., O'Reilly, F.J., Yatskevich, S., Rappsilber, J., Hu, B., Nasmyth, K., and Löwe, J. (2019). A folded conformation of MukBEF and cohesin. Nat Struct Mol Biol *26*, 227-236.
Bustard, D.E., Menolfi, D., Jeppsson, K., Ball, L.G., Dewey, S.C., Shirahige, K., Sjögren, C., Branzei, D., and Cobb, J.A. (2012). During replication stress, non-SMC element 5 (NSE5) is required for Smc5/6 protein complex functionality at stalled forks. The Journal of biological chemistry *287*, 11374-11383.
Butler, M.G., Rafi, S.K., and Manzardo, A.M. (2015). High-resolution chromosome ideogram representation of currently recognized genes for autism spectrum disorders. Int J Mol Sci *16*, 6464-6495.
Bzymek, M., Thayer, N.H., Oh, S.D., Kleckner, N., and Hunter, N. (2010). Double Holliday junctions are intermediates of DNA break repair. Nature *464*, 937-941.
Casper, A.M., Nghiem, P., Arlt, M.F., and Glover, T.W. (2002). ATR regulates fragile site stability. Cell *111*, 779-789.
Castells-Roca, L., Mueller, M.M., and Schumacher, B. (2015). Longevity through DNA damage tolerance. Cell cycle (Georgetown, Tex.) *14*, 467-468.
Cejka, P., Plank, J.L., Bachrati, C.Z., Hickson, I.D., and Kowalczykowski, S.C. (2010). Rmi1 stimulates decatenation of double Holliday junctions during dissolution by Sgs1-Top3. Nature structural & molecular biology *17*, 1377-1382.
Cha, R.S., and Kleckner, N. (2002). ATR homolog Mec1 promotes fork progression, thus averting breaks in replication slow zones. Science *297*, 602-606.
Champoux, J.J. (2001). DNA topoisomerases: structure, function, and mechanism. Annu Rev Biochem *70*, 369-413.
Chan, K.L., Palmai-Pallag, T., Ying, S., and Hickson, I.D. (2009). Replication stress induces sister-chromatid bridging at fragile site loci in mitosis. Nature cell biology *11*, 753-760.
Chang, M., Bellaoui, M., Zhang, C., Desai, R., Morozov, P., Delgado-Cruzata, L., Rothstein, R., Freyer, G.A., Boone, C., and Brown, G.W. (2005). RMI1/NCE4, a suppressor of genome instability, encodes a member of the RecQ helicase/Topo III complex. The EMBO journal *24*, 2024-2033.

Chen, Y.-H., Szakal, B., Castellucci, F., Branzei, D., and Zhao, X. (2013). DNA damage checkpoint and recombinational repair differentially affect the replication stress tolerance of Smc6 mutants. Molecular biology of the cell *24*, 2431-2441.
Chen, Y.H., Choi, K., Szakal, B., Arenz, J., Duan, X., Ye, H., Branzei, D., and Zhao, X. (2009). Interplay between the Smc5/6 complex and the Mph1 helicase in recombinational repair. Proc Natl Acad Sci U S A *106*, 21252-21257.
Cheng, E., Vaisica, J.A., Ou, J., Baryshnikova, A., Lu, Y., Roth, F.P., and Brown, G.W. (2012). Genome rearrangements caused by depletion of essential DNA replication proteins in Saccharomyces cerevisiae. Genetics *192*, 147-160.
Cho, W.H., Kang, Y.H., An, Y.Y., Tappin, I., Hurwitz, J., and Lee, J.K. (2013). Human Tim-Tipin complex affects the biochemical properties of the replicative DNA helicase and DNA polymerases. Proc Natl Acad Sci U S A *110*, 2523-2527.
Choi, K., Batke, S., Szakal, B., Lowther, J., Hao, F., Sarangi, P., Branzei, D., Ulrich, H.D., and Zhao, X. (2015). Concerted and differential actions of two enzymatic domains underlie Rad5 contributions to DNA damage tolerance. Nucleic Acids Res *43*, 2666-2677.
Choi, K., Szakal, B., Chen, Y.-H., Branzei, D., and Zhao, X. (2010). The Smc5/6 complex and Esc2 influence multiple replication-associated recombination processes in Saccharomyces cerevisiae. Molecular biology of the cell *21*, 2306-2314.
Chu, W.K., and Hickson, I.D. (2009). RecQ helicases: multifunctional genome caretakers. Nat Rev Cancer *9*, 644-654.
D'Ambrosio, C., Kelly, G., Shirahige, K., and Uhlmann, F. (2008). Condensin-dependent rDNA decatenation introduces a temporal pattern to chromosome segregation. Current biology : CB *18*, 1084-1089.
Daee, D.L., Ferrari, E., Longerich, S., Zheng, X.F., Xue, X., Branzei, D., Sung, P., and Myung, K. (2012). Rad5-dependent DNA repair functions of the Saccharomyces cerevisiae FANCM protein homolog Mph1. J Biol Chem *287*, 26563-26575.
Daghsni, M., Lahbib, S., Fradj, M., Sayeb, M., Kelmemi, W., Kraoua, L., Kchaou, M., Maazoul, F., Echebbi, S., Ben Ali, N.*, et al.* (2018). TOP3B: A Novel Candidate Gene in Juvenile Myoclonic Epilepsy? Cytogenet Genome Res *154*, 1-5.
Daigaku, Y., Davies, A.A., and Ulrich, H.D. (2010). Ubiquitin-dependent DNA damage bypass is separable from genome replication. Nature *465*, 951-955.
Dalgaard, J.Z., and Klar, A.J. (2001). A DNA replication-arrest site RTS1 regulates imprinting by determining the direction of replication at mat1 in S. pombe. Genes Dev *15*, 2060-2068.
Das, S.P., and Sinha, P. (2005). The budding yeast protein Chl1p has a role in transcriptional silencing, rDNA recombination, and aging. Biochem Biophys Res Commun *337*, 167-172.
De Antoni, A., and Gallwitz, D. (2000). A novel multi-purpose cassette for repeated integrative epitope tagging of genes in Saccharomyces cerevisiae. Gene *246*, 179-185.
de la Loza, M.C.D., Wellinger, R.E., and Aguilera, A. (2009). Stimulation of direct-repeat recombination by RNA polymerase III transcription. DNA repair *8*, 620-626.
De Piccoli, G., Cortes-Ledesma, F., Ira, G., Torres-Rosell, J., Uhle, S., Farmer, S., Hwang, J.-Y., Machin, F., Ceschia, A., McAleenan, A.*, et al.* (2006). Smc5-Smc6 mediate DNA double-strand-break repair by promoting sister-chromatid recombination. Nature cell biology *8*, 1032-1034.
De Piccoli, G., Katou, Y., Itoh, T., Nakato, R., Shirahige, K., and Labib, K. (2012). Replisome stability at defective DNA replication forks is independent of S phase checkpoint kinases. Mol Cell *45*, 696-704.

Defossez, P.A., Prusty, R., Kaeberlein, M., Lin, S.J., Ferrigno, P., Silver, P.A., Keil, R.L., and Guarente, L. (1999). Elimination of replication block protein Fob1 extends the life span of yeast mother cells. Mol Cell *3*, 447-455.
Dekker, N.H., Rybenkov, V.V., Duguet, M., Crisona, N.J., Cozzarelli, N.R., Bensimon, D., and Croquette, V. (2002). The mechanism of type IA topoisomerases. Proceedings of the National Academy of Sciences of the United States of America *99*, 12126-12131.
Deshpande, A.M., and Newlon, C.S. (1996). DNA replication fork pause sites dependent on transcription. Science *272*, 1030-1033.
Di Marco, S., Hasanova, Z., Kanagaraj, R., Chappidi, N., Altmannova, V., Menon, S., Sedlackova, H., Langhoff, J., Surendranath, K., Huhn, D.*, et al.* (2017). RECQ5 Helicase Cooperates with MUS81 Endonuclease in Processing Stalled Replication Forks at Common Fragile Sites during Mitosis. Mol Cell *66*, 658-671 e658.
DiNardo, S., Voelkel, K., and Sternglanz, R. (1984). DNA topoisomerase II mutant of Saccharomyces cerevisiae: topoisomerase II is required for segregation of daughter molecules at the termination of DNA replication. Proceedings of the National Academy of Sciences of the United States of America *81*, 2616-2620.
Doyle, J.M., Gao, J., Wang, J., Yang, M., and Potts, P.R. (2010). MAGE-RING protein complexes comprise a family of E3 ubiquitin ligases. Molecular cell *39*, 963-974.
Duan, X., Sarangi, P., Liu, X., Rangi, G.K., Zhao, X., and Ye, H. (2009a). Structural and functional insights into the roles of the Mms21 subunit of the Smc5/6 complex. Molecular cell *35*, 657-668.
Duan, X., Yang, Y., Chen, Y.-H., Arenz, J., Rangi, G.K., Zhao, X., and Ye, H. (2009b). Architecture of the Smc5/6 Complex of Saccharomyces cerevisiae Reveals a Unique Interaction between the Nse5-6 Subcomplex and the Hinge Regions of Smc5 and Smc6. The Journal of biological chemistry *284*, 8507-8515.
Dubarry, M., Loiodice, I., Chen, C.L., Thermes, C., and Taddei, A. (2011). Tight protein-DNA interactions favor gene silencing. Genes Dev *25*, 1365-1370.
Fachinetti, D., Bermejo, R., Cocito, A., Minardi, S., Katou, Y., Kanoh, Y., Shirahige, K., Azvolinsky, A., Zakian, V.A., and Foiani, M. (2010). Replication termination at eukaryotic chromosomes is mediated by Top2 and occurs at genomic loci containing pausing elements. Mol Cell *39*, 595-605.
Fasching, C.L., Cejka, P., Kowalczykowski, S.C., and Heyer, W.-D. (2015). Top3-Rmi1 dissolve Rad51-mediated D loops by a topoisomerase-based mechanism. Molecular cell *57*, 595-606.
Feng, Y., Gao, J., and Yang, M. (2011). When MAGE meets RING: insights into biological functions of MAGE proteins. Protein Cell *2*, 7-12.
Fricke, W.M., and Brill, S.J. (2003). Slx1-Slx4 is a second structure-specific endonuclease functionally redundant with Sgs1-Top3. Genes & development *17*, 1768-1778.
Fritze, C.E., Verschueren, K., Strich, R., and Easton Esposito, R. (1997). Direct evidence for SIR2 modulation of chromatin structure in yeast rDNA. EMBO J *16*, 6495-6509.
Fukuchi, K., Martin, G.M., and Monnat, R.J., Jr. (1989). Mutator phenotype of Werner syndrome is characterized by extensive deletions. Proceedings of the National Academy of Sciences of the United States of America *86*, 5893-5897.
Gallego-Paez, L.M., Tanaka, H., Bando, M., Takahashi, M., Nozaki, N., Nakato, R., Shirahige, K., and Hirota, T. (2014). Smc5/6-mediated regulation of replication progression contributes to chromosome assembly during mitosis in human cells. Molecular biology of the cell *25*, 302-317.
Gallo, D., and Brown, G.W. (2019). Post-replication repair: Rad5/HLTF regulation, activity on undamaged templates, and relationship to cancer. Crit Rev Biochem Mol Biol *54*, 301-332.

Gallo, D., Kim, T., Szakal, B., Saayman, X., Narula, A., Park, Y., Branzei, D., Zhang, Z., and Brown, G.W. (2019). Rad5 Recruits Error-Prone DNA Polymerases for Mutagenic Repair of ssDNA Gaps on Undamaged Templates. Mol Cell *73*, 900-914.e909.
Gangloff, S., McDonald, J.P., Bendixen, C., Arthur, L., and Rothstein, R. (1994). The yeast type I topoisomerase Top3 interacts with Sgs1, a DNA helicase homolog: a potential eukaryotic reverse gyrase. Molecular and cellular biology *14*, 8391-8398.
García-Gómez, S., Reyes, A., Martínez-Jiménez, M.I., Chocrón, E.S., Mourón, S., Terrados, G., Powell, C., Salido, E., Méndez, J., Holt, I.J.*, et al.* (2013). PrimPol, an archaic primase/polymerase operating in human cells. Molecular cell *52*, 541-553.
Giannattasio, M., and Branzei, D. (2017). S-phase checkpoint regulations that preserve replication and chromosome integrity upon dNTP depletion. Cell Mol Life Sci *74*, 2361-2380.
Giannattasio, M., Zwicky, K., Follonier, C., Foiani, M., Lopes, M., and Branzei, D. (2014a). Visualization of recombination-mediated damage bypass by template switching. Nature structural & molecular biology *21*, 884-892.
Giannattasio, M., Zwicky, K., Follonier, C., Foiani, M., Lopes, M., and Branzei, D. (2014b). Visualization of recombination-mediated damage bypass by template switching. Nature structural & molecular biology *21*, 884-892.
Gietz, R.D., Schiestl, R.H., Willems, A.R., and Woods, R.A. (1995). Studies on the transformation of intact yeast cells by the LiAc/SS-DNA/PEG procedure. Yeast *11*, 355-360.
Gligoris, T.G., Scheinost, J.C., Bürmann, F., Petela, N., Chan, K.-L., Uluocak, P., Beckouët, F., Gruber, S., Nasmyth, K., and Löwe, J. (2014). Closing the cohesin ring: structure and function of its Smc3-kleisin interface. Science (New York, N.Y.) *346*, 963-967.
Glover, T.W., Berger, C., Coyle, J., and Echo, B. (1984). DNA polymerase alpha inhibition by aphidicolin induces gaps and breaks at common fragile sites in human chromosomes. Hum Genet *67*, 136-142.
Gonzalez-Huici, V., Szakal, B., Urulangodi, M., Psakhye, I., Castellucci, F., Menolfi, D., Rajakumara, E., Fumasoni, M., Bermejo, R., Jentsch, S.*, et al.* (2014). DNA bending facilitates the error-free DNA damage tolerance pathway and upholds genome integrity. The EMBO journal *33*, 327-340.
Gravel, S., Chapman, J.R., Magill, C., and Jackson, S.P. (2008). DNA helicases Sgs1 and BLM promote DNA double-strand break resection. Genes & development *22*, 2767-2772.
Greenfeder, S.A., and Newlon, C.S. (1992). Replication forks pause at yeast centromeres. Molecular and cellular biology *12*, 4056-4066.
Groh, M., Lufino, M.M., Wade-Martins, R., and Gromak, N. (2014). R-loops associated with triplet repeat expansions promote gene silencing in Friedreich ataxia and fragile X syndrome. PLoS Genet *10*, e1004318.
Groth, A., Corpet, A., Cook, A.J., Roche, D., Bartek, J., Lukas, J., and Almouzni, G. (2007). Regulation of replication fork progression through histone supply and demand. Science *318*, 1928-1931.
Guo, M., Hundseth, K., Ding, H., Vidhyasagar, V., Inoue, A., Nguyen, C.-H., Zain, R., Lee, J.S., and Wu, Y. (2015). A distinct triplex DNA unwinding activity of ChlR1 helicase. The Journal of biological chemistry *290*, 5174-5189.
Haase, S.B., and Reed, S.I. (2002). Improved flow cytometric analysis of the budding yeast cell cycle. Cell cycle (Georgetown, Tex.) *1*, 132-136.
Haering, C.H., Schoffnegger, D., Nishino, T., Helmhart, W., Nasmyth, K., and Löwe, J. (2004). Structure and stability of cohesin's Smc1-kleisin interaction. Molecular cell *15*, 951-964.

Handa, N., Morimatsu, K., Lovett, S.T., and Kowalczykowski, S.C. (2009). Reconstitution of initial steps of dsDNA break repair by the RecF pathway of E. coli. Genes & development *23*, 1234-1245.
Harada, Y., Ohara, O., Takatsuki, A., Itoh, H., Shimamoto, N., and Kinosita, K., Jr. (2001). Direct observation of DNA rotation during transcription by Escherichia coli RNA polymerase. Nature *409*, 113-115.
Harmon, F.G., DiGate, R.J., and Kowalczykowski, S.C. (1999). RecQ helicase and topoisomerase III comprise a novel DNA strand passage function: a conserved mechanism for control of DNA recombination. Molecular cell *3*, 611-620.
Harvey, S.H., Sheedy, D.M., Cuddihy, A.R., and O'Connell, M.J. (2004). Coordination of DNA damage responses via the Smc5/Smc6 complex. Molecular and cellular biology *24*, 662-674.
Hashash, N., Johnson, A.L., and Cha, R.S. (2012). Topoisomerase II- and condensin-dependent breakage of MEC1ATR-sensitive fragile sites occurs independently of spindle tension, anaphase, or cytokinesis. PLoS genetics *8*, e1002978-e1002978.
Hiasa, H., and Marians, K.J. (1994). Topoisomerase III, but not topoisomerase I, can support nascent chain elongation during theta-type DNA replication. J Biol Chem *269*, 32655-32659.
Hodgson, B., Calzada, A., and Labib, K. (2007). Mrc1 and Tof1 regulate DNA replication forks in different ways during normal S phase. Mol Biol Cell *18*, 3894-3902.
Hoege, C., Pfander, B., Moldovan, G.-L., Pyrowolakis, G., and Jentsch, S. (2002). RAD6-dependent DNA repair is linked to modification of PCNA by ubiquitin and SUMO. Nature *419*, 135-141.
Holm, C., Stearns, T., and Botstein, D. (1989). DNA topoisomerase II must act at mitosis to prevent nondisjunction and chromosome breakage. Molecular and cellular biology *9*, 159-168.
Hu, B., Liao, C., Millson, S.H., Mollapour, M., Prodromou, C., Pearl, L.H., Piper, P.W., and Panaretou, B. (2005). Qri2/Nse4, a component of the essential Smc5/6 DNA repair complex. Mol Microbiol *55*, 1735-1750.
Huang, J., Brito, I.L., Villen, J., Gygi, S.P., Amon, A., and Moazed, D. (2006). Inhibition of homologous recombination by a cohesin-associated clamp complex recruited to the rDNA recombination enhancer. Genes Dev *20*, 2887-2901.
Hwang, J.-Y., Smith, S., Ceschia, A., Torres-Rosell, J., Aragon, L., and Myung, K. (2008). Smc5-Smc6 complex suppresses gross chromosomal rearrangements mediated by break-induced replications. DNA repair *7*, 1426-1436.
Iossifov, I., Ronemus, M., Levy, D., Wang, Z., Hakker, I., Rosenbaum, J., Yamrom, B., Lee, Y.-H., Narzisi, G., Leotta, A.*, et al.* (2012). De novo gene disruptions in children on the autistic spectrum. Neuron *74*, 285-299.
Ivessa, A.S., Lenzmeier, B.A., Bessler, J.B., Goudsouzian, L.K., Schnakenberg, S.L., and Zakian, V.A. (2003). The Saccharomyces cerevisiae helicase Rrm3p facilitates replication past nonhistone protein-DNA complexes. Mol Cell *12*, 1525-1536.
Ivessa, A.S., Zhou, J.-Q., Schulz, V.P., Monson, E.K., and Zakian, V.A. (2002). Saccharomyces Rrm3p, a 5' to 3' DNA helicase that promotes replication fork progression through telomeric and subtelomeric DNA. Genes & development *16*, 1383-1396.
Jacome, A., Gutierrez-Martinez, P., Schiavoni, F., Tenaglia, E., Martinez, P., Rodríguez-Acebes, S., Lecona, E., Murga, M., Méndez, J., Blasco, M.A.*, et al.* (2015). NSMCE2 suppresses cancer and aging in mice independently of its SUMO ligase activity. The EMBO journal *34*, 2604-2619.
Janke, C., Magiera, M.M., Rathfelder, N., Taxis, C., Reber, S., Maekawa, H., Moreno-Borchart, A., Doenges, G., Schwob, E., Schiebel, E.*, et al.* (2004). A versatile toolbox for

PCR-based tagging of yeast genes: new fluorescent proteins, more markers and promoter substitution cassettes. Yeast *21*, 947-962.
Jasencakova, Z., and Groth, A. (2010). Replication stress, a source of epigenetic aberrations in cancer? Bioessays *32*, 847-855.
Jasencakova, Z., Scharf, A.N., Ask, K., Corpet, A., Imhof, A., Almouzni, G., and Groth, A. (2010). Replication stress interferes with histone recycling and predeposition marking of new histones. Mol Cell *37*, 736-743.
Jentsch, S., and Psakhye, I. (2013). Control of nuclear activities by substrate-selective and protein-group SUMOylation. Annu Rev Genet *47*, 167-186.
Jeppsson, K., Carlborg, K.K., Nakato, R., Berta, D.G., Lilienthal, I., Kanno, T., Lindqvist, A., Brink, M.C., Dantuma, N.P., Katou, Y.*, et al.* (2014a). The chromosomal association of the Smc5/6 complex depends on cohesion and predicts the level of sister chromatid entanglement. PLoS genetics *10*, e1004680-e1004680.
Jeppsson, K., Kanno, T., Shirahige, K., and Sjogren, C. (2014b). The maintenance of chromosome structure: positioning and functioning of SMC complexes. Nat Rev Mol Cell Biol *15*, 601-614.
Johnson, C., Gali, V.K., Takahashi, T.S., and Kubota, T. (2016). PCNA Retention on DNA into G2/M Phase Causes Genome Instability in Cells Lacking Elg1. Cell reports *16*, 684-695.
Johnson, F.B., Lombard, D.B., Neff, N.F., Mastrangelo, M.A., Dewolf, W., Ellis, N.A., Marciniak, R.A., Yin, Y., Jaenisch, R., and Guarente, L. (2000). Association of the Bloom syndrome protein with topoisomerase IIIalpha in somatic and meiotic cells. Cancer Res *60*, 1162-1167.
Ju, L., Wing, J., Taylor, E., Brandt, R., Slijepcevic, P., Horsch, M., Rathkolb, B., Rácz, I., Becker, L., Hans, W.*, et al.* (2013). SMC6 is an essential gene in mice, but a hypomorphic mutant in the ATPase domain has a mild phenotype with a range of subtle abnormalities. DNA repair *12*, 356-366.
Kaliraman, V., Mullen, J.R., Fricke, W.M., Bastin-Shanower, S.A., and Brill, S.J. (2001). Functional overlap between Sgs1-Top3 and the Mms4-Mus81 endonuclease. Genes & development *15*, 2730-2740.
Kanno, T., Berta, D.G., and Sjögren, C. (2015). The Smc5/6 Complex Is an ATP-Dependent Intermolecular DNA Linker. Cell reports *12*, 1471-1482.
Kannouche, P.L., Wing, J., and Lehmann, A.R. (2004). Interaction of human DNA polymerase eta with monoubiquitinated PCNA: a possible mechanism for the polymerase switch in response to DNA damage. Molecular cell *14*, 491-500.
Kaplan, D.L. (2006). Replication termination: mechanism of polar arrest revealed. Curr Biol *16*, R684-686.
Karras, G.I., Fumasoni, M., Sienski, G., Vanoli, F., Branzei, D., and Jentsch, S. (2013). Noncanonical role of the 9-1-1 clamp in the error-free DNA damage tolerance pathway. Molecular cell *49*, 536-546.
Karras, G.I., and Jentsch, S. (2010). The RAD6 DNA damage tolerance pathway operates uncoupled from the replication fork and is functional beyond S phase. Cell *141*, 255-267.
Katou, Y., Kaneshiro, K., Aburatani, H., and Shirahige, K. (2006). Genomic approach for the understanding of dynamic aspect of chromosome behavior. Methods Enzymol *409*, 389-410.
Kaufman, C.S., Genovese, A., and Butler, M.G. (2016). Deletion of TOP3B Is Associated with Cognitive Impairment and Facial Dysmorphism. Cytogenet Genome Res *150*, 106-111.
Kegel, A., Betts-Lindroos, H., Kanno, T., Jeppsson, K., Ström, L., Katou, Y., Itoh, T., Shirahige, K., and Sjögren, C. (2011). Chromosome length influences replication-induced topological stress. Nature *471*, 392-396.

Kennedy, J.A., Syed, S., and Schmidt, K.H. (2015). Structural Motifs Critical for In Vivo Function and Stability of the RecQ-Mediated Genome Instability Protein Rmi1. PLoS One *10*, e0145466-e0145466.
Kim, R.A., and Wang, J.C. (1992). Identification of the yeast TOP3 gene product as a single strand-specific DNA topoisomerase. The Journal of biological chemistry *267*, 17178-17185.
Kitao, S., Shimamoto, A., Goto, M., Miller, R.W., Smithson, W.A., Lindor, N.M., and Furuichi, Y. (1999). Mutations in RECQL4 cause a subset of cases of Rothmund-Thomson syndrome. Nature genetics *22*, 82-84.
Kliszczak, M., Stephan, A.K., Flanagan, A.-M., and Morrison, C.G. (2012). SUMO ligase activity of vertebrate Mms21/Nse2 is required for efficient DNA repair but not for Smc5/6 complex stability. DNA repair *11*, 799-810.
Kobayashi, T. (2006). Strategies to maintain the stability of the ribosomal RNA gene repeats--collaboration of recombination, cohesion, and condensation. Genes Genet Syst *81*, 155-161.
Kobayashi, T., and Ganley, A.R. (2005). Recombination regulation by transcription-induced cohesin dissociation in rDNA repeats. Science *309*, 1581-1584.
Kobayashi, T., and Horiuchi, T. (1996). A yeast gene product, Fob1 protein, required for both replication fork blocking and recombinational hotspot activities. Genes Cells *1*, 465-474.
Kobayashi, T., Horiuchi, T., Tongaonkar, P., Vu, L., and Nomura, M. (2004). SIR2 regulates recombination between different rDNA repeats, but not recombination within individual rRNA genes in yeast. Cell *117*, 441-453.
Kötter, P., Weigand, J.E., Meyer, B., Entian, K.-D., and Suess, B. (2009). A fast and efficient translational control system for conditional expression of yeast genes. Nucleic Acids Res *37*, e120-e120.
Koundrioukoff, S., Carignon, S., Techer, H., Letessier, A., Brison, O., and Debatisse, M. (2013). Stepwise activation of the ATR signaling pathway upon increasing replication stress impacts fragile site integrity. PLoS Genet *9*, e1003643.
Krings, G., and Bastia, D. (2004). swi1- and swi3-dependent and independent replication fork arrest at the ribosomal DNA of Schizosaccharomyces pombe. Proc Natl Acad Sci U S A *101*, 14085-14090.
Labbé, D.P., Sweeney, C.J., Brown, M., Galbo, P., Rosario, S., Wadosky, K.M., Ku, S.-Y., Sjöström, M., Alshalalfa, M., Erho, N.*, et al.* (2017). TOP2A and EZH2 Provide Early Detection of an Aggressive Prostate Cancer Subgroup. Clin Cancer Res *23*, 7072-7083.
Laemmli, U.K. (1970). Cleavage of Structural Proteins during the Assembly of the Head of Bacteriophage T4. Nature *227*, 680-685.
Lai, E., Birren, B.W., Clark, S.M., Simon, M.I., and Hood, L. (1989). Pulsed field gel electrophoresis. Biotechniques *7*, 34-42.
Lambert, S., and Carr, A.M. (2005). Checkpoint responses to replication fork barriers. Biochimie *87*, 591-602.
Lambert, S., Watson, A., Sheedy, D.M., Martin, B., and Carr, A.M. (2005). Gross chromosomal rearrangements and elevated recombination at an inducible site-specific replication fork barrier. Cell *121*, 689-702.
Langlois, R.G., Bigbee, W.L., Jensen, R.H., and German, J. (1989). Evidence for increased in vivo mutation and somatic recombination in Bloom's syndrome. Proceedings of the National Academy of Sciences of the United States of America *86*, 670-674.
Larcher, M.V., and Pasero, P. (2020). Top1 and Top2 promote replication fork arrest at a programmed pause site. Genes & development *34*, 1-3.

Lavrukhin, O.V., Fortune, J.M., Wood, T.G., Burbank, D.E., Van Etten, J.L., Osheroff, N., and Lloyd, R.S. (2000). Topoisomerase II from Chlorella virus PBCV-1. Characterization of the smallest known type II topoisomerase. The Journal of biological chemistry *275*, 6915-6921.
Lee, K.-y., and Myung, K. (2008). PCNA modifications for regulation of post-replication repair pathways. Mol Cells *26*, 5-11.
Lehmann, A.R., Walicka, M., Griffiths, D.J., Murray, J.M., Watts, F.Z., McCready, S., and Carr, A.M. (1995). The rad18 gene of Schizosaccharomyces pombe defines a new subgroup of the SMC superfamily involved in DNA repair. Molecular and cellular biology *15*, 7067-7080.
Lemoine, F.J., Degtyareva, N.P., Lobachev, K., and Petes, T.D. (2005). Chromosomal translocations in yeast induced by low levels of DNA polymerase a model for chromosome fragile sites. Cell *120*, 587-598.
Leon-Ortiz, A.M., Svendsen, J., and Boulton, S.J. (2014). Metabolism of DNA secondary structures at the eukaryotic replication fork. DNA Repair (Amst) *19*, 152-162.
Liberi, G., Maffioletti, G., Lucca, C., Chiolo, I., Baryshnikova, A., Cotta-Ramusino, C., Lopes, M., Pellicioli, A., Haber, J.E., and Foiani, M. (2005a). Rad51-dependent DNA structures accumulate at damaged replication forks in sgs1 mutants defective in the yeast ortholog of BLM RecQ helicase. Genes & development *19*, 339-350.
Liberi, G., Maffioletti, G., Lucca, C., Chiolo, I., Baryshnikova, A., Cotta-Ramusino, C., Lopes, M., Pellicioli, A., Haber, J.E., and Foiani, M. (2005b). Rad51-dependent DNA structures accumulate at damaged replication forks in sgs1 mutants defective in the yeast ortholog of BLM RecQ helicase. Genes Dev *19*, 339-350.
Lindroos, H.B., Ström, L., Itoh, T., Katou, Y., Shirahige, K., and Sjögren, C. (2006). Chromosomal association of the Smc5/6 complex reveals that it functions in differently regulated pathways. Molecular cell *22*, 755-767.
Litwin, I., Bakowski, T., Maciaszczyk-Dziubinska, E., and Wysocki, R. (2017). The LSH/HELLS homolog Irc5 contributes to cohesin association with chromatin in yeast. Nucleic Acids Res *45*, 6404-6416.
Liu, B., and Alberts, B.M. (1995). Head-on collision between a DNA replication apparatus and RNA polymerase transcription complex. Science (New York, N.Y.) *267*, 1131-1137.
Liu, L.F., and Wang, J.C. (1987). Supercoiling of the DNA template during transcription. Proceedings of the National Academy of Sciences of the United States of America *84*, 7024-7027.
Lobachev, K.S., Stenger, J.E., Kozyreva, O.G., Jurka, J., Gordenin, D.A., and Resnick, M.A. (2000). Inverted Alu repeats unstable in yeast are excluded from the human genome. EMBO J *19*, 3822-3830.
Longtine, M.S., McKenzie, A., 3rd, Demarini, D.J., Shah, N.G., Wach, A., Brachat, A., Philippsen, P., and Pringle, J.R. (1998). Additional modules for versatile and economical PCR-based gene deletion and modification in Saccharomyces cerevisiae. Yeast *14*, 953-961.
Lopes, M., Cotta-Ramusino, C., Liberi, G., and Foiani, M. (2003). Branch migrating sister chromatid junctions form at replication origins through Rad51/Rad52-independent mechanisms. Molecular cell *12*, 1499-1510.
Lopes, M., Cotta-Ramusino, C., Pellicioli, A., Liberi, G., Plevani, P., Muzi-Falconi, M., Newlon, C.S., and Foiani, M. (2001). The DNA replication checkpoint response stabilizes stalled replication forks. Nature *412*, 557-561.
Losada, A., and Hirano, T. (2005). Dynamic molecular linkers of the genome: the first decade of SMC proteins. Genes & development *19*, 1269-1287.

Lu, J., Kobayashi, R., and Brill, S.J. (1996). Characterization of a high mobility group 1/2 homolog in yeast. The Journal of biological chemistry *271*, 33678-33685.
Lucas, I., and Hyrien, O. (2000). Hemicatenanes form upon inhibition of DNA replication. Nucleic Acids Res *28*, 2187-2193.
Luke, B., Versini, G., Jaquenoud, M., Zaidi, I.W., Kurz, T., Pintard, L., Pasero, P., and Peter, M. (2006). The cullin Rtt101p promotes replication fork progression through damaged DNA and natural pause sites. Curr Biol *16*, 786-792.
Makovets, S., Herskowitz, I., and Blackburn, E.H. (2004). Anatomy and dynamics of DNA replication fork movement in yeast telomeric regions. Mol Cell Biol *24*, 4019-4031.
Mankouri, H.W., and Hickson, I.D. (2006). Top3 processes recombination intermediates and modulates checkpoint activity after DNA damage. Mol Biol Cell *17*, 4473-4483.
Marko, J.F., De Los Rios, P., Barducci, A., and Gruber, S. (2019). DNA-segment-capture model for loop extrusion by structural maintenance of chromosome (SMC) protein complexes. Nucleic Acids Res *47*, 6956-6972.
Matsuzaki, H., Kassavetis, G.A., and Geiduschek, E.P. (1994). Analysis of RNA chain elongation and termination by Saccharomyces cerevisiae RNA polymerase III. J Mol Biol *235*, 1173-1192.
Mayer, V.W., and Goin, C.J. (1988). Investigations of aneuploidy-inducing chemical combinations in Saccharomyces cerevisiae. Mutat Res *201*, 413-421.
McAleenan, A., Cordon-Preciado, V., Clemente-Blanco, A., Liu, I.C., Sen, N., Leonard, J., Jarmuz, A., and Aragón, L. (2012). SUMOylation of the α-kleisin subunit of cohesin is required for DNA damage-induced cohesion. Current biology : CB *22*, 1564-1575.
McDonald, W.H., Pavlova, Y., Yates, J.R., 3rd, and Boddy, M.N. (2003). Novel essential DNA repair proteins Nse1 and Nse2 are subunits of the fission yeast Smc5-Smc6 complex. The Journal of biological chemistry *278*, 45460-45467.
McVey, M., Kaeberlein, M., Tissenbaum, H.A., and Guarente, L. (2001). The short life span of Saccharomyces cerevisiae sgs1 and srs2 mutants is a composite of normal aging processes and mitotic arrest due to defective recombination. Genetics *157*, 1531-1542.
Menolfi, D., Delamarre, A., Lengronne, A., Pasero, P., and Branzei, D. (2015). Essential Roles of the Smc5/6 Complex in Replication through Natural Pausing Sites and Endogenous DNA Damage Tolerance. Molecular cell *60*, 835-846.
Merz, K., Hondele, M., Goetze, H., Gmelch, K., Stoeckl, U., and Griesenbeck, J. (2008). Actively transcribed rRNA genes in S. cerevisiae are organized in a specialized chromatin associated with the high-mobility group protein Hmo1 and are largely devoid of histone molecules. Genes & development *22*, 1190-1204.
Mieczkowski, P.A., Lemoine, F.J., and Petes, T.D. (2006). Recombination between retrotransposons as a source of chromosome rearrangements in the yeast Saccharomyces cerevisiae. DNA Repair (Amst) *5*, 1010-1020.
Mimitou, E.P., and Symington, L.S. (2008). Sae2, Exo1 and Sgs1 collaborate in DNA double-strand break processing. Nature *455*, 770-774.
Mohanty, B.K., Bairwa, N.K., and Bastia, D. (2006). The Tof1p-Csm3p protein complex counteracts the Rrm3p helicase to control replication termination of Saccharomyces cerevisiae. Proc Natl Acad Sci U S A *103*, 897-902.
Mourón, S., Rodriguez-Acebes, S., Martínez-Jiménez, M.I., García-Gómez, S., Chocrón, S., Blanco, L., and Méndez, J. (2013). Repriming of DNA synthesis at stalled replication forks by human PrimPol. Nature structural & molecular biology *20*, 1383-1389.
Mullen, J.R., Kaliraman, V., Ibrahim, S.S., and Brill, S.J. (2001). Requirement for three novel protein complexes in the absence of the Sgs1 DNA helicase in Saccharomyces cerevisiae. Genetics *157*, 103-118.

Mullen, J.R., Nallaseth, F.S., Lan, Y.Q., Slagle, C.E., and Brill, S.J. (2005). Yeast Rmi1/Nce4 controls genome stability as a subunit of the Sgs1-Top3 complex. Molecular and cellular biology *25*, 4476-4487.
Mundbjerg, K., Jorgensen, S.W., Fredsoe, J., Nielsen, I., Pedersen, J.M., Bentsen, I.B., Lisby, M., Bjergbaek, L., and Andersen, A.H. (2015). Top2 and Sgs1-Top3 Act Redundantly to Ensure rDNA Replication Termination. PLoS Genet *11*, e1005697.
Murayama, Y., and Uhlmann, F. (2015). DNA Entry into and Exit out of the Cohesin Ring by an Interlocking Gate Mechanism. Cell *163*, 1628-1640.
Murugesapillai, D., McCauley, M.J., Huo, R., Nelson Holte, M.H., Stepanyants, A., Maher, L.J., 3rd, Israeloff, N.E., and Williams, M.C. (2014). DNA bridging and looping by HMO1 provides a mechanism for stabilizing nucleosome-free chromatin. Nucleic Acids Res *42*, 8996-9004.
Narayanan, V., Mieczkowski, P.A., Kim, H.M., Petes, T.D., and Lobachev, K.S. (2006). The pattern of gene amplification is determined by the chromosomal location of hairpin-capped breaks. Cell *125*, 1283-1296.
Nedelcheva, M.N., Roguev, A., Dolapchiev, L.B., Shevchenko, A., Taskov, H.B., Shevchenko, A., Stewart, A.F., and Stoynov, S.S. (2005). Uncoupling of unwinding from DNA synthesis implies regulation of MCM helicase by Tof1/Mrc1/Csm3 checkpoint complex. J Mol Biol *347*, 509-521.
Nicholls, T.J., Nadalutti, C.A., Motori, E., Sommerville, E.W., Gorman, G.S., Basu, S., Hoberg, E., Turnbull, D.M., Chinnery, P.F., Larsson, N.-G*., et al.* (2018). Topoisomerase 3α Is Required for Decatenation and Segregation of Human mtDNA. Molecular cell *69*, 9-23.e26.
Nikolov, I., and Taddei, A. (2016). Linking replication stress with heterochromatin formation. Chromosoma *125*, 523-533.
Nimonkar, A.V., Genschel, J., Kinoshita, E., Polaczek, P., Campbell, J.L., Wyman, C., Modrich, P., and Kowalczykowski, S.C. (2011). BLM-DNA2-RPA-MRN and EXO1-BLM-RPA-MRN constitute two DNA end resection machineries for human DNA break repair. Genes & development *25*, 350-362.
Nimonkar, A.V., Ozsoy, A.Z., Genschel, J., Modrich, P., and Kowalczykowski, S.C. (2008). Human exonuclease 1 and BLM helicase interact to resect DNA and initiate DNA repair. Proceedings of the National Academy of Sciences of the United States of America *105*, 16906-16911.
Nitiss, J.L. (1998). Investigating the biological functions of DNA topoisomerases in eukaryotic cells. Biochim Biophys Acta *1400*, 63-81.
Nurse, P., Levine, C., Hassing, H., and Marians, K.J. (2003). Topoisomerase III can serve as the cellular decatenase in Escherichia coli. J Biol Chem *278*, 8653-8660.
O'Reilly, N., Charbin, A., Lopez-Serra, L., and Uhlmann, F. (2012). Facile synthesis of budding yeast a-factor and its use to synchronize cells of α mating type. Yeast *29*, 233-240.
Oakley, T.J., and Hickson, I.D. (2002). Defending genome integrity during S-phase: putative roles for RecQ helicases and topoisomerase III. DNA repair *1*, 175-207.
Oliveira, R., and Johansson, B. (2012). Quantitative DNA damage and repair measurement with the yeast comet assay. Methods Mol Biol *920*, 101-109.
Omont, N., and Képès, F. (2004). Transcription/replication collisions cause bacterial transcription units to be longer on the leading strand of replication. Bioinformatics *20*, 2719-2725.
Onoda, F., Takeda, M., Seki, M., Maeda, D., Tajima, J.-i., Ui, A., Yagi, H., and Enomoto, T. (2004). SMC6 is required for MMS-induced interchromosomal and sister chromatid recombinations in Saccharomyces cerevisiae. DNA repair *3*, 429-439.

Onodera, R., Seki, M., Ui, A., Satoh, Y., Miyajima, A., Onoda, F., and Enomoto, T. (2002). Functional and physical interaction between Sgs1 and Top3 and Sgs1-independent function of Top3 in DNA recombination repair. Genes & genetic systems *77*, 11-21.
Ooi, S.L., Shoemaker, D.D., and Boeke, J.D. (2003). DNA helicase gene interaction network defined using synthetic lethality analyzed by microarray. Nature Genetics *35*, 277-286.
Paeschke, K., Bochman, M.L., Garcia, P.D., Cejka, P., Friedman, K.L., Kowalczykowski, S.C., and Zakian, V.A. (2013). Pif1 family helicases suppress genome instability at G-quadruplex motifs. Nature *497*, 458-462.
Palecek, J., Vidot, S., Feng, M., Doherty, A.J., and Lehmann, A.R. (2006). The Smc5-Smc6 DNA repair complex. bridging of the Smc5-Smc6 heads by the KLEISIN, Nse4, and non-Kleisin subunits. The Journal of biological chemistry *281*, 36952-36959.
Papadopoulou, C., Guilbaud, G., Schiavone, D., and Sale, J.E. (2015). Nucleotide Pool Depletion Induces G-Quadruplex-Dependent Perturbation of Gene Expression. Cell Rep *13*, 2491-2503.
Papouli, E., Chen, S., Davies, A.A., Huttner, D., Krejci, L., Sung, P., and Ulrich, H.D. (2005). Crosstalk between SUMO and ubiquitin on PCNA is mediated by recruitment of the helicase Srs2p. Molecular cell *19*, 123-133.
Park, S., Han, J.E., Kim, H.-G., Kim, H.-Y., Kim, M.-G., Park, J.-K., Cho, G.-J., Huang, H., Kim, M.O., Ryoo, Z.Y.*, et al.* (2020). Inhibition of MAGEA2 regulates pluripotency, proliferation, apoptosis, and differentiation in mouse embryonic stem cells. J Cell Biochem, 10.1002/jcb.29692.
Pasero, P., Bensimon, A., and Schwob, E. (2002). Single-molecule analysis reveals clustering and epigenetic regulation of replication origins at the yeast rDNA locus. Genes Dev *16*, 2479-2484.
Paul Solomon Devakumar, L.J., Gaubitz, C., Lundblad, V., Kelch, B.A., and Kubota, T. (2019). Effective mismatch repair depends on timely control of PCNA retention on DNA by the Elg1 complex. Nucleic Acids Res *47*, 6826-6841.
Payne, F., Colnaghi, R., Rocha, N., Seth, A., Harris, J., Carpenter, G., Bottomley, W.E., Wheeler, E., Wong, S., Saudek, V.*, et al.* (2014). Hypomorphism in human NSMCE2 linked to primordial dwarfism and insulin resistance. J Clin Invest *124*, 4028-4038.
Pebernard, S., McDonald, W.H., Pavlova, Y., Yates, J.R., 3rd, and Boddy, M.N. (2004). Nse1, Nse2, and a novel subunit of the Smc5-Smc6 complex, Nse3, play a crucial role in meiosis. Molecular biology of the cell *15*, 4866-4876.
Pebernard, S., Perry, J.J.P., Tainer, J.A., and Boddy, M.N. (2008). Nse1 RING-like domain supports functions of the Smc5-Smc6 holocomplex in genome stability. Molecular biology of the cell *19*, 4099-4109.
Pebernard, S., Wohlschlegel, J., McDonald, W.H., Yates, J.R., 3rd, and Boddy, M.N. (2006). The Nse5-Nse6 dimer mediates DNA repair roles of the Smc5-Smc6 complex. Molecular and cellular biology *26*, 1617-1630.
Peng, J., and Feng, W. (2016). Incision of damaged DNA in the presence of an impaired Smc5/6 complex imperils genome stability. Nucleic Acids Res *44*, 10216-10229.
Peng, X.P., Lim, S., Li, S., Marjavaara, L., Chabes, A., and Zhao, X. (2018). Acute Smc5/6 depletion reveals its primary role in rDNA replication by restraining recombination at fork pausing sites. PLoS genetics *14*, e1007129-e1007129.
Petes, T.D. (1979). Yeast ribosomal DNA genes are located on chromosome XII. Proc Natl Acad Sci U S A *76*, 410-414.
Pfander, B., Moldovan, G.-L., Sacher, M., Hoege, C., and Jentsch, S. (2005). SUMO-modified PCNA recruits Srs2 to prevent recombination during S phase. Nature *436*, 428-433.

Phillips, J.A., Chan, A., Paeschke, K., and Zakian, V.A. (2015). The pif1 helicase, a negative regulator of telomerase, acts preferentially at long telomeres. PLoS Genet *11*, e1005186.
Piazza, A., Shah, S.S., Wright, W.D., Gore, S.K., Koszul, R., and Heyer, W.-D. (2019). Dynamic Processing of Displacement Loops during Recombinational DNA Repair. Molecular cell *73*, 1255-1266.e1254.
Pilzecker, B., Buoninfante, O.A., and Jacobs, H. (2019). DNA damage tolerance in stem cells, ageing, mutagenesis, disease and cancer therapy. Nucleic Acids Res *47*, 7163-7181.
Plank, J.L., Wu, J., and Hsieh, T.-S. (2006). Topoisomerase IIIalpha and Bloom's helicase can resolve a mobile double Holliday junction substrate through convergent branch migration. Proceedings of the National Academy of Sciences of the United States of America *103*, 11118-11123.
Postow, L., Crisona, N.J., Peter, B.J., Hardy, C.D., and Cozzarelli, N.R. (2001). Topological challenges to DNA replication: conformations at the fork. Proceedings of the National Academy of Sciences of the United States of America *98*, 8219-8226.
Postow, L., Hardy, C.D., Arsuaga, J., and Cozzarelli, N.R. (2004). Topological domain structure of the Escherichia coli chromosome. Genes & development *18*, 1766-1779.
Potts, P.R., Porteus, M.H., and Yu, H. (2006). Human SMC5/6 complex promotes sister chromatid homologous recombination by recruiting the SMC1/3 cohesin complex to double-strand breaks. The EMBO journal *25*, 3377-3388.
Potts, P.R., and Yu, H. (2005). Human MMS21/NSE2 is a SUMO ligase required for DNA repair. Molecular and cellular biology *25*, 7021-7032.
Potts, P.R., and Yu, H. (2007). The SMC5/6 complex maintains telomere length in ALT cancer cells through SUMOylation of telomere-binding proteins. Nature structural & molecular biology *14*, 581-590.
Prado, F., and Aguilera, A. (2005). Impairment of replication fork progression mediates RNA polII transcription-associated recombination. EMBO J *24*, 1267-1276.
Räschle, M., Smeenk, G., Hansen, R.K., Temu, T., Oka, Y., Hein, M.Y., Nagaraj, N., Long, D.T., Walter, J.C., Hofmann, K.*, et al.* (2015). DNA repair. Proteomics reveals dynamic assembly of repair complexes during bypass of DNA cross-links. Science (New York, N.Y.) *348*, 1253671-1253671.
Raveendranathan, M., Chattopadhyay, S., Bolon, Y.T., Haworth, J., Clarke, D.J., and Bielinsky, A.K. (2006). Genome-wide replication profiles of S-phase checkpoint mutants reveal fragile sites in yeast. EMBO J *25*, 3627-3639.
Reid, G.A., and Schatz, G. (1982). Import of proteins into mitochondria. Yeast cells grown in the presence of carbonyl cyanide m-chlorophenylhydrazone accumulate massive amounts of some mitochondrial precursor polypeptides. The Journal of biological chemistry *257*, 13056-13061.
Reyes-Lamothe, R., Possoz, C., Danilova, O., and Sherratt, D.J. (2008). Independent positioning and action of Escherichia coli replisomes in live cells. Cell *133*, 90-102.
Rossi, F., Helbling-Leclerc, A., Kawasumi, R., Jegadesan, N.K., Xu, X., Devulder, P., Abe, T., Takata, M., Xu, D., Rosselli, F.*, et al.* (2020). SMC5/6 acts jointly with Fanconi anemia factors to support DNA repair and genome stability. EMBO Rep *21*, e48222.
Roy, M.-A., and D'Amours, D. (2011). DNA-binding properties of Smc6, a core component of the Smc5-6 DNA repair complex. Biochem Biophys Res Commun *416*, 80-85.
Roy, M.-A., Siddiqui, N., and D'Amours, D. (2011). Dynamic and selective DNA-binding activity of Smc5, a core component of the Smc5-Smc6 complex. Cell cycle (Georgetown, Tex.) *10*, 690-700.
Sabouri, N., McDonald, K.R., Webb, C.J., Cristea, I.M., and Zakian, V.A. (2012). DNA replication through hard-to-replicate sites, including both highly transcribed RNA Pol II and Pol III genes, requires the S. pombe Pfh1 helicase. Genes Dev *26*, 581-593.

San-Segundo, P.A., and Clemente-Blanco, A. (2020). Resolvases, Dissolvases, and Helicases in Homologous Recombination: Clearing the Road for Chromosome Segregation. Genes (Basel) *11*, 71.
Sasaki, M., and Kobayashi, T. (2017). Ctf4 Prevents Genome Rearrangements by Suppressing DNA Double-Strand Break Formation and Its End Resection at Arrested Replication Forks. Molecular cell *66*, 533-545.e535.
Saunus, J.M., Quinn, M.C.J., Patch, A.-M., Pearson, J.V., Bailey, P.J., Nones, K., McCart Reed, A.E., Miller, D., Wilson, P.J., Al-Ejeh, F.*, et al.* (2015). Integrated genomic and transcriptomic analysis of human brain metastases identifies alterations of potential clinical significance. J Pathol *237*, 363-378.
Scappaticci, S., Cerimele, D., and Fraccaro, M. (1982). Clonal structural chromosomal rearrangements in primary fibroblast cultures and in lymphocytes of patients with Werner's Syndrome. Human genetics *62*, 16-24.
Schalbetter, S.A., Mansoubi, S., Chambers, A.L., Downs, J.A., and Baxter, J. (2015). Fork rotation and DNA precatenation are restricted during DNA replication to prevent chromosomal instability. Proc Natl Acad Sci U S A *112*, E4565-4570.
Schmidt, K.H., and Kolodner, R.D. (2004). Requirement of Rrm3 helicase for repair of spontaneous DNA lesions in cells lacking Srs2 or Sgs1 helicase. Mol Cell Biol *24*, 3213-3226.
Schvartzman, J.B., Martínez-Robles, M.-L., Hernández, P., and Krimer, D.B. (2013). The benefit of DNA supercoiling during replication. Biochem Soc Trans *41*, 646-651.
Schvartzman, J.B., and Stasiak, A. (2004). A topological view of the replicon. EMBO Rep *5*, 256-261.
Schwab, R.A., Nieminuszczy, J., Shin-ya, K., and Niedzwiedz, W. (2013). FANCJ couples replication past natural fork barriers with maintenance of chromatin structure. J Cell Biol *201*, 33-48.
Sergeant, J., Taylor, E., Palecek, J., Fousteri, M., Andrews, E.A., Sweeney, S., Shinagawa, H., Watts, F.Z., and Lehmann, A.R. (2005). Composition and architecture of the Schizosaccharomyces pombe Rad18 (Smc5-6) complex. Molecular and cellular biology *25*, 172-184.
Shyian, M., Albert, B., Zupan, A.M., Ivanitsa, V., Charbonnet, G., Dilg, D., and Shore, D. (2020). Fork pausing complex engages topoisomerases at the replisome. Genes & development *34*, 87-98.
Sinclair, D.A., Mills, K., and Guarente, L. (1997). Accelerated aging and nucleolar fragmentation in yeast sgs1 mutants. Science (New York, N.Y.) *277*, 1313-1316.
Sista, P.R., Mukherjee, S., Patel, P., Khatri, G.S., and Bastia, D. (1989). A host-encoded DNA-binding protein promotes termination of plasmid replication at a sequence-specific replication terminus. Proc Natl Acad Sci U S A *86*, 3026-3030.
Sollier, J., Driscoll, R., Castellucci, F., Foiani, M., Jackson, S.P., and Branzei, D. (2009). The Saccharomyces cerevisiae Esc2 and Smc5-6 proteins promote sister chromatid junction-mediated intra-S repair. Molecular biology of the cell *20*, 1671-1682.
Somasagara, R.R., Spencer, S.M., Tripathi, K., Clark, D.W., Mani, C., Madeira da Silva, L., Scalici, J., Kothayer, H., Westwell, A.D., Rocconi, R.P.*, et al.* (2017). RAD6 promotes DNA repair and stem cell signaling in ovarian cancer and is a promising therapeutic target to prevent and treat acquired chemoresistance. Oncogene *36*, 6680-6690.
Song, W., Dominska, M., Greenwell, P.W., and Petes, T.D. (2014). Genome-wide high-resolution mapping of chromosome fragile sites in Saccharomyces cerevisiae. Proc Natl Acad Sci U S A *111*, E2210-2218.
Stelter, P., and Ulrich, H.D. (2003). Control of spontaneous and damage-induced mutagenesis by SUMO and ubiquitin conjugation. Nature *425*, 188-191.

Stephan, A.K., Kliszczak, M., Dodson, H., Cooley, C., and Morrison, C.G. (2011). Roles of vertebrate Smc5 in sister chromatid cohesion and homologous recombinational repair. Molecular and cellular biology *31*, 1369-1381.
Stoimenov, I., and Helleday, T. (2009). PCNA on the crossroad of cancer. Biochem Soc Trans *37*, 605-613.
Stoll, G., Pietiläinen, O.P.H., Linder, B., Suvisaari, J., Brosi, C., Hennah, W., Leppä, V., Torniainen, M., Ripatti, S., Ala-Mello, S*., et al.* (2013). Deletion of TOP3β, a component of FMRP-containing mRNPs, contributes to neurodevelopmental disorders. Nat Neurosci *16*, 1228-1237.
Sung, P., and Klein, H. (2006). Mechanism of homologous recombination: mediators and helicases take on regulatory functions. Nat Rev Mol Cell Biol *7*, 739-750.
Suski, C., and Marians, K.J. (2008). Resolution of converging replication forks by RecQ and topoisomerase III. Molecular cell *30*, 779-789.
Szakal, B., and Branzei, D. (2013a). Premature Cdk1/Cdc5/Mus81 pathway activation induces aberrant replication and deleterious crossover. Embo j *32*, 1155-1167.
Szakal, B., and Branzei, D. (2013b). Premature Cdk1/Cdc5/Mus81 pathway activation induces aberrant replication and deleterious crossover. The EMBO journal *32*, 1155-1167.
Szilard, R.K., Jacques, P.E., Laramee, L., Cheng, B., Galicia, S., Bataille, A.R., Yeung, M., Mendez, M., Bergeron, M., Robert, F*., et al.* (2010). Systematic identification of fragile sites via genome-wide location analysis of gamma-H2AX. Nat Struct Mol Biol *17*, 299-305.
Takahashi, Y., Dulev, S., Liu, X., Hiller, N.J., Zhao, X., and Strunnikov, A. (2008). Cooperation of sumoylated chromosomal proteins in rDNA maintenance. PLoS genetics *4*, e1000215-e1000215.
Takeuchi, Y., Horiuchi, T., and Kobayashi, T. (2003). Transcription-dependent recombination and the role of fork collision in yeast rDNA. Genes Dev *17*, 1497-1506.
Tan, T.Y., Collins, A., James, P.A., McGillivray, G., Stark, Z., Gordon, C.T., Leventer, R.J., Pope, K., Forbes, R., Crolla, J.A*., et al.* (2011). Phenotypic variability of distal 22q11.2 copy number abnormalities. Am J Med Genet A *155A*, 1623-1633.
Taylor, E.M., Copsey, A.C., Hudson, J.J.R., Vidot, S., and Lehmann, A.R. (2008). Identification of the proteins, including MAGEG1, that make up the human SMC5-6 protein complex. Molecular and cellular biology *28*, 1197-1206.
Tomas-Roca, L., Tsaalbi-Shtylik, A., Jansen, J.G., Singh, M.K., Epstein, J.A., Altunoglu, U., Verzijl, H., Soria, L., van Beusekom, E., Roscioli, T*., et al.* (2015). De novo mutations in PLXND1 and REV3L cause Möbius syndrome. Nat Commun *6*, 7199-7199.
Tong, A.H., Evangelista, M., Parsons, A.B., Xu, H., Bader, G.D., Page, N., Robinson, M., Raghibizadeh, S., Hogue, C.W., Bussey, H*., et al.* (2001). Systematic genetic analysis with ordered arrays of yeast deletion mutants. Science *294*, 2364-2368.
Torres, J.Z., Schnakenberg, S.L., and Zakian, V.A. (2004). Saccharomyces cerevisiae Rrm3p DNA helicase promotes genome integrity by preventing replication fork stalling: viability of rrm3 cells requires the intra-S-phase checkpoint and fork restart activities. Mol Cell Biol *24*, 3198-3212.
Torres-Rosell, J., De Piccoli, G., Cordon-Preciado, V., Farmer, S., Jarmuz, A., Machin, F., Pasero, P., Lisby, M., Haber, J.E., and Aragón, L. (2007a). Anaphase onset before complete DNA replication with intact checkpoint responses. Science (New York, N.Y.) *315*, 1411-1415.
Torres-Rosell, J., Machín, F., Farmer, S., Jarmuz, A., Eydmann, T., Dalgaard, J.Z., and Aragón, L. (2005). SMC5 and SMC6 genes are required for the segregation of repetitive chromosome regions. Nature Cell Biology *7*, 412-419.
Torres-Rosell, J., Sunjevaric, I., De Piccoli, G., Sacher, M., Eckert-Boulet, N., Reid, R., Jentsch, S., Rothstein, R., Aragón, L., and Lisby, M. (2007b). The Smc5-Smc6 complex and

SUMO modification of Rad52 regulates recombinational repair at the ribosomal gene locus. Nature cell biology *9*, 923-931.
Tourriere, H., and Pasero, P. (2007). Maintenance of fork integrity at damaged DNA and natural pause sites. DNA Repair (Amst) *6*, 900-913.
Tsukamoto, Y., Taggart, A.K., and Zakian, V.A. (2001). The role of the Mre11-Rad50-Xrs2 complex in telomerase- mediated lengthening of Saccharomyces cerevisiae telomeres. Curr Biol *11*, 1328-1335.
van der Crabben, S.N., Hennus, M.P., McGregor, G.A., Ritter, D.I., Nagamani, S.C.S., Wells, O.S., Harakalova, M., Chinn, I.K., Alt, A., Vondrova, L.*, et al.* (2016). Destabilized SMC5/6 complex leads to chromosome breakage syndrome with severe lung disease. J Clin Invest *126*, 2881-2892.
van der Lelij, P., Chrzanowska, K.H., Godthelp, B.C., Rooimans, M.A., Oostra, A.B., Stumm, M., Zdzienicka, M.Z., Joenje, H., and de Winter, J.P. (2010). Warsaw breakage syndrome, a cohesinopathy associated with mutations in the XPD helicase family member DDX11/ChlR1. Am J Hum Genet *86*, 262-266.
Venegas, A.B., Natsume, T., Kanemaki, M., and Hickson, I.D. (2020). Inducible Degradation of the Human SMC5/6 Complex Reveals an Essential Role Only during Interphase. Cell Rep *31*, 107533.
Vennos, E.M., and James, W.D. (1995). Rothmund-Thomson syndrome. Dermatol Clin *13*, 143-150.
Verver, D.E., Zheng, Y., Speijer, D., Hoebe, R., Dekker, H.L., Repping, S., Stap, J., and Hamer, G. (2016). Non-SMC Element 2 (NSMCE2) of the SMC5/6 Complex Helps to Resolve Topological Stress. Int J Mol Sci *17*, 1782.
Verzijl, H.T.F.M., van der Zwaag, B., Cruysberg, J.R.M., and Padberg, G.W. (2003). Möbius syndrome redefined: a syndrome of rhombencephalic maldevelopment. Neurology *61*, 327-333.
Visakorpi, T. (1992). Proliferative activity determined by DNA flow cytometry and proliferating cell nuclear antigen (PCNA) immunohistochemistry as a prognostic factor in prostatic carcinoma. J Pathol *168*, 7-13.
Vuorela, M., Pylkäs, K., and Winqvist, R. (2011). Mutation screening of the RNF8, UBC13 and MMS2 genes in Northern Finnish breast cancer families. BMC Med Genet *12*, 98-98.
Wang, F., Yang, Y., Singh, T.R., Busygina, V., Guo, R., Wan, K., Wang, W., Sung, P., Meetei, A.R., and Lei, M. (2010). Crystal structures of RMI1 and RMI2, two OB-fold regulatory subunits of the BLM complex. Structure *18*, 1159-1170.
Wang, J.C. (2002a). Cellular roles of DNA topoisomerases: a molecular perspective. Nat Rev Mol Cell Biol *3*, 430-440.
Wang, J.C. (2002b). Cellular roles of DNA topoisomerases: a molecular perspective. Nature reviews. Molecular cell biology *3*, 430-440.
Wang, S.-C. (2014). PCNA: a silent housekeeper or a potential therapeutic target? Trends Pharmacol Sci *35*, 178-186.
Wani, S., Maharshi, N., Kothiwal, D., Mahendrawada, L., Kalaivani, R., and Laloraya, S. (2018). Interaction of the Saccharomyces cerevisiae RING-domain protein Nse1 with Nse3 and the Smc5/6 complex is required for chromosome replication and stability. Curr Genet *64*, 599-617.
Waters, L.S., Minesinger, B.K., Wiltrout, M.E., D'Souza, S., Woodruff, R.V., and Walker, G.C. (2009). Eukaryotic translesion polymerases and their roles and regulation in DNA damage tolerance. Microbiol Mol Biol Rev *73*, 134-154.
Wong, R.P., García-Rodríguez, N., Zilio, N., Hanulová, M., and Ulrich, H.D. (2020). Processing of DNA Polymerase-Blocking Lesions during Genome Replication Is Spatially and Temporally Segregated from Replication Forks. Mol Cell *77*, 3-16.e14.

Wright, J.H., Gottschling, D.E., and Zakian, V.A. (1992). Saccharomyces telomeres assume a non-nucleosomal chromatin structure. Genes Dev *6*, 197-210.
Wu, L., Davies, S.L., North, P.S., Goulaouic, H., Riou, J.F., Turley, H., Gatter, K.C., and Hickson, I.D. (2000). The Bloom's syndrome gene product interacts with topoisomerase III. The Journal of biological chemistry *275*, 9636-9644.
Wu, L., and Hickson, I.D. (2003). The Bloom's syndrome helicase suppresses crossing over during homologous recombination. Nature *426*, 870-874.
Wyse, B., Oshidari, R., Rowlands, H., Abbasi, S., and Yankulov, K. (2016). RRM3 regulates epigenetic conversions in Saccharomyces cerevisiae in conjunction with Chromatin Assembly Factor I. Nucleus *7*, 405-414.
Xu, G., Chapman, J.R., Brandsma, I., Yuan, J., Mistrik, M., Bouwman, P., Bartkova, J., Gogola, E., Warmerdam, D., Barazas, M*., et al.* (2015). REV7 counteracts DNA double-strand break resection and affects PARP inhibition. Nature *521*, 541-544.
Xu, W., Ma, C., Zhang, Q., Zhao, R., Hu, D., Zhang, X., Chen, J., Liu, F., Wu, K., Liu, Y*., et al.* (2018). PJA1 Coordinates with the SMC5/6 Complex To Restrict DNA Viruses and Episomal Genes in an Interferon-Independent Manner. J Virol *92*, e00825-00818.
Xue, X., Choi, K., Bonner, J., Chiba, T., Kwon, Y., Xu, Y., Sanchez, H., Wyman, C., Niu, H., Zhao, X*., et al.* (2014). Restriction of replication fork regression activities by a conserved SMC complex. Molecular cell *56*, 436-445.
Yadav, S., Thakur, S., Kohlhase, J., Bhari, N., Kabra, M., and Gupta, N. (2019). Report of Two Novel Mutations in Indian Patients with Rothmund-Thomson Syndrome. J Pediatr Genet *8*, 163-167.
Yang, W., and Gao, Y. (2018). Translesion and Repair DNA Polymerases: Diverse Structure and Mechanism. Annu Rev Biochem *87*, 239-261.
Ying, S., Minocherhomji, S., Chan, K.L., Palmai-Pallag, T., Chu, W.K., Wass, T., Mankouri, H.W., Liu, Y., and Hickson, I.D. (2013). MUS81 promotes common fragile site expression. Nat Cell Biol *15*, 1001-1007.
Yong-Gonzales, V., Hang, L.E., Castellucci, F., Branzei, D., and Zhao, X. (2012). The Smc5-Smc6 complex regulates recombination at centromeric regions and affects kinetochore protein sumoylation during normal growth. PLoS One *7*, e51540-e51540.
Zabrady, K., Adamus, M., Vondrova, L., Liao, C., Skoupilova, H., Novakova, M., Jurcisinova, L., Alt, A., Oliver, A.W., Lehmann, A.R*., et al.* (2016). Chromatin association of the SMC5/6 complex is dependent on binding of its NSE3 subunit to DNA. Nucleic Acids Res *44*, 1064-1079.
Zhao, X., and Blobel, G. (2005). A SUMO ligase is part of a nuclear multiprotein complex that affects DNA repair and chromosomal organization. Proceedings of the National Academy of Sciences of the United States of America *102*, 4777-4782.
Zhu, Z., Chung, W.-H., Shim, E.Y., Lee, S.E., and Ira, G. (2008). Sgs1 helicase and two nucleases Dna2 and Exo1 resect DNA double-strand break ends. Cell *134*, 981-994.
Zou, S., Yang, J., Guo, J., Su, Y., He, C., Wu, J., Yu, L., Ding, W.-Q., and Zhou, J. (2018). RAD18 promotes the migration and invasion of esophageal squamous cell cancer via the JNK-MMPs pathway. Cancer Lett *417*, 65-74.

Appendix 1

1.1 Comet Assay

1.1.1 Introduction

Comet assay is a single cell electrophoresis assay: the cells are incorporated in agarose on a glass slide, lysed with lysis buffer and the DNA from single cells is run in an electrophoresis chamber. As the DNA is negatively charged, it moves towards positive charge and while the chromosomal DNA is slower in movement, DNA breaks create smaller fragments of DNA that can move faster. This forms a particular pattern where the chromosomal/intact DNA forms a concentrated area while the broken DNA fragments appear as comet tails. As the pattern formed resembles comets, the assay is named "comet assay" (Olive et al., 1990; Ostling and Johanson, 1984). Comets for mammalian cells appear more clearly than *S. cerevisiae* cells as the size of the mammalian cells is larger. Nonetheless, we have tried to perform comet assay in yeast cells following the protocol by (Oliveira and Johansson, 2012).

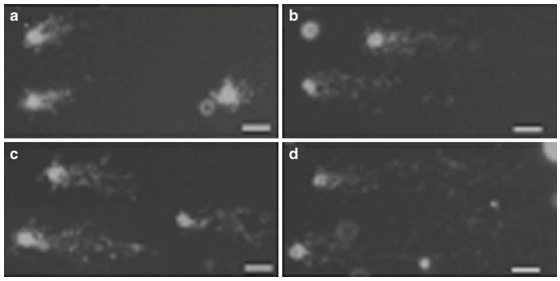

Fig1.1: examples of Comets acquired by (Oliveira and Johansson, 2012)

As observed in fig1.1 acquired and analyzed by (Oliveira and Johansson, 2012), various DNA damaging agents, specifically 300 mM, 500 mM, and 1 mM $KMnO_4$ shown in (1.1b, c, d respectively), create longer comets than untreated WT (1.1a). With ImageJ we can automatically quantify the lengths of comets for each sample and compare the mean length between WT and mutants or between treated and untreated samples.

1.1.2 Materials and methods:

Protocol for Comet assay is adapted from (Oliveira and Johansson, 2012).

- Cells were grown overnight in YPD media, diluted to 10^7 cells per ml and 50 ml of diluted cultures were centrifuged and washed twice with ice cold water.
- Cells were then resuspended in 1ml Zymolyase buffer {Zymolyase buffer: Dissolve 2 mg Zymolyase (ImmunO™—20 T) in 1 mL S buffer (1 M sorbitol, 25 mM KH_2PO_4 in ultrapure water and adjust to pH 6.5 with NaOH. Autoclave at 120°C, 1 atm for 20 min) and 50 mM β-mercaptoethanol.} and incubated at 30ºC for 30'.

- The spheroblasts are collected by centrifugation, washed once with S buffer and then treated with 1ml 10 mM H_2O_2 (for positive control samples, optional) or other DNA damaging reagents at 4ºC for 20'.
- Cells are collected by centrifugation, resuspended in 1.5% low melting agarose (w/v in S buffer). About 100 µl cells resuspended in agarose are spread on the precoated Comet assay slides (Comet assay 4250-050-K from Merce).
- The slides are dried at 4ºC for 30' and then incubated at 4ºC for 20' each in Lysis buffer (30 mM NaOH, 1 M NaCl, 0.05 % (w/v) lauroylsarcosine, 50 mM EDTA, and 10 mM Tris–HCl, pH 10. This buffer should be prepared just before use by mixing appropriate volumes of stock solutions of 300 mM NaOH, 5 M NaCl, 500 mM EDTA, and 100 mM Tris–HCl.) and freshly prepared Electrophoresis buffer (30 mM NaOH, 10 mM EDTA, and 10 mM Tris–HCl, pH 10).
- Electrophoresis is carried out by applying the voltage to the slides in an electrophoresis chamber 21V for 10'.
- Following the electrophoresis, the slides are washed for 10' each in Neutralization buffer (10 mM Tris-HCl, pH 7.4) at 4ºC, 76% v/v ethanol at RT and 96% v/v ethanol at RT. Slides are then dried at room temperature.
- Cells are stained with DAPI and images are acquired with DeltaVision microscope at 40X magnification.
- The comets are analyzed with ImageJ.

1.1.3 Results and conclusions

1.1.3.1 *smc6/5* mutants show longer comet tails compared to WT

We compared the comets from WT log culture and *smc6-56* log culture to compare the lengths of comet tails observed. The results showed that compared to WT, *smc6-56* showed longer mean comet tail length.

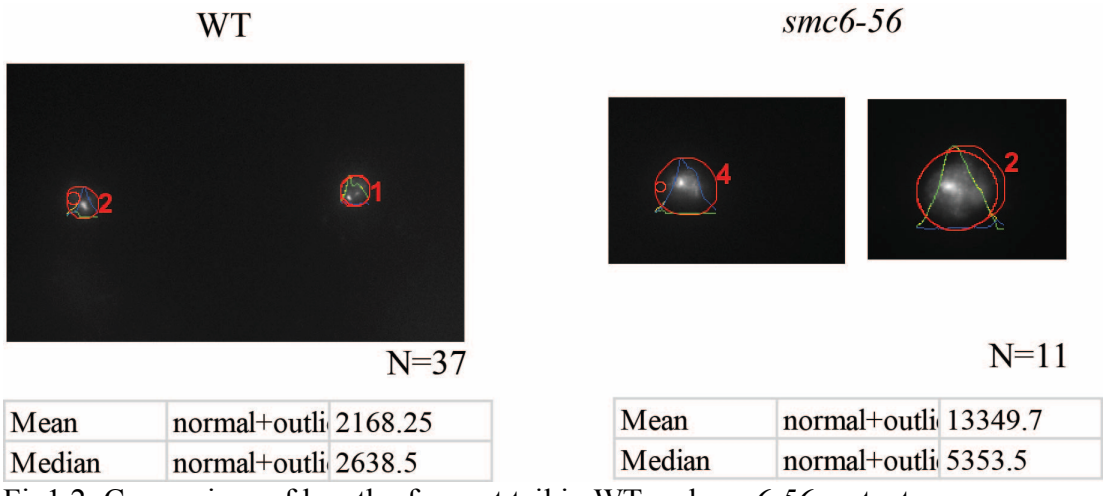

Fig1.2: Comparison of length of comet tail in WT and *smc6-56* mutants.

Although we found that in unperturbed conditions *smc6-56* showed longer comet tails than WT cells, we faced several problems while getting the results. Moreover, the number of comets analyzed was unequal due to several technical issues.

1.1.3.2 Technical issues that prevented us from getting conclusive results with Comet Assay

As mentioned in the previous section, we faced several technical issues while acquiring and analyzing images for Comet Assay. One of the major problems was that *S. cerevisiae* cells were very small compared to mammalian cells. Due to smaller size of cells, the nucleus was smaller, genome size was smaller therefore the DAPI signal was much weaker than that of mammalian cells. We tried to use magnification as high as 400X (40X plus 10X objective). Even at such high magnification, many cells were not detected by the analysis software as comets.

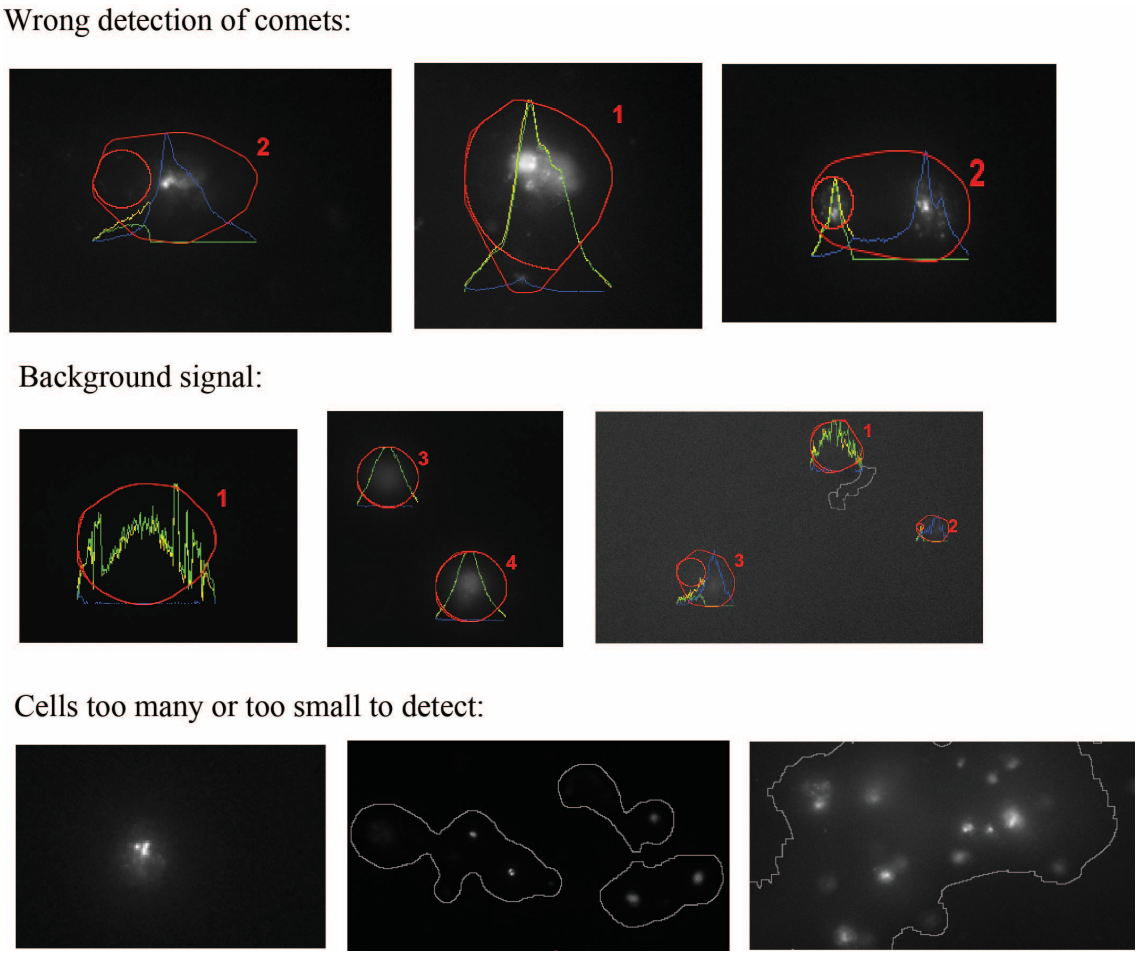

Fig1.3: Summary of problems faced with Comet Assay

We faced problems while automatically detecting signals with the Comets with ImageJ/Fiji, as sometimes several comets were detected as same signal, sometimes smaller cells were not detected at all. There was also high background signal. As our cells had low intensity of DAPI signal, the background was creating noisy analysis.

Due to several problems faced, we decided not to include the Comet Assay as a major strategy for analysis of fragility for our mutants. Instead, we used PFGE at rDNA among other analyses.

1.2 Recombination assay

1.2.1 Introduction

To understand the effect of Smc5/6 (and possibly STR later on) on the recombination at a particular tRNA, we decided to use a recombination assay in our system. This is a plasmid-based assay: under a Galactose promoter, tRNA is cloned with *BglII* cloning site flanking 5' and 3' of *leu2* gene, the tRNA is either in 'in' orientation (transcription to collide with replication) or 'out' orientation (transcription not to collide with replication). The empty vector along with the two constructs is transformed in WT or mutant cells and the colonies are plated on YPD and selection plate. If DNA breaks at tRNA due to replication stress, recombination can occur between the flanking *leu2* regions giving a WT *LEU2* gene. We therefore select for colonies with recombination event on -Leu2 plate.

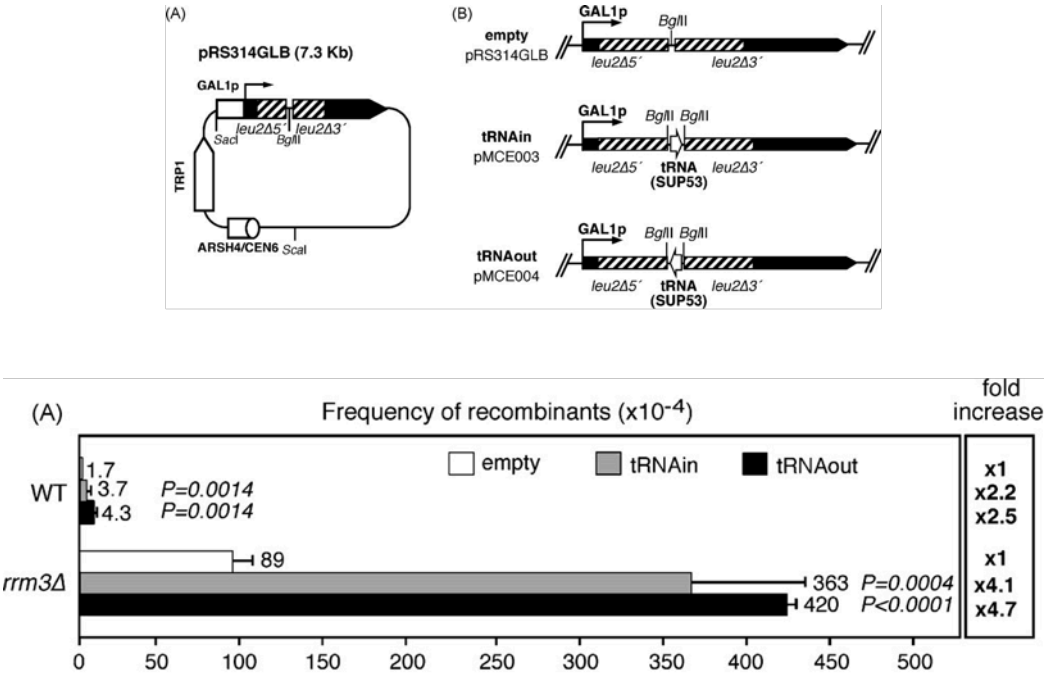

Fig1.4: Construct of recombination assay as described by (de la Loza et al., 2009) and the results for WT and *rrm3* from (de la Loza et al., 2009).

We received the constructs from (de la Loza et al., 2009), and we transformed the plasmids in WT and *rrm3* along with *smc6-56*. We repeated the experiment of (de la Loza et al., 2009) including our strain of interest *smc6-56*.

1.2.2 Results

We carried out the assay by generating single colonies of strains to be tested. Eight colonies for each strain were inoculated for 16 hr in YPD medium and then diluted 1:20 times before plating on selection plate and diluted 1:100000 times before plating on control plates. We then waited for 3-4 days for colonies to arise.

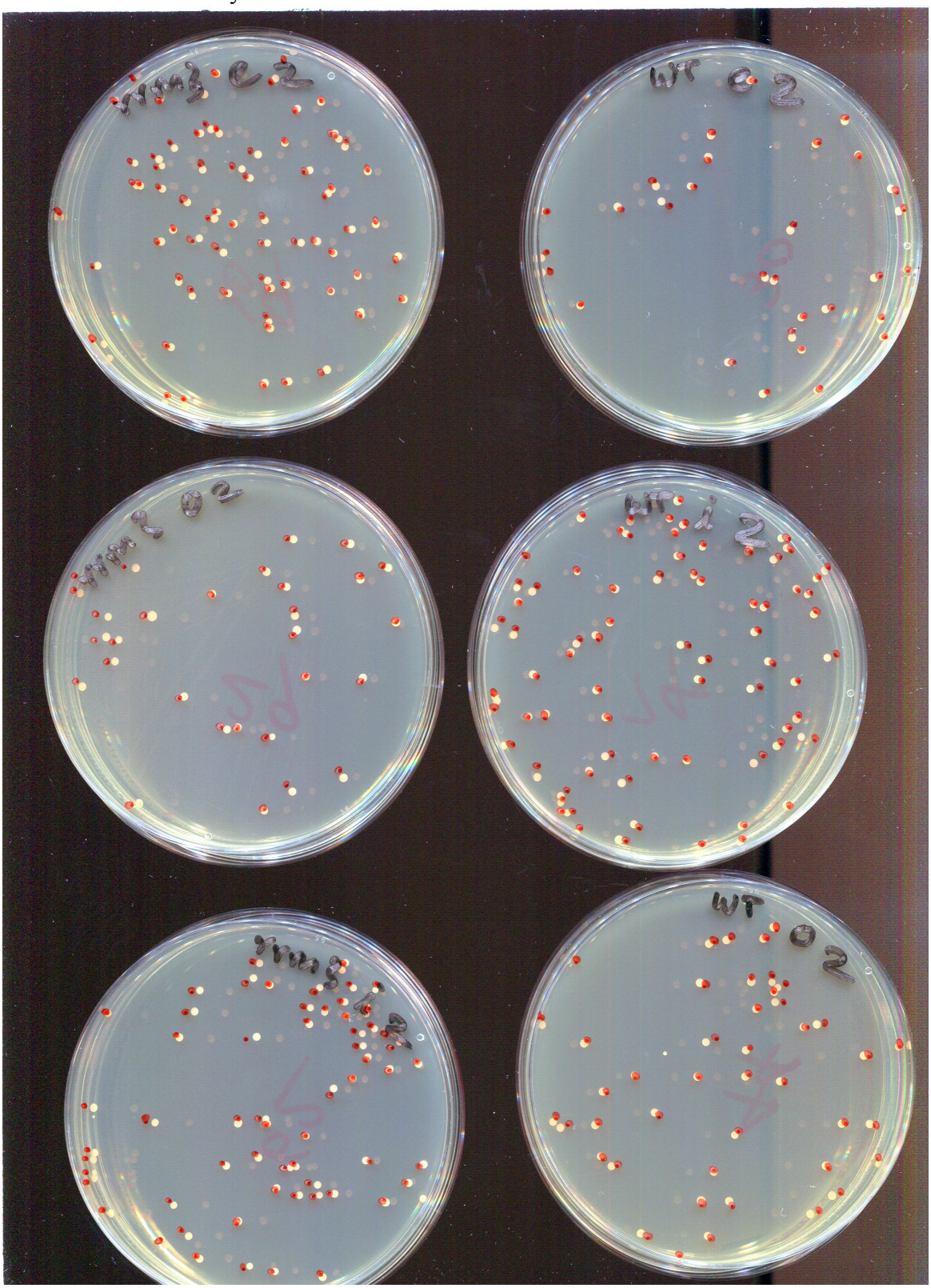

Fig1.5: Examples of colony formation on -Leu plates for recombination assay

We then counted the colonies formed for eight independent biological replicates and for each of WT + empty vector, WT + tRNA in, *rrm3* + empty vector, *rrm3* + tRNA in, *smc6-56* + empty vector and *smc6-56* + tRNA in. The median of eight colonies was plotted for each sample.

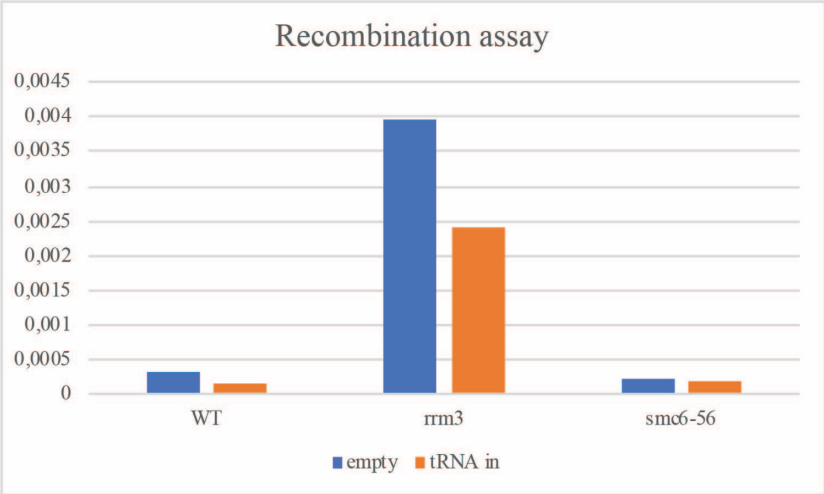

	WT	rrm3	smc6-56
empty	0,0003129	0,00396552	0,00024003
tRNA in	0,00016716	0,00239535	0,00019649

Fig1.6: Recombination assay for WT, *rrm3* and *smc6-56*

We observed that *rrm3* showed high recombination frequency with both empty vector and tRNA in. On the other hand, WT and *smc6-56* showed low frequency of recombination, and also no effect of the tRNA in but no increase in recombination frequencies caused by tRNA. As these results were different from from what is published or expected from the literature at least in regard to WT and *rrm3*, we decided not to pursue with this assay.

1.3 PFGE at other chromosomes

1.3.1 Introduction

As previously mentioned in results, we used PFGE to visualize DSBs formed during replication in WT and mutants. While at rDNA (chromosome 12) we visualized a clear phenotype, we also checked other chromosomes for formation of breaks. The results were not as clear or as we expected. Therefore, we keep these results in Appendix instead of main results.

1.3.2 Chromosome 3

For chromosome 3, we separated the chromosomes with a specific program to separate the small chromosomes. Then we probed for ARS305 and TER302 to see the breaks formed in chromosome 3 in WT, *S-mms21* and *sgs1*.

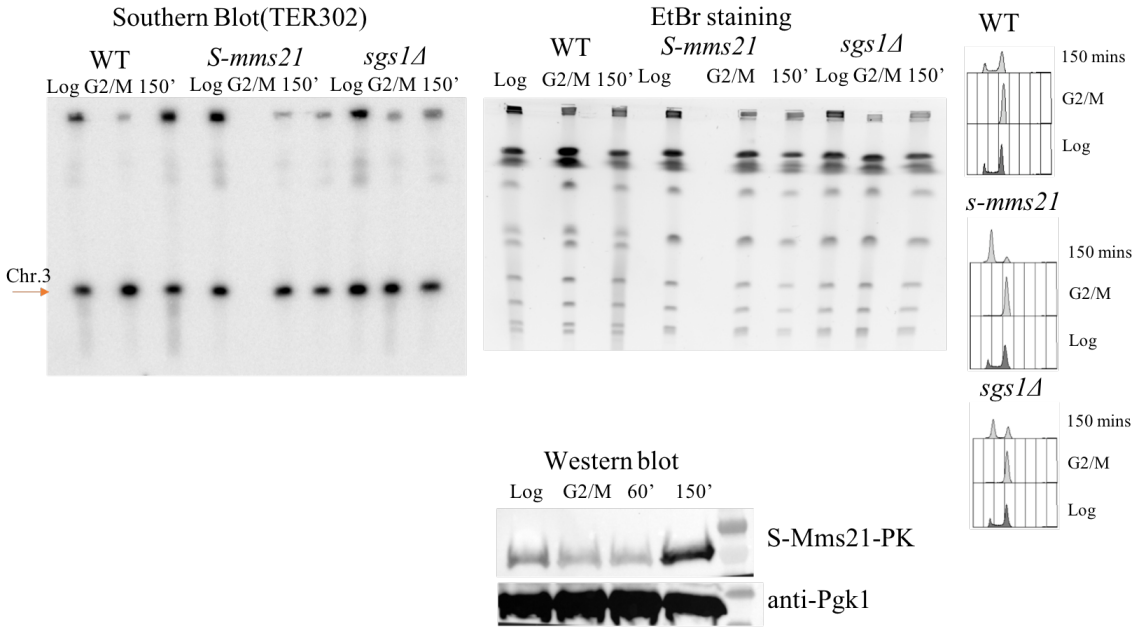

Fig1.7: PFGE analysis to visualize breaks in chromosome 3, with TER302 probe. Cells with indicated genotype were arrested with Nocodazole (G2/M) and samples were collected after release in YPD at indicated timepoints and plugs were prepared. Cell cycle progression and protein expression were confirmed by FACS acquisition and western blot respectively.

We observed breaks in log phase WT and also S-phase WT cells, there were no breaks observed for *S-mms21* which is in contrast with (Menolfi et al., 2015) and we observed little bit of signals from breaks in G2/M phase for *sgs1*. We also tried to probe with another probe, ARS305 to confirm the results and to understand if there was issue with our WT strain.

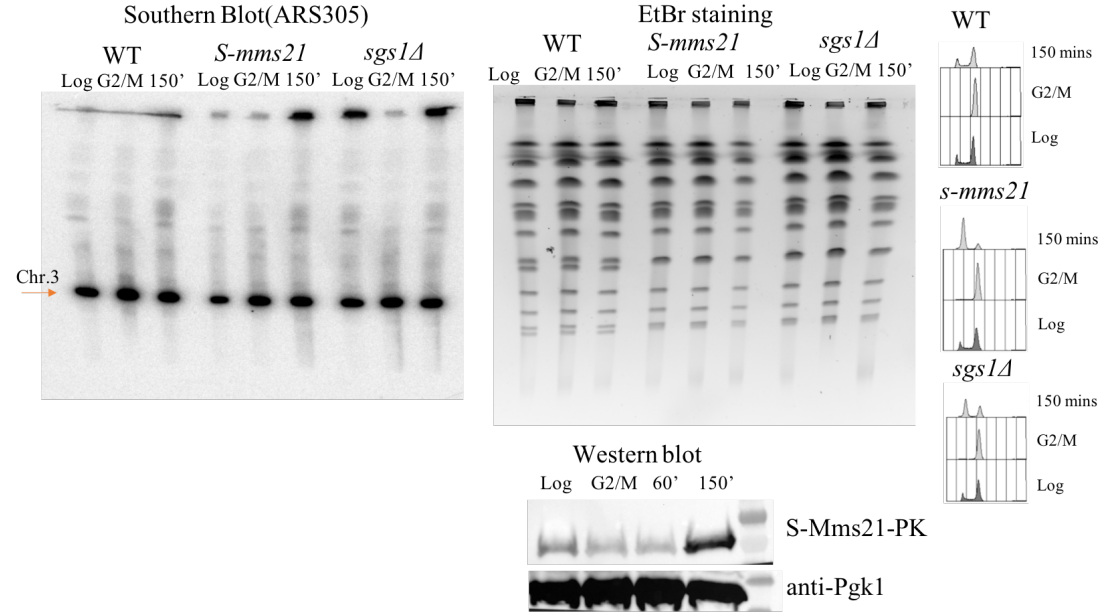

Fig1.8: PFGE analysis to visualize breaks in chromosome 3, with ARS305 probe. Cells with indicated genotype were arrested with Nocodazole (G2/M) and samples were collected after release in YPD at indicated timepoints and plugs were prepared. Cell cycle progression and protein expression were confirmed by FACS acquisition and western blot respectively.

We observed that WT showed no breaks with ARS305 probe, *S-mms21* showed breaks in 150' sample while *sgs1* showed breaks in both G2/M and 150' samples. This agreed with what we expected, indicating that both Smc5/6 and STR protein complexes are involved in preventing breaks in unperturbed cell cycle, however there were problems with the consistency of the results.

1.3.3 Chromosome 6

We further checked formation of breaks on chromosome 6 with TER603 probe.

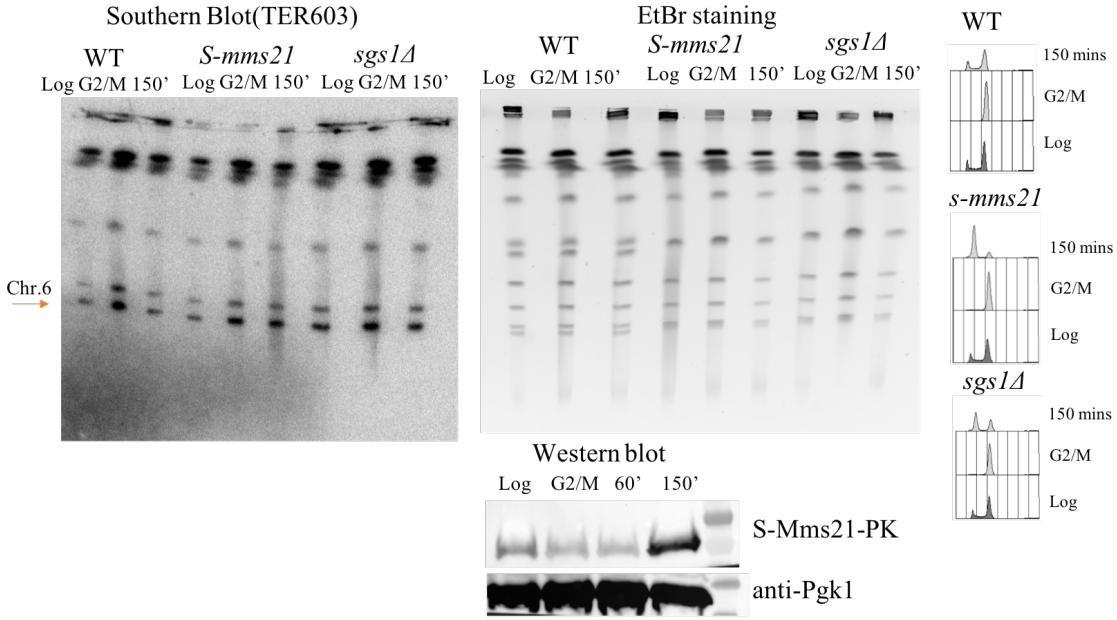

Fig1.9: PFGE analysis to visualize breaks in chromosome 6, with TER603 probe. Cells with indicated genotype were arrested with Nocodazole (G2/M) and samples were collected after release in YPD at indicated timepoints and plugs were prepared. Cell cycle progression and protein expression were confirmed by FACS acquisition and western blot respectively.

We observed that WT showed little or no signal of breaks at all the timepoints, *S-mms21* showed signal of breaks at 150' while *sgs1* showed DNA breaks in G2/M. However, the TER603 probe was probing nonspecific chromosomes and the blot itself showed a lot of background signal in my hand.

1.3.4 Conclusions

We observed with the EtBr stained PF gels that *smc5/6* and *sgs1* showed defects in sizes of small chromosomes. In each of our run at all timepoints, the smallest two chromosomes were merged as one for *S-mms21* and *sgs1*. This indicated changes in sizes of the small chromosomes. However, probing with chromosome 3 or chromosome 6 specific probes did

not show a strong phenotype for *S-mms21* and *sgs1*. Along with this, the results were not consistent and there was background signal due to the weakness of the signal from smaller chromosomes. We decided to only include rDNA results (due to repeats, the signal was strong and phenotype was reproducible and apparent) in the main results while we included the PFGE for small chromosomes in the appendix.

1.4 Mms4 binds to TERs and its binding is independent of Smc5/6

1.4.1 Introduction

Sgs1-Top3-Rmi1 plays a role in removing recombination intermediates upon DNA damage by dissolution. While this is a predominant pathway of dissolution of recombination intermediates, Mus81/Mms4 complex that is active in G2/M resolves the recombination intermediates through the endonuclease activity of Mus81. This pathway acts a backup pathway for persistent double Holliday Junctions structures that escape dissolution by the STR complex and for Holliday Junctions that are not resolved by STR (Szakal and Branzei, 2013). Mus81/Eme1 (human Mus81/Mms4 complex) was previously shown to be important for replication of mammalian common fragile sites in RecQ5 dependent manner (Di Marco et al., 2017). In this study we observed that the STR complex localizes to TERs and other NPSs (which are similar to mammalian CFSs) in G2/M phase. In a different study in the lab it was observed that Mus81/Mms4 associates with NPSs. We asked if Mms4 recruitment or retention may be influenced by Smc5/6.

1.4.2 Results and conclusion

We conducted a ChIP-qPCR experiment with Mms4-PK in G2/M phase in WT and *smc6-56* background. We compared the amount of Mms4 bound to TER302 in unperturbed G2/M cells.

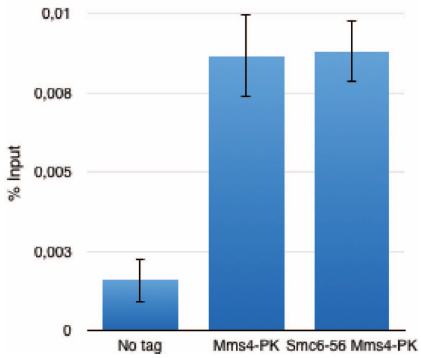

Fig1.10: Quantification of Mms4 binding to TER302 by ChIP-qPCR (N=3)

We observed that Mms4 was enriched at TER302 and the amount of Mms4 did not reduce upon the *smc6-56* mutation in *SMC6*. This was opposite from our observation for Top3 of the STR complex.

After checking the aggravation of genetic interactions between smc6-56-sup sgs1Δ, we decided to check the effect of smc6-56, smc6-56-sup on accumulation of Mms4 to NPSs. We conducted the ChIP-qPCR experiment with the Mms4-10xFlag strain in various backgrounds.

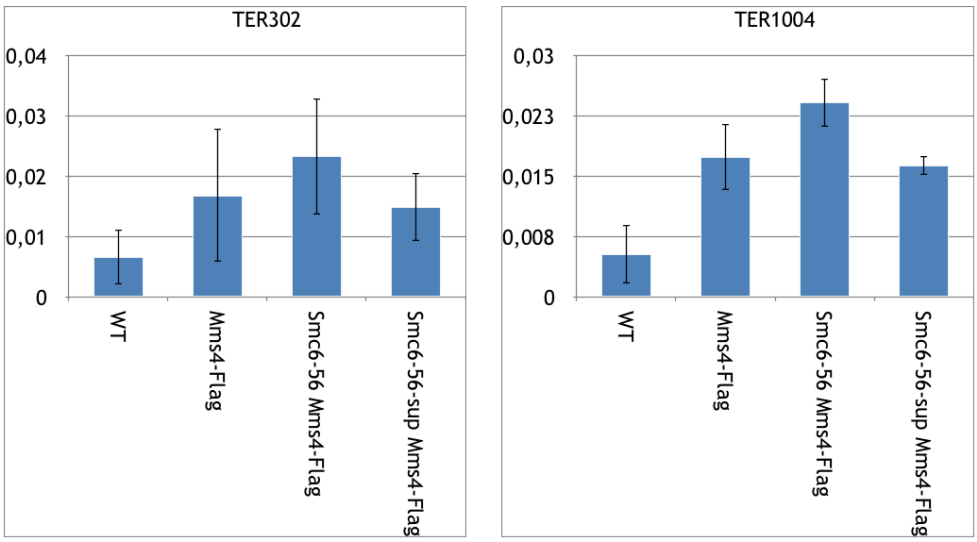

Fig1.11: Quantification of Mms4 binding to TER302/TER1004 by ChIP-qPCR (N=3)

We observed no effect of *SMC6* mutations on the recruitment of Mms4 to NPSs. We further checked the genome-wide effect of Mms4 DNA binding by chromatin fractionation.

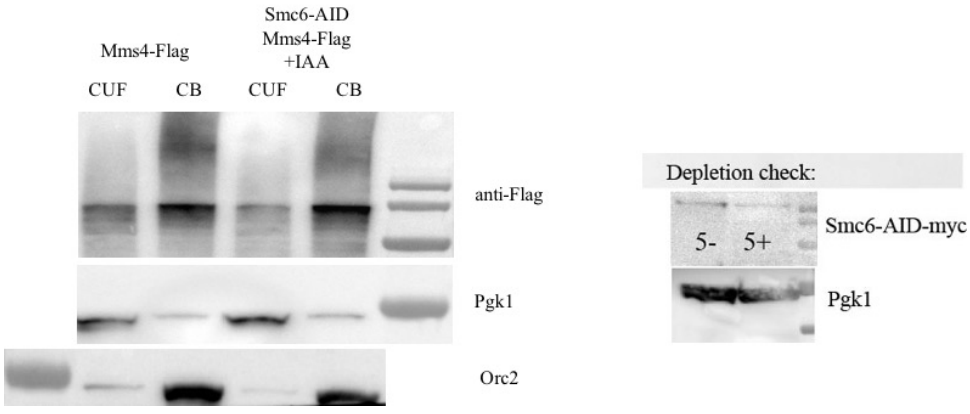

Fig1.12: Visualization of Mms4 chromatin binding by chromatin fractionation. Chromatin Unbound Fraction (CUF) and Chromatin Bound Fraction (CB) loaded on the western blot and Pgk1 and Orc2 used as loading control for CUF and CB respectively. Depletion of Smc6 checked by western blot with(+)/without (-) auxin.

We did not observe any effect of Smc6 depletion on the genome-wide chromatin binding of Mms4. As we did not follow these experiments to understand the role of Mus81/Mms4 at NPSs in detail, we decided to place the result in the appendix. In conclusion, we observe that Smc5/6 affects enrichment of STR but not Mus81/Mms4 to NPSs.

1.5 References:

1. de la Loza, M.C.D., Wellinger, R.E., and Aguilera, A. (2009). Stimulation of direct-repeat recombination by RNA polymerase III transcription. DNA repair *8*, 620-626.
2. Di Marco, S., Hasanova, Z., Kanagaraj, R., Chappidi, N., Altmannova, V., Menon, S., Sedlackova, H., Langhoff, J., Surendranath, K., Huhn, D*., et al.* (2017). RECQ5 Helicase Cooperates with MUS81 Endonuclease in Processing Stalled Replication Forks at Common Fragile Sites during Mitosis. Mol Cell *66*, 658-671 e658.
3. Menolfi, D., Delamarre, A., Lengronne, A., Pasero, P., and Branzei, D. (2015). Essential Roles of the Smc5/6 Complex in Replication through Natural Pausing Sites and Endogenous DNA Damage Tolerance. Molecular cell *60*, 835-846.
4. Olive, P.L., Banáth, J.P., and Durand, R.E. (1990). Heterogeneity in radiation-induced DNA damage and repair in tumor and normal cells measured using the "comet" assay. Radiat Res *122*, 86-94.
5. Oliveira, R., and Johansson, B. (2012). Quantitative DNA damage and repair measurement with the yeast comet assay. Methods Mol Biol *920*, 101-109.
6. Ostling, O., and Johanson, K.J. (1984). Microelectrophoretic study of radiation-induced DNA damages in individual mammalian cells. Biochem Biophys Res Commun *123*, 291-298.
7. Szakal, B., and Branzei, D. (2013). Premature Cdk1/Cdc5/Mus81 pathway activation induces aberrant replication and deleterious crossover. The EMBO journal *32*, 1155-1167.

Appendix 2

ChIP-qPCR trouble shooting

2.1 Problems in ChIP-qPCR

While performing the ChIP-qPCR experiments with protocol mentioned before (materials and methods, 2.6.3), we faced some problems with the ChIP-qPCR technique. The major issue was that the no tag (control) values were increasing compared to the old experiments. This caused a problem as the tag values were not extremely high and increasing no tag values meant the different between binding of our protein of interest and background was now less than 2-fold.

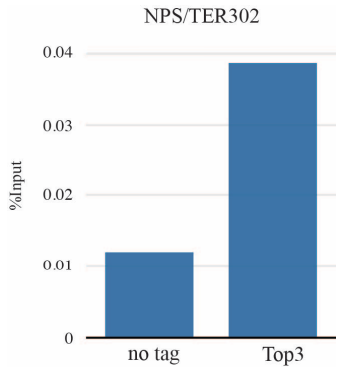

Fig2.1: binding of Top3 to TER302 compared to no tag control checked by ChIP-qPCR

As seen in figure 2.1, previously we observed at least 3-fold change between no tag and Top3 tagged strains. However, starting from one of our experiment, we started to observe much higher values for no tag.

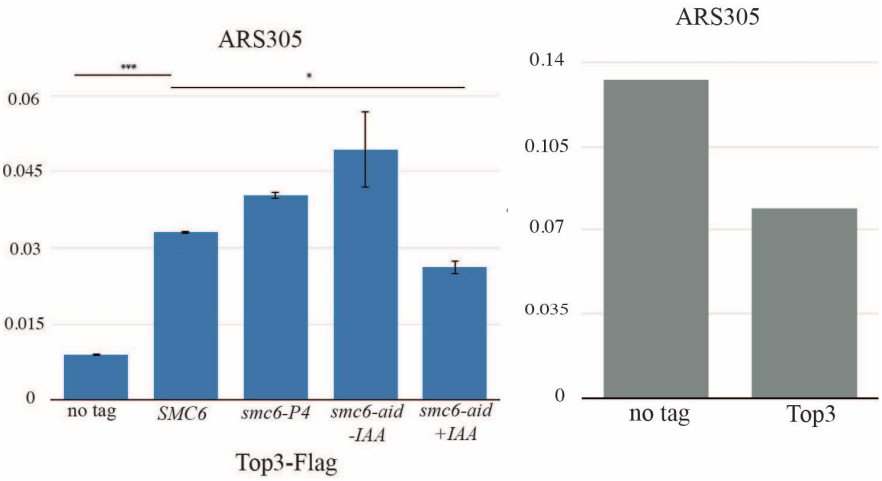

Fig2.2: Comparison of old (left) and new (right) qPCR results for Top3 binding to ARS305 upon HU treatment.

While we were checking the binding of Top3 to ARS305 upon HU treatment, we observed that Top3-Flag in WT background showed less enrichment to ARS305 than the WT strains. We compared this result with our old results for Top3-Flag (repeated three times,

plotted mean and standard error). We observed that the values for the no tag (background) signals were very high. First, we confirmed the strains used in this experiment by western blot. Once the results were confirmed (by checking western blot of the ChIP experiment for no tag vs Top3-Flag), we started the trouble shooting for ChIP-qPCR.

2.2 Changes in WT strains and preventing cross contamination between the samples

Our first hypothesis was that we might be facing problems with cross-contamination between the no tag and tagged strains. We decided to conduct an experiment with only WT no tag strain. Now there was still a highly unlikely possibility that the glycerol stock of the strain in use (my personal stock) was also contaminated with Top3-Flag. We therefore included two other strains of W303 WT from our database (the glycerol stocks were commonly used by others in our lab). The strains were confirmed with several selection markers, we observed no suppressor colonies on any selection plates. Another possibility was degradation of formaldehyde, giving rise to faulty crosslinking (this had happened once before in the lab where an old bottle of formaldehyde was not effective anymore). We ordered fresh formaldehyde and only used this formaldehyde for all further experiments. It was used successfully in mammalian cells by another member of the lab confirming that there was no issue with newly ordered formaldehyde. I also freshly prepared all the ChIP buffers and discarded the old buffers. I also performed an extra step of preclearing lysate to reduce background caused by beads.

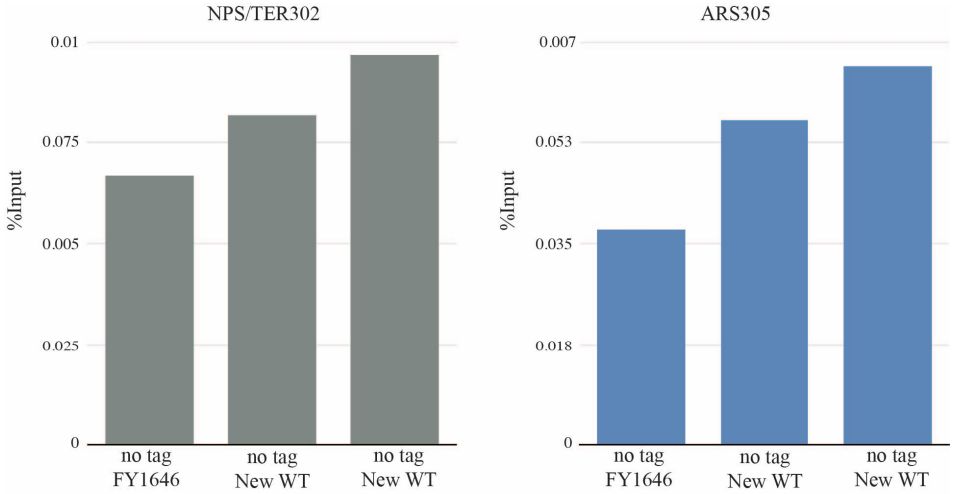

Fig2.3: ChIP-qPCR experiment with WT strains in G2/M phase for trouble shooting

We observed that the newly included WT strains also showed considerable background signal. We observed this signal at TER302 as well, indicating that the signal was not locus specific for ARS305 and it was not related to HU treatment either. Furthermore, the signal did not arise from cross-contamination as there was no tagged strain to contaminate this experiment. We had tested this region with G2/M arrest several times before and the no tag

signal was considerably low. We decided to change the other reagents of ChIP-qPCR experiment one by one.

2.3 Changing the antibody used for ChIP-qPCR experiments

After confirming that the problem was neither due to cross contamination nor to our WT no tag strain, we decided to change the antibody aliquot. The activity of the antibody is crucial for ChIP experiments. Usually we ordered a large volume of the antibody, confirmed the antibody repeating an experiment and then aliquoted the antibody for ChIP use only. There was a possibility that our current aliquot was degraded. We decided to use old and new aliquoted anti-Flag antibody and anti-Myc antibody as another control.

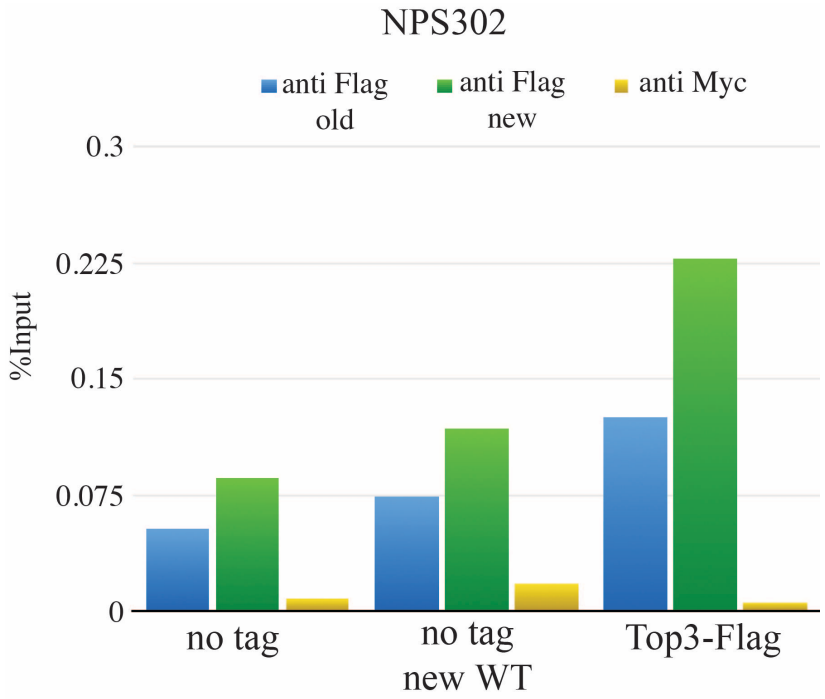

Fig2.4: ChIP-qPCR experiment with different antibody aliquots in G2/M phase for trouble shooting

We observed that both the aliquots of anti-Flag antibody showed larger background signal than the anti-Myc antibody, at least the signals for Top3-Flag were higher in the new aliquot. However, the ratio of no tag to tagged Top3 still remained lower than 2. We decided to use an antibody recently used successfully by a staff scientist in the institute, Danielle Piccini, as additional control.

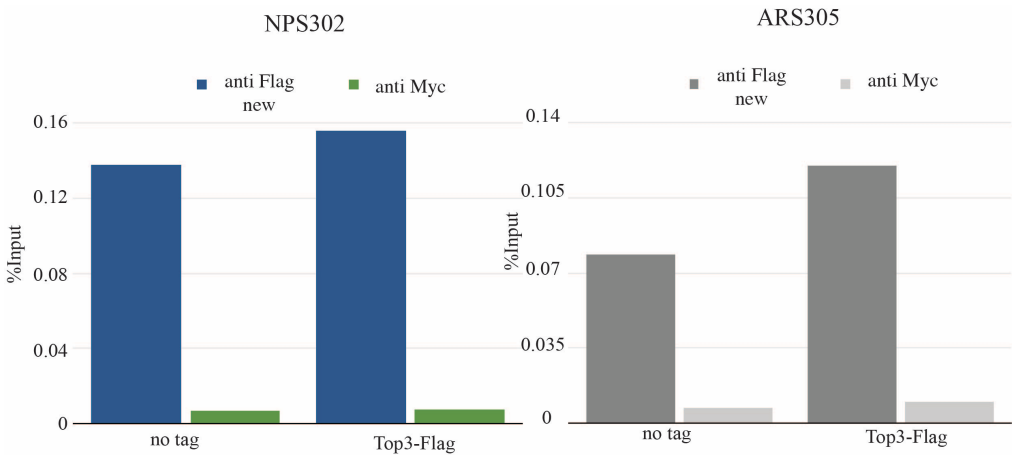

Fig2.5: ChIP-qPCR experiment with new Flag antibody in G2/M phase for trouble shooting

We observed that even after using an antibody that was recently used for the ChIP experiments, we did not manage to reduce the no tag signal. Whereas, consistent with previous results anti-Myc antibody showed lower values throughout the experiments so far. We suspected that the batch antibody may be an issue and we decided to order a new aliquot of anti-Flag M2 antibody (F1804) from Sigma.

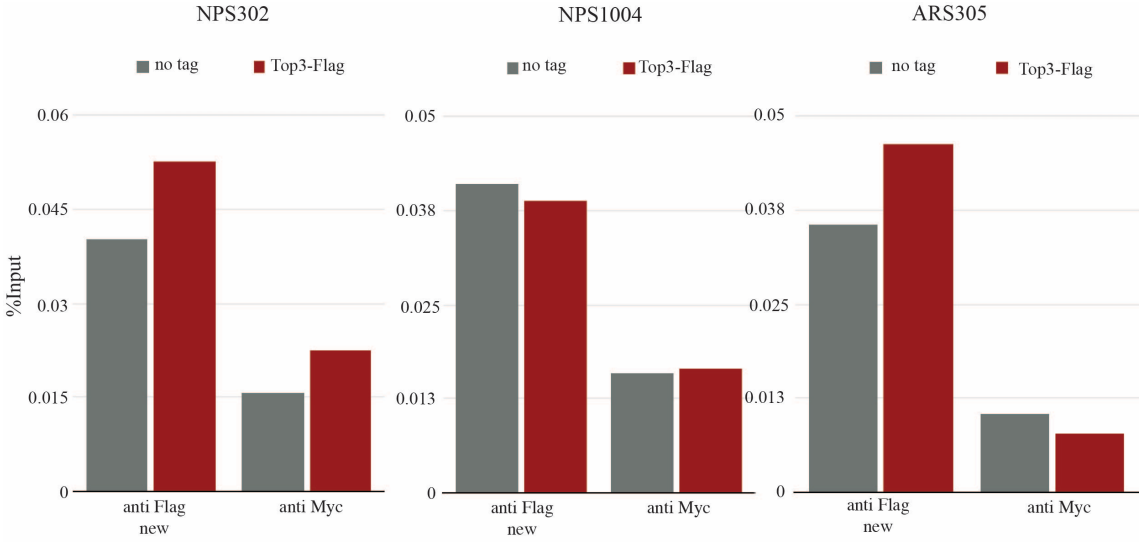

Fig2.6: ChIP-qPCR experiment with new Flag antibody in G2/M phase for trouble shooting

We observed that ordering a fresh antibody did not reduce the background signal from our experiments. We still observed high values for no tag samples. Next, we decided to include a different protein with stronger DNA binding capacity, Rad9-Flag, as a positive control and to address whether the tagged strains had any issues.

2.4 Including Rad9-Flag as a positive control

We conducted the next experiment including Rad9-Flag as a positive control.

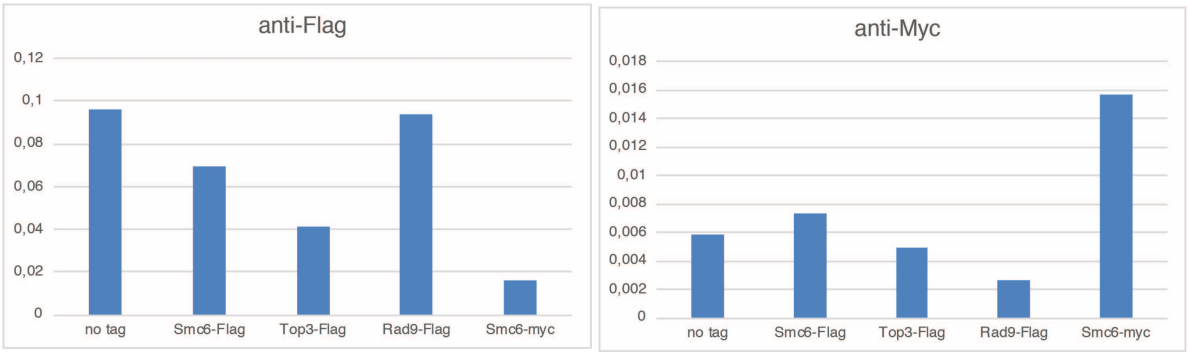

Fig2.7: ChIP-qPCR experiment in G2/M with positive controls phase for trouble shooting at TER302

For this experiment in particular, I was followed by a post-doctoral researcher from the lab to make sure there was no mistake in the execution of the ChIP protocol. Together, we repeated the ChIP experiment with no tag, Top3-Flag, Smc6-Flag and Rad9-Flag strains. We also used Smc6-Myc strain as a positive control and conducted the ChIP with both anti-Flag and anti-Myc antibody.

We observed that there were high values for no tag strains even higher than the Rad9 signal. However, the Smc6-Myc strain showed much lower signal in the Flag ChIP. This encouraged us to try to use Smc6-Myc as our negative control. We also observed that the ChIP experiment with anti-Myc antibody was giving us consistent results. There was low no tag value and enrichment of Smc6 at TER302 was consistent with previous experiments. Next, we changed the magnetic beads used for the experiment and repeated the ChIP.

2.5 Changing the magnetic beads used for ChIP-qPCR experiments

We used Protein A dynabeads from Invitrogen for all the previous experiments. We decided to use two different aliquots of ProteinA dynabeads with beads only control to rule out the possibility of background signal coming from beads. We also used Protein G beads and Flag antibody coupled beads (referred here as Flag beads slurry).

TER302	Beads A	Beads B	Myc Beads A	Beads only
WT	0,0222817	0,035206926	0,001902356	0,002903
Top3-Flag	0,044873362	0,046455818	0,002325897	0,003625
TER603	Beads A	Beads B	Myc Beads A	Beads only
WT	0,012534108	0,019130297	0,002053076	0,00231
Top3-Flag	0,03988536	0,037214356	0,001762701	0,002709
ARS305	Beads A	Beads B	Myc Beads A	Beads only
WT	0,012976122	0,020081392	0,001876166	0,002326
Top3-Flag	0,029400879	0,028996108	0,002215738	0,003155
ARS304	Beads A	Beads B	Myc Beads A	Beads only
WT	0,012361547	0,016311159	0,00153452	0,002082
Top3-Flag	0,023389472	0,022749885	0,002140262	0,002924

Fig2.8: Table for ChIP-qPCR values with two aliquots of proteinA beads (Beads A and Beads B) with Flag and Myc antibody and beads A only control at different regions of genome for trouble shooting

Protein G beads	TER302	TER603	TER1004	ARS1
WT	0,044873362	0,031077259	0,008561	0,012797
Top3-Flag	0,057193821	0,036957298	0,008502	0,011064

Flag beads slurry	TER302	TER603	TER1004	ARS1
WT	0,018736601	0,014802689	0,009632	0,013716
Top3-Flag	0,052629047	0,049446187	0,046135	0,033539

Fig2.9: Table for ChIP-qPCR values with proteinG dynabeads with Flag antibody and Flag-beads slurry at different regions of genome for trouble shooting

We observed that the no tag values for both aliquots of ProteinA dynabeads were similar to each other and the fold increase between no tag and tagged strain was less than 2. The results with anti-Myc antibody with proteinA beads were consistently low and there was very low background signal with beads only samples. With ProteinG beads we observed very low fold increase even as low as 1 or 1.5, which proved that the issue with background was not due to incompatible dynabeads. Flag-beads slurry gave us promising results where the fold increase was as close to 3. It was not as high as our previous results but still higher than recent experiments. We decided to try the Flag-beads slurry for some more experiments to see the consistency of the results.

2.6 Experiment repeated by a senior researcher including a strong positive control

We requested a staff scientist who was guiding us in the trouble shooting process to repeat the experiment independently from our trouble shooting efforts, using his conditions of experiments and his reagents. He used a strong positive control Rpc25-Flag which is a subunit of RNA polymerase II and is known to bind strongly to tRNA genes. He checked

two TERs overlapping with tRNA as a positive control. The experiment was done in asynchronous cultures. He used WT from our lab (DB) and from Marco Foiani (MF) lab to rule out the possibility of contaminated WT strains.

TER302	WT (MF)	wt(DB)	Rpc25-Flag	Top3-Flag
	0,068488382	0,07090362	1,571348403	0,042453
TER603	WT (MF)	wt(DB)	Rpc25-Flag	Top3-Flag
	0,063460517	0,060875397	20,8503991	0,110491
ARS304	WT (MF)	wt(DB)	Rpc25-Flag	Top3-Flag
	0,045816247	0,045185481	0,599571243	0,068015

Fig2.10: Table for ChIP-qPCR values done by Daniele Piccini at different regions of genome for trouble shooting

We observed that consistent with our results, there was value of no tag that was as high as Top3-Flag strain. However, when we included a strong DNA binder Rpc25, we observed large fold increase (no tag vs tag) at positive control locus. This indicated a possibility that the protein of our interest (Top3) was probably binding weakly to DNA and the conditions used in the ChIP were not suitable for ChIP of Top3. Another possibility was that Flag tag was not exposed properly when we pulled down Top3 and thus the ChIP failed. However, the western blot for each ChIP experiment confirmed that the IP of Top3-Flag worked very well and we were able to pull down the protein.

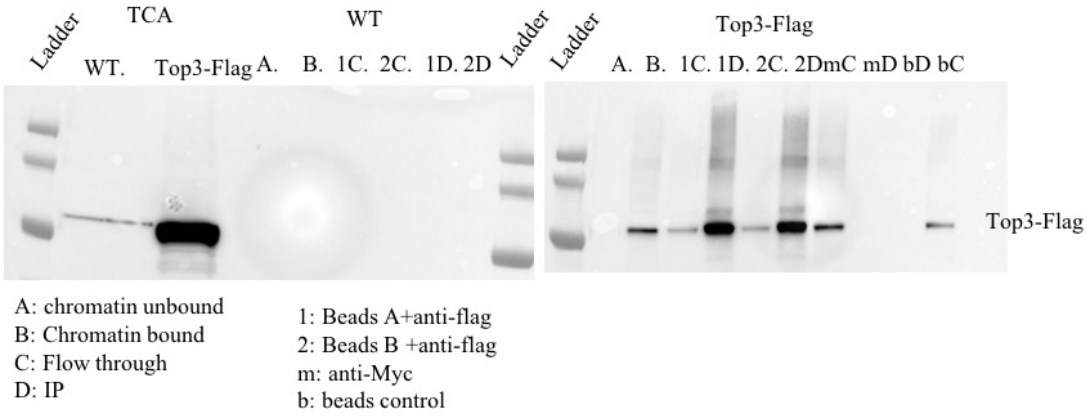

Fig2.11: Western blot for a ChIP experiment with WT and Top3-Flag with different ProteinA dynabeads aliquots

As seen in fig2.11, the western blot indicated enrichment of Top3-Flag in sample D, the IP samples. This indicated that the protein was pulled down but the DNA was either not

pulled down well or there was an issue with detection of DNA. We decided to check the qPCR machines and qPCR master mix before the next ChIP experiment.

2.7 Repeating the previous ChIP samples with two qPCR machines and new qPCR master mix

We wanted to confirm that the qPCR master mix did not get degraded and the qPCR reactions worked well. We therefore used a fresh vial of qPCR master mix and performed qPCR with two qPCR instruments (LC480 and LC96) in parallel for a previous set of samples. We compared the new and old values to understand whether the issue of no tag values was occurring because of mistakes in the final step of ChIP-qPCR.

TER302 LC96		
Old samples		previous value
no tag	0,025418154	0,024895056
Top3-Flag	0,064346393	0,041965505
sgs1-KR Top3-Flag	0,045499771	0,061469355
sgs1-SIM Top3-Flag	0,020503345	0,027071159
smc6-AID Top3-Flag	0,03545181	0,029667316
LC480		
Old sample		Previous value
no tag	0,01490565	0,024895056
Top3-Flag	0,048765447	0,041965505
sgs1-KR Top3-Flag	0,036957298	0,061469355
sgs1-SIM Top3-Flag	0,014802689	0,027071159

Fig2.12: Table for old and new qPCR values acquired with two qPCR instruments for trouble shooting

We observed that repeating qPCR experiments for previous ChIP samples gave us values similar to the previous values. The background values were not extremely high as observed in the recent results. The previous ChIP experiments were reproducible and the qPCR set up and acquisition was not creating the high background signal in our experiments.

2.8 Shifting to Myc tags for further ChIP experiments

We consistently observed that the ChIP-qPCR experiments with anti-Myc antibody showed us promising results. The background values were consistently low. We repeated an experiment previously done for Smc6-Myc with no tag control checking several regions of genome.

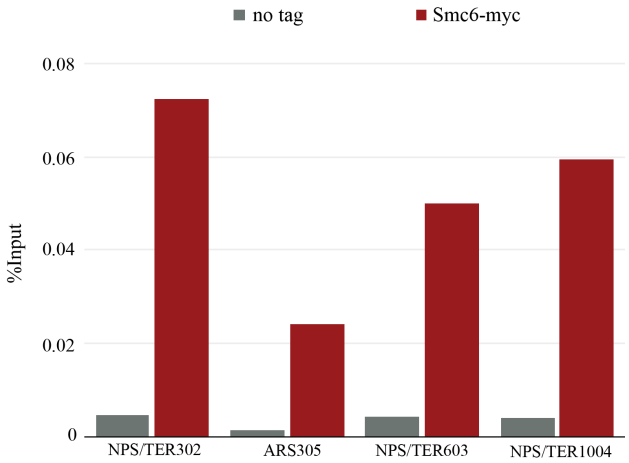

Fig2.13: ChIP-qPCR experiment with Myc tag for various genomic regions

We observed that the no tag values for ChIP-qPCR with Myc were low at all the tested genomic loci. The tag values for Smc6 were high and the fold increase was satisfactory. We therefore decided to construct a Top3-Myc strain and try to repeat the ChIP-qPCR for Top3 with Myc tag.

In parallel with these experiments we had also ordered a new anti-Flag antibody from Euroclone/Cell signaling (Same monoclonal Flag M2 antibody from a different company). We also tried this new vial of antibody in the same experiment with Top3-Flag strain.

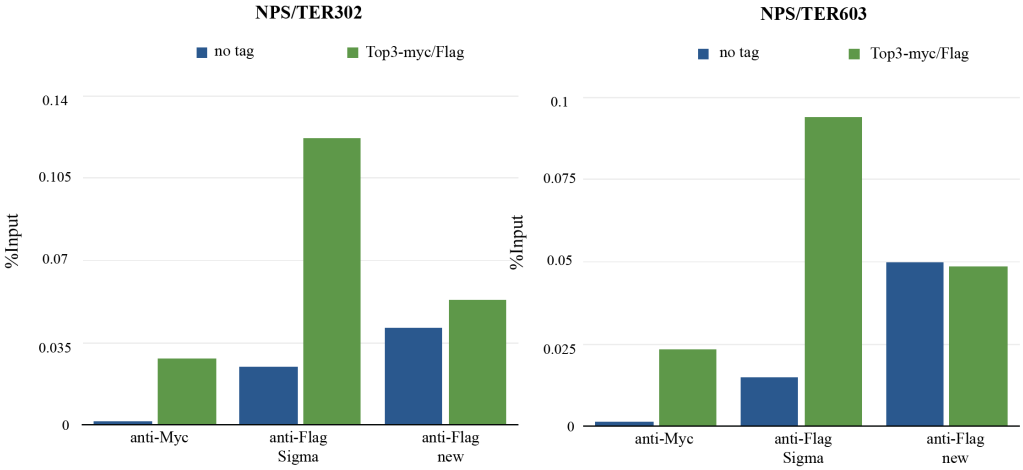

Fig2.14: ChIP-qPCR experiment with Top3-Myc and new Flag antibody for trouble shooting

We observed that compared to Flag antibody from Sigma, the new antibody did not give better results. In this particular experiment the Flag ChIP with Top3 worked well, but the consistency in the results was missing. We therefore decided not to use anti-Flag for Top3 ChIP anymore.

The ChIP-qPCR experiment with Top3-Myc gave us low background/no tag value and the tag value was higher at both TERs checked. We had two options for using anti-Myc antibody. The purified and concentrated anti-myc or anti-myc antibody that was not

purified (both from IFOM facilities). We checked whether one had an advantage over the other.

	TER302	TER603	TER1004	ARS314
Purified				
WT	0,007299448	0,006905699	0,007556863	0,005532
Top3-Myc	0,029197792	0,082583827	0,07090362	0,045185
fold change	4	11,95879399	9,382679594	8,168097
not purified				
WT	0,01039478	0,013066378	0,01210715	0,008043
Top3-Myc	0,038260594	0,041579122	0,038526718	0,024047
fold change	3,680750602	3,182145935	3,182145935	2,989698

Fig2.15: ChIP-qPCR experiment with Top3-Myc with purified or not purified antibody for trouble shooting

We observed that the purified and concentrated antibody gave better results than the not purified. We decided to use the purified anti-Myc antibody for further experiments.

2.9 Repeating the experiments with Top3-Myc

We repeated the experiment with for enrichment of Top3 to NPSs with *smc6-56/P4* variants with anti-Myc ChIP.

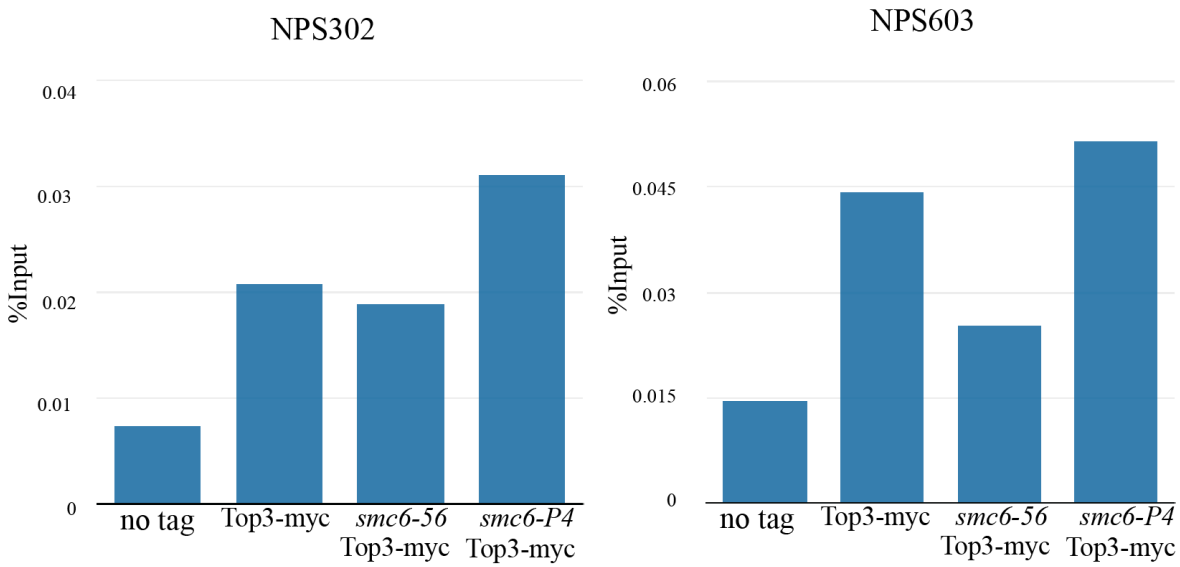

Fig2.16: ChIP-qPCR experiment with Top3-Myc for trouble shooting (N=2)

We observed that the overall values for Top3-myc were lower. The enrichment of Top3 in WT conditions was so low that it was difficult to see the reduction in the mutant backgrounds. There was 8 to 10-fold change between the no tag and tag value but the ChIP for Top3 was weaker with Myc tag. We decided not to use the ChIP with Top3-myc anymore.

2.9 New protocol for ChIP-qPCR

We decided to try a different protocol from Maria Pia Longhese lab, as reported in (Villa et al., 2018). We repeated the experiment with no tag, Smc6-Flag and Top3-Flag.

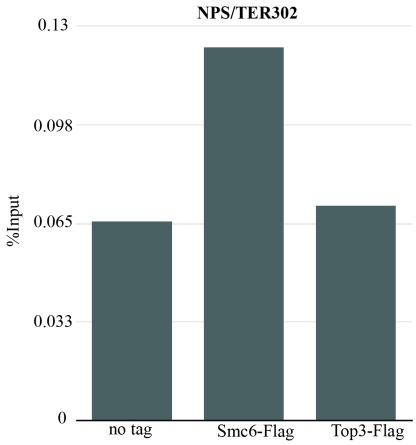

Fig2.17: ChIP-qPCR experiment with new protocol for trouble shooting

We observed that the no tag values were comparable to Top3-Flag values while Smc6-Flag showed about 2-fold increase. This was not encouraging and we decided to stop the process of trouble shooting at this stage.

2.10 Repeat ChIP after several months, changed everything started fresh

After completely stopping the experiments for about two months while in the lockdown due to Corona virus, we decided to restart with ChIP-qPCR analysis with all new reagents using the protocol used since the beginning (materials and methods, 2.6.3). We tried to ChIP Mms4 with four available tagging methods. We compared ChIP with Flag, PK and HA antibody for the Mms4 protein. We observed low background for all three no tag controls in a comparable manner.

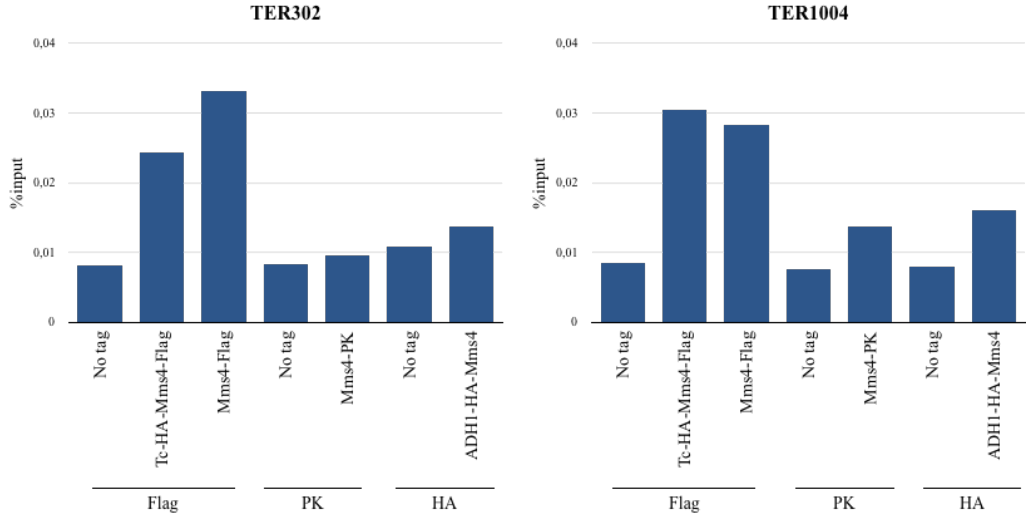

Fig2.18: ChIP-qPCR experiment with Flag/PK/HA tagged Mms4 to find out best tag for Mms4 (N=1).

We observed about 0.008 %input for no tag controls for two regions checked while Mms4-Flag showed 3 or 4-fold increase. Although the fold increase was lower than before, we still observed a reduced no-tag value. This suggested that even though the ChIP efficiency was low, the problems we were facing for ChIP were eliminated. Unfortunately, we did not understand why the problems occurred and what specific change eliminated them. The most probable explanation is that changing the batch of beads and antibody may have fixed the issue, however we are not sure. Nonetheless, we obtained good no-tag to tagged strain ratio for this experiment. Looking at this result we decided to proceed with ChIP again and address one remaining question about Top3 recruitment by Flag ChIP. These experiments worked well, as previously, and the results are reported in the thesis.

2.11 References:

Villa, M., Bonetti, D., Carraro, M., and Longhese, M.P. (2018). Rad9/53BP1 protects stalled replication forks from degradation in Mec1/ATR-defective cells. EMBO Rep *19*, 351-367.